

Surface polysaccharide biosynthesis and function, and regulation by DmxA and c-di-GMP in *Myxococcus xanthus*

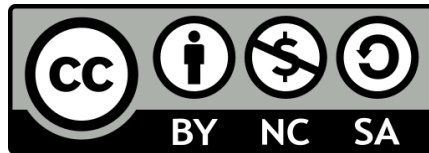
DISSERTATION
zur Erlangung des Doktorgrades
der Naturwissenschaften
(Dr. rer. nat.)

des Fachbereichs Biologie
der Philipps-Universität Marburg

vorgelegt von
María Pérez Burgos
aus Barcelona/Spanien

Marburg an der Lahn, 2020

Originaldokument gespeichert auf dem Publikationsserver der
Philipps-Universität Marburg
<http://archiv.ub.uni-marburg.de>



Dieses Werk bzw. Inhalt steht unter einer
Creative Commons
Namensnennung
Keine kommerzielle Nutzung
Weitergabe unter gleichen Bedingungen
4.0 Deutschland Lizenz.

Die vollständige Lizenz finden Sie unter:

<https://creativecommons.org/licenses/by-nc-sa/4.0/deed.de>

Die Untersuchungen zur vorliegenden Arbeit wurden von Januar 2015 bis Januar 2020 am Max-Planck-Institut für terrestrische Mikrobiologie unter der Leitung von Prof. Dr. Lotte Søgaard-Andersen durchgeführt.

Vom Fachbereich Biologie der Philipps-Universität Marburg

als Dissertation angenommen am: 16.03.2020

Erstgutachterin: Prof. Dr. Lotte Søgaard-Andersen
Zweitgutachter: Prof. Dr. Erhard Bremer

Weitere Mitglieder der Prüfungskommission:
Prof. Dr. Lars-Oliver Essen
Prof. Dr. Hans-Ulrich Mösch
Prof. Dr. Johann Heider

Tag der mündlichen Prüfung: 14.07.2020

Parts of this thesis have been published or are in preparation for publication:

Pérez-Burgos, M. & Søgaaard-Andersen, L. (2020). Regulation by c-di-GMP in *Myxococcus xanthus*. In: Microbial Cyclic Di-Nucleotide Signaling. S.-H. Chou, N. Guiliani, V.T. Lee & U. Römling (eds). Cham: Springer International Publishing, pp. 293-309.

Pérez-Burgos, M., García-Romero, I., Jung, J. Valvano, M.A. & Søgaaard-Andersen, L. (2019). Identification of the lipopolysaccharide O-antigen biosynthesis priming enzyme and the O-antigen ligase in *Myxococcus xanthus*: Critical role of LPS O-antigen in motility and development. Mol Microbiol, 112, 1178-1198

Pérez-Burgos M., García-Romero I., Valvano M.A., Søgaaard-Andersen L. Identification of the Wzx flippase, Wzy polymerase and sugar-modifying enzymes for spore coat polysaccharide biosynthesis in *Myxococcus xanthus*. Mol Microbiol (in press)

Pérez-Burgos M., García-Romero I., Jung J., Schander E., Valvano M.A., Søgaaard-Andersen L. Identification of the exopolysaccharide biosynthesis pathway in *Myxococcus xanthus* (in preparation)

Erklärung

Ich versichere, dass ich meine Dissertation mit dem Titel "Surface polysaccharide biosynthesis and function, and regulation by DmxA and c-di-GMP in *Myxococcus xanthus*" selbstständig, ohne unerlaubte Hilfe angefertigt und mich dabei keiner anderen als der von mir ausdrücklich bezeichneten Quellen und Hilfsmittel bedient habe. Diese Dissertation wurde in der jetzigen oder einer ähnlichen Form noch bei keiner anderen Hochschule eingereicht und hat noch keinen sonstigen Prüfungszwecken gedient.

Marburg den ____ ____ ____

María Pérez Burgos

Ami familia

Table of contents

Erklärung.....	3
Abbreviations	7
Abstract.....	9
Zusammenfassung	10
1. Introduction	12
1.1 Introduction to bacterial cell surface polysaccharides	12
1.1.1 Introduction to the bacterial cell envelope	12
1.1.2 Glycans and glycoconjugates in bacteria	12
1.1.3 General pathways for surface polysaccharide biosynthesis	14
1.1.4 Synthesis of lipopolysaccharide.....	18
1.2 Introduction to c-di-GMP	19
1.2.1 Regulation of surface polysaccharide synthesis by c-di-GMP	20
1.2.2 Regulation of motility by c-di-GMP	21
1.3 <i>Myxococcus xanthus</i> as a model organism.....	22
1.3.1 <i>M. xanthus</i> motility systems	22
1.3.2 Polarity and reversals in <i>M. xanthus</i>	24
1.3.3 Development.....	25
1.3.4 <i>M. xanthus</i> surface polysaccharides.....	26
1.3.5 Regulation by c-di-GMP in <i>M. xanthus</i>	33
2. Scope of this study.....	51
3. Results	52
3.1 Identification of the lipopolysaccharide O-antigen biosynthesis priming enzyme and the O-antigen ligase in <i>Myxococcus xanthus</i> : Critical role of LPS O-antigen in motility and development.....	52
3.1.1 Supplementary material.....	74
3.2 Identification of the Wzx flippase, Wzy polymerase and sugar-modifying enzymes for spore coat polysaccharide biosynthesis in <i>Myxococcus xanthus</i>	81
3.2.1 Supplementary material.....	102
3.3 Identification of the exopolysaccharide biosynthesis pathway in <i>Myxococcus xanthus</i> ..	112

3.3.1 Summary	113
3.3.2 Introduction	113
3.3.3 Results	116
3.3.4 Discussion	130
3.4.5 Acknowledgement	131
3.3.6 Experimental procedures	132
3.3.7 Supplementary material	138
3.4 Regulation by the diguanylate cyclase DmxA and c-di-GMP in <i>M. xanthus</i>	146
3.4.1 Results	146
3.4.2 Discussion	162
3.4.3 Experimental procedures	163
4. Discussion of the study	171
5. References.....	172
Acknowledgments	187
Curriculum Vitae	189

Abbreviations

ABC:	ATP-binding cassette
ATP/ADP:	Adenosin tri-/diphosphate
c-di-GMP:	Bis-(3'-5')-cyclic dimeric guanosine monophosphate
CPS:	capsular polysaccharides
CTT:	Casitone Tris medium
DGC:	diguanylate cyclase
DNA:	deoxyribonucleic acid
DRaCALA:	differential radial capillary action of ligand assay
DTT:	dithiothreitol
ECM:	extracellular matrix
EPS:	exopolysaccharide
Gal:	galactose
Glc:	glucose
GalNAc:	<i>N</i> -acetylgalactosamine
GlcNAc:	<i>N</i> -acetylglucosamine
GT:	glycotransferase
GTP/GDP/GMP:	Guanosine tri-/di-/ monophosphate
h:	hours
IM:	inner membrane
IPTG:	Isopropyl β -D-1-thiogalaktopyranoside
kDa:	kilodalton
Km:	kanamycin
l	litre
LOS:	lipooligosaccharide
LPS:	lipopolysaccharide
Man:	mannose
min:	minutes
MOPS:	3-(<i>N</i> -morpholino) propanesulfonic acid
MurNAc:	<i>N</i> -acetylmuramic acid
OD:	optical density
OM:	outer membrane
OMV:	outer membrane vesicles
OPX:	outer membrane polysaccharide export
OPG:	osmoregulated periplasmic glucans
PDE:	phosphodiesterase
PG:	peptidoglycan
PHPT:	polyisoprenyl-phosphate hexose-1-phosphate transferase
PNAG:	poly- β -D- <i>N</i> -acetylglucosamine
PNPT:	polyisoprenyl-phosphate <i>N</i> -acetylaminosugar-1-phosphate transferase
PST:	polysaccharide transporter
Rha:	rhamnose
s:	seconds
SD:	standard deviation
SDS-PAGE	sodium dodecyl sulfate polyacrilamide gel electrophoresis

Abbreviations

T4P:	type IV pili
TA:	teichoic acid
Tet:	tetracycline
TLC:	thin layer chromatography
TMH:	transmembrane helices
Und-P:	undecaprenyl phosphate
Xyl:	xylose
WT:	Wild type

Abstract

Bacteria possess surface polysaccharides that fulfill different functions, e.g. mediate host/pathogen interactions and protect cells from desiccation stress, predation or immunological reactions. *Myxococcus xanthus* is a Gram-negative deltaproteobacterium with a complex and nutrient-dependent life cycle. In the presence of nutrients, cells grow, divide and form coordinately spreading colonies on a solid surface. Upon starvation, cells initiate a developmental program that culminates in the formation of spore-filled fruiting bodies. Both parts of the lifecycle involve extensive cell-cell interactions. So far, three different surface polysaccharides have been identified in *M. xanthus*: lipopolysaccharide (LPS), exopolysaccharide (EPS) and spore coat polysaccharide. However little is known about their biosynthetic machineries, regulation and composition.

To understand how these polysaccharides are synthesized in *M. xanthus*, we identified homologs of proteins involved in surface polysaccharide biosynthesis (i.e. proteins of Wzx/Wzy or ABC-transporter dependent pathways). Bioinformatics, genetic analyses, heterologous expression, and biochemical experiments, in combination with detection of LPS, EPS or spore coat polysaccharide biosynthesis, allowed us to elucidate the biosynthetic pathways for LPS O-antigen and EPS. Moreover, we identified the missing components of the spore coat polysaccharide biosynthesis machinery. While synthesis of LPS O-antigen depends on an ABC-transporter-dependent pathway, synthesis of EPS and spore coat polysaccharide involves Wzx/Wzy-dependent pathways. Each individual pathway is dedicated to the biosynthesis of one polysaccharide. We also identified a polysaccharide biosynthesis locus of unknown function encoding homologs of a Wzx/Wzy-dependent pathway. Using selected mutants exclusively blocked in the synthesis of one of these sugars, we reevaluated the role of these surface glycans. We show that O-antigen is essential for development and gliding motility, but conditionally important for type IV pili (T4P)-dependent motility. By contrast, EPS is important for agglutination, T4P-dependent motility and T4P formation, and is conditionally important for development.

The nucleotide-based second messenger c-di-GMP has critical functions in *M. xanthus*. During growth, the diguanylate cyclase (DGC) DmxA is important for motility. We show that DGC activity of DmxA is important for motility and that DmxA is involved in regulation of the polarity of the two motility systems. Because DmxA-mVenus localizes to mid-cell and this localization depends on FtsZ, and DmxA does not contribute to the overall c-di-GMP pool, we suggest that DmxA function may be restricted to a local pool.

Zusammenfassung

Bakterien besitzen Oberflächenpolysaccharide, die unterschiedliche Funktionen erfüllen, z.B. Vermittlung von Wirt/ Pathogen-Interaktionen, und Schutz der Zellen vor Austrocknungsstress, vor Prädation oder vor immunologischen Reaktionen. *Myxococcus xanthus* ist ein gramnegatives Deltaproteobakterium mit einem komplexen und nährstoffabhängigen Lebenszyklus. In Gegenwart von Nährstoffen wachsen Zellen, teilen sich und bilden koordiniert ausbreitende Kolonien auf einer festen Oberfläche. Bei Nährstoffmangel initiieren die Zellen ein Entwicklungsprogramm, welches in der Bildung sporengefüllter Fruchtkörper gipfelt. Beide Teile des Lebenszyklus beinhalten umfangreiche Zell-Zell-Wechselwirkungen. Bisher wurden in *M. xanthus* drei verschiedene Oberflächenpolysaccharide identifiziert: Lipopolysaccharid (LPS), Exopolysaccharid (EPS) und Sporenhüllenpolysaccharid. Über ihre Biosynthesemaschinen, ihre Regulierung und Zusammensetzung ist jedoch wenig bekannt.

Um zu verstehen, wie diese Polysaccharide in *M. xanthus* synthetisiert werden, haben wir Homologe von Proteinen identifiziert, die an der Biosynthese von Oberflächenpolysacchariden beteiligt sind (Proteine von Wzx/Wzy- oder ABC-Transporter-abhängigen Wegen). Bioinformatik, genetische Analysen, heterologe Expression und biochemische Experimente in Kombination mit dem Nachweis der Biosynthese von LPS-, EPS- oder Sporenhüllenpolysaccharid, ermöglichten es uns die Biosynthesewege für LPS O-Antigen und EPS aufzuklären. Darüber hinaus identifizierten wir die fehlenden Komponenten der Biosynthesemaschine des Sporenbeschichtungspolysaccharids. Während LPS O-Antigen von einem ABC-Transporter-abhängigen Weg synthetisiert wird, involviert die Synthese von EPS und Sporenhüllenpolysaccharid Wzx/Wzy-abhängige Wege. Jeder einzelne Weg ist der Biosynthese eines Polysaccharids gewidmet. Zusätzlich identifizierten wir einen Polysaccharid-Biosyntheselokus mit unbekannter Funktion, der Homologe eines Wzx/Wzy-abhängigen Weges kodiert. Unter Verwendung ausgewählter Mutanten, die ausschließlich in der Synthese eines dieser Zucker blockiert sind, haben wir die Rolle dieser Oberflächenglykane neu evaluiert. Wir zeigen, dass O-Antigen für die Entwicklung und die gleitende Bewegung essentiell ist, aber bedingt wichtig für die Typ IV Pili (T4P) abhängige Motilität ist. Im Gegensatz dazu ist EPS wichtig für die Agglutination, die T4P-abhängige Motilität und die T4P-Bildung und ist bedingt wichtig für die Entwicklung.

Der auf Nukleotiden basierende sekundärer Botenstoff c-di-GMP hat bei *M. xanthus* wichtige Funktionen. Während des Wachstums ist die Diguanylatzyklase (DGC) DmxA bedeutend für die

Motilität. Wir zeigen, dass die DGC-Aktivität von DmxA für die Motilität wichtig ist und, dass DmxA an der Regulierung der Polarität beider Motilitätssysteme beteiligt ist. Da sich DmxA-mVenus in der Mitte der Zelle befindet und diese Lokalisierung von FtsZ abhängt, und DmxA nicht zum gesamten c-di-GMP-Pool beiträgt, schlagen wir vor, dass die DmxA-Funktion auf einen lokalen Pool beschränkt ist.

1. Introduction

1.1 Introduction to bacterial cell surface polysaccharides

1.1.1 Introduction to the bacterial cell envelope

In bacteria, the cell envelope serves as the first barrier of protection against the environment and is also an important site of interaction of cells with the environment. Glycosylated macromolecules located within the cell envelope, coupled to the cell envelope or loosely associated with the envelope, have important protective functions (Silhavy *et al.*, 2010). Moreover, surface glycans are in most pathogenic bacteria one of the principle virulence factors (Tytgat & Lebeer, 2014, Whitfield, 2006, Reid & Szymanski, 2010, Liang, 2015).

Gram-positive bacteria possess a single membrane composed of phospholipids surrounded by a thick peptidoglycan (PG) layer and also contain wall teichoic acids (WTA) and lipoteichoic acids (LTA) covalently coupled to the PG and membrane lipids, respectively. By contrast, Gram-negative bacteria possess an inner membrane (IM) composed of phospholipids, a thinner PG layer and an asymmetric outer membrane (OM) that confers additional protection. While proteins are present in all three layers, a modified phospholipid, lipopolysaccharide (LPS), is found exclusively in the outer leaflet of the OM (Silhavy *et al.*, 2010, Whitfield & Trent, 2014).

1.1.2 Glycans and glycoconjugates in bacteria

Bacteria synthesize different polysaccharides, oligosaccharides and glycoconjugates (Fig. 1) (Schmid *et al.*, 2015, Rehm, 2010, Tytgat & Lebeer, 2014). While polysaccharides and oligosaccharides are mainly composed of repeat units of monosaccharides, glycoconjugates are formed by polysaccharides covalently linked to other chemical species such as proteins, peptides and lipids.

An example of an intracellular metabolic reserve in bacteria is glycogen, which consists of an α -1,4-linked glucose homopolysaccharide with α -1,6-linked glucose branches (Wilson *et al.*, 2010). Osmoregulated periplasmic glucans (OPGs) are oligosaccharides formed by a glucose backbone and are found in the periplasm of many Gram-negative bacteria in response to low osmolarity. In *Escherichia coli*, OPGs are substituted by phosphoglycerol, phosphoethanolamine and succinyl residues (Bontemps-Gallo *et al.*, 2013).

Exopolysaccharides (EPS) are secreted polysaccharides that are classified into two types: Those closely associated with the cell surface including capsular polysaccharides (CPS), which are covalently linked to a phospholipid, and those polysaccharides that are secreted and only loosely associated with the cell surface through electrostatic interactions (slime or free EPS). Of note, it is challenging to differentiate CPS and free EPS because the phosphodiester bond between a polysaccharide and a phospholipid anchor can easily break releasing CPS or, alternatively, free EPS can be found closely associated with the cell surface (Knirel & Valvano, 2013).

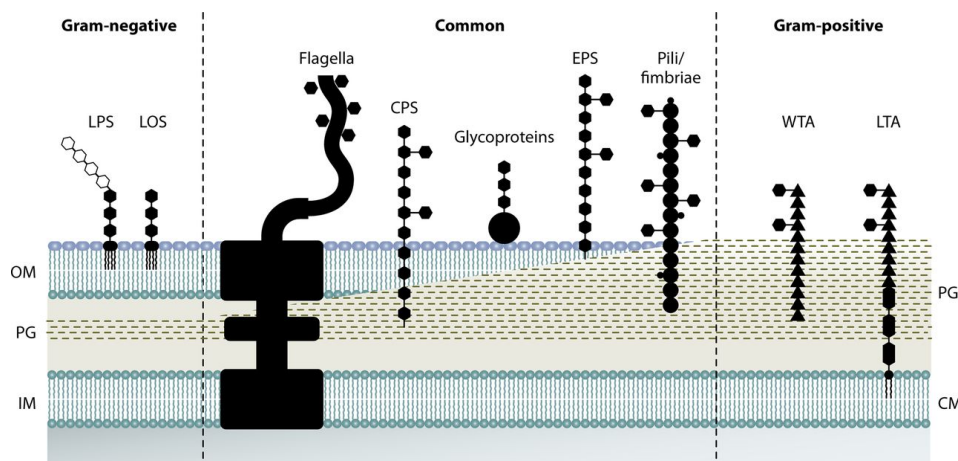


Figure 1. Bacterial glycans and glycoconjugates. LPS, lipopolysaccharide; LOS, lipooligosaccharide; WTA, wall teichoic acid; LTA, lipoteichoic acid; CPS, capsular polysaccharide; EPS, exopolysaccharide, and glycoproteins. Proteins (round dots), ribitol phosphate or glycerol phosphate moieties (triangles), and glycans (hexamers) are indicated. Figure was reproduced from (Tytgat & Lebeer, 2014) with permission of the publisher.

TAs are anionic polymers found in the wall of Gram-positive bacteria with low G+C content. They are made of poly(glycerol phosphate) or poly(ribitol phosphate) and can be classified into wall teichoic acids (WTA) that are covalently linked to the PG, and lipoteichoic acids (LTA), which are covalently coupled to phospholipids in the cytoplasmic membrane. Both WTA and LTA can be modified by glycosylation (Tytgat & Lebeer, 2014).

LPS are glycoconjugates formed by lipids and polysaccharides. LPS, also referred to as endotoxin, is found in the outer leaflet of the OM of Gram-negative bacteria and is generally composed of three different parts: the O-antigen polysaccharide, which is attached to an oligosaccharide part called core, which, in turn, is linked to lipid A that is responsible for anchoring LPS molecules in the OM (Knirel & Valvano, 2013). Alternatively, some bacteria have lipooligosaccharide (LOS), which lacks the O-antigen region and has an altered core oligosaccharide (Tytgat & Lebeer, 2014).

Glycoproteins in bacteria typically include surface layer proteins, pilins and flagellins. The type of glycosylation varies depending on the amino acid that is glycosylated. If the reaction occurs on serine, threonine or tyrosine, it is known as *O*-glycosylation; whereas it is referred to as *N*-/S-glycosylation if the reaction occurs on asparagine or cysteine, respectively (Tytgat & Lebeer, 2014). Proteins can be directly glycosylated by glycosyltransferases (GTs). Additionally, a glycan molecule can also be synthesized on an undecaprenyl phosphate (Und-P) (see below) and subsequently transferred to a protein in a reaction referred to as *en bloc* glycosylation. The latter one is catalyzed by an oligosaccharide transferase containing a Wzy_C domain, similarly to O-antigen ligases and Wzy polymerases (see below) (Hug & Feldman, 2011, Tytgat & Lebeer, 2014).

PG or murein is a rigid polymer that makes up the bacterial cell wall, defines the cell shape and confers resistance to internal turgor pressure. It is formed by alternating residues of *N*-acetylglucosamine (GlcNAc) and *N*-acetylmuramic acid (MurNAc) containing a short peptide of three to five amino acids. Peptide chains are cross-linked forming a large biopolymer (Knirel & Valvano, 2013, Sobhanifar *et al.*, 2013, Vollmer *et al.*, 2008).

1.1.3 General pathways for surface polysaccharide biosynthesis

Surface polysaccharides and glycoconjugates in bacteria are synthesized using different biosynthetic pathways, which involve different membrane and soluble proteins. So far, three synthetic machineries have been described for polysaccharide synthesis in bacteria (Schmid *et al.*, 2015, Valvano, 2011). Note that extracellular synthesis of glycans through a single sucrose protein from hydrolyzed oligosaccharides (e.g. dextran synthesis) (Schmid *et al.*, 2015) is not going to be discussed in this work.

1) The Wzx/Wzy-dependent pathway: The Wzx/Wzy dependent pathway (Fig. 2) is involved in the synthesis of polysaccharides and glycoconjugates. The synthesis of the repeat unit begins with the covalent coupling of a phosphorylated monosaccharide (sugar-P) to the recyclable undecaprenyl phosphate (Und-P), also known as bactoprenol or C₅₅-lipid linker, by a polyprenol phosphate C-1-phosphoglycosyltransferases (Lukose *et al.*, 2017) in the IM. The sugar-P moiety is typically derived from a uridine diphosphate (UDP)-sugar, and the product of the reaction is the formation of a phosphoanhydride bond between the bactoprenol and the sugar transferred (Und-PP-sugar) (Valvano, 2011, Valvano *et al.*, 2011).

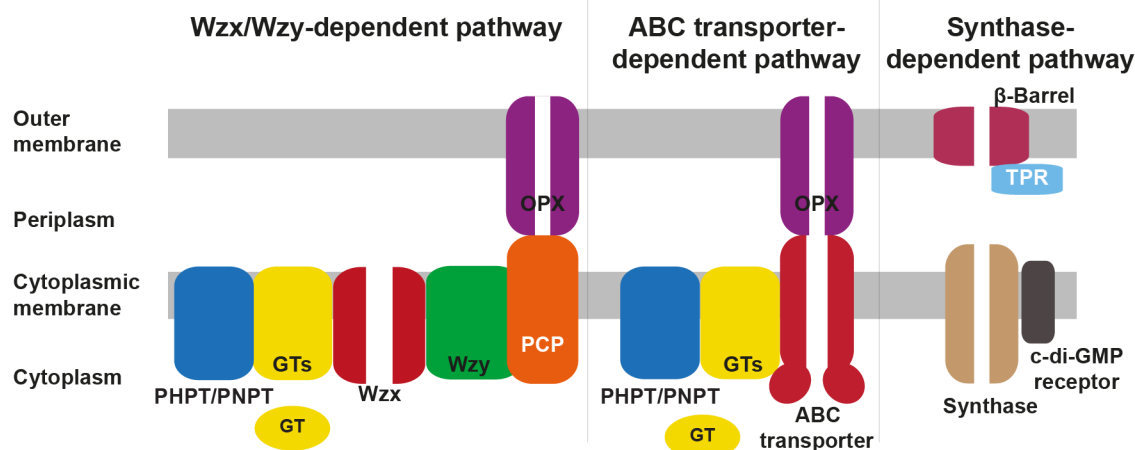


Figure 2. Model for surface polysaccharide biosynthesis (see text) based on (Whitfield, 2010, Cuthbertson *et al.*, 2007, Whitney & Howell, 2013).

The starting enzymes can be divided into two protein families: the polyisoprenyl-phosphate hexose-1-phosphate transferases (PHPTs) or the polyisoprenyl-phosphate *N*-acetylhexosamine-1-phosphate transferases (PNPTs) (Valvano, 2011, Patel *et al.*, 2012, Whitfield, 2010). Generally, PHPTs have hexose-1-P transferase activity. WbaP from *Salmonella enterica* (WbaP_{Se}) and WcaJ from *E. coli* (WcaJ_{Ec}) are prototypes for this family of enzymes. WbaP_{Se} transfers Galactose-1-P (Gal-1-P) and is involved in the synthesis of O-antigen (Saldías *et al.*, 2008), and WcaJ_{Ec} is involved in the synthesis of colanic acid by transferring Glucose-1-P (Glc-1-P) to Und-P. WcaJ_{Ec} contains an N-terminal domain with four transmembrane helices (TMHs), a large cytoplasmic loop and a C-terminal domain (containing one TMH that does not fully span the membrane and a cytosolic tail). The C-terminal domain is conserved among other PHPT and is responsible and sufficient for sugar transferase activity (Furlong *et al.*, 2015, Saldías *et al.*, 2008).

By contrast, PNPTs primarily transfer *N*-acetyl amino sugars. WecA from *E. coli* serves as the prototype for this family of enzymes. It is involved in initiation of synthesis of enterobacterial common antigen (ECA) and O-antigen by transferring GlcNAc to Und-P. Additionally, WecA contains eleven TMHs and five cytoplasmic loops. The second cytoplasmic loop contains the conserved DDxxD motif conserved among PHPTs, the fifth loop shows more diversity and it was proposed to participate in carbohydrate recognition (Valvano *et al.*, 2011). While PHPTs are exclusively found in bacteria, PNPTs are also found in eukaryotes associated with the membrane of the rough endoplasmic reticulum where they initiate synthesis of glycans important for *N*-glycosylation of proteins (Valvano *et al.*, 2011). PNPTs in bacteria transfer a sugar-1-phosphate to Und-P, whereas eukaryote homologs use dolichyl phosphate attached to the endoplasmic reticulum membrane (Valvano *et al.*, 2011, Hug & Feldman, 2011).

After completion of the first reaction in the Wzx/Wzy dependent pathway, different glycosyltransferases (GTs) add sugars to the non-reducing end to form the Und-PP-linked repeat unit, which is, subsequently, translocated by the Wzx flippase across the IM. Generally, Wzx proteins contain 12 trans-membrane helices (TMHs) (Valvano, 2011, Marolda *et al.*, 2010) and belong to the polysaccharide transporter (PST) family, which are substrate/H⁺ or Na⁺ antiporters to energize transport (Hvorup *et al.*, 2003, Islam & Lam, 2014). Wzx flippases are thought to recognize the repeat unit through the first sugar linked to the bactoprenol (Islam & Lam, 2014, Marolda *et al.*, 2004) and the amino acid sequence of Wzx homologs is highly variable consistent with the broad substrate specificity of the family members (Islam & Lam, 2014).

On the periplasmic side of the IM, the repeat units are polymerized to form the high molecular weight glycan chains. Polymerization is realized by the Wzy polymerase (Whitfield, 2010), which is an IM GT that contains 9-14 predicted TMHs (Whitfield, 2010, Islam & Lam, 2014), a large periplasmic loop in the C-terminal half of the protein and a second periplasmic loop at the N-terminus (Islam & Lam, 2014). Wzy polymerases transfer the reducing end of the growing polymer to the non-reducing end of the Und-PP-linked unit (Valvano *et al.*, 2011). They are not abundant in the cell and have high specificity for their respective substrates (Islam & Lam, 2014).

Polymerization and glycan chain length control involve the action of the polysaccharide co-polymerase (PCP) protein in the periplasm. Wzz is a PCP-1 protein that possesses two TMHs and a middle periplasmic loop (Whitfield, 2010, Islam & Lam, 2014). Wzc is a PCP-2 protein, which in addition to the mentioned domains contains an ATP-binding domain (either located in the C-terminus of the protein or as a separate polypeptide) and functions as an autophosphorylating tyrosine kinase (Reid & Szymanski, 2010, Morona *et al.*, 2000). While the exact mechanism of PCP proteins is not known, it was suggested that PCPs recruit Wzy subunits thereby increasing the polymerization efficiency of Wzy polymerases (Whitfield & Larue, 2008, Whitfield, 2010, Morona *et al.*, 2000). This idea is supported by the observation that Wzy and Wzz from *Rhizobium leguminosum* interact (Marczak *et al.*, 2013).

Finally, the glycan chain is transported through an OM polysaccharide export (OPX) protein in the OM to the cell surface (Schmid *et al.*, 2015, Whitfield, 2006). Note that the amphipathic LPS molecules follow a different translocation system and do not use OPX proteins (see below). Interestingly, differently than other OM proteins, the octamer of the OPX protein Wza forms an α -helical barrel that facilitates transport of the glycan to the outer leaflet of the OM (Reid & Cuthbertson, 2012).

2) The ATP-binding cassette (ABC) transporter-dependent pathway: Typically, glycan synthesis in this pathway (Fig. 2) also starts with the activity of a PHTP or PNPT (e.g. *E. coli* O8, O9, O9a) by transferring the first sugar-1-phosphate to Und-P (Reid & Szymanski, 2010). Alternatively, KpsC and KpsS initiate the synthesis of CPS by coupling 3-deoxy-D-manno-oct-2-ulosonic acid (Kdo) to a phosphatidylglycerol acceptor to form the poly-Kdo linker (Willis & Whitfield, 2013a).

Subsequently, the entire full-length polysaccharide molecule is synthesized through the sequential action of different GTs in the cytoplasm followed by its translocation across the IM by an ABC transporter (Willis & Whitfield, 2013b). The ABC transporter is composed of the membrane-spanning permease and an ATPase divided into two polypeptides (Wzm/KpsM and Wzt/KpsT, respectively) or in a single polypeptide (PglK from *Campylobacter jejuni* or Wzk from *Helicobacter pylori*) and depends on ATP hydrolysis for function (Reid & Szymanski, 2010, Tytgat & Lebeer, 2014, Valvano, 2011, Cuthbertson *et al.*, 2010). Finally, the polysaccharide is transported across the OM by an OPX protein.

ABC transporters generally have low specificity for the glycan chain. However, in some O-antigen biosynthesis systems (i.e. *E. coli* serotypes O8, O9 and O9a and *Klebsiella pneumoniae* serotypes O3 and O5), an additional C-terminal carbohydrate binding motif in the Wzt ATPase defines specificity for the glycan chain (Fig. 2). In those systems polymerization of the O-antigen can be terminated by a non-reducing terminal modification (i.e. methyl or methyl-phosphate), incorporated by the methyltransferase/kinase-methyltransferase WbdD. This modification can be specifically recognized by the carbohydrate binding motif of Wzt prior to its transport to the periplasm. Additionally, through terminal modification, WbdD regulates chain length control (Cuthbertson *et al.*, 2005, Clarke *et al.*, 2004, Greenfield & Whitfield, 2012).

3) The synthase-dependent pathway: In this pathway, the synthase complex (Fig. 2) that span the complete cell envelope, catalyzes the initiation, polymerization, and transport of usually rather simple glycans (e.g. composed of only one type of monosaccharide such as cellulose) (Schmid *et al.*, 2015). Differently from the previously described pathways, polymerization and transport through the cell wall occur simultaneously and may occur independently of a lipid carrier (Whitney & Howell, 2013).

In *Pseudomonas aeruginosa*, the alginate polymer is synthesized independently of a lipid carrier and transported across the IM by the Alg8 synthase while the PilZ protein Alg44, which binds and is regulated by c-di-GMP (see below), controls its synthesis. In the periplasm, where the TPR-

containing protein AlgK may facilitate protein-protein interactions, the polysaccharide is modified by the action of different enzymes. The mature alginate polymer crosses the OM through a β -barrel protein, AlgE (Tytgat & Lebeer, 2014, Whitney & Howell, 2013).

1.1.4 Synthesis of lipopolysaccharide

LPS is a modified glycolipid present in the outer leaflet of the OM in Gram-negative bacteria. LPS is responsible for protection of the cell, the interaction with the environment, forms a permeability barrier and it plays an important role in pathogenesis in many bacteria. Biosynthesis of its three distinct regions (lipid A, core (inner and outer) and O-antigen) requires >100 genes (Okuda *et al.*, 2016, Ruiz *et al.*, 2009), and biosynthesis of the lipid A-core and the O-antigen takes place separately before they are joined in the periplasm (Fig. 3).

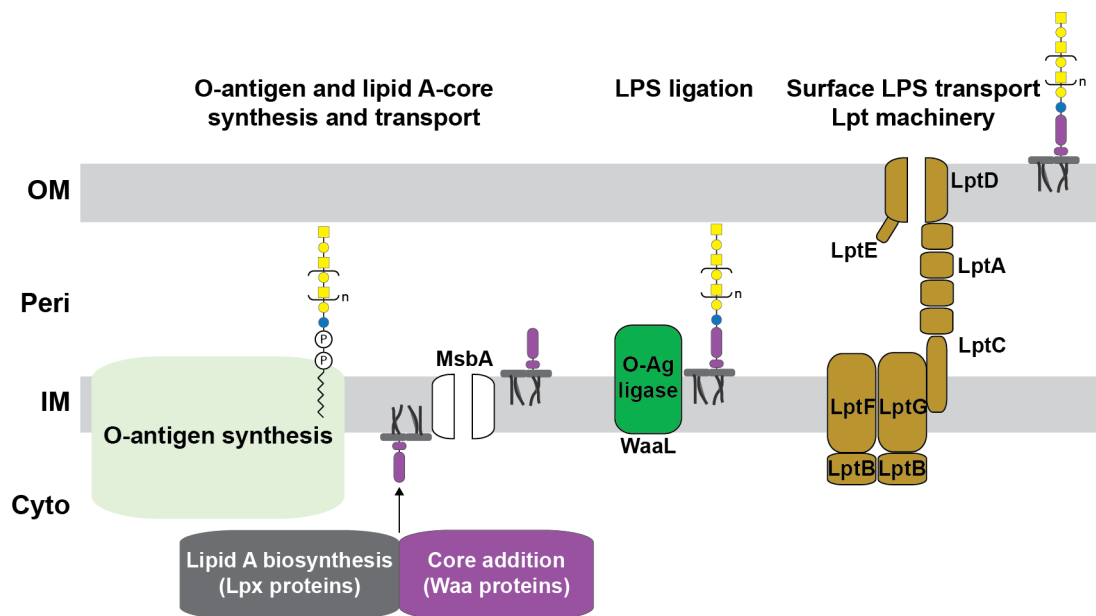


Figure 3. LPS biosynthesis in Gram negative bacteria (see text) based on (Okuda *et al.*, 2016, Ruiz *et al.*, 2009, Whitfield & Trent, 2014). In the O-antigen, the initiating sugar (blue) added by a PHPT or a PNPT, and the monosaccharides (yellow) added by GTs are indicated. Lipid A and core are depicted in dark grey and purple.

O-antigen can be synthesized by either of the three surface polysaccharide machineries while lipid A-core biosynthesis always depends on the so-called Raetz pathway (Whitfield & Trent, 2014). In the majority of species investigated, O-antigen is synthesized by either a Wzx/Wzy dependent pathway or an ABC-transporter dependent pathway; however, at least *S. enterica* serovar Borreze O:54 uses a synthase dependent pathway (Raetz & Whitfield, 2002, Valvano, 2011, Kalynych *et al.*, 2014, Whitfield & Trent, 2014, Keenleyside & Whitfield, 1996). In parallel, lipid A-core synthesis starts with the synthesis of the Kdo₂-lipid A intermediate at the cytoplasmic

side of the IM by the Lpx and Waa proteins (Raetz pathway). Synthesis of Kdo₂-lipid A depends on nine steps that are conserved among Gram-negative bacteria. GTs transfer sugars onto the Kdo₂-lipid A to form the lipid A-core, which is translocated through the ABC transporter MsbA (Whitfield & Trent, 2014). Transport through MsbA requires the presence of two Kdo residues which makes up for the quality control step of the lipid A-core synthesis (Tytgat & Lebeer, 2014).

In the periplasm, the O-antigen ligase WaaL ligates O-antigen and lipid A-core by forming a glycosidic bond between the core and the first sugar in the O-antigen (Raetz & Whitfield, 2002), followed by transport of the mature LPS molecule from the periplasmic side of the IM to the surface of the cell via the Lpt (LPS transport) pathway (Fig. 3) (Okuda *et al.*, 2016, Ruiz *et al.*, 2009). For this step, the LptB₂FG ABC transporter, formed by the ATPase LptB and the LptFG permease, extracts LPS molecules from the IM. The LPS molecule is transferred from LptC to LptA to cross the periplasmic space. Finally, at the OM, LptD and LptE interact in order to allow transport of the LPS to the outer leaflet of the OM, where the lipoprotein LptE acts as a plug (Okuda *et al.*, 2016, Ruiz *et al.*, 2009).

1.2 Introduction to c-di-GMP

Cyclic-di-GMP is a second messenger involved in regulation of different physiological processes in response to environmental and cell cycle signals in bacteria (Fig. 4). It is often associated with regulating the transition between motile and sessile lifestyles. Generally, it stimulates the biosynthesis of extracellular matrix (ECM) substances (e.g. exopolysaccharides and adhesins) during biofilm formation while inhibiting motility (see below). Additionally, c-di-GMP is involved in regulation of development, cell differentiation, cell cycle progression, and virulence (Römling *et al.*, 2013, Hengge, 2009, Jenal *et al.*, 2017, McDougald *et al.*, 2012).

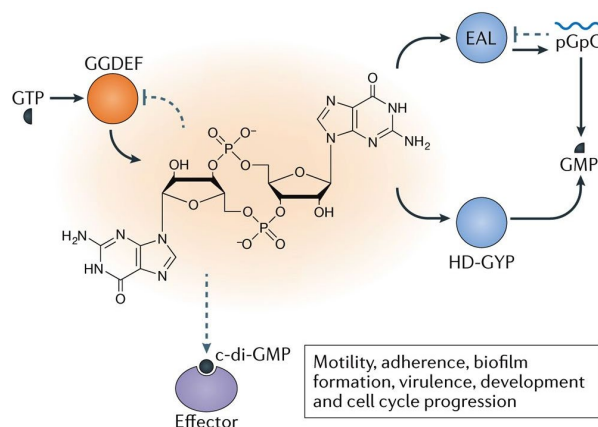


Figure 4. Principles of c-di-GMP signaling. Figure was reproduced and modified from (Jenal *et al.*, 2017) with permission of the publisher.

C-di-GMP is produced from two GTP molecules by diguanylate cyclases (DGCs) that contain a GGDEF or GGEEF motif at the active site (A-site) and often also an allosteric RxxD motif (I-site), which allows product inhibition to control DGC activity. c-di-GMP is hydrolyzed by phosphodiesterases (PDEs) with an EAL or HD-GYP domain to 5'-phosphoguanylyl-(3'-5')-guanosine (pGpG) (Hengge, 2009, Jenal *et al.*, 2017, Römling *et al.*, 2013) and then further degraded to 2 GMP molecules, which may depend on an oligoribonuclease (Cohen *et al.*, 2015, Orr *et al.*, 2015).

C-di-GMP regulates processes at the transcriptional, post-transcriptional and post-translational level by binding to effectors, which include riboswitches and proteins (Römling *et al.*, 2013, Jenal *et al.*, 2017). Proteinaceous effectors are highly diverse and include PilZ (Amikam & Galperin, 2006) and MshEN domain proteins (Wang *et al.*, 2016), various families of transcription factors, and proteins with degenerate and enzymatically inactive GGDEF and EAL domains (Jenal *et al.*, 2017, Römling *et al.*, 2013, Hengge, 2009).

1.2.1 Regulation of surface polysaccharide synthesis by c-di-GMP

An increase in c-di-GMP is often associated with inhibition of motility (see below) and increased biofilm formation by enhancing ECM production including EPS synthesis (Römling *et al.*, 2013, Liang, 2015). Since c-di-GMP was first identified as an allosteric activator of the cellulose synthase in *Komagataeibacter xylinus* (previously *Gluconacetobacter xylinus*) (Ross *et al.*, 1987), many more polysaccharide biosynthesis proteins have been described to be regulated by c-di-GMP. As mentioned, the synthase dependent pathway involved in glycan synthesis is usually controlled by c-di-GMP. While the cellulose synthase BcsA of *E. coli* contains an additional C-terminal PilZ domain (Steiner *et al.*, 2013), the alginate synthase in *P. aeruginosa* is controlled by the stand-alone PilZ protein Alg44 (Whitney & Howell, 2013, Liang, 2015). In both pathways, polysaccharide synthesis and transport is regulated by binding of c-di-GMP to the PilZ domains (Whitney & Howell, 2013). By contrast, during Pel polysaccharide synthesis in *P. aeruginosa*, the synthase PelF is controlled by the degenerate GGDEF protein PelD, which binds c-di-GMP (Liang, 2015). Finally, in the poly- β -D-N-acetylglucosamine (PNAG) synthesis pathway of *E. coli*, c-di-GMP mediates protein-protein interaction between the synthase PgaC and the PgaD protein to stimulate polysaccharide production (Steiner *et al.*, 2013). Importantly, c-di-GMP does not only regulate polysaccharide production at the post-translational level but also at the transcriptional level (Liang, 2015, Römling *et al.*, 2013). For instance, in *P. aeruginosa* transcription of the *psl* operon, that encodes proteins proposed to form part of a Wzx/Wzy-dependent pathway for Psl synthesis (Franklin *et al.*, 2011), and the *pel* operon, involved in Pel polysaccharide synthesis, is

regulated by c-di-GMP binding to the transcriptional regulator FleQ (Liang, 2015, Römling *et al.*, 2013).

C-di-GMP is not only involved in turning on and off polysaccharide synthesis, but is also implicated in regulation of modifications of polysaccharides. In *Caulobacter crescentus*, c-di-GMP regulates the cohesive properties of the holdfast by controlling the localization of the acetyltransferase HfsK during the cell cycle (Sprecher *et al.*, 2017). Additionally, in *P. aeruginosa*, the O-antigen methyltransferase WarA, which together with the kinase WarB regulate O-antigen chain length distribution, binds c-di-GMP resulting in an increase in its activity (McCarthy *et al.*, 2017).

1.2.2 Regulation of motility by c-di-GMP

C-di-GMP can regulate motility (i.e. flagellar, twitching and gliding motility) at different levels through complex signaling cascades and usually this regulation results in motility inhibition.

First, c-di-GMP can regulate assembly and activity of the flagellar motor. In *E. coli* and *S. enterica*, c-di-GMP binds to the YcgR PilZ effector to decrease motility by obstructing the flagellar motor; in *C. crescentus*, the flagellum is lost during the swarmer to stalked transition through an increase in c-di-GMP produced by the DGC PleD and the flagellum is assembled at low c-di-GMP levels established by the PDE PdeA (Jenal *et al.*, 2017, Hengge, 2009, Römling *et al.*, 2013). In *P. aeruginosa*, the DGC SadC and the PDE BifA oppositely regulate EPS synthesis and swarming motility (Merritt *et al.*, 2007). Interestingly, SadC was suggested to be controlled by signaling through the type IV pilus (T4P) apparatus by the PilY1 protein, which forms part of the T4P together with the minor and major pilins (Luo *et al.*, 2015, Leighton *et al.*, 2015). Additionally, c-di-GMP can regulate polarity of flagella assembly in *Bdellovibrio bacteriovorus* through the DGC DgcC (Hobley *et al.*, 2012) and at the transcriptional level, c-di-GMP binding to the transcription factor VspT inhibits transcription of flagellar genes in *Vibrio cholerae*.

The second messenger c-di-GMP can also regulate pili assembly and function in different organisms such as *M. xanthus* (see below), *P. aeruginosa*, *C. crescentus*, *Clostridium difficile* and *V. cholerae*. In *P. aeruginosa*, the PilZ protein that gave the name to the PilZ domain family, despite it doesn't bind c-di-GMP itself (Amikam & Galperin, 2006), and FimX, a two-domain protein with a degenerate GGDEF and an EAL domain, regulate T4P assembly and twitching motility. In contrast to PilZ, FimX is a c-di-GMP receptor (Navarro *et al.*, 2009) that localizes at the piliated pole (Kazmierczak *et al.*, 2006) and interacts with the PilB ATPase to regulate T4P assembly at low c-di-GMP concentrations (Jain *et al.*, 2017, Jain *et al.*, 2012). Similarly, in *Xanthomonas axonopodis*, PilZ interacts with PilB and FimX (Guzzo *et al.*, 2009).

The recently discovered MshEN domain proteins, named after the MshE ATPase involved in mannose-sensitive hemagglutinin (MshA) pilus assembly in *V. cholerae*, can bind c-di-GMP. MshEN domains are found among others in ATPases involved in type II secretion and in formation of T4P. Supporting this, direct binding of c-di-GMP to the PilB ATPase involved in T4P assembly in *Clostridium perfringens* was recently shown (Hendrick *et al.*, 2017).

Finally, regulation of gliding and pili assembly by c-di-GMP in the predatory cells of *B. bacteriovorus* occurs at several levels: the DGC DgcA regulates gliding motility to exit the prey (Hobley *et al.*, 2012). Binding of c-di-GMP to the degenerate GGDEF protein CdgA, which forms part of a protein complex at the leading pole including the response regulator RomR and the GTPase MglA (see below), has been shown to regulate predation. Importantly, MglA regulates predation, gliding reversals and pilus extrusion (Milner *et al.*, 2014, Hobley *et al.*, 2012) and it is possible that c-di-GMP and CdgA participate in those processes as well.

1.3 *Myxococcus xanthus* as a model organism

M. xanthus is a Gram-negative rod-shaped deltaproteobacterium with a social lifecycle regulated by nutrient availability that includes a vegetative and a developmental stage. In the presence of nutrients the cells grow, divide and form coordinately spreading colonies on solid surfaces. Upon starvation, cells initiate a multicellular developmental program and aggregate to form fruiting bodies inside which the cells differentiate to spores that germinate in the presence of nutrients (Wireman & Dworkin, 1977, Konovalova *et al.*, 2010). Development depends on motility, intercellular signaling, temporal regulation of gene expression and regulated proteolysis (Konovalova *et al.*, 2010, Zhang *et al.*, 2012, Kroos, 2017), synthesis of polysaccharides (Lu *et al.*, 2005, Fink & Zissler, 1989b, Müller *et al.*, 2012), as well as intracellular signaling by the nucleotide-based second messengers c-di-GMP (Skotnicka *et al.*, 2016, Skotnicka *et al.*, 2015) and (p)ppGpp (Harris *et al.*, 1998, Singer & Kaiser, 1995). Due to its complex and social life style, *M. xanthus* serves as a model for investigating motility, cell polarity, development and cell differentiation.

1.3.1 *M. xanthus* motility systems

M. xanthus cells move in the direction of their long axis by means of two genetically distinct motility systems, one is for type IV pili (T4P)-dependent motility and one is for gliding motility (Schumacher & Søgaard-Andersen, 2017, Zhang *et al.*, 2012). The two motility systems function synergistically, but confer different advantages depending on the surface conditions. The gliding motility system

promotes the motility of single cells on hard and dry surfaces (1.5-2.0% agar), whereas the T4P-dependent motility system favors the movement of groups of cells on soft and wet surfaces (e.g. 0.5% agar) (Shi & Zusman, 1993).

Gliding motility depends on assembly of a protein complex spanning the cell envelope and formed by two subcomplexes, the Agl motor formed by AglR, AglQ and AglS and 11 Glt proteins (GltA-K) (Fig. 5). The Agl-Glt proteins additionally interact with a cytoplasmic subcomplex formed by the AglZ protein, the Ras-like GTPase MglA (see below), and the actin-like protein MreB. The machinery, powered by proton motive force, assembles at the leading cell pole, adheres to the underlying substratum forming so-called focal adhesion complexes, moves directionally along the cell to propel the cell and disassembles at the lagging cell pole (Treuner-Lange *et al.*, 2015, Schumacher & S gaard-Andersen, 2017, Zhang *et al.*, 2012, Faure *et al.*, 2016, Luciano *et al.*, 2011, Jakobczak *et al.*, 2015).

Slime deposition is a general means for gliding organisms to adhere and move over surfaces. The deposition of a trail or so-called “slime” containing polysaccharides and OM vesicles (OMV), which other cells tend to preferably follow, has been associated with the movement of single cells by gliding (Ducret *et al.*, 2012, Ducret *et al.*, 2013).

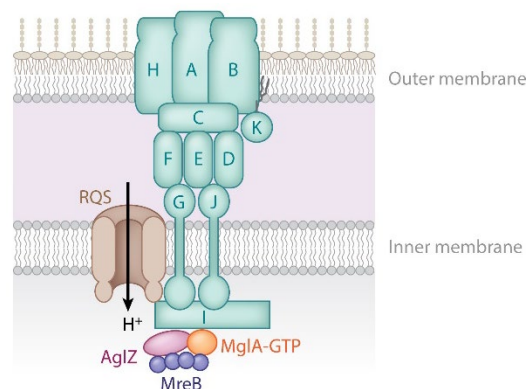


Figure 5. Model of the *M. xanthus* gliding motility machinery. Agl and Glt proteins are in brown and aqua, respectively. Figure was reproduced from (Schumacher & S gaard-Andersen, 2017) with permission of the publisher.

The T4P-dependent motility system of *M. xanthus* depends on three different components: T4P, LPS O-antigen and EPS (Konovalova *et al.*, 2010, Li *et al.*, 2003, Lu *et al.*, 2005, Bowden & Kaplan, 1998) and it is additionally regulated by the second messenger c-di-GMP (see below) (Skotnicka *et al.*, 2015). The T4P is a cell surface appendage that undergoes cycles of extension, adhesion and retraction. The current model proposes that EPS stimulates T4P retraction and that upon attachment of T4P to the EPS on a neighboring cell, pili retraction is triggered promoting the

movement of groups of cells (Li *et al.*, 2003). However, it is not clear how LPS O-antigen influences T4P-dependent motility.

The T4P function depends on a highly conserved envelope-spanning machinery consisting of 10 proteins that localize polarly in *M. xanthus* (Fig. 6) (Friedrich *et al.*, 2014, Chang *et al.*, 2016, Siewering *et al.*, 2014). The PilQ secretin forms an OM pore around which TsaP forms a periplasmic ring. The lipoprotein Tgl facilitates PilQ multimerization (Wall *et al.*, 1998). The periplasmic domains of PilQ together with PilP, and PilO and PilN constitute the mid-periplasmic and the lower periplasmic rings, respectively. The IM protein PilC constitute the cytoplasmic dome and PilM forms a ring in the cytoplasm. Finally, the PilB and PilT ATPases bind in a mutually exclusive manner to the base of the T4P machinery to extend or retract the T4P (Friedrich *et al.*, 2014, Chang *et al.*, 2016, Bulyha *et al.*, 2009, Siewering *et al.*, 2014, Bischof *et al.*, 2016).

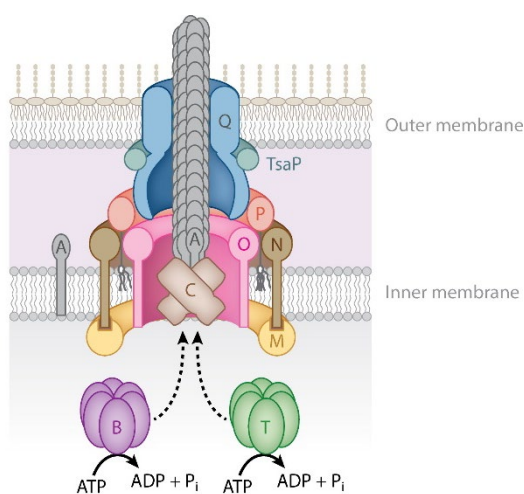


Figure 6. Architectural model of the T4aP machine of *M. xanthus* (see text). Proteins labeled with single letters have the Pil prefix. Figure was reproduced from (Schumacher & Sogaard-Andersen, 2017) with permission of the publisher.

1.3.2 Polarity and reversals in *M. xanthus*

Both motility systems in *M. xanthus* are polarized and only assemble at the leading cell pole. However, in response to signaling by the Frz chemosensory system, *M. xanthus* cells undergo a so-called reversal process in which the direction of motility is changed and the leading and lagging cell poles are inverted.

Regulation of cell polarity in *M. xanthus* depends on the polarity module MglA/MglB/RomR-RomX (Schumacher & Sogaard-Andersen, 2017, Szadkowski *et al.*, 2019). MglA is a Ras-like GTPase that localizes at the leading cell pole and binds its effectors when it is in the GTP-bound state to stimulate both motility systems. MglB is its cognate GTPase activating (GAP) protein, which

mainly localizes to the lagging cell pole and stimulates the low intrinsic GTPase activity of MglA resulting in the conversion of active MglA-GTP to inactive MglA-GDP. By contrast, the complex formed by the response regulator RomR and RomX, possesses guanine nucleotide exchange factor (GEF) activity and stimulates the exchange of GDP for GTP by MglA and, thus, MglA-GTP formation (Szadkowski *et al.*, 2019, Schumacher & Søgaard-Andersen, 2017).

1.3.3 Development

In response to scarce nutrients, *M. xanthus* cells start a multicellular developmental program with distinct morphological stages. During the first 4-6 h, motile cells aggregate into translucent mounds. By 24 h the fruiting body is formed and inside it, cells undergo morphological changes to differentiate into myxospores. By 72 h sporulation is complete and the mature fruiting body has been formed (Wireman & Dworkin, 1977, Konovalova *et al.*, 2010). Not all the cells that start the developmental program turn into spores, instead there are three different cell subpopulations. Around 10% of the cells differentiate into spores; 30% remains outside of the fruiting bodies, shows a rod-shaped morphology and are known as 'peripheral rods' (O'Connor & Zusman, 1991a, O'Connor & Zusman, 1991b), while the remaining cells undergo cell lysis (Wireman & Dworkin, 1977).

The developmental program is a complex process regulated by different signaling cues. As a response to starvation, RelA synthesizes (p)ppGpp, which affects gene transcription important for development and starts the developmental program (Harris *et al.*, 1998, Singer & Kaiser, 1995). Fruiting body formation depends on the intercellular A-E signals, which affect regulation of motility and gene expression, and regulated proteolysis (Konovalova *et al.*, 2010, Zhang *et al.*, 2012, Kroos, 2017, Bretl & Kirby, 2016). (p)ppGpp accumulation is necessary and sufficient to start the developmental program and two of the main intercellular signaling cascades (A and C) depend on (p)ppGpp (Harris *et al.*, 1998, Singer & Kaiser, 1995, Manoil & Kaiser, 1980, Konovalova *et al.*, 2012).

Additionally, motility (Hodgkin & Kaiser, 1979), LPS O-antigen and EPS (Lu *et al.*, 2005, Fink & Zissler, 1989b, Müller *et al.*, 2012), as well as intracellular signaling by the nucleotide-based second messengers c-di-GMP (Skotnicka *et al.*, 2016, Skotnicka *et al.*, 2015) are essential for fruiting body formation. Myxospore formation depends on MreB, peptidoglycan degradation and spore coat polysaccharide synthesis (Müller *et al.*, 2010, Bui *et al.*, 2009, Müller *et al.*, 2012).

1.3.4 *M. xanthus* surface polysaccharides

M. xanthus cells are surrounded by an ECM (Merroun *et al.*, 2003, Arnold & Shimkets, 1988a, Hu *et al.*, 2013), mostly composed of EPS and proteins (1:1) (previously known as fibrils) (Behmlander & Dworkin, 1994), but also extracellular lipids (Gloag *et al.*, 2016), OM vesicles (Remis *et al.*, 2014, Ducret *et al.*, 2013, Gloag *et al.*, 2016, Palsdottir *et al.*, 2009, Kahnt *et al.*, 2010) and extracellular DNA (Hu *et al.*, 2012a, Gloag *et al.*, 2016). In addition to EPS, *M. xanthus* synthesizes two other additional surface polysaccharides (LPS and spore coat polysaccharide). LPS O-antigen and EPS are important for motility and development, whereas the spore coat polysaccharide is essential for formation of heat and sonic resistant spores (Müller *et al.*, 2012, Fink & Zissler, 1989b, Lu *et al.*, 2005, Yang *et al.*, 2000a). Additionally gliding cells deposit a slime trail, whose composition and function are unknown, but contains at least polysaccharides and OMV (Ducret *et al.*, 2012, Ducret *et al.*, 2013, Gloag *et al.*, 2016).

1.3.4.1 The *M. xanthus* LPS

M. xanthus possesses an LPS molecule composed of lipid A, core and O-antigen (Maclean *et al.*, 2007, Fink & Zissler, 1989a) (Fig. 7). Little is known about LPS synthesis in *M. xanthus*, except that a Wzm and a Wzt homolog were implicated in polymeric O-antigen synthesis suggesting that the synthesis depends on an ABC-transporter dependent pathway (Guo *et al.*, 1996, Kaplan *et al.*, 1991, Bowden & Kaplan, 1998). Additionally, the two GTs WbgA and WbgB are essential for O-antigen synthesis (Guo *et al.*, 1996, Kaplan *et al.*, 1991).

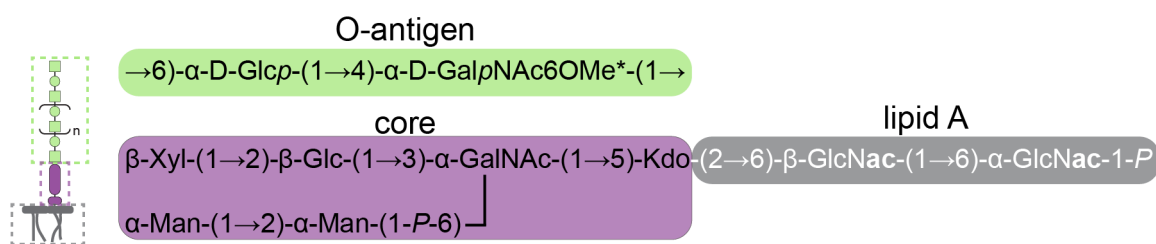


Figure 7. Structure of the LPS molecule in *M. xanthus*, where ac are 13-methyl-C14-3OH (*iso*-C15-3OH), C16-3OH, or 15-methyl-C16-3OH (*iso*-C17-3OH) based on (Maclean *et al.*, 2007).

LPS is essential in *M. xanthus* (Vassallo *et al.*, 2015). Moreover, LPS O-antigen has been suggested to be important for motility and development (Guo *et al.*, 1996, Kaplan *et al.*, 1991, Bowden & Kaplan, 1998, Vassallo *et al.*, 2015, Fink & Zissler, 1989a). While it is not known how LPS O-antigen affects these processes, it was observed that *M. xanthus* LPS undergoes several modifications during early development (e.g. methylation) (Panassenko, 1985, Sutherland, 1976, Panassenko *et al.*, 1989). Additionally, LPS has been suggested to be removed during differentiation into spores (Sutherland, 1976, Sutherland & Thomson, 1975).

1.3.4.2 The *M. xanthus* spore coat polysaccharide

In the first step of cell differentiation to form spores, the rod-shaped *M. xanthus* cells shorten and eventually become spherical spores with a diameter of 1-2 μm (Dworkin & Voelz, 1962, Dworkin & Gibson, 1964, Müller *et al.*, 2012). During this process, the PG is degraded (Bui *et al.*, 2009) and the spore coat containing a thick layer of polysaccharide (Holkenbrink *et al.*, 2014, Müller *et al.*, 2012) and various proteins (i.e. protein C, S2, and U) (McCleary *et al.*, 1991, Inouye *et al.*, 1979a, Leng *et al.*, 2011) is synthesized. Importantly, while none of these proteins are essential for spore formation (Komano *et al.*, 1984, Inouye *et al.*, 1979b, Leng *et al.*, 2011, Lee *et al.*, 2011, Curtis *et al.*, 2007), the spore coat polysaccharide made of 1-3-, 1-4-linked *N*-acetylgalactosamine (GalNAc), 1-4-linked Glc (GalNAc:Glc ratio 17:1) and glycine is essential for myxospore formation and confers resistance to heat, sonic and ultraviolet light treatments (Holkenbrink *et al.*, 2014, Müller *et al.*, 2012).

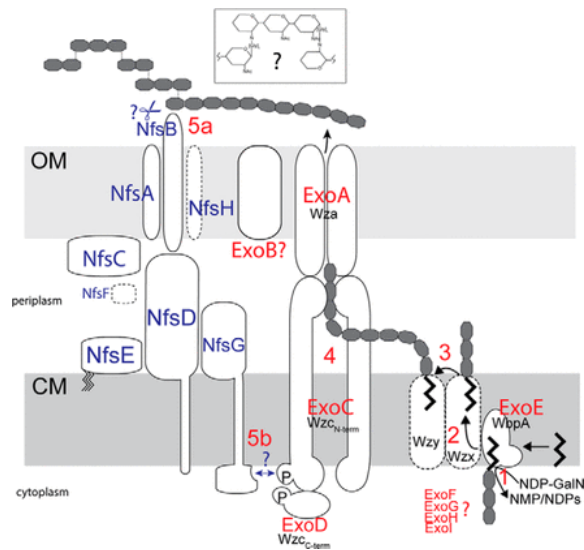


Figure 8. Model for spore coat polysaccharide synthesis and modification in *M. xanthus*. Figure was reproduced from (Holkenbrink *et al.*, 2014) with permission of the publisher.

Synthesis of the *M. xanthus* spore coat polysaccharide depends on the ExoA-I and the NfsA-H/AgIQRS proteins (Holkenbrink *et al.*, 2014, Ueki & Inouye, 2005, Müller *et al.*, 2012, Licking *et al.*, 2000, Wartel *et al.*, 2013). The ExoA-I proteins form part of an incomplete Wzx/Wzy-dependent pathway essential for spore coat polysaccharide synthesis (Fig. 8) (Holkenbrink *et al.*, 2014, Müller *et al.*, 2012), where ExoE, a sugar transferase homologue, links UDP-sugar to the Und-P lipid carrier, starting the synthesis of the repeat unit. The repeat unit is transported across the IM by an unidentified Wzx flippase, it is assembled into a higher molecular weight polysaccharide by an unknown Wzy polymerase in the periplasm and it is transported through ExoA (Wza) across the OM. Polymerization and/or transport may be regulated by ExoC (PCP-2)

under the control of the tyrosine kinase ExoD (Kimura *et al.*, 2011). On the cell surface, the NfsA-H machinery, which is homologous to the Glt motility machinery and powered by the AglQRS proteins, assembles the polysaccharides into a rigid structure (Holkenbrink *et al.*, 2014, Müller *et al.*, 2012, Müller *et al.*, 2010, Wartel *et al.*, 2013, Ueki & Inouye, 2005).

1.3.4.3 The *M. xanthus* EPS

EPS forms part of the ECM; however, it is not known whether it is covalently attached to the OM (Merroun *et al.*, 2003, Arnold & Shimkets, 1988a, Kim *et al.*, 1999, Behmlander & Dworkin, 1994) or whether it is released into the ECM (Berleman *et al.*, 2016, Gloag *et al.*, 2016, Hu *et al.*, 2013, Berleman *et al.*, 2011, Lux *et al.*, 2004).

Little is known about the structure and synthesis of EPS in *M. xanthus*. Its monosaccharidic composition has been studied multiple times with various approaches and different results (Table 1) and while the exact EPS biosynthesis machinery has not been identified, an *eps* locus, identified by transposon mutagenesis, has been implicated with its synthesis and export (Lu *et al.*, 2005). Since the biosynthetic machinery is unknown, the majority of the studies investigating EPS function has been performed using mutants involved in the regulation of EPS metabolism (see below).

EPS is essential for cell-cell cohesion (Shimkets, 1986a, Arnold & Shimkets, 1988a, Hu *et al.*, 2012b, Yang *et al.*, 2000b) and it is important at both stages of the *M. xanthus* social life cycle to regulate T4P-dependent motility and development (Arnold & Shimkets, 1988b, Chang & Dworkin, 1994, Shimkets, 1986b, Yang *et al.*, 1998b, Dana & Shimkets, 1993, Yang *et al.*, 1998a, Lu *et al.*, 2005). Additionally, while EPS is not required *per se* for predation on solid surfaces (Müller *et al.*, 2016), the adhesive properties of EPS are required in aqueous environments through formation of aggregates with the prey (Pan *et al.*, 2013).

Table 1. Analysis of the EPS composition in *M. xanthus*.

Reference	GalN	GlcN	Gal	Glc	Man	Rha	Xyl
(Sutherland & Thomson, 1975)	X	X	X	X	X		
(Behmlander & Dworkin, 1994)		X	X	X		X	X

Because, as mentioned, different regulatory mutants have been analyzed without considering potential pleiotropic effects of the mutations, there are many controversies regarding the exact

function of EPS. Large amounts of EPS are found in fruiting bodies (Lux *et al.*, 2004) and it was suggested that EPS keeps the structure and the spores within the fruiting body together (Burchard, 1975, Berleman *et al.*, 2016). However, while some EPS⁻ mutants (i.e. *dsp* or *difA-C*, *sglK*, *cds*, *rasA/sgmO*) are completely blocked in fruiting body formation (Yang *et al.*, 1998a, Shimkets, 1986b, Downard *et al.*, 1993, Ramaswamy *et al.*, 1997, Pham *et al.*, 2005, Bellenger *et al.*, 2002), an *epsZ* mutant, which lacks the PHPT important for EPS synthesis, formed translucent aggregates on agar with apparent reduced sporulation (Berleman *et al.*, 2016, Zhou & Nan, 2017).

Because EPS affects the overall colony structure and the motility pattern as well (Hu *et al.*, 2016, Hu *et al.*, 2012b), the mechanism by which EPS regulates T4P-dependent motility has been studied in numerous studies leading to different conclusions. First, polysaccharides containing amino sugars (i.e. EPS) have been suggested to trigger retraction of T4P in *M. xanthus* cells enhancing the collective movement by T4P-dependent motility (Li *et al.*, 2003). This was concluded from the observation that different mutants lacking EPS ($\Delta difA$, *dsp*, *difE* and *sglK*) showed hyperpiliation and that the defect in pili retraction could be rescued by addition of isolated EPS material or chitin, a GlcNAc polymer (Li *et al.*, 2003, Hu *et al.*, 2011). However, the $\Delta difA$ hyperpiliation results reported by Li *et al.* (Li *et al.*, 2003) are in disagreement with a previous study, in which it was shown that WT and $\Delta difA$ cells assembled similar levels of T4P (Yang *et al.*, 2000b). Also, a shear-off assay on other EPS⁻ mutants (i.e. *esg*, *cds* and *epsZ* strains) showed the same level of T4P as in WT cells (Ramaswamy *et al.*, 1997, Kim *et al.*, 1999, Zhou & Nan, 2017). Even though GlcNAc was proposed to bind to the PilA protein of *M. xanthus* (Hu *et al.*, 2012c), it remains unclear how EPS is actually affecting T4P-dependent motility.

The second model for how EPS is important for motility is based on the importance of EPS for cell-cell cohesion. It has been debated whether *M. xanthus* EPS has glue-like properties or whether it works as a lubricant (Hu *et al.*, 2016, Gibiansky *et al.*, 2013). While some studies support that an increase in the EPS level leads to an increase in colony expansion by means of collective movement by T4P (Berleman *et al.*, 2016, Patra *et al.*, 2016), others showed a reduction in T4P-dependent motility (Black & Yang, 2004, Xu *et al.*, 2005, Moak *et al.*, 2015). Interestingly, based on single cell analysis, EPS has been proposed to regulate single cell velocity and cell directionality of T4P-dependent motility (Berleman *et al.*, 2016, Hu *et al.*, 2016, Hu *et al.*, 2011).

The third proposal considers the implication of EPS in the regulation of cell reversals. However, this is controversial. While Zhou & Nan (Zhou & Nan, 2017) observed an increase in the reversal frequency of $\Delta epsZ$ cells on soft and hard agar, Berleman *et al.* (Berleman *et al.*, 2016) observed

no changes in the reversal frequency of *epsZ* cells in comparison to WT. Moreover, either no effects (Yang *et al.*, 1998b, Yang *et al.*, 1998a) or a decrease (Shi *et al.*, 2000, Kearns *et al.*, 2000) in the reversal frequency of gliding cells were observed for the *sglK*, *difE*, *difA* or *difC* mutants.

In conclusion, it is not clear if the T4P-dependent motility defects observed result exclusively from lack of EPS or from pleiotropic effects as a result of the corresponding mutation(s).

1.3.4.4 Regulation of EPS synthesis

EPS synthesis increases upon surface contact, high cell density and calcium (Behmlander & Dworkin, 1991, Arnold & Shimkets, 1988a, Kim *et al.*, 1999, Berleman *et al.*, 2011, Patra *et al.*, 2016, Hillesland & Velicer, 2005). There are several proteins extensively described to influence EPS synthesis: proteins encoded by the *eps* and *eas* loci (Lu *et al.*, 2005), the Dif chemosensory pathway (see below) (Yang *et al.*, 1998b), the DnaK orthologs SglK (Weimer *et al.*, 1998, Yang *et al.*, 1998a) and StkA (Dana & Shimkets, 1993, Moak *et al.*, 2015) together with FibR, StkB and StkC (Weimer *et al.*, 1998, Moak *et al.*, 2015), the Pil proteins (i.e. *pilA*, *pilB*, *tgl*, *pilQ*, *pilR*, *pilR2* and *pilT*) (Black *et al.*, 2006, Wallace *et al.*, 2014, Dana & Shimkets, 1993, Bretl *et al.*, 2016, Wu *et al.*, 1997, Shimkets, 1986a, Black *et al.*, 2017) and the NtrC-like transcriptional activators Nla24/EpsI and Nla19 (Lancero *et al.*, 2004, Lancero *et al.*, 2005, Lu *et al.*, 2005). Additionally, other proteins have been implicated in EPS synthesis: RasA/SgmO (Pham *et al.*, 2005), FrzS (Berleman *et al.*, 2011), the Che7 chemosensory system (Black *et al.*, 2009), the tyrosine phosphatase PhpA (Mori *et al.*, 2012), the tyrosine kinases BtkB (Kato *et al.*, 2015) and Mask (Thomasson *et al.*, 2002), the Clp/Hsp100 chaperone MXAN_4832 (Yan *et al.*, 2012), a CRISPR system (Wallace *et al.*, 2014), the RppA transducer homolog together with the MmrA multidrug transporter homolog (Kimura *et al.*, 2004), the DNA-binding response regulator DigR (Overgaard *et al.*, 2006) and its partner kinase SgmT (Petters *et al.*, 2012). Also, the second messenger c-di-GMP was described to be involved in regulation of EPS accumulation during growth and development in *M. xanthus* (Skotnicka *et al.*, 2016, Skotnicka *et al.*, 2015) (see below). Importantly, it is not clear whether these regulators are directly involved in EPS synthesis or regulate a different process (e.g. regulation of metabolism to synthesize sugar precursors), which indirectly affects EPS.

Among the different regulators of EPS synthesis, the Dif (Defective in fruiting/fibril) chemosensory pathway is the most studied regulator of EPS synthesis and many of the functions assigned to EPS (i.e. essential for T4P-dependent motility, T4P-retraction, aggregation and fruiting body formation) have been determined using *dif* (previously *dsp* (Lancero *et al.*, 2002, Yang *et al.*,

2000b)) mutants (Fig. 9). The Dif system (Yang & Li, 2005, Yang *et al.*, 1998b) consists of at least six proteins: DifA (a methyl-accepting chemotaxis (MCP)-like protein), DifE (CheA-like) and DifC (CheW-like) form a membrane signaling complex (Lancero *et al.*, 2005, Yang & Li, 2005, Xu *et al.*, 2005, Xu *et al.*, 2011) and are positive regulators of EPS synthesis (Yang *et al.*, 1998b, Bellenger *et al.*, 2002). Two response regulators, DifD and EpsW (both CheY-like), are phosphorylated by the DifE histidine kinase (Lancero *et al.*, 2005, Yang & Li, 2005, Black *et al.*, 2010, Black *et al.*, 2015); additionally DifE also weakly interacts with the Ntrc-like response regulator Nla19 (Lancero *et al.*, 2005). While phosphorylation of EpsW positively regulates EPS metabolism (Black *et al.*, 2015), DifD is suggested to be a phosphate sink (Black *et al.*, 2010). Lack of DifD or DifG (a CheC-like phosphatase that accelerates the dephosphorylation of phosphorylated DifD) causes an increase in EPS accumulation (Black & Yang, 2004). However, the model does not address why a $\Delta difD \Delta difG$ double mutant, has a significant stronger phenotype on EPS production than the single mutations (Black *et al.*, 2006). Additionally, Mcp7 and DifA were suggested to compete for interactions with DifC in the absence of Che7 (Black *et al.*, 2009). Similarly, the signals transmitting through the Dif pathway affect the Frz chemosensory systems (Xu *et al.*, 2008) suggesting that signaling through the Dif pathway is very complex.

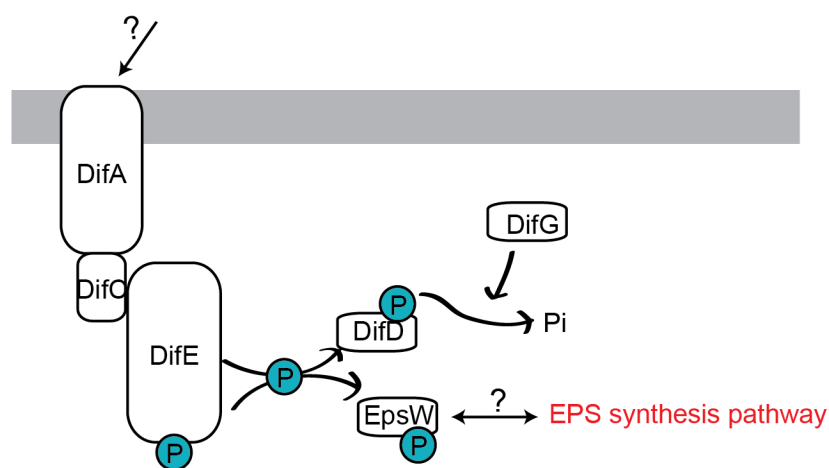


Figure 9. Model for Dif signaling pathway in *M. xanthus*, (see text) based on (Zusman *et al.*, 2007, He & Bauer, 2014, Black *et al.*, 2015, Lancero *et al.*, 2005).

Mutants impaired in T4P show a defect in EPS biosynthesis, while StkA inhibits EPS synthesis (Moak *et al.*, 2015, Dana & Shimkets, 1993) and SglK stimulates EPS production (Weimer *et al.*, 1998, Yang *et al.*, 1998a). Through combination of double or triple mutations and epistasis, it was possible to infer that the T4P or the T4P machinery function upstream of the Dif pathway in the regulation of EPS synthesis (Black *et al.*, 2006, Dana & Shimkets, 1993, Black *et al.*, 2009). Interestingly, PilB was recently shown to work downstream of T4P and upstream of the Dif system (Black *et al.*, 2017). Moreover, StkA and CRISPR3 function downstream of T4P but upstream of

the Dif pathway (Moak *et al.*, 2015, Dana & Shimkets, 1993, Wallace *et al.*, 2014). Specifically, CRISPR3 also functions downstream of the EPS stimulator SglK and PilB (Wallace *et al.*, 2014).

1.3.4.5 The *M. xanthus* slime

Gliding cells deposit a so-called slime (Fluegel, 1963) that contains polysaccharides and OMV, and promotes adherence of cells to the substratum (Ducret *et al.*, 2013, Gloag *et al.*, 2016) (Fig. 10). For a long time it was discussed whether slime deposition occurred by a passive release of attached surface polysaccharides caused by friction against the surface or whether it was actively secreted through some nozzle structures at the poles which provide propulsive force to cells (Wolgemuth *et al.*, 2002). Recently it was shown that the Agl/Glt gliding machinery is not necessary for slime deposition (Ducret *et al.*, 2012), and that slime is most probably deposited from beneath cells, and functions as an adhesive and not to propel cells (Ducret *et al.*, 2012). A better understanding of the biosynthesis machinery is necessary in order to understand the function of the slime.

Slime has been detected in a triple LPS O-antigen *wzm wzt wbgA* mutant and an EPS⁻ *difA* strain implying the presence of an additional unidentified polymer (Ducret *et al.*, 2012). However, it would be interesting to study a double mutant affected in synthesis of both, LPS O-antigen and EPS.

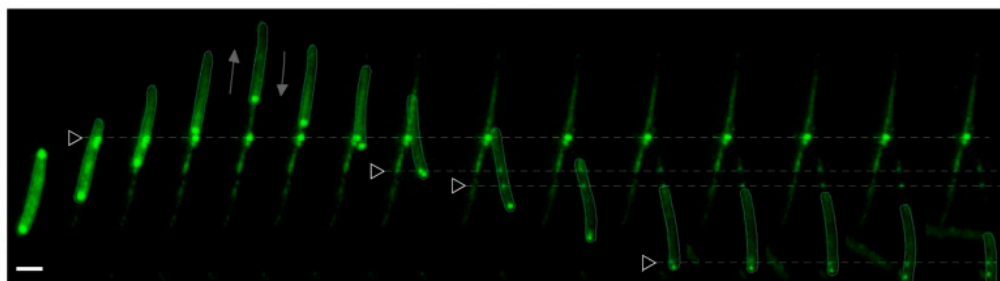


Figure 10. Polysaccharide staining of the *M. xanthus* slime trail at different time points using the polysaccharide binding protein ConA that selectively binds to α -D-mannosyl or α -D-glucosyl residues. Figure was reproduced from (Ducret *et al.*, 2012) with permission of the publisher.

1.3.5 Regulation by c-di-GMP in *M. xanthus*

In this section, I make use of our review article (Pérez-Burgos & Søgaard-Andersen, 2020), which compiles the results of c-di-GMP signaling in *M. xanthus*.

Regulation by c-di-GMP in *Myxococcus xanthus*

Pérez-Burgos, M. & Søgaard-Andersen, L.

This part of the thesis is written as part of a book chapter published in Springer in March 2020. I contributed to this work by doing literature research, preparing the figures and manuscript. The article was reused with permission of the publisher.

Chapter 18

Regulation by Cyclic di-GMP in *Myxococcus xanthus*



María Pérez-Burgos and Lotte Søgaard-Andersen

Abstract *Myxococcus xanthus* has a complex lifecycle that is regulated by nutrient availability. In the presence of nutrients, *M. xanthus* cells grow, divide, and move to assemble into colonies that feed cooperatively either saprophytically or on prey. In response to starvation, a developmental program is initiated that culminates in formation of multicellular spore-filled fruiting bodies. The nucleotide-based second messenger cyclic di-GMP accumulates in *M. xanthus* and has critical functions in both stages of the lifecycle. Here, we describe the roles of cyclic di-GMP, its metabolizing proteins, and receptor proteins. During growth, the correct level of cyclic di-GMP is important for type IV pili-dependent motility. During development, the cyclic di-GMP level increases and a threshold concentration of cyclic di-GMP is essential for completion of the developmental program. By individually inactivating the genes involved in cyclic di-GMP synthesis or degradation, two diguanylate cyclases, DmxA and DmxB, were identified to function at specific stages of the lifecycle with DmxA involved in type IV pili-dependent motility and DmxB in development. Similarly, the phosphodiesterase PmxA is specifically important for development but functions independently of DmxB. Bioinformatics analyses suggest the existence of various cyclic di-GMP receptor proteins, a few of which have been confirmed experimentally while the remainder are still uncharacterized. We are only just beginning to understand regulation by cyclic di-GMP in *M. xanthus* and it will be exciting to identify all the processes regulated by cyclic di-GMP and the underlying mechanisms.

Keywords Cyclic di-GMP · Myxobacteria · *Myxococcus xanthus* · Type IV pili · Motility · Development · Exopolysaccharide · Sporulation

M. Pérez-Burgos · L. Søgaard-Andersen (✉)
Department of Ecophysiology, Max Planck Institute for Terrestrial Microbiology, Marburg,
Germany
e-mail: sogaard@mpi-marburg.mpg.de

18.1 Introduction

Bis-(3'-5')-cyclic dimeric guanosine monophosphate (cyclic di-GMP) is an exceptionally versatile nucleotide-based second messenger that regulates a multitude of physiological processes in bacteria in response to environmental and cell-intrinsic signals. In many species, cyclic di-GMP is involved in regulating the transition between planktonic and surface-associated lifestyles by enhancing the production of extracellular matrix components and inhibiting motility [1–3]. However, cyclic di-GMP is also involved in controlling more complex lifecycle changes such as the transition between growth and multicellular development in *Streptomyces* spp. [4, 5] and *Myxococcus xanthus* [6] and between axenic growth and predation in *Bdellovibrio bacteriovorus* [7]. While these changes occur in response to alterations in the external environment, cyclic di-GMP can also regulate cell-intrinsic processes including cell cycle progression in *Caulobacter crescentus* [3] and possibly also unipolar growth in *Sinorhizobium meliloti* [8].

Cyclic di-GMP is produced from two GTP molecules by diguanylate cyclases (DGCs) that contain a GGDEF domain named after the conserved GG[E/D]EF motif in the active site (A-site). Often these proteins also contain an allosteric I-site with the conserved RxxD motif that allows product feedback inhibition. Cyclic di-GMP is hydrolyzed by phosphodiesterases (PDEs) with either an EAL or HD-GYP domain (again named after conserved sequences in the active site) to 5'-phosphoguanylyl-(3'-5')-guanosine (pGpG) and then further degraded to 2 GMP molecules [1–3]. The latter step may depend on an oligoribonuclease [9, 10]. In order for cyclic di-GMP to elicit a response, it binds to downstream effectors. Effectors include riboswitches and proteins [1, 3]. Proteinaceous effectors are functionally and sequence wise highly diverse encompassing PilZ domain proteins, MshEN domain proteins, various families of transcription factors, various ATPases, and proteins with degenerate and enzymatically inactive GGDEF and EAL domains [1–3]. Upon effector binding, cyclic di-GMP can regulate processes at the transcriptional, posttranscriptional or posttranslational level [1, 3].

Here, we focus on regulation by cyclic di-GMP in *M. xanthus*, a model organism for motility and multicellular development in bacteria. We will describe the role of cyclic di-GMP during the two stages of the lifecycle, the different cellular networks in which cyclic di-GMP is involved and conclude with open questions.

18.2 Introduction to *Myxococcus xanthus*

M. xanthus is a Gram-negative rod-shaped deltaproteobacterium with a lifecycle that includes two stages and with the switch between the two stages being regulated by nutrient availability. In the presence of nutrients, cells grow, divide, and move forming coordinately spreading colonies on a solid surface and cells feeding saprophytically or by preying in a wolf pack-like manner on other microorganisms

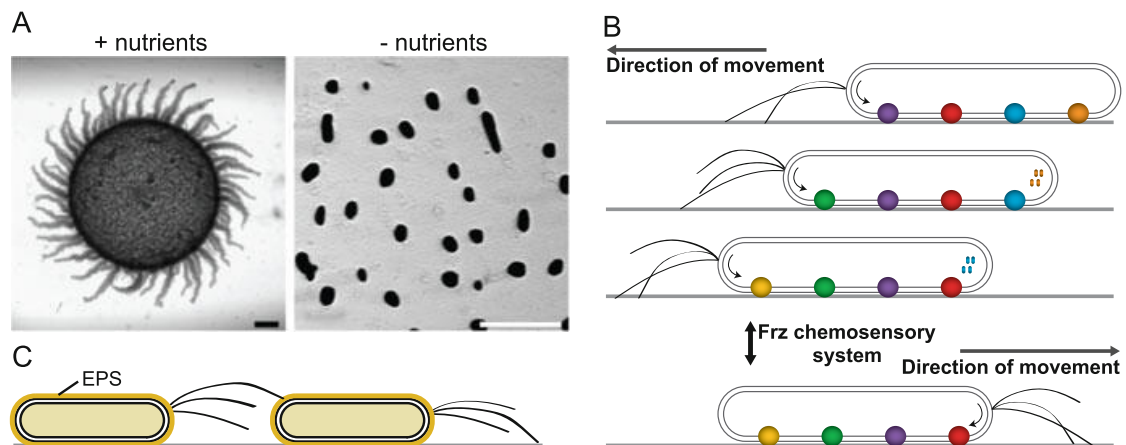


Fig. 18.1 Overview of *M. xanthus* life cycle and motility. (a) Colony morphology (left) and fruiting body formation (right) are regulated by nutrient availability. Scale bars: 0.5 mm. (b) *M. xanthus* has two polarized motility systems. T4P assembles at the leading cell pole. Agl/Glt complexes (colored circles) assemble at the leading cell pole, adhere to the substratum, remain stationary as a cell moves forward, and disassemble at the lagging pole. Leading-lagging polarity is inverted during Frz-induced reversals. (c) T4P retractions are induced by EPS on a neighboring cell

(Fig. 18.1a) [11]. When nutrients become scarce, *M. xanthus* initiates a multicellular developmental program that culminates in the formation of spore-filled fruiting bodies (Fig. 18.1a) [12]. Completion of this developmental program depends on motility, temporally regulated gene expression, regulated proteolysis, intercellular signaling [12–14] as well as intracellular signaling by the nucleotide-based second messengers cyclic di-GMP [6] and (p)ppGpp [15, 16]. Motility and its regulation are important for both stages of the lifecycle. *M. xanthus* cells move in the direction of their long axis by means of two distinct motility systems, type IV pili (T4P)-dependent motility (T4 PM) and gliding motility (Fig. 18.1b) [13, 17]. T4 PM favors the movement of groups of cells in a cell–cell contact-dependent manner on soft, moist surfaces (e.g. 0.5% agar), whereas gliding motility promotes the motility of single cells on firm and dry surfaces (e.g. 1.5–2.0% agar) [18]. T4 PM depends on T4P, exopolysaccharides (EPS) and possibly also the O-antigen part of the lipopolysaccharide (LPS) [12]. The current model suggests that upon attachment of T4P to the EPS on a neighboring cell, pili retraction is triggered enhancing the movement of cells within groups (Fig. 18.1c) [19]. Gliding motility depends on the Agl/Glt machinery that assembles at the leading cell pole, adheres to the substratum, moves rearwards as cells move, and finally disassembles at the lagging cell pole [13, 17, 20]. Both motility systems are highly polarized and only assemble at the leading cell pole. Occasionally, and in response to signaling by the Frz chemosensory system, cells reverse their direction of movement; during a reversal, the polarity of the two motility systems is inverted, and after a reversal, T4P and the Agl/Glt machinery assemble at the former lagging cell pole [17].

18.3 Bioinformatics-Based Analysis of Cyclic di-GMP Metabolism in *M. xanthus*

The first evidence that cyclic di-GMP could play a role in *M. xanthus* came from investigations of the two component signal transduction system (TCS) SgmT/DigR, which regulates extracellular matrix composition [21, 22]. The histidine protein kinase SgmT contains a C-terminal GGDEF domain with a degenerate A-site and an intact I-site. This domain binds cyclic di-GMP in vitro and SgmT variants in which this domain is mutated are affected in localization, but not in function [21]. These findings motivated further research into the possible functions of cyclic di-GMP in *M. xanthus*.

Genome-wide analyses of the *M. xanthus* genome have revealed a large capacity for regulation by cyclic di-GMP. This genome encodes 26 proteins with a GGDEF, EAL, or HD-GYP domain (Fig. 18.2) (https://www.ncbi.nlm.nih.gov/Complete_Genomes/c-di-GMP.html) [23]. Among the 18 GGDEF domain-containing proteins, 11 are predicted to have DGC activity based on sequence analysis. Four of the predicted enzymatically inactive proteins possess the I-site motif and may function as cyclic di-GMP effectors. Additionally, *M. xanthus* has two and six proteins with an EAL or HD-GYP domain, respectively. Six of these eight proteins are predicted to be enzymatically active based on sequence analysis. Many bacteria contain hybrid proteins with both a GGDEF and an EAL domain [27]. Interestingly, no such proteins have been identified in *M. xanthus*. However, the majority (22 out of 24) of the GGDEF and HD-GYP domain-containing proteins in *M. xanthus* possesses additional N-terminal domains, the majority of which belong to TCS (13 out of 22), whereas the EAL domain proteins do not contain additional identified domains (Fig. 18.2) [23]. Three of the 26 proteins are predicted to be integral membrane proteins (Fig. 18.2). These two observations suggest that the activity of the majority of these 26 proteins could be directly regulated by phosphorylation or ligand binding and that this regulation may not directly depend on extracellular cues.

The diversity among cyclic di-GMP binding effector proteins makes it difficult to predict how many potential effectors the *M. xanthus* genome encodes. However, in the case of PilZ and MshEN domains, which typically function as cyclic di-GMP effectors [28, 29], the *M. xanthus* genome is predicted to encode a surprisingly high number of PilZ and MshEN domain proteins (https://www.ncbi.nlm.nih.gov/Complete_Genomes/c-di-GMP.html). Among the predicted 24 PilZ domain-containing proteins, 14 are stand-alone PilZ domain proteins while 10 contain additional domains. Among the predicted 22 MshEN domain proteins [28], MXAN2513 is predicted to be an ATPase important for type II secretion based on the genetic context of the gene and MXAN5788 encodes the PilB ATPase of the T4P system [30] while the remaining proteins contain other domains.

Proteins with GGDEF domain		A site GGDEF	<i>In vitro</i> activity	I site RxxD	<i>In vitro</i> binding of cyclic di-GMP
MXAN1525		GGEEF		RxxQ	
MXAN2643 HyprB		GGDEF	cAG synth	RxxD	
MXAN2997		GGEEF		RxxD	
MXAN3705 DmxA		GGEEF	DGC	RxxD	+ / DRaCALA
MXAN3735 DmxB		GGDEF	DGC	RxxD	+ / DRaCALA
MXAN4029		GGEEF		RxxD	
MXAN4463 HyprA		GGDEY	cAG synth	RxxD	
MXAN5199		GGEEF		RxxD	
MXAN5366		GGEEF		RxxD	
MXAN5791		GGEEF		RxxD	
MXAN7362		GGEEF		RxxD	
MXAN3213 ActA		GDCQF		RxxD	
MXAN4257		EGGAF		VxxG	
MXAN4445 TmoK		AGDDF	- DGC	AxxD	- / DRaCALA
MXAN4640 SgmT		GGGVF	- DGC	RxxD	+ / DRaCALA/cdG-CC
MXAN5053		SDQEF		RxxD	
MXAN5340		ADSRF		RxxD	
MXAN5347		HADAF		YxxA	

Proteins with EAL domain		Predicted PDE activity	<i>In vitro</i> activity
MXAN2424		+	
MXAN2530		+	

Proteins with HD-GYP domain		Predicted PDE activity	<i>In vitro</i> activity
MXAN2061 PmxA		+	PDE
MXAN4232		+	
MXAN4675		+	
MXAN6298		+	
MXAN2807		-	
MXAN3353		-	

	GGDEF		Hpt		PAS		FHA		Cache
	EAL		HPK		RPT		GAF		HAMP
	HD-GYP		REC		TMH		GSPII_E/MshEN		

Fig. 18.2 Proteins containing GGDEF, EAL, or HD-GYP domains in *M. xanthus*. Domain organization of *M. xanthus* GGDEF, EAL, and HD-GYP proteins modified from [23]. Locus tags and protein names are listed on the left. Predicted domain structures are indicated and domains are not drawn to scale. Domain predictions were done by using the SMART [24] and TMHMM 2.0 web tools (<http://www.cbs.dtu.dk/services/TMHMM/>). For GGDEF proteins, A- and I-site residues labeled in red indicate residues that do not match with the consensus. Enzyme activity *in vitro* is only listed for proteins that have been tested; cAG synth is short for 3', 3'-cGMP-AMP synthase. Predicted PDE activity is based on conservation of conserved active site residues [23]. Cyclic di-GMP binding *in vitro* is listed for proteins tested together with the method used, DRaCALA [25] and cyclic di-GMP capture compound (cdG-CC) methodology [26]

18.4 Cyclic di-GMP Accumulates in *M. xanthus* and Is Important for Motility and Development

As expected based on the bioinformatics analysis, wild-type cells of *M. xanthus* accumulate cyclic di-GMP during growth as well as development [6, 23]. The cyclic di-GMP level does not change during the switch from exponential to stationary growth phase [23]. By contrast, the level of cyclic di-GMP increases more than 20-fold during development [6].

To begin to understand, whether the precise level of cyclic di-GMP is important for specific processes in *M. xanthus*, an approach in which a heterologous DGC or PDE was expressed was used [23]. Expression of DgcA, an active DGC from *C. crescentus* [31], or PA5295, an active PDE from *Pseudomonas aeruginosa* [32] in otherwise wild-type cells, demonstrated that a significant increase or decrease in the cyclic di-GMP level in growing cells caused a decrease in T4 PM [23] (Figs. 18.3a, b). The mechanistic basis for the motility defect in response to increased cyclic di-GMP was tracked down to reduced *pilA* transcription, causing reduced accumulation of the major pilin, PilA, and reduced T4P formation. By contrast, EPS was not affected by the increased cyclic di-GMP level. Transcription of *pilA* is regulated by the TCS PilS/PilR

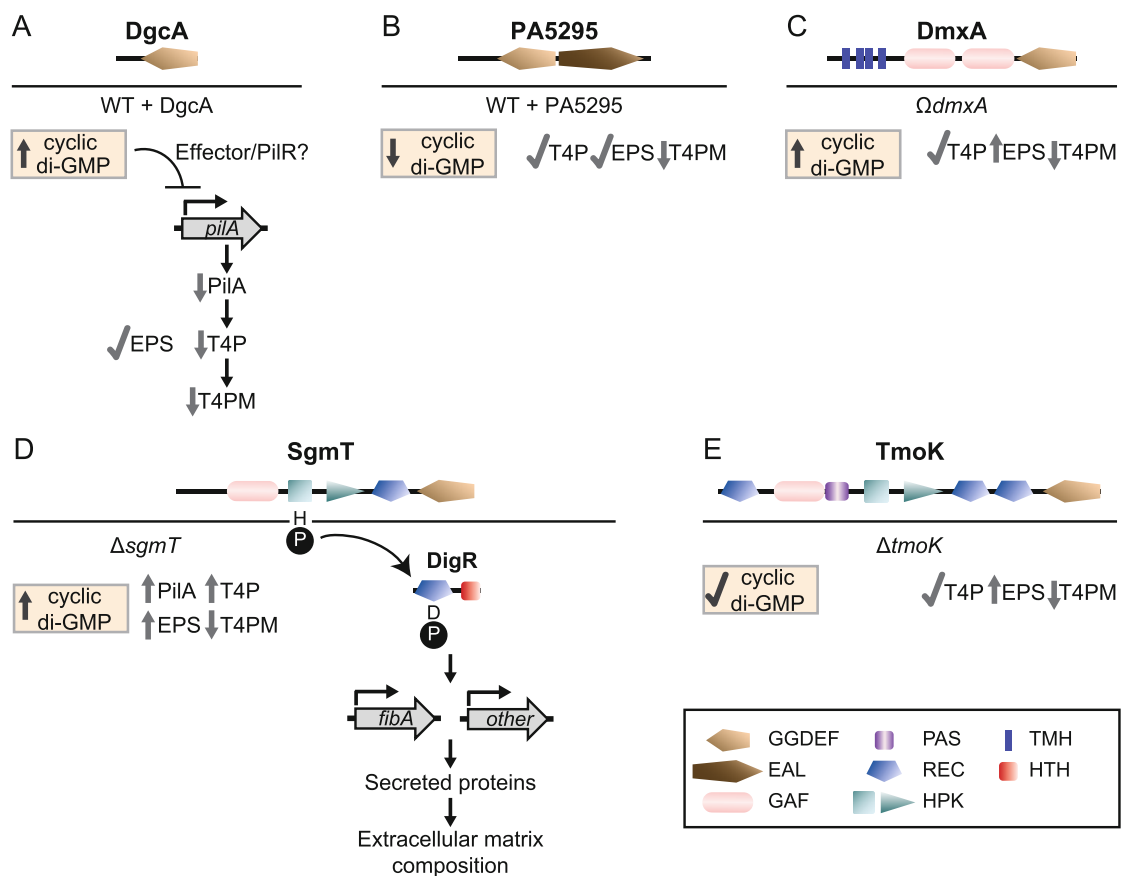


Fig. 18.3 Cyclic di-GMP is important for T4 PM in growing cells. (a, b) Expression of the heterologous DGC DgcA (a) or the heterologous PDE PA5295 (b) affects T4 PM. See text for details. (c, d, e) Lack of DmxA (c), SgmT (d) or TmoK (e) causes defect in T4 PM. See text for details

[33]. Inactivation of the transcriptional regulator PilR causes a reduction in *pilA* transcription [33, 34]. Interestingly, PilR belongs to the family of NtrC-like transcriptional regulators several of which bind cyclic di-GMP [1]. Therefore, it would be interesting to study whether a high cyclic di-GMP level influences *pilA* transcription by directly binding to PilR. A reduced cyclic di-GMP level affected neither T4P formation nor EPS accumulation [23]. Thus, the mechanism underlying this motility defect remains unknown. During starvation, an increased level of cyclic di-GMP resulting from expression of DgcA did not interfere with development (Fig. 18.4a). By contrast, a reduction of the cyclic di-GMP level caused by expression of PA5295 resulted in delayed fruiting body formation and reduced sporulation [6] (Fig. 18.4b). The mechanism(s) underlying this defect has not been analyzed (but see also below). Thus, based on these analyses, the precise level of cyclic di-GMP is important for T4 PM during growth and a sufficiently high level is important for development, whereas a higher level does not interfere with development.

Whereas the genes encoding PilZ- or MshEN domain proteins have not been systematically analyzed genetically, the systematic inactivation of 24 of the 26 genes (the two exceptions being MXAN5347 and MXAN3353) encoding proteins with a GGDEF, EAL, or HD-GYP domain followed by phenotypic description of their growth, motility, and developmental characteristics, identified proteins specifically important for motility, development, or for motility as well as development [6, 21, 23]. These observations lend support to the idea that different proteins involved in cyclic di-GMP metabolism and/or regulation have distinct functions during the two stages of the life cycle. Moreover, they suggest that either the remaining proteins function redundantly or their function(s) is not evident under laboratory conditions.

18.5 GGDEF Domain Proteins Important for T4P-Dependent motility

DmxA is a predicted integral membrane protein composed of two N-terminal GAF domains and a C-terminal GGDEF domain (Fig. 18.3c). A variant of DmxA comprising the two GAF domains, and the GGDEF domain has DGC activity in vitro and binds cyclic di-GMP in vitro likely via the intact I-site [23] (Fig. 18.2). Surprisingly, insertional inactivation of *dmxA* caused a 1.5-fold increase in the cyclic di-GMP level (Fig. 18.3c). The Ω *dmxA* cells displayed a defect in T4 PM and assembled T4P at wild-type levels but a higher level of EPS. Therefore, it was suggested that the increase in EPS causes the defect in T4 PM [23]. How the lack of DmxA causes an increase in EPS accumulation remains to be elucidated.

SgmT is a cytoplasmic hybrid histidine protein kinase that functions together with the DNA binding response regulator DigR [21, 22] (Fig. 18.3d). The *sgmT* and *digR* mutants were originally identified based on their defect in T4 PM [22, 35]. SgmT contains an N-terminal GAF domain, the two canonical domains of histidine protein kinases [36], a receiver domain, and a C-terminal degenerate GGDEF domain

[21, 35]. While the GAF domain and kinase activity are important for SgmT function in T4 PM, the receiver domain and the GGDEF domain are not [21]. As expected based on sequence analyses (Fig. 18.2), the GGDEF domain does not have DGC activity, but it binds cyclic di-GMP through the intact I-site [21, 23]. In vitro full-length SgmT engages in phosphotransfer to DigR independently of the presence or absence of cyclic di-GMP [21] (Fig. 18.3d). So far, the only function attributed to the SgmT GGDEF domain is that it brings about the localization of SgmT to one or more clusters distributed along the cell length; because SgmT variants that no longer localize to these clusters still function as the wild-type protein under all conditions tested, the relevance of this localization pattern is not known [21].

Lack of SgmT or DigR results in a defect in T4 PM [21, 22]. To begin to understand the underlying mechanism(s), global transcriptomics analyses together with in vitro DNA binding experiments were performed [21]. These analyses provided evidence that SgmT/DigR directly regulates the expression of genes coding for proteins secreted to the extracellular matrix including the FibA protease, which is among the most abundant proteins in the extracellular matrix [37], as well as enzymes involved in secondary metabolism [21]. Among these proteins, only the FibA protein has been analyzed in some details and lack of this protein does not cause a defect in T4 PM [38]; for the remainder proteins, it is not known whether they have a function in T4 PM or EPS accumulation. Lack of SgmT or DigR also causes an increase in PilA accumulation, increased T4P formation, and increased EPS accumulation [23] without affecting *pilA* transcription or transcription of genes for EPS synthesis. Finally, a Δ *sgmT* mutant displays a 1.5-fold increase in cyclic di-GMP accumulation [23]. It has been speculated that lack of certain secreted proteins may cause a compensatory response involving the increased accumulation of EPS and T4P and that this increase would be responsible for the motility defect (Fig. 18.3d) [21]. How lack of SgmT causes an increase in the cyclic di-GMP level remains to be investigated.

TmoK is a cytoplasmic hybrid histidine protein kinase, that contains a GGDEF domain with degenerate A- and I-sites, and neither synthesizes nor binds cyclic di-GMP in vitro (Figs. 18.2 and 18.3e) [23]. Lack of TmoK does not affect the cyclic di-GMP level [23]. However, lack of TmoK results in a T4 PM defect and increased accumulation of EPS, whereas PilA accumulation and T4P formation are as in wild type. These observations suggest that also in the case of the Δ *tmoK* mutant the altered EPS accumulation may cause the defect in T4 PM. Interaction partners of TmoK remain to be identified.

Altogether, lack of DmxA, SgmT/DigR, or TmoK affects T4 PM. However, the molecular mechanism(s) underlying this effect still needs to be precisely defined. The available evidence suggests that they could be diverse and possibly indirect, i.e., the primary function of these four proteins may not be regulation of T4 PM, but rather regulation of extracellular matrix composition and EPS accumulation. Similarly, it is not clear how lack of DmxA or SgmT causes a change in the cyclic di-GMP level and how these changes in cyclic di-GMP may affect T4P formation and/or EPS accumulation and in that way T4 PM.

18.6 GGDEF Domain Proteins Important for Development

The systematic inactivation of genes coding for proteins with GGDEF, EAL, or HD-GYP domains demonstrated that DmxB is the only GGDEF domain protein that specifically caused a developmental defect. Previous research suggested that ActA, which contains a degenerate GGDEF domain with an intact I-site (Fig. 18.2) is important for development [39]. Posterior reannotation of *actA* suggested that the original *actA* mutation affected the promoter of the *act* operon causing a polar effect on *actB*, which is required for fruiting body formation [6, 39]. Consistently, an *actA* in-frame deletion mutant had no developmental defect [6].

DmxB is a cytoplasmic protein with an N-terminal receiver domain of TCS systems and a C-terminal GGDEF domain. Full-length DmxB has DGC activity and binds cyclic di-GMP via its I-site in vitro (Fig. 18.2). Lack of DmxB causes a defect in fruiting body formation and sporulation [6]. Importantly, Δ *dmxB* cells do not progressively accumulate cyclic di-GMP during development and the level is comparable to that in growing cells, suggesting that DmxB is the DGC responsible for the 20-fold increase of cyclic di-GMP during development (Fig. 18.4c). Lack of DmxB specifically causes developmental defects. This specificity has been tracked down to transcriptional regulation of *dmxB* expression, which is upregulated during development ensuring that DmxB specifically accumulates during development [6] (Fig. 18.4c).

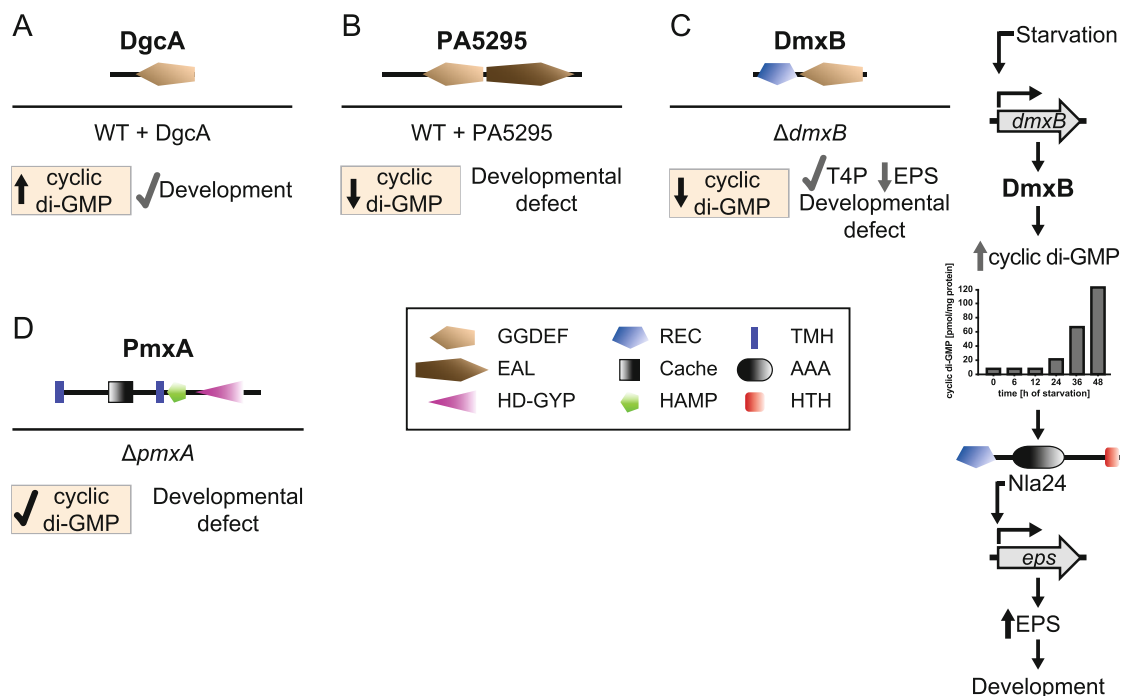


Fig. 18.4 Cyclic di-GMP is important for development. (a) Expression of the heterologous DGC DgcA does not affect development. See text for details. (b) Expression of the heterologous PDE PA5295 interferes with development. See text for details. (c, d) Lack of DmxB (c) or PmxA (d) causes developmental defects. See text for details

Consistently, a DmxB variant with a substitution in the active site did not restore development of the $\Delta dmxB$ mutant and did not support the increase in cyclic di-GMP. By contrast, a DmxB variant with a mutated I-site developed as wild type, but accumulated cyclic di-GMP at a much-increased level compared to wild type suggesting that this variant was not subject to feedback inhibition by cyclic di-GMP. Moreover, genetic evidence supports that phosphorylation of the N-terminal receiver domain does not have an impact on DmxB function in vivo and in vitro. The developmental defects of the $\Delta dmxB$ mutant were partially restored by expression of the heterologous DGC DgcA. Altogether, these findings suggested a model in which DmxB *per se* is not important for development but rather its DGC activity is important. Taken together with the observation that a reduction in the cyclic di-GMP level caused by expression of the heterologous PDE PA5295 inhibited development, it was concluded that the important function of DmxB is to generate a minimal threshold level of cyclic di-GMP that is essential for development to proceed successfully. Of note, an even higher increase in cyclic di-GMP level does not interfere with development.

Lack of DmxB caused reduced EPS accumulation during development due to reduced expression of a subset of *eps* genes, which code for enzymes important for EPS synthesis and export. Guided by these observations and the observations that NtrC-like transcriptional factors such as FleQ in *P. aeruginosa* [40, 41] and VpsR of *Vibrio cholerae* [42] bind cyclic di-GMP, the NtrC-like transcriptional activator Nla24/EpsI, which is encoded in the *eps* locus and was previously shown to be important for *eps* expression or EPS accumulation [43–45], was identified as a cyclic di-GMP binding protein.

Altogether, in the current model for the function of DmxB during development, *dmxB* transcription is upregulated early during development leading to accumulation of DmxB. DmxB activity allows the cyclic di-GMP level to reach the minimal threshold level that is essential for development. One of the effectors for cyclic di-GMP during development is Nla24/EpsI, which, in turn, activates *eps* transcription and EPS accumulation [6]. Because an artificial increase in cyclic di-GMP levels in growing cells does not initiate the developmental program [23], it is clear that an increase in cyclic di-GMP is required for development but it is not sufficient to initiate development. By contrast, accumulation of (p)ppGpp is required and sufficient for initiating development [15, 16]. Interestingly, cyclic di-GMP also regulates multicellular development in *Streptomyces* spp. [4, 5]. While an increase in cyclic di-GMP is necessary for the multicellular developmental program in *M. xanthus*, it has the opposite effect in *Streptomyces* spp. in which a high level of cyclic di-GMP inhibits multicellular development by binding to the transcription factor BldD, which, in turn, inhibits expression of sporulation genes. Thus, cyclic di-GMP appears to have opposite effects on multicellular development in *Streptomyces* spp. and *M. xanthus*.

Although the current model for the function of DmxB during development explains all experimental observations, several questions remain open: Given that Nla24/EpsI has been implicated in regulation of *eps* expression in growing cells [43], how does cyclic di-GMP modulate the activity of Nla24/EpsI during development? How is *dmxB* expression activated during development? Are there other cyclic di-GMP effectors that are important for development?

Among the 18 GGDEF domain-containing proteins in *M. xanthus*, lack of SgmT (as well as its cognate response regulator DigR) and TmoK also causes defects in development [6, 21, 22]. Lack of SgmT/DigR and TmoK also causes defects in EPS accumulation and T4 PM (see above), which are important for development [46, 47]. Therefore, it has been speculated that the developmental defects observed in the Δ *sgmT* and Δ *tmoK* mutants are caused by the defect in EPS accumulation and/or T4 PM.

18.7 PmxA, an HD-GYP Type PDE Is Important for Development

Inactivation of seven of the eight genes containing either an EAL or HD-GYP domain identified PmxA as important for development, whereas lack of any single one of the remaining six proteins neither caused defects in growing cells nor in development [6, 23]. PmxA is a membrane protein with an HD-GYP domain, and N-terminal CaChe (domain named after the first proteins in which it was identified: Calcium channels and chemotaxis receptors [48]) and HAMP (domain named after its presence in histidine kinases, adenyl cyclases, methyl-accepting proteins, and phosphatases [49]) domains (Figs. 18.2, 18.4d). In vitro the HD-GYP domain has PDE activity and degrades cyclic di-GMP [6] (Fig. 18.2). Nevertheless, inactivation of *pmxA* had no effect on the level of cyclic di-GMP during development (Fig. 18.4d) [6]. It is currently not known which processes during development are affected by lack of PmxA or how PmxA may act at the molecular level. However, it has been speculated that PmxA may regulate a local pool of cyclic di-GMP—opposed to DmxB that regulates the global pool of cyclic di-GMP—and possibly engage in protein complex formation [6].

18.8 Cyclic di-GMP Effectors in *M. xanthus*

Little is known about cyclic di-GMP effectors in *M. xanthus*. So far, the only experimentally verified effectors are SgmT and Nla24/EpsI [6, 21, 23]. No systematic study of the 24 PilZ domain-containing proteins in *M. xanthus* has been done and only three of these proteins have been analyzed experimentally.

PlpA is a cytoplasmic stand-alone PilZ domain protein and contains all the residues predicted to be important for cyclic di-GMP binding (RxxxR and D/NxS/AxxG separated by 20–30 amino acid residues) [1, 50] (Fig. 18.5a). Nevertheless, the purified protein was reported not to bind cyclic di-GMP in vitro [50]. The deletion of *plpA* results in strong defects in both motility systems; however, motility *per se* is not affected rather the mutant has a defect in regulation of motility and reverses more frequently than wild-type cells [50]. Consistent with the observation in vitro that

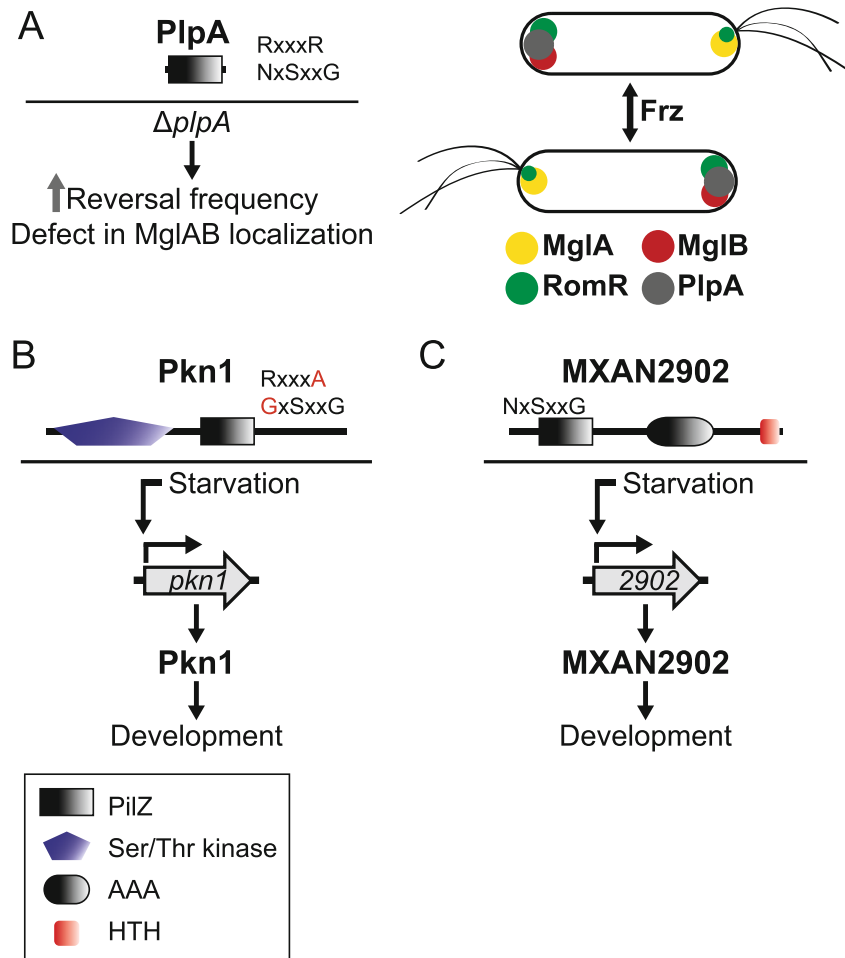


Fig. 18.5 PilZ domain-containing proteins are involved in motility regulation and development. (a) PlpA is important for regulation of motility. Based on sequence alignments, the two motifs important for cyclic di-GMP binding in PilZ domains are indicated. See text for details. (b, c) Pkn1 and MXAN2902 are important for development. Based on sequence alignments, the two motifs important for cyclic di-GMP binding in PilZ domains are indicated. Residues in red indicate non-conserved residues; in MXAN2902, the N-terminal conserved motif is missing. See text for details

PlpA does not bind cyclic di-GMP; expression of predicted nonbinding PlpA variants did not cause motility defects [50].

In *M. xanthus*, the leading-lagging polarity axis for motility is established by a protein module comprised of three proteins, the Ras-like GTPase MglA, its cognate GTPase Activating Protein (GAP) MglB, and the response regulator RomR [17]. All three proteins localize asymmetrically to the cell poles and their polarity is switched in response to signaling by the Frz chemosensory system causing the cells to change the direction of movement (Fig. 18.5a). Interestingly, PlpA localizes to the lagging cell pole and also interacts with the gliding motility protein AglS (Fig. 18.5a) [50] and in the absence of PlpA MglA and MglB localize more symmetrically to both cell poles [50]. How PlpA is targeted to one of the poles remains unknown; similarly, it is not known whether PlpA interacts with any of the proteins in the polarity module.

Interestingly, regulation of leading-lagging polarity in the predatory delta-proteobacterium *Bdellovibrio bacteriovorus* depends on the interplay between the cyclic di-GMP-binding protein CdgA, which contains a degenerate GGDEF domain, a RomR homolog, an MglA homolog, and a tetratricopeptide repeat (TPR) domain protein, Bd2492. These proteins localize and interact at the leading cell pole, which is the prey invasion pole [7, 51]. Based on this comparison, it will be interesting to explore whether any cyclic di-GMP binding protein is involved in regulating cell polarity in *M. xanthus*.

The Ser/Thr kinase Pkn1 is important for development [52, 53] and contains a C-terminal PilZ domain. Transcription of *pkn1* is induced during development [52]. The Pkn1 PilZ domain lacks consensus residues important for cyclic di-GMP binding (Fig. 18.5b) and it is not known whether the PilZ domain binds cyclic di-GMP or whether the domain is important for development. Nevertheless, the domain structure of Pkn1 suggests that regulation by cyclic di-GMP could potentially be coupled to signaling by a Ser/Thr kinase during development.

MXAN2902 is a σ^{54} dependent transcriptional factor with an N-terminal PilZ domain that also lacks the consensus residues important for cyclic di-GMP binding. Transcription of *MXAN2902* increases during development, and a mutant containing an insertion in *MXAN2902* has a defect in fruiting body morphology (Fig. 18.5c) [54]. As for Pkn1, it is not currently known whether the PilZ domain binds cyclic di-GMP or whether this domain is important for development.

The MshEN domain was recently identified as a new cyclic di-GMP binding domain typically associated with ATPases involved in type II secretion or T4P function [28, 55]. The *M. xanthus* genome encodes 22 MshEN-containing proteins [28]. As discussed above, MXAN2513 is predicted to be an ATPase important for type II secretion, and MXAN5788 encodes the PilB ATPase of the T4P system [30]; however, none of these two proteins have been tested for cyclic di-GMP binding. Interestingly, one of the proteins containing an MshEN domain is the HD-GYP domain-containing protein MXAN2807 (Fig. 18.2). Lack of this protein does not cause defects in growth, motility, or development (see above) [6, 23]. By contrast, inactivation of *MXAN6627* (*sgnC*), which encodes a response regulator with a C-terminal MshEN domain, has been reported to result in a defect in T4 PM by an unknown mechanism [35]. None of the remaining proteins have been analyzed experimentally and it is not known whether they bind cyclic di-GMP.

18.9 Conclusions and Outlook

In this review, we have described the role of cyclic di-GMP during the *M. xanthus* lifecycle. Looking forward, it will not only be important to determine the function of all 26 proteins with a GGDEF, EAL, or HD-GYP domain, it will also be important to determine when during the lifecycle they accumulate in order to understand to what extent the activity of these proteins is temporally separated. Along the same lines, it will be of interest to understand if they contribute to a global cellular pool of cyclic

di-GMP or act more locally in confined protein complexes. The identification of cyclic di-GMP binding effectors in different signaling pathways will also be an important goal for the future. Currently, this research area is understudied and it is largely not clear how different effects of alterations in cyclic di-GMP concentrations are implemented. Along the same lines, sporadic evidence suggests that cyclic di-GMP signaling in *M. xanthus* may connect to signaling by Ser/Thr kinases for regulating development and to a small GTPase/GAP module to regulate cell polarity. It will be interesting to follow up on these leads to obtain a complete picture of how cyclic di-GMP interfaces with other signaling modalities. Finally, it was recently reported that *M. xanthus* cells accumulate cyclic AMP-GMP (3', 3'-cGMP-AMP), and that the two GGDEF domain proteins MXAN2643 (HyprB) and MXAN4463 (HyprA) synthesize this molecule in vitro [56] (Fig. 18.2). Lack of MXAN2643 and MXAN4463 does not cause defects in growth, motility, or development [6, 23]. Therefore, up to now, it is a completely open question of what the function of cyclic AMP-GMP could be in *M. xanthus*.

Acknowledgments We thank Dorota Skotnicka for many helpful discussions. Work on cyclic di-GMP signaling in the authors' laboratory is supported by Deutsche Forschungsgemeinschaft (DFG, German Research Council) within the framework of the SFB987 Microbial Diversity in Environmental Signal Response and the Priority Programme SPP 1879 Nucleotide Second Messenger Signaling in Bacteria as well as by the Max Planck Society.

References

1. Römling U, Galperin MY, Gomelsky M (2013) Cyclic di-GMP: the first 25 years of a universal bacterial second messenger. *Microbiol Mol Biol Rev* 77(1):1–52. <https://doi.org/10.1128/MMBR.00043-12>
2. Hengge R (2009) Principles of c-di-GMP signalling in bacteria. *Nat Rev Microbiol* 7:263–273. <https://doi.org/10.1038/nrmicro2109>
3. Jenal U, Reinders A, Lori C (2017) Cyclic di-GMP: second messenger extraordinaire. *Nat Rev Microbiol* 15:271–284. <https://doi.org/10.1038/nrmicro.2016.190>
4. Tschowri N, Schumacher MA, Schlimpert S, Chinnam NB, Findlay KC, Brennan RG, Buttner MJ (2014) Tetrameric c-di-GMP mediates effective transcription factor dimerization to control *Streptomyces* development. *Cell* 158:1136–1147. <https://doi.org/10.1016/j.cell.2014.07.022>
5. Tschowri N (2016) Cyclic dinucleotide-controlled regulatory pathways in *Streptomyces* species. *J Bacteriol* 198:47–54. <https://doi.org/10.1128/JB.00423-15>
6. Skotnicka D, Smaldone GT, Petters T, Trampari E, Liang J, Kaeffer V, Malone JG, Singer M, Søgaaard-Andersen L (2016) A minimal threshold of c-di-GMP is essential for fruiting body formation and sporulation in *Myxococcus xanthus*. *PLoS Genet* 12:e1006080. <https://doi.org/10.1371/journal.pgen.1006080>
7. Hogley L, Fung RK, Lambert C, Harris MA, Dabhi JM, King SS, Basford SM, Uchida K, Till R, Ahmad R, Aizawa S, Gomelsky M, Sockett RE (2012) Discrete cyclic di-GMP-dependent control of bacterial predation versus axenic growth in *Bdellovibrio bacteriovorus*. *PLoS Pathog* 8:e1002493. <https://doi.org/10.1371/journal.ppat.1002493>
8. Schäper S, Yau HCL, Krol E, Skotnicka D, Heimerl T, Gray J, Kaeffer V, Søgaaard-Andersen L, Vollmer W, Becker A (2018) Seven-transmembrane receptor protein RgsP and cell wall-

- binding protein RgsM promote unipolar growth in Rhizobiales. *PLoS Genet* 14:e1007594. <https://doi.org/10.1371/journal.pgen.1007594>
9. Cohen D, Mechold U, Nevenzal H, Yarmiyhu Y, Randall TE, Bay DC, Rich JD, Parsek MR, Kaever V, Harrison JJ, Banin E (2015) Oligoribonuclease is a central feature of cyclic diguanylate signaling in *Pseudomonas aeruginosa*. *Proc Natl Acad Sci U S A* 112:11359–11364. <https://doi.org/10.1073/pnas.1421450112>
 10. Orr MW, Donaldson GP, Severin GB, Wang J, Sintim HO, Waters CM, Lee VT (2015) Oligoribonuclease is the primary degradative enzyme for pGpG in *Pseudomonas aeruginosa* that is required for cyclic-di-GMP turnover. *Proc Natl Acad Sci U S A* 112(36):E5048–E5057. <https://doi.org/10.1073/pnas.1507245112>
 11. Berleman JE, Kirby JR (2009) Deciphering the hunting strategy of a bacterial wolfpack. *FEMS Microbiol Rev* 33:942–957. <https://doi.org/10.1111/j.1574-6976.2009.00185.x>
 12. Konovalova A, Petters T, Søggaard-Andersen L (2010) Extracellular biology of *Myxococcus xanthus*. *FEMS Microbiol Rev* 34:89–106. <https://doi.org/10.1111/j.1574-6976.2009.00194.x>
 13. Zhang Y, Ducret A, Shaevitz J, Mignot T (2012) From individual cell motility to collective behaviors: insights from a prokaryote, *Myxococcus xanthus*. *FEMS Microbiol Rev* 36:149–164. <https://doi.org/10.1111/j.1574-6976.2011.00307.x>
 14. Kroos L (2017) Highly signal-responsive gene regulatory network governing *Myxococcus* development. *Trends Genet* 33:3–15. <https://doi.org/10.1016/j.tig.2016.10.006>
 15. Harris BZ, Kaiser D, Singer M (1998) The guanosine nucleotide (p)ppGpp initiates development and A-factor production in *Myxococcus xanthus*. *Genes Dev* 12:1022–1035. <https://doi.org/10.1101/gad.12.7.1022>
 16. Singer M, Kaiser D (1995) Ectopic production of guanosine penta- and teraphosphate can initiate early developmental gene expression in *Myxococcus xanthus*. *Genes Dev* 9:1633–1644. <https://doi.org/10.1101/gad.9.13.1633>
 17. Schumacher D, Søggaard-Andersen L (2017) Regulation of cell polarity in motility and cell division in *Myxococcus xanthus*. *Annu Rev Microbiol* 71:61–78. <https://doi.org/10.1146/annurev-micro-102215-095415>
 18. Shi W, Zusman DR (1993) The two motility systems of *Myxococcus xanthus* show different selective advantages on various surfaces. *Proc Natl Acad Sci U S A* 90:3378–3382. <https://doi.org/10.1073/pnas.90.8.3378>
 19. Li Y, Sun H, Ma X, Lu A, Lux R, Zusman D, Shi W (2003) Extracellular polysaccharides mediate pilus retraction during social motility of *Myxococcus xanthus*. *Proc Natl Acad Sci U S A* 100:5443–5448. <https://doi.org/10.1073/pnas.0836639100>
 20. Faure LM, Fiche J-B, Espinosa L, Ducret A, Anantharaman V, Luciano J, Lhospice S, Islam ST, Tréguier J, Sotes M, Kuru E, Van Nieuwenhze MS, Brun YV, Théodoly O, Aravind L, Nollmann M, Mignot T (2016) The mechanism of force transmission at bacterial focal adhesion complexes. *Nature* 539:530–535. <https://doi.org/10.1038/nature20121>
 21. Petters T, Zhang X, Nesper J, Treuner-Lange A, Gomez-Santos N, Hoppert M, Jenal U, Søggaard-Andersen L (2012) The orphan histidine protein kinase SgmT is a c-di-GMP receptor and regulates composition of the extracellular matrix together with the orphan DNA binding response regulator DigR in *Myxococcus xanthus*. *Mol Microbiol* 84:147–165. <https://doi.org/10.1111/j.1365-2958.2012.08015.x>
 22. Overgaard M, Wegener-Feldbrügge S, Søggaard-Andersen L (2006) The orphan response regulator DigR is required for synthesis of extracellular matrix fibrils in *Myxococcus xanthus*. *J Bacteriol* 188:4384–4394. <https://doi.org/10.1128/JB.00189-06>
 23. Skotnicka D, Petters T, Heering J, Hoppert M, Kaever V, Søggaard-Andersen L (2015) c-di-GMP regulates type IV pili-dependent-motility in *Myxococcus xanthus*. *J Bacteriol* 198:77–90. <https://doi.org/10.1128/JB.00281-15>
 24. Letunic I, Doerks T, Bork P (2015) SMART: recent updates, new developments and status in 2015. *Nucleic Acids Res* 43(Database issue):D257–D260. <https://doi.org/10.1093/nar/gku949>

25. Roelofs KG, Wang JX, Sintim HO, Lee VT (2011) Differential radial capillary action of ligand assay for high-throughput detection of protein-metabolite interactions. *Proc Natl Acad Sci U S A* 108:15528–15533. <https://doi.org/10.1073/pnas.1018949108>
26. Nesper J, Reinders A, Glatter T, Schmidt A, Jenal U (2012) A novel capture compound for the identification and analysis of cyclic di-GMP binding proteins. *J Proteome* 75:4874–4878. <https://doi.org/10.1016/j.jprot.2012.05.033>
27. Seshasayee AS, Fraser GM, Luscombe NM (2010) Comparative genomics of cyclic-di-GMP signalling in bacteria: post-translational regulation and catalytic activity. *Nucl Acids Res* 38:5970–5981. <https://doi.org/10.1093/nar/gkq382>
28. Wang YC, Chin KH, Tu ZL, He J, Jones CJ, Sanchez DZ, Yildiz FH, Galperin MY, Chou SH (2016) Nucleotide binding by the widespread high-affinity cyclic di-GMP receptor MshEN domain. *Nat Com* 7:12481. <https://doi.org/10.1038/ncomms12481>
29. Chou S-H, Galperin MY (2016) Diversity of cyclic di-GMP-binding proteins and mechanisms. *J Bacteriol* 198:32–46. <https://doi.org/10.1128/jb.00333-15>
30. Jakovljevic V, Leonardy S, Hoppert M, Søgaaard-Andersen L (2008) PilB and PilT are ATPases acting antagonistically in type IV pili function in *Myxococcus xanthus*. *J Bacteriol* 190:2411–2421. <https://doi.org/10.1128/JB.01793-07>
31. Christen B, Christen M, Paul R, Schmid F, Folcher M, Jenoe P, Meuwly M, Jenal U (2006) Allosteric control of cyclic di-GMP signaling. *J Biol Chem* 281:32015–32024. <https://doi.org/10.1074/jbc.M603589200>
32. Kulasakara H, Lee V, Brencic A, Liberati N, Urbach J, Miyata S, Lee DG, Neely AN, Hyodo M, Hayakawa Y, Ausubel FM, Lory S (2006) Analysis of *Pseudomonas aeruginosa* diguanylate cyclases and phosphodiesterases reveals a role for bis-(3'-5')-cyclic-GMP in virulence. *Proc Natl Acad Sci U S A* 103:2839–2844. <https://doi.org/10.1073/pnas.0511090103>
33. Wu SS, Kaiser D (1997) Regulation of expression of the *pilA* gene in *Myxococcus xanthus*. *J Bacteriol* 179:7748–7758. <https://doi.org/10.1128/jb.179.24.7748-7758.1997>
34. Bretl DJ, Muller S, Ladd KM, Atkinson SN, Kirby JR (2016) Type IV-pili dependent motility is co-regulated by PilSR and PilS2R2 two-component systems via distinct pathways in *Myxococcus xanthus*. *Mol Microbiol* 102:37–53. <https://doi.org/10.1111/mmi.13445>
35. Youderian P, Hartzell PL (2006) Transposon insertions of magellan-4 that impair social gliding motility in *Myxococcus xanthus*. *Genetics* 172:1397–1410. <https://doi.org/10.1534/genetics.105.050542>
36. Stock AM, Robinson VL, Goudreau PN (2000) Two-component signal transduction. *Annu Rev Biochem* 69:183–215. <https://doi.org/10.1146/annurev.biochem.69.1.183>
37. Behmlander RM, Dworkin M (1994) Biochemical and structural analyses of the extracellular matrix fibrils of *Myxococcus xanthus*. *J Bacteriol* 176:6295–6303. <https://doi.org/10.1128/jb.176.20.6295-6303.1994>
38. Kearns DB, Bonner PJ, Smith DR, Shimkets LJ (2002) An extracellular matrix-associated zinc metalloprotease is required for dilauroyl phosphatidylethanolamine chemotactic excitation in *Myxococcus xanthus*. *J Bacteriol* 184:1678–1684. <https://doi.org/10.1128/JB.184.6.1678-1684.2002>
39. Gronewold TM, Kaiser D (2001) The *act* operon controls the level and time of C-signal production for *Myxococcus xanthus* development. *Mol Microbiol* 40:744–756. <https://doi.org/10.1046/j.1365-2958.2001.02428.x>
40. Hickman JW, Harwood CS (2008) Identification of FleQ from *Pseudomonas aeruginosa* as a c-di-GMP-responsive transcription factor. *Mol Microbiol* 69:376–389. <https://doi.org/10.1111/j.1365-2958.2008.06281.x>
41. Matsuyama BY, Krasteva PV, Baraquet C, Harwood CS, Sondermann H, Navarro MV (2016) Mechanistic insights into c-di-GMP-dependent control of the biofilm regulator FleQ from *Pseudomonas aeruginosa*. *Proc Natl Acad Sci U S A* 113:E209–E218. <https://doi.org/10.1073/pnas.1523148113>

42. Srivastava D, Harris RC, Waters CM (2011) Integration of cyclic di-GMP and quorum sensing in the control of *vpsT* and *aphA* in *Vibrio cholerae*. *J Bacteriol* 193:6331–6341. <https://doi.org/10.1128/JB.05167-11>
43. Lancero H, Caberoy NB, Castaneda S, Li YN, Lu A, Dutton D, Duan XY, Kaplan HB, Shi WY, Garza AG (2004) Characterization of a *Myxococcus xanthus* mutant that is defective for adventurous motility and social motility. *Microbiol-Sgm* 150:4085–4093. <https://doi.org/10.1099/mic.0.27381-0>
44. Caberoy NB, Welch RD, Jakobsen JS, Slater SC, Garza AG (2003) Global mutational analysis of NtrC-like activators in *Myxococcus xanthus*: identifying activator mutants defective for motility and fruiting body development. *J Bacteriol* 185:6083–6094. <https://doi.org/10.1128/JB.185.20.6083-6094.2003>
45. Lu A, Cho K, Black WP, Duan XY, Lux R, Yang Z, Kaplan HB, Zusman DR, Shi W (2005) Exopolysaccharide biosynthesis genes required for social motility in *Myxococcus xanthus*. *Mol Microbiol* 55:206–220. <https://doi.org/10.1111/j.1365-2958.2004.04369.x>
46. Hodgkin J, Kaiser D (1979) Genetics of gliding motility in *Myxococcus xanthus* (Myxobacterales) - 2 gene systems control movement. *Mol Gen Genet* 171:177–191. <https://doi.org/10.1007/Bf00270004>
47. Shimkets LJ (1986) Role of cell cohesion in *Myxococcus xanthus* fruiting body formation. *J Bacteriol* 166:842–848. <https://doi.org/10.1128/jb.166.3.842-848.1986>
48. Anantharaman V, Aravind L (2000) Cache – a signaling domain common to animal Ca²⁺–channel subunits and a class of prokaryotic chemotaxis receptors. *Trends Biochem Sci* 25:535–537. [https://doi.org/10.1016/S0968-0004\(00\)01672-8](https://doi.org/10.1016/S0968-0004(00)01672-8)
49. Aravind L, Ponting CP (1999) The cytoplasmic helical linker domain of receptor histidine kinase and methyl-accepting proteins is common to many prokaryotic signalling proteins. *FEMS Microbiol Lett* 176:111–116. <https://doi.org/10.1111/j.1574-6968.1999.tb13650.x>
50. Pogue CB, Zhou T, Nan B (2018) PlpA, a PilZ-like protein, regulates directed motility of the bacterium *Myxococcus xanthus*. *Mol Microbiol* 107:214–228. <https://doi.org/10.1111/mmi.13878>
51. Milner DS, Till R, Cadby I, Lovering AL, Basford SM, Saxon EB, Liddell S, Williams LE, Sockett RE (2014) Ras GTPase-like protein MglA, a controller of bacterial social-motility in Myxobacteria, has evolved to control bacterial predation by *Bdellovibrio*. *PLoS Genet* 10:e1004253. <https://doi.org/10.1371/journal.pgen.1004253>
52. Munoz-Dorado J, Inouye S, Inouye M (1991) A gene encoding a protein Serine Threonine kinase is required for normal development of *M. xanthus*, a Gram-negative bacterium. *Cell* 67:995–1006. [https://doi.org/10.1016/0092-8674\(91\)90372-6](https://doi.org/10.1016/0092-8674(91)90372-6)
53. Escalante AE, Inouye S, Travisano M (2012) A spectrum of pleiotropic consequences in development due to changes in a regulatory pathway. *PLoS One* 7:e43413. <https://doi.org/10.1371/journal.pone.0043413>
54. Jakobsen JS, Jelsbak L, Jelsbak L, Welch RD, Cummings C, Goldman B, Stark E, Slater S, Kaiser D (2004) Sigma54 enhancer binding proteins and *Myxococcus xanthus* fruiting body development. *J Bacteriol* 186:4361–4368. <https://doi.org/10.1128/JB.186.13.4361-4368.2004>
55. Roelofs KG, Jones CJ, Helman SR, Shang X, Orr MW, Goodson JR, Galperin MY, Yildiz FH, Lee VT (2015) Systematic identification of cyclic-di-GMP binding proteins in *Vibrio cholerae* reveals a novel class of cyclic-di-GMP-binding ATPases associated with type II secretion systems. *PLoS Pathog* 11:e1005232. <https://doi.org/10.1371/journal.ppat.1005232>
56. Hallberg ZF, Wang XC, Wright TA, Nan B, Ad O, Yeo J, Hammond MC (2016) Hybrid promiscuous (Hypr) GGDEF enzymes produce cyclic AMP-GMP (3', 3'-cGAMP). *Proc Natl Acad Sci U S A* 113:1790–1795. <https://doi.org/10.1073/pnas.1515287113>

2. Scope of this study

M. xanthus is a model organism to study social behaviors, cell-cell communication, motility, development and cell differentiation in bacteria. *M. xanthus* synthesizes different surface polysaccharides including LPS, EPS and spore coat polysaccharide that are important at different steps of its life cycle. While many studies have addressed the function of these glycans, little is known about how they are synthesized. Here, we focused on elucidation of the biosynthesis pathways of EPS, LPS and spore coat polysaccharide as the first step to understand the differences between their composition, structure and function. We bioinformatically identified homologs of Wzx/Wzy- and ABC-transporter-dependent pathways encoded by the *M. xanthus* genome and potentially involved in synthesis of EPS, LPS and spore coat polysaccharide. Experimentally, we sought to assign individual proteins to EPS, LPS and spore coat polysaccharide biosynthetic pathways. Additionally, because mutations blocking the synthesis of one polysaccharide can cause pleiotropic effects through Und-P sequestration and because in many studies regulatory mutants were used, we reevaluated the role of these polysaccharides in the *M. xanthus* life cycle using mutants affected at different steps of the synthesis of these molecules.

Previously, it had been suggested that c-di-GMP and the DGC DmxA regulated motility during growth via changes in EPS synthesis. Here, we reevaluated these results and found that DmxA may regulate motility by affecting cell polarity during growth and effects on EPS may be indirect.

3. Results



3.1 Identification of the lipopolysaccharide O-antigen biosynthesis priming enzyme and the O-antigen ligase in *Myxococcus xanthus*: Critical role of LPS O-antigen in motility and development

Pérez-Burgos, M., García-Romero, I., Jung, J., Valvano, M.A., & Søgaard-Andersen, L.

This chapter contains our advances in the identification of the LPS biosynthesis components and the role of LPS O-antigen in the life cycle of *M. xanthus* (Pérez-Burgos et al., 2019). The article was reused with permission of the publisher. This part of the thesis is written in a manuscript style and was published in *Molecular Microbiology* in 2019. I contributed to this work by designing, performing and analyzing experiments, preparing the figures and the manuscript.

Specifically, I carried out all the experiments and analysis shown in Fig. 1, 2A, 4, 5 and 6 as well as in Fig. S1-S3. Jana Jung carried out the experiment in Fig. 2B-C under my direct supervision. Heterologous experiments (Fig. 3) were carried out by Dr. Inmaculada García Romero at the Wellcome-Wolfson Institute for Experimental Medicine (Queen's University Belfast) and I generated the plasmid expressing the *M. xanthus* PHPT homolog used for the heterologous experiments.

Identification of the lipopolysaccharide O-antigen biosynthesis priming enzyme and the O-antigen ligase in *Myxococcus xanthus*: critical role of LPS O-antigen in motility and development

María Pérez-Burgos,¹ Inmaculada García-Romero,² Jana Jung,¹ Miguel A. Valvano ² and Lotte Søgaard-Andersen ^{1*}

¹Department of Ecophysiology, Max Planck Institute for Terrestrial Microbiology, Karl-von-Frisch Str. 10, 35043, Marburg, Germany.

²Wellcome-Wolfson Institute for Experimental Medicine, Queen's University Belfast, Belfast, BT9 7BL, UK.

Summary

Myxococcus xanthus is a model bacterium to study social behavior. At the cellular level, the different social behaviors of *M. xanthus* involve extensive cell–cell contacts. Here, we used bioinformatics, genetics, heterologous expression and biochemical experiments to identify and characterize the key enzymes in *M. xanthus* implicated in O-antigen and lipopolysaccharide (LPS) biosynthesis and examined the role of LPS O-antigen in *M. xanthus* social behaviors. We identified WbaP_{Mx} (MXAN_2922) as the polyisoprenyl-phosphate hexose-1-phosphate transferase responsible for priming O-antigen synthesis. In heterologous expression experiments, WbaP_{Mx} complemented a *Salmonella enterica* mutant lacking the endogenous WbaP that primes O-antigen synthesis, indicating that WbaP_{Mx} transfers galactose-1-P to undecaprenyl-phosphate. We also identified WaaL_{Mx} (MXAN_2919), as the O-antigen ligase that joins O-antigen to lipid A-core. Our data also support the previous suggestion that Wzm_{Mx} (MXAN_4622) and Wzt_{Mx} (MXAN_4623) form the Wzm/Wzt ABC transporter. We show that mutations that block different steps in LPS O-antigen synthesis can cause pleiotropic phenotypes. Also, using a *wbaP*_{Mx} deletion mutant, we revisited the role of LPS O-antigen and demonstrate that it is important for

gliding motility, conditionally important for type IV pili-dependent motility and required to complete the developmental program leading to the formation of spore-filled fruiting bodies.

Introduction

The Gram-negative deltaproteobacterium *Myxococcus xanthus* is a model organism to study social behavior in bacteria. Social behaviors of *M. xanthus* include the formation of saprophytically feeding colonies in which cells spread outward in a highly coordinated fashion, predation and starvation-induced development with the formation of multicellular spore-filled fruiting bodies (Berleman and Kirby, 2009; Konovalova *et al.*, 2010; Cao *et al.*, 2015). At the cellular level, these social behaviors of *M. xanthus* require extensive and diverse cell–cell contact-dependent interactions.

The rod-shaped *M. xanthus* cells harbor two systems for motility: one for type IV pili (T4P)-dependent motility and one for gliding motility (Zhang *et al.*, 2012; Schumacher and Søgaard-Andersen, 2017). T4P supports the movement of groups of cells in a cell–cell contact-dependent manner and not only depends on T4P (Kaiser, 1979), but also on exopolysaccharide (EPS) (Shimkets, 1986; Arnold and Shimkets, 1988). In addition, T4P-dependent motility may also depend on the O-antigen moiety of the lipopolysaccharide (LPS), although this is still debated. Using different mutants and motility assays, several groups reported that O-antigen is important for T4P-dependent motility (Bowden and Kaplan, 1998; Yang *et al.*, 2000; Youderian and Hartzell, 2006; Vassallo *et al.*, 2015) while Fink and Zissler (1989b) reported that the O-antigen is not required. In the current model, contact by a T4P on one cell to EPS on a neighboring cell triggers pilus retraction, enhancing the movement of cells within groups (Li *et al.*, 2003). By contrast, gliding motility promotes the movement of single cells and depends on the Agl/Glt machinery that assembles at the leading cell pole, adheres to the substratum, moves rearwards as cells move and finally disassembles at the lagging cell pole

Accepted 19 July, 2019. *For correspondence. E-mail sogaard@mpi-marburg.mpg.de, Tel. (+49) 6421 178 201; Fax (+49) 6421 178 209.

(Zhang *et al.*, 2012; Faure *et al.*, 2016; Schumacher and Søgaard-Andersen, 2017). LPS O-antigen has also been implicated in gliding motility (Fink and Zissler, 1989b; Yang *et al.*, 2000; Yu and Kaiser, 2007), while Bowden and Kaplan (1998) reported that O-antigen is not important for gliding. The process referred to as 'outer membrane exchange' also involves cell–cell contact. Here, the outer membrane (OM) of neighboring cells are thought to fuse to allow the bidirectional exchange of OM lipids, lipoproteins and LPS (Nudleman *et al.*, 2005; Wei *et al.*, 2011; Pathak *et al.*, 2012; Vassallo *et al.*, 2015; 2017). This exchange can have positive effects on recipient cells, i.e., LPS transfer can help recipient cells with damaged OMs to regain fitness (Vassallo *et al.*, 2015) and transferred lipoproteins can stimulate assembly of the T4P and Agl/Glt machineries for motility (Nudleman *et al.*, 2005; 2006; Jakobczak *et al.*, 2015). Conversely, transfer of lipoproteins may also have negative effects on recipients, as is the case for the transfer of toxins that kill non-immune recipient cells (Vassallo *et al.*, 2017). Other toxins that kill non-immune cells are transferred in a contact-dependent manner by the type VI secretion system (Gong *et al.*, 2018; Troselj *et al.*, 2018). Finally, during the starvation-induced formation of spore-filled fruiting bodies, transmission of the cell–cell contact-dependent C-signal is essential for the completion of this developmental program (Kim and Kaiser, 1990a; 1990b).

Here, we focused on the elucidation of the pathway for O-antigen and LPS biosynthesis to better understand the role of LPS in contact-dependent social behaviors in *M. xanthus*. LPS is the main component of the outer leaflet of the OM of most Gram-negative bacteria and is also found in a few diderm phyla that belong to the Firmicutes while the inner leaflet of the OM is composed of phospholipids (Raetz and Whitfield, 2002; Valvano, 2011; Antunes *et al.*, 2016). Generally, LPS has a protective function and helps maintain OM stability, relative impermeability and also plays an important role in virulence (Raetz and Whitfield, 2002; Valvano, 2011; Okuda *et al.*, 2016). LPS molecules encompass three regions: the hydrophobic lipid A, a core oligosaccharide that is attached to lipid A, and the highly variable O-antigen polysaccharide that is attached to the core. The O-antigen is composed of repeating oligosaccharide units. While the lipid A-core is structurally conserved, the composition of the repeat units and the length of the O-antigen chain vary within and between species (Raetz and Whitfield, 2002; Whitfield and Trent, 2014). Unlike lipid A-core, the O-antigen is typically not essential for viability (Raetz and Whitfield, 2002; Whitfield and Trent, 2014). Biosynthesis and membrane translocation of lipid A-core and O-antigen occur in separate pathways, and the two moieties are joined at the periplasmic side of the inner membrane (IM) followed by the transport of the complete LPS molecules to the OM via the Lpt system

(Raetz and Whitfield, 2002; Ruiz *et al.*, 2009; Valvano, 2011; Whitfield and Trent, 2014; Okuda *et al.*, 2016).

Lipid A-core biosynthesis begins with the synthesis of the lipid A-Kdo₂ intermediate at the cytoplasmic side of the IM via the conserved Raetz pathway (Whitfield and Trent, 2014). Subsequently, heptosyl- and glycosyltransferases add sugars onto lipid A-Kdo₂ followed by translocation of lipid A-core to the periplasmic side of the IM by the MsbA flippase (Whitfield and Trent, 2014). O-antigen synthesis and assembly follows one of two pathways (Raetz and Whitfield, 2002; Valvano, 2011; Kalynych *et al.*, 2014; Whitfield and Trent, 2014). These pathways share the same mechanism for initiation of synthesis of the repeating units, but differ in how these units are extended, joined and transported to the periplasm. The initiation of O-antigen synthesis involves a reaction in which a sugar-1-phosphate (sugar-1-P) from an activated sugar-nucleotide donor is transferred to the lipid carrier undecaprenyl-phosphate (Und-P) giving rise to an Und-PP sugar intermediate. Und-P is also used as a sugar lipid carrier for the synthesis of EPS, capsular polysaccharides and peptidoglycan. The priming enzymes that initiate O-antigen biosynthesis, also referred to as polyprenol phosphate C-1-phosphoglycosyltransferases (Lukose *et al.*, 2017), can be broadly placed into two protein families, the polyisoprenyl-phosphate hexose-1-phosphate transferases (PHPTs) or the polyisoprenyl-phosphate *N*-acetylhexosamine-1-phosphate transferases (PNPTs) (Valvano, 2011). The synthesis of the rest of the O-antigen requires specific glycosyltransferases and also depends on the specific membrane translocation pathway. In the Wzx/Wzy pathway, specific glycosyltransferases act sequentially to transfer the relevant sugar building blocks from nucleotide-sugar donors to the Und-PP-sugar primer molecule to generate the Und-PP-O-repeat unit. The Wzx flippase translocates individual Und-PP-O-repeat units to the periplasmic side of the IM. There, the O-antigen polymerase Wzy joins and polymerizes the repeat units. O-antigen chain length is regulated by the protein Wzz resulting in the formation of O-antigen molecules with a range of lengths. Finally, the O-antigen chain is ligated to the lipid A-core by the WaaL O-antigen ligase in a reaction in which the O-antigen chain is transferred from Und-PP and the proximal sugar joined to a sugar molecule in the lipid A-core acceptor. The Und-PP molecules arising after ligation are dephosphorylated into Und-P in the periplasm, translocated to the cytoplasmic leaflet of the IM by an unknown mechanism, and then reused (Tatar *et al.*, 2007; Valvano, 2008; Manat *et al.*, 2015). In the ABC transporter-dependent pathway, the full-length O-antigen is synthesized on the cytoplasmic side of the IM by various glycosyltransferases. Termination of extension may involve addition of a methyl or methyl-phosphate residue to the non-reducing terminus of the O-antigen by

homologs of the methyltransferase/kinase-methyltransferase WbdD (Clarke *et al.*, 2004; Greenfield and Whitfield, 2012). By terminating extension, WbdD is also involved in controlling O-antigen chain length (Clarke *et al.*, 2004; Greenfield and Whitfield, 2012). Translocation of the O-antigen across the IM depends on an ABC transporter composed of the membrane-spanning permease Wzm and the Wzt ATPase; subsequently O-antigen is ligated to the lipid A-core by the WaaL ligase following the same scheme as in the Wzx/Wzy pathway. In systems with a modification at the non-reducing end of the O-antigen, transport to the periplasm depends on recognition of this modification by a C-terminal carbohydrate binding domain in Wzt (Cuthbertson *et al.*, 2005).

M. xanthus synthesizes an LPS molecule composed of lipid A, core and O-antigen (Fink and Zissler, 1989a). Four proteins implicated in O-antigen synthesis have been identified in *M. xanthus* (Fig. 1A). Wzm_{Mx} (MXAN_4622) and Wzt_{Mx} (MXAN_4623) were suggested to form the Wzm/Wzt ABC transporter while the glycosyltransferases WbgA (MXAN_4621) and WbgB (MXAN_4619) were suggested to be involved in the formation of the O-antigen unit (Guo *et al.*, 1996; Bowden and Kaplan, 1998; Yang *et al.*, 2000).

Here, we identify two additional key proteins for *M. xanthus* LPS synthesis, MXAN_2922 and MXAN_2919, as the PHPT homolog responsible for priming O-antigen synthesis and the O-antigen ligase respectively. Heterologous expression experiments in *Salmonella enterica* support that MXAN_2922 transfers galactose-1-P (Gal-1-P) to Und-P. We renamed MXAN_2922 and MXAN_2919 as WbaP_{Mx} and WaaL_{Mx} respectively (Reeves *et al.*, 1996). Finally, using a mutant that lacks WbaP_{Mx}, we demonstrate that LPS O-antigen is important for gliding, conditionally important for T4P-dependent motility and required for development.

Results

Identification of PHPT and ligase candidates for LPS O-antigen synthesis

Prior studies by transposon mutagenesis identified genes potentially required for T4P-dependent and/or gliding motility that by sequence homology could be involved in LPS synthesis (Youderian and Hartzell, 2006; Yu and Kaiser, 2007). These genes map to two regions on the *M. xanthus* genome, one of which encodes the proposed Wzm/Wzt ABC transporter (Fig. 1A).

In LPS gene cluster I (Fig. 1A; Table S1), the genes MXAN_4623–MXAN_4619 form a putative operon encoding the proposed Wzm/Wzt ABC transporter, the WbgA (MXAN_4621) and WbgB (MXAN_4619) glycosyltransferases, and a putative sugar methyltransferase SgmR

(MXAN_4620). Interestingly, genes encoding glycosyltransferases and sugar methyltransferases involved in O-antigen biosynthesis are often found in close association with Wzm/Wzt ABC transporter encoding genes (Greenfield and Whitfield, 2012). According to the CAZy database, WbgA contains two glycosyltransferase domains of the GT2 and one of the GT4 family, while WbgB contains a single GT2 glycosyltransferase domain. SgmR has an N-terminal methyltransferase domain (Pfam domain PF13489), similar to WbdD homologs such as *Escherichia coli* WbdD_{O8} involved in the terminal methylation of O8-antigen synthesis (Clarke *et al.*, 2004) (Fig. S1), suggesting this protein could be involved in sugar methylation.

LPS gene cluster II (Fig. 1A; Table S1) revealed that MXAN_2920 and MXAN_2921 encode putative glycosyltransferases and MXAN_2922 encodes a PHPT homolog. In agreement with (Vassallo *et al.*, 2015), MXAN_2919 encodes a protein with a Wzy_C domain. This domain is present in O-antigen ligases, Wzy O-antigen polymerases and O-linked oligosaccharyltransferases (Schild *et al.*, 2005). MXAN_2917 and MXAN_2918 encode homologs of LptF and LptG, respectively that form part of the ABC transporter involved in translocating LPS to the OM (Okuda *et al.*, 2016). The remaining homologs of Lpt proteins were identified using combined orthology searches in the KEGG database and BlastP searches (Experimental procedures). We identified three additional genomic regions containing *lpt* genes (Fig. S2A), which together with the *lptFG* genes in LPS gene cluster II encode a complete Lpt pathway (Fig. S2B).

To better understand LPS O-antigen biosynthesis in *M. xanthus*, we focused on the Wzm/Wzt ABC transporter encoded by cluster I, and the MXAN_2922 and MXAN_2919 proteins encoded by cluster II. We carried out a detailed domain analysis of MXAN_4623 and MXAN_4622, renamed Wzm_{Mx} and Wzt_{Mx} respectively. Wzm_{Mx} has six predicted trans-membrane helices (TMH) and the ABC2_{membrane} domain (Pfam domain PF01061) characteristic of Wzm proteins (Fig. 1B). Wzt_{Mx} contains the ABC_{transporter} domain (Pfam domain PF00005) and the Wzt_C domain involved in recognition of the terminal modification of the O-antigen chain (Pfam domain PF14524) (Fig. 1C). Similar domain architectures are found in the *E. coli* Wzm_{O8} and Wzt_{O8} proteins involved in O8-antigen transport (Cuthbertson *et al.*, 2005; 2007) (Fig. 1C).

MXAN_2922 is a PHPT homolog with five TMH, a CoA binding domain (Pfam domain PF02629) and a Bacterial Sugar Transferase domain (Pfam domain PF02397) similar to the two best-studied PHPTs WbaP of *Salmonella enterica* (WbaP_{Se}) that synthesizes Und-PP-Gal and WcaJ of *E. coli* (WcaJ_{Ec}) that synthesizes Und-PP-glucose (Und-PP-Glc) (Fig. 1D) (Saldías *et al.*, 2008; Furlong *et al.*, 2015).

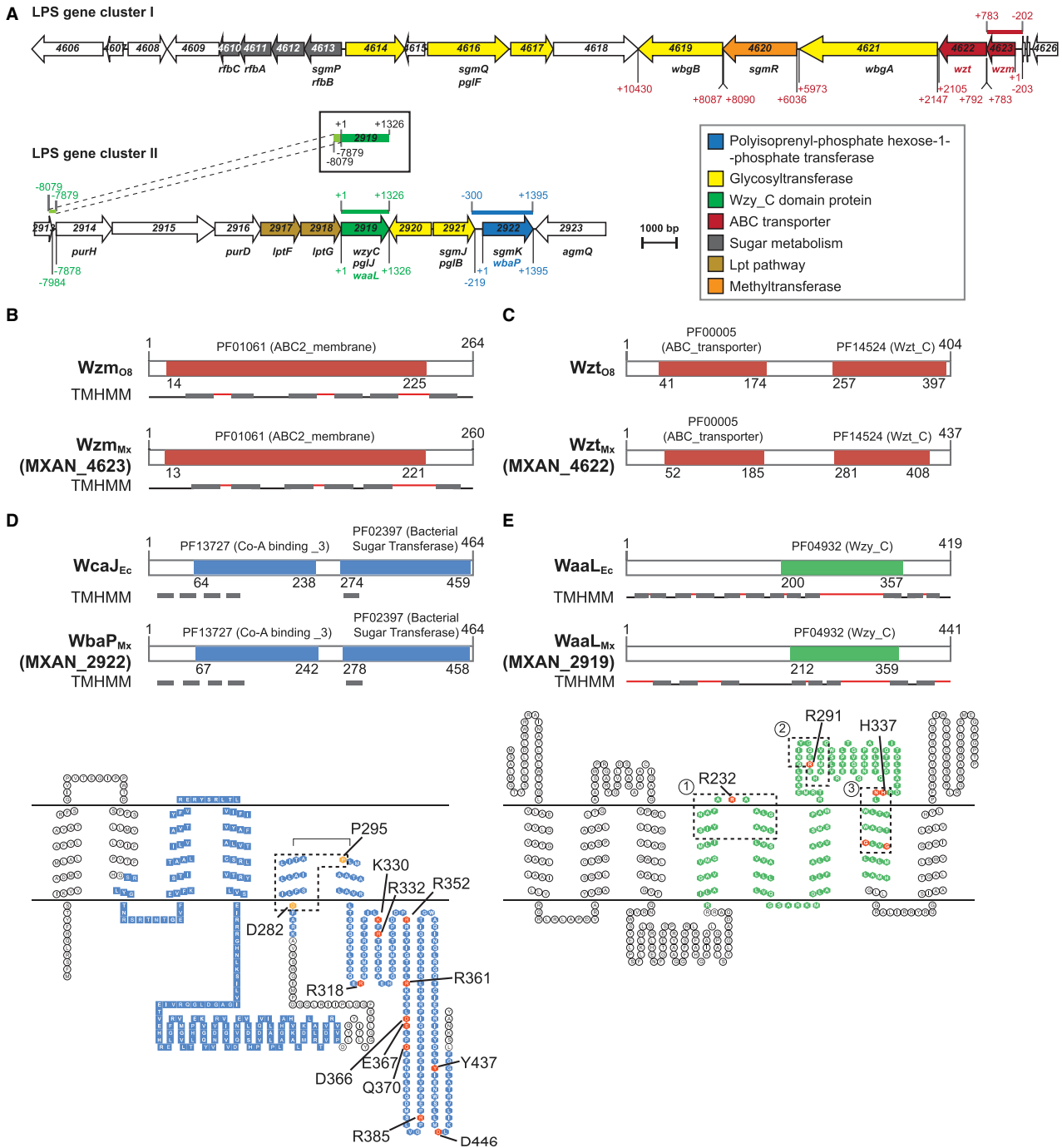


Fig. 1. Bioinformatic analysis of gene clusters and proteins involved in LPS synthesis. (A) LPS gene cluster I and II. Genes are drawn to scale and MXAN number or gene name indicated (Table S1). Coordinates are relative to the first nucleotide of each corresponding gene except for MXAN_4622, _4621, _4620 and _4619 for which coordinates are relative to the first nucleotide of MXAN_4623. DNA fragments comprising promoter and structural gene used in complementation experiments are indicated by a blue, green or red line above the corresponding region. Note that MXAN_2919 is likely in an operon with the upstream genes and, therefore, the promoter used for ectopic expression of MXAN_2919 is the region upstream of MXAN_2914. (B-E) Domain and TMH prediction of Wzm_{Mx} and Wzm_{O8} from *E. coli* (B), Wzt_{Mx} and Wzt_{O8} from *E. coli* (C), WbaP_{Mx} (MXAN_2922) and WcaJ_{Ec} (D) and WaaL_{Mx} (MXAN_2919) and WaaL_{Ec} (E). Grey rectangles indicate TMH, red and black lines indicate periplasmic and cytoplasmic domains respectively. In D and E, the lower schematics indicate topology predictions for MXAN_2922 and MXAN_2919. Domains are indicated in blue and green. Conserved amino acids important for structure or activity of the protein are marked with orange and red respectively. Sequence alignment of the C-terminal region of MXAN_2922 with WcaJ_{Ec} and WbaP_{Se}, or MXAN_2919 with WaaL_{Ec} (sequences in boxes) are shown in Fig. S3.

The fifth TMH of WcaJ_{Ec} does not fully span the IM but has a helix-break-helix structure resulting in the cytoplasmic localization of the C-terminal domain (Furlong *et al.*, 2015). In WbaP_{Se}, the C-terminal domain also localizes to the cytoplasm and is sufficient for catalytic activity (Wang *et al.*, 1996; Saldías *et al.*, 2008; Patel *et al.*, 2010). The residue P291 in WcaJ_{Ec} has been implicated in the helix-break-helix structure and together with D278, forms part of a DX₁₂P motif that is conserved among PHPTs (Furlong *et al.*, 2015). Both residues are conserved in MXAN_2922 (P295 and D282) suggesting that the C-terminal domain of this protein is also cytoplasmic (Figs 1D and S3A). In the C-terminal, catalytic domain of WbaP_{Se} several amino acids have been identified that are essential for activity and conserved among PHPTs (Patel *et al.*, 2010). All these residues are conserved in MXAN_2922 (Figs 1D and S3B). Based on these comparisons, we suggest that MXAN_2922 has a membrane topology similar to WcaJ_{Ec} and WbaP_{Se} (Fig. 1D) and a C-terminal domain with PHPT activity. We hypothesized that MXAN_2922 is the PHPT that primes the first step in O-antigen synthesis in *M. xanthus*.

MXAN_2919 is a membrane protein with eight putative TMHs and a C-terminal Wzy_C domain (Pfam domain PF04932) containing a relatively large predicted periplasmic loop (Fig. 1E). O-antigen synthesis in *M. xanthus* depends on the proposed Wzm/Wzt ABC transporter, and, therefore, is predicted to not involve a Wzy O-antigen polymerase. Therefore, we speculated that MXAN_2919 is an O-antigen ligase. The amino acid sequences of WaaL ligases are not highly conserved, but they are all predicted integral IM proteins with eight or more TMH (Raetz and Whitfield, 2002). The WaaL ligases of *Pseudomonas aeruginosa* and *E. coli* (WaaL_{Pa} and WaaL_{Ec} respectively) contain a partially periplasmic Wzy_C domain, responsible for catalytic activity and 12 TMHs (Islam *et al.*, 2010; Pan *et al.*, 2012; Ruan *et al.*, 2012; Ruan *et al.*, 2018) (Fig. 1E). Three amino acid residues in the Wzy_C domain of WaaL_{Ec}, Arg215, Arg288 and His338, are important for activity and His338 is also part of the conserved H³³⁸[NSQ] X₉GXX[GTY] motif in the last TMH of the Wzy_C domain; moreover, Asp389 in the TMH following the Wzy_C domain is important for activity (Perez *et al.*, 2008; Ruan *et al.*, 2012). MXAN_2919 contains all these residues with the exception of that corresponding to Asp389 (Figs 1E and S3C). Similarly, WaaL_{Pa} also contains all these residues except for the residue corresponding to Asp389 (Ruan *et al.*, 2012). Based on these comparisons, we hypothesized that MXAN_2919 is the *M. xanthus* O-antigen ligase.

Lack of MXAN_2919 (WaaL_{Mx}), MXAN_2922 (WbaP_{Mx}) and Wzm_{Mx} affects LPS synthesis

To evaluate the role of MXAN_2919, MXAN_2922 and the proposed Wzm/Wzt ABC transporter in LPS synthesis,

we generated in-frame deletions in the MXAN_2919, MXAN_2922 and wzm_{Mx} genes in the wild-type strain DK1622. If MXAN_2922 is responsible for initiating O-antigen synthesis, the ΔMXAN_2922 mutant should lack LPS O-antigen, but still synthesize lipid A-core. If MXAN_2919 is the O-antigen ligase, a ΔMXAN_2919 mutant should accumulate Und-PP-linked O-antigen in the periplasm and produce LPS devoid of O-antigen polysaccharide. LPS extracted from the WT strain DK1622 and the various mutants, separated by SDS-PAGE, was visualized using Emerald staining (Marolda *et al.*, 2006; Davis and Goldberg, 2012). In contrast to WT, none of the three mutants made LPS O-antigen while they all made lipid A-core (Fig. 2A). We investigated these phenotypes in more detail by immunoblot analysis with two monoclonal antibodies (MAbs), MAb783 and MAb2254 that specifically recognize O-antigen and lipid A-core oligosaccharide respectively (Gill and Dworkin, 1986; Fink and Zissler, 1989a).

In cell extracts from the WT strain separated by SDS-PAGE, MAb783 detected polymeric O-antigen forming a characteristic ladder, as previously reported (Fink and Zissler, 1989a), while no O-antigen was detected in the extract of the Δwzm_{Mx} mutant, also in agreement with previous results (Guo *et al.*, 1996) (Fig. 2B). O-antigen was absent in the extract of the ΔMXAN_2922 mutant but detected in extract of the ΔMXAN_2919 mutant (Fig. 2B).

In the extract from WT, MAb2254 recognized the fast migrating lipid A-core band devoid of O-antigen, as well as the polymeric LPS O-antigen (Fig. 2C). As expected based on previous research (Guo *et al.*, 1996), only the lipid A-core band was detected in the Δwzm_{Mx} mutant (Fig. 2C). Lack of polymeric LPS O-antigen was also observed in the ΔMXAN_2922 and ΔMXAN_2919 mutants.

From the combined results of LPS detection by Emerald staining and immunoblotting, we concluded that the ΔMXAN_2922 and Δwzm_{Mx} mutants do not synthesize O-antigen. These results support the hypothesis that MXAN_2922 is the PHPT enzyme for the initiation of O-antigen synthesis. The absence of O-antigen in Δwzm_{Mx} confirms previous findings indicating that loss of the Wzm_{Mx}/Wzt_{Mx} ABC transporter affects O-antigen synthesis (Guo *et al.*, 1996). By contrast, the ΔMXAN_2919 mutant synthesizes O-antigen that is not linked to lipid A-core, explaining its lack of detection with MAb2254 and Emerald staining and the detection of O-antigen bands when LPS was examined with MAb783. This phenotype is consistent with the absence of O-antigen ligase function resulting in Und-PP-linked O-antigen polysaccharide accumulation and demonstrating that MXAN_2919 is the O-antigen ligase.

The loss of O-antigen synthesis in the ΔMXAN_2922 and Δwzm_{Mx} mutants was generally corrected by the ectopic expression of the full-length proteins from their native promoters on plasmids integrated in single copy at

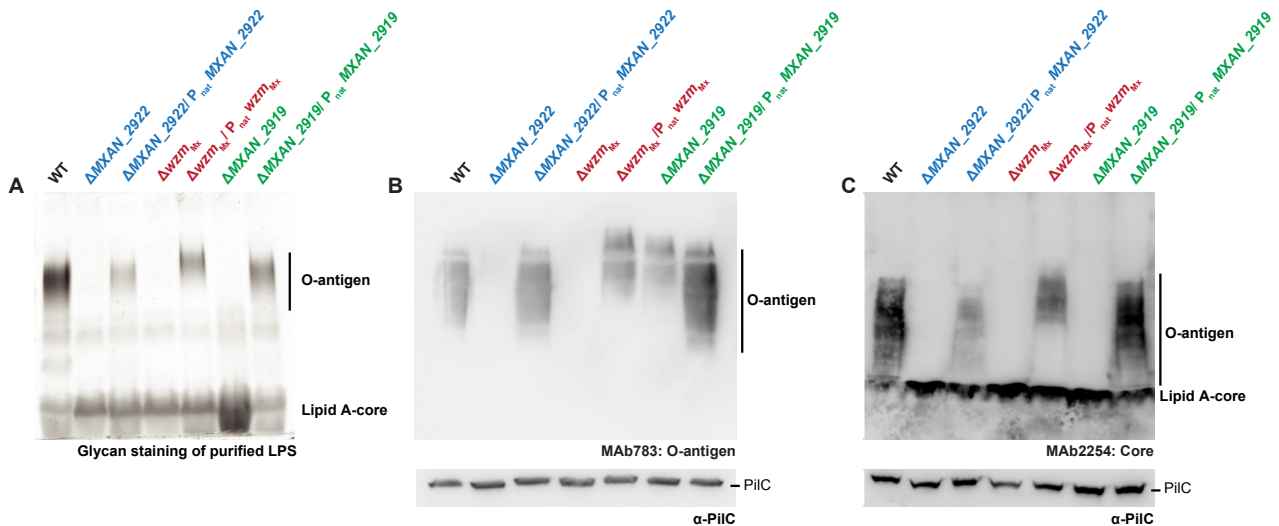


Fig. 2. Detection of LPS O-antigen and lipid A-core from *M. xanthus*.

A. Detection of LPS, which was extracted following (Davis and Goldberg, 2012). Samples from the same number of cells were separated by SDS-PAGE and detected with Pro-Q Emerald 300.

B. Immunoblot detection of LPS O-antigen using MAb783.

C. Immunoblot detection of lipid A-core using MAb2254. For (B) and (C), cell extracts were isolated from exponentially growing bacteria, and aliquots representing the same number of cells were loaded per lane and separated by SDS-PAGE. Blots were probed with MAb783, MAb2254 and α -PilC (45.2 kDa, loading control). MXAN_2922 is WbaP_{Mx} and MXAN_2919 is WaaL_{Mx}.

the Mx8 *attB* site (Figs 1A and 2). The total amount of LPS in the Δ MXAN_2922/MXAN_2922 strain was lower than in WT (Fig. 2A and C), which could be due to reduced expression of the ectopic MXAN_2922 gene. Also, the differences in the migration of LPS O-antigen polysaccharides in the Δ wzm_{Mx}/wzm_{Mx} strain, that appeared of higher molecular mass than in WT (Fig. 2), could be due to an altered accumulation level of Wzm_{Mx} in the complementation strain compared to WT (see discussion). Ectopic expression of MXAN_2919 complemented the defect in LPS O-antigen synthesis in the Δ MXAN_2919 mutant (Fig. 2A and C). The differences in the O-antigen bands between the Δ MXAN_2919 mutant and the complemented strain (Fig. 2B) can be explained by the different nature of the O-antigen link, Und-PP in the former and lipid A-core in the latter. Together, the results of the experiments described above support the notion that MXAN_2922 and MXAN_2919 are the PHPT O-antigen initiating enzyme and O-antigen ligase respectively. These proteins were herein renamed WbaP_{Mx} (see details below) and WaaL_{Mx} respectively.

WbaP_{Mx} transfers galactose-1-P to Und-P

The majority of PHPTs utilize either UDP-galactose or UDP-glucose (Valvano, 2011; Lukose *et al.*, 2017). To functionally determine the specificity of WbaP_{Mx}, we performed complementation experiments using *S. enterica* serovar Typhimurium Δ wbaP_{Se} and *E. coli* Δ wcaJ_{Ec} mutants. WbaP_{Se} initiates O-antigen synthesis

in *S. enterica* by catalysing the transfer of Gal-1-P onto Und-P, while WcaJ_{Ec} initiates synthesis of the colanic acid exopolysaccharide by transferring glucose-1-phosphate (Glc-1-P) onto Und-P generating Und-PP-Glc.

Disruption of *wbaP*_{Se} in *S. enterica* (Δ wbaP_{Se} mutant) results in the loss of LPS O-antigen (Fig. 3A). As described previously (Saldías *et al.*, 2008), this defect is partially corrected by complementation with plasmid pJD132, which encodes the *E. coli* O9:K30 WbaP homolog (WbaP_{Ec} O9:K30), and with the plasmid pSM13, which encodes WbaP_{Se} (Fig. 3A). The *wbaP*_{Mx} gene was cloned into pBADNTF resulting in plasmid pMP139, which encodes WbaP_{Mx} with an N-terminal FLAG tag (FLAG-WbaP_{Mx}) to facilitate detection by immunoblot and under the control of an arabinose inducible promoter. pMP139 was introduced into the *S. enterica* Δ wbaP_{Se} mutant. In the presence of 0.2% arabinose, FLAG-WbaP_{Mx} expressed from pMP139 resulted in an LPS banding profile similar to that obtained with pSM13 (Fig. 3A, left panel), while the pBADNTF vector control did not affect the LPS profile. These results were further validated by immunoblotting with *Salmonella* O-antigen rabbit antibodies. The specificity of the antibodies was verified by the lack of reactivity with O-antigen and lipid A-core in the Δ wbaP_{Se} mutant with no plasmid and in the presence of the vector control with no insert (Fig. 3A, right panel). Importantly, WbaP_{Se}, FLAG-WbaP_{Mx} and WbaP_{Ec} O9:K30 restored O-antigen synthesis in the Δ wbaP_{Se} mutant (Fig. 3A, right panel). The difference in the O-antigen profile between the strains complemented with WbaP_{Se} and FLAG-WbaP_{Mx} compared to the strain

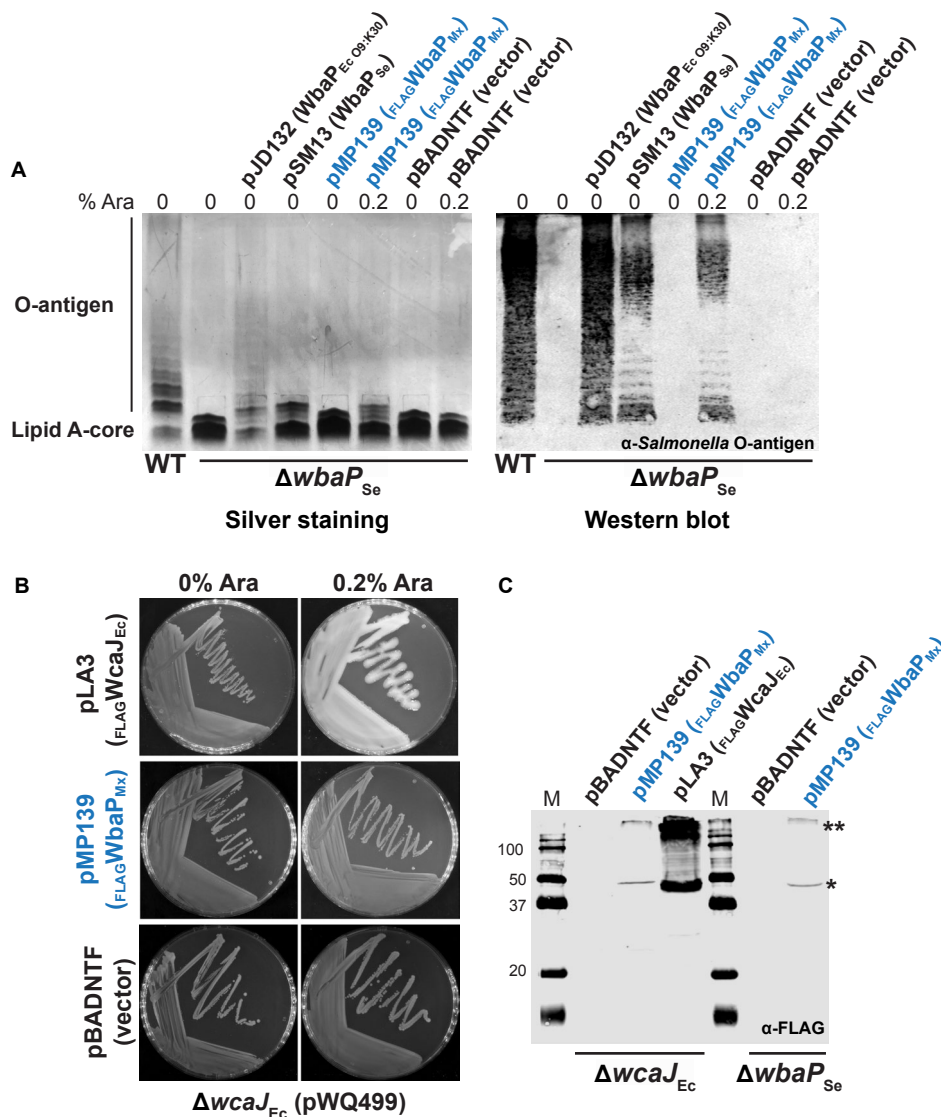


Fig. 3. Complementation of O-antigen and colanic acid synthesis in *S. enterica* LT2 ($\Delta wbaP_{Se}$) and *E. coli* K-12 W3110 ($\Delta wcaJ_{Ec}$) mutants, respectively, by plasmids encoding the indicated PHPT proteins.

A. Complementation of $\Delta wbaP_{Se}$ mutant in *S. enterica* Typhimurium LT2 containing the indicated plasmids. LPS samples were extracted, separated by electrophoresis on SDS–14% polyacrylamide gels and silver stained (left panel) or examined by immunoblotting using rabbit *Salmonella* O antiserum group B (right panel). Each lane corresponds to LPS extracted from 10^8 cells. Cultures included addition of arabinose as indicated.

B. $\Delta wcaJ_{Ec}$ mutant XBF1 containing pWQ499 (RcsA⁺) and the indicated complementing plasmids or vector control was incubated overnight at 37°C on LB plates with $10 \mu\text{g ml}^{-1}$ tetracycline (to maintain pWQ499) and with or without arabinose (Ara) to induce gene expression. Incubation was extended to 24–48 h at room temperature to further increase colanic capsule formation.

C. Immunoblot using α -FLAG monoclonal antibody to confirm expression of FLAG-WbaP_{Mx} and FLAG-WcaJ_{Ec} in the $\Delta wcaJ_{Ec}$ mutant, and the expression of FLAG-WbaP_{Mx} in *S. enterica* WbaP_{Se} expressed from pSM13 was not tested since it does not have a FLAG tag. * and ** denote the monomeric and oligomeric forms of the PHPT proteins, usually present under the gel conditions required to ensure their visualization.

complemented with WbaP_{Ec O9:K30} are likely due to different processing of the O-antigen, as previously reported (Saldías *et al.*, 2008), and not to a defect in the initiation of its synthesis. We conclude from these experiments that WbaP_{Mx} transfers Gal-1-P onto Und-P.

An *E. coli* $\Delta wcaJ_{Ec}$ mutant was used to test whether FLAG-WbaP_{Mx} can transfer Glc-1-P to Und-P. Colanic acid

formation is readily apparent by a strong mucoid phenotype in *wcaJ*⁺ cells containing the plasmid pWQ499, which encodes the positive regulator RcsA of the colanic acid biosynthesis gene cluster (Furlong *et al.*, 2015). In the presence of arabinose, a mucoid phenotype was detected in the $\Delta wcaJ_{Ec}$ (pWQ499) mutant complemented with the plasmid pLA3, which encodes FLAG-WcaJ_{Ec} under the

control of the arabinose inducible promoter (Fig. 3B). By contrast, no complementation was observed in the presence of arabinose with pMP139, and this strain had the same phenotype as $\Delta wcaJ_{Ec}$ (pWQ499) containing the vector control pBADNTF (Fig. 3B). This result suggests that WbaP_{Mx} does not have UDP-Glc transferase activity.

When grown in the presence of arabinose, FLAG-WbaP_{Mx} was detected in the *S. enterica* $\Delta wbaP_{Se}$ mutant with α -FLAG antibodies at similar expression levels as in $\Delta wcaJ_{Ec}$ (pWQ499) *E. coli* strain (Fig. 3C). However, compared to FLAG-WcaJ_{Ec}, FLAG-WbaP_{Mx} was less abundant, which could be due to differences in codon usage, as previously shown for other PHTP proteins heterologously expressed in *E. coli* or in *S. enterica* (Steiner *et al.*, 2007; Patel *et al.*, 2012). FLAG-WcaJ_{Ec} as well as FLAG-WbaP_{Mx} showed the characteristic oligomeric and monomeric bands of similar apparent mass, as previously reported for PHPTs (Saldías *et al.*, 2008). The combined results presented above support the notion that WbaP_{Mx} transfers Gal-1-P and not Glc-1-P onto Und-P.

Loss of WaaL_{Mx} and WbaP_{Mx} do not affect EPS and spore coat formation

In addition to LPS, *M. xanthus* produces two other surface polysaccharides, EPS and spore coat (Dworkin and Gibson, 1964; Fink and Zissler, 1989a; Lu *et al.*, 2005; Holkenbrink *et al.*, 2014). We investigated whether lack of WaaL_{Mx}, Wzm_{Mx} or WbaP_{Mx} affect EPS synthesis, spore coat formation and cell morphology.

We determined EPS production using a plate-based colorimetric assay with Congo red that binds EPS. The $\Omega difE$ mutant, which does not accumulate EPS (Yang *et al.*, 1998), was used as a negative control. Cells lacking WbaP_{Mx} or WaaL_{Mx} produced EPS as the WT, while cells lacking Wzm_{Mx} showed reduced EPS (Fig. 4A). The defect in EPS production in the Δwzm_{Mx} mutant was complemented by ectopic expression of *wzm_{Mx}* (Fig. 4A).

The spore coat is essential for spore formation (Licking *et al.*, 2000; Müller *et al.*, 2012). To follow spore coat synthesis, we used an assay in which spore formation is induced in response to a high concentration of glycerol (Dworkin and Gibson, 1964). Although these chemically-induced spores are not identical to the spores formed in response to starvation, their morphogenesis results from the same cellular remodeling process in which rod-shaped cells are remodeled into spherical cells and the composition of the spore coat is similar in both types of spores (Kottel *et al.*, 1975; Inouye *et al.*, 1979a; 1979b; McCleary *et al.*, 1991; Otani *et al.*, 1998; Müller *et al.*, 2012). We generated an in-frame deletion mutation in *exoE*, which encodes the PHPT suggested to be responsible for initiation of spore coat polysaccharide synthesis (Holkenbrink

et al., 2014), as a negative control for spore coat accumulation. Compared to WT, cells lacking WbaP_{Mx} or WaaL_{Mx} were not affected in the formation of resistant, phase bright spherical spores while cells lacking Wzm_{Mx} formed spores at a reduced level and most of which were less spherical than those formed by WT (Fig. 4B). This defect in spore morphology and formation was not complemented by ectopic expression of *wzm_{Mx}* (Fig. 4B).

We used cell morphology and length as a readout to determine whether the $\Delta wbaP_{Mx}$, $\Delta waaL_{Mx}$ and Δwzm_{Mx} mutants had altered peptidoglycan synthesis. Cells of all three mutants had a rod-shaped morphology (Fig. 4B). In the $\Delta wbaP_{Mx}$ mutant, the cell length distribution was shifted marginally but significantly toward shorter cells and this effect was slightly exacerbated in the complemented strain (Fig. 4C). In the $\Delta waaL_{Mx}$ mutant, the cell length distribution was shifted marginally but significantly toward longer cells and this defect was partially corrected in the complemented strain (Fig. 4C). Cells of the Δwzm_{Mx} mutant were significantly longer than WT cells and this defect was not corrected in the complementation strain (Fig. 4C).

Together, these observations suggest that lack of WbaP_{Mx} and WaaL_{Mx} neither causes defects in EPS synthesis nor in spore coat synthesis, while the $\Delta wbaP_{Mx}$ and $\Delta waaL_{Mx}$ mutants have slightly abnormal cell length. By contrast, lack of Wzm_{Mx} causes pleiotropic effects and reduced EPS synthesis and also had an effect on spore formation and cell length.

Lack of LPS O-antigen causes defects in both motility systems and development

Previous reports on the importance of LPS O-antigen for the two motility systems in *M. xanthus* came to opposite conclusions. Because the mutations used in previous reports were not examined for pleiotropic effects on EPS synthesis and cell length, we reevaluated the importance of LPS O-antigen for motility. To this end, we employed the $\Delta wbaP_{Mx}$ mutant because our data support that the $\Delta wbaP_{Mx}$ mutation does not cause significant pleiotropic effects and the mutant does not accumulate Und-PP O-antigen intermediates.

To analyze the motility of the $\Delta wbaP_{Mx}$ mutant, cells were spotted on 1.5% and 0.5% agar, which are favorable for gliding motility and T4P-dependent motility respectively (Shi and Zusman, 1993). On 1.5% of agar, WT displayed the single cells at the colony edge characteristic of gliding motility, in contrast to the $\Delta aglQ$ mutant, which lacks an essential component of the gliding machinery (Sun *et al.*, 2011; Nan *et al.*, 2013). The $\Delta wbaP_{Mx}$ mutant displayed small groups of cells at the colony edge, but fewer single cells and colony expansion was strongly reduced compared to WT (Fig. 5A). On 0.5% of agar, WT displayed the long flares at the edge

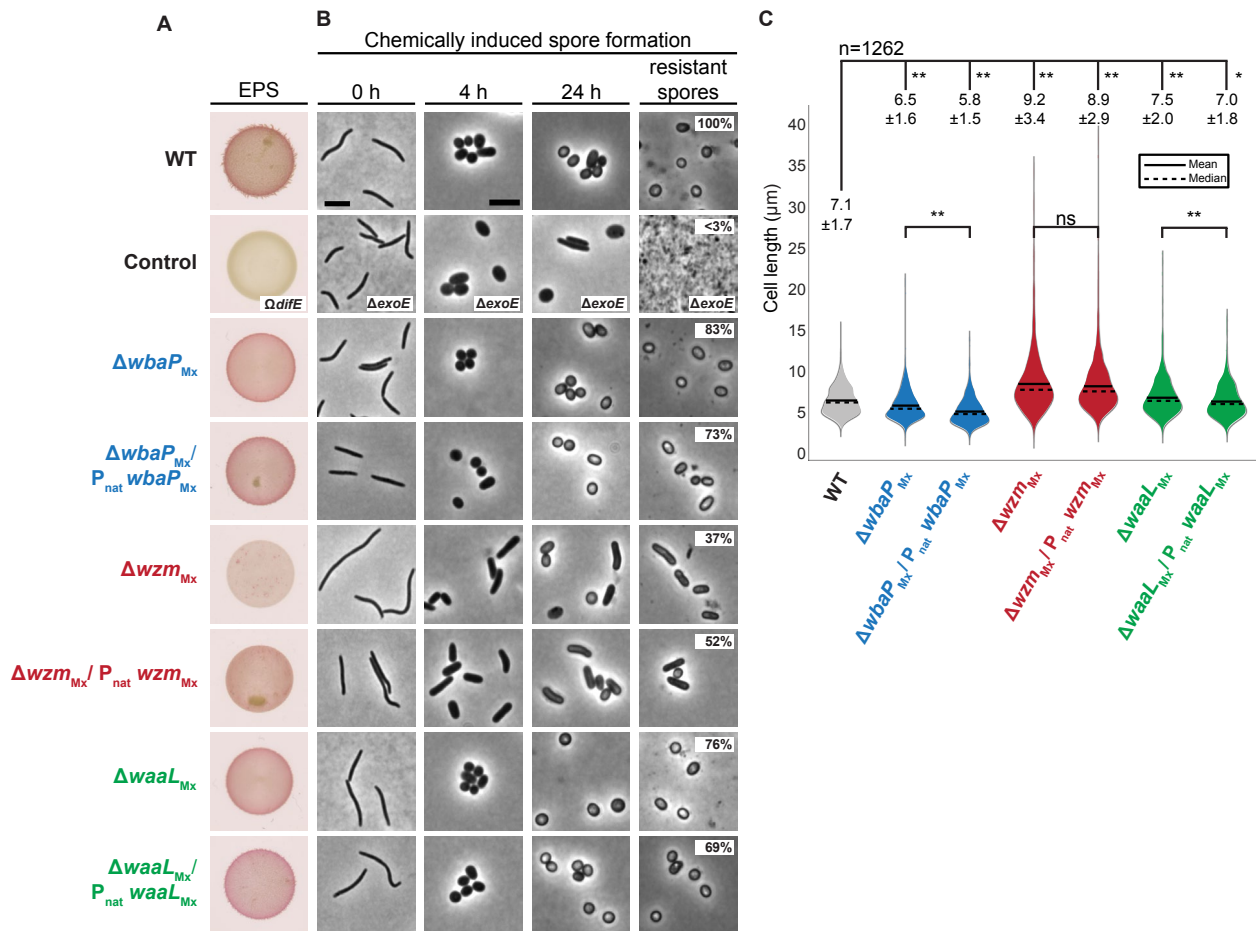


Fig. 4. EPS accumulation, chemically induced sporulation and cell length determination in the $\Delta wbaP_{Mx}$, $\Delta waaL_{Mx}$ and Δwzm_{Mx} mutants.

A. Determination of EPS accumulation. 20 μ l aliquots of cell suspensions at 7×10^9 cells/ml were spotted on 0.5% agar supplemented with 0.5% CTT and Congo red and incubated at 32°C for 24 h. The $\Delta difE$ mutant was used as a negative control.

B. Chemically induced sporulation. Sporulation was induced by addition of glycerol to a final concentration of 0.5 M. At 0, 4 and 24 h after induction cell morphology was observed. In images labeled resistant spores, cells were exposed to sonic and heat treatment before microscopy. Sporulation frequency after sonic and heat treatment is indicated as the mean of three technical replicates relative to WT. Scale bars, 5 μ m.

C. Cell length determination. Cell length distribution is shown in a violin plot. Each violin indicates the probability density of the data at different cell length values. Mean and median values are represented by a continuous and dashed line respectively. For each strain, mean cell length \pm standard deviation is indicated; $n = 1262$ combined from three biological replicates. Samples were compared using a Mann–Whitney test, * and **, p value < 0.01 and < 0.001, respectively; ns, not significant.

of colonies characteristic of T4P-dependent motility while the $\Delta pilA$ mutant, which lacks the major pilin of T4P (Wu and Kaiser, 1996) and served as a negative control, generated a colony edge without flares; by contrast, the $\Delta wbaP_{Mx}$ mutant only formed short flares (Fig. 5A).

Because motility defects observed in the two previous assays can be caused by either *bona fide* motility defects or improper regulation of the reversal frequency, we analyzed the motility characteristics of the $\Delta wbaP_{Mx}$ mutant at the single cell level. On 1.5% of agar, the $\Delta aglQ$ mutant was strongly reduced in single cell gliding motility (Fig. 5B). Less than 50% of cells of the $\Delta wbaP_{Mx}$ mutant displayed active movement and cells moved a significantly shorter cumulative distance than WT cells but reversed like WT cells (Fig. 5B).

Because *M. xanthus* does not move as single cells by means of T4P on agar surfaces, cells were placed on a polystyrene surface and covered with 1% of methylcellulose (Sun *et al.*, 2000) to analyze motility of single cells moving by T4P. $\Delta pilA$ cells showed very little movement on this surface (Fig. 5C). Surprisingly, the $\Delta wbaP_{Mx}$ mutant moved similarly to WT under this condition. Moreover, both strains had the same reversal frequency as WT cells. In an assay in which T4P were sheared off the cell surface, the $\Delta wbaP_{Mx}$ mutant contained slightly more PilA protein in the sheared T4P fraction and in total cell extracts compared to WT (Fig. 5D). Thus, the $\Delta wbaP_{Mx}$ mutant accumulates PilA and assemble T4P.

We conclude that $WbaP_{Mx}$ and, therefore, LPS O-antigen, is important for gliding motility, while $WbaP_{Mx}$

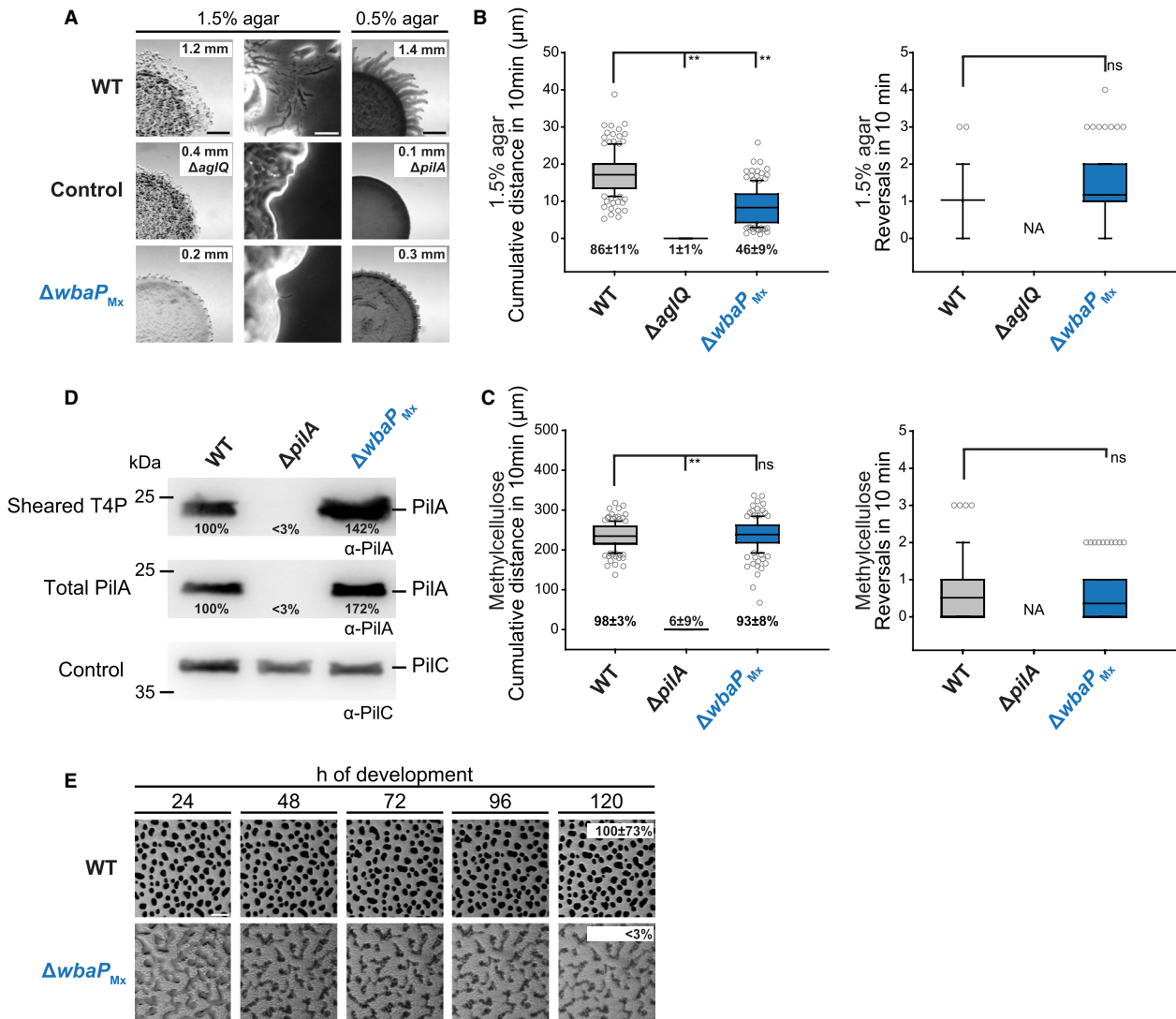


Fig. 5. Functional characterization of the $\Delta wbaP_{Mx}$ mutant. (A) Colony-based motility assays. T4P-dependent motility and gliding motility were analyzed on 0.5% and 1.5% agar respectively. The $\Delta pilA$ and $\Delta aglQ$ mutants served as negative controls. Images were recorded at 24 h. Numbers indicate increase in colony radius calculated from three technical replicates. Scale bars, 1 mm, 50 μ m and 1 mm (left to right). (B) Movement of single cells by gliding motility or (C) by T4P-dependent motility. Cells on 1.5% TPM agar supplemented with 0.5% CTT or in methylcellulose were imaged for 10 min with 20 or 10 s intervals respectively. Cumulative distance and number of reversals were calculated for $n = 150$ from three biological replicates. Only cells moving during the entire recording interval were included. In the box plot, boxes enclose the 25th and 75th percentile with the black line representing the mean; whiskers represent the 10th and 90th percentile. Samples were compared using a Mann-Whitney test, **, p value < 0.001 ; ns, not significant. In the left panel, % of cells displaying movement is indicated as the mean \pm standard deviation; $n = 1200$ combined from three biological replicates. (D) T4P shear off assay. Immunoblot detection of PiIA in sheared T4P (top) and in total cell extract (middle). Total protein was isolated from the indicated strains grown on 1% CTT 1.5% agar plates. In all three blots, protein from the same number of cells was loaded per lane. The top and middle blots were probed with α -PiIA antibodies. The bottom blot was probed against PiIC (45.2 kDa), as a loading control. Numbers indicate mean level of PiIA from two biological replicates normalized to the loading control (PiIC) and relative to WT (100%). PiIA has a calculated molecular mass of 23.4 kDa. (E) Development of $\Delta wbaP_{Mx}$ mutant. Cells on TPM agar were followed during development. Images were recorded at the indicated time points. Sporulation efficiency after heat and sonic treatment is indicated as the mean \pm standard deviation from three biological replicates relative to WT. Scale bar, 500 μ m.

(and therefore, LPS O-antigen) is conditionally important for T4P-dependent motility.

Different O-antigen deficient mutants have been described to be deficient in fruiting body formation and sporulation (Fink and Zissler, 1989b; Bowden and

Kaplan, 1998). While WT cells had aggregated to form darkened mounds after 24 h of starvation, the $\Delta wbaP_{Mx}$ mutant had only aggregated to form abnormally shaped translucent mounds after 24 h and even after 120 h, the $\Delta wbaP_{Mx}$ mutant had not formed regular and darkened

fruiting bodies (Fig. 5E). In addition, the $\Delta wbaP_{Mx}$ mutant was strongly reduced in sporulation compared to WT.

Discussion

This study focused on elucidating key steps of LPS O-antigen biosynthesis in *M. xanthus* and determining the functional consequences of LPS O-antigen loss. We demonstrated that *MXAN_2919* encodes the *WaaL_{Mx}* O-antigen ligase, which contains all the critical residues for O-antigen ligase activity found in other members of the family. Further, the $\Delta waaL_{Mx}$ mutant produced Und-PP-linked O-polysaccharide that was not transferred to lipid A-core, and LPS O-antigen synthesis was restored by ectopic expression of *waaL_{Mx}*. Therefore, we also suggest that *WaaL_{Mx}* is the sole O-antigen ligase in *M. xanthus*. *MXAN_2922* encodes the *WbaP* homolog for the initiation of O-antigen synthesis in *M. xanthus*. This is based on three lines of evidence. First, the predicted protein contains all the residues known to be important for enzymatic activity in the PHPT family. Second, a mutant lacking *WbaP_{Mx}* synthesized lipid A-core but lacked polymeric O-antigen. LPS O-antigen synthesis was restored by ectopic expression of *wbaP_{Mx}*, except that the complemented strain displayed a lower level of LPS O-antigen than WT, which could be due to differences in expression associated with the ectopic expression of *wbaP_{Mx}*. The absence of LPS O-antigen in the $\Delta wbaP_{Mx}$ mutant supports the idea that *WbaP_{Mx}* is the only PHPT involved in O-antigen synthesis. Moreover, neither *WaaL_{Mx}* nor *WbaP_{Mx}* are required for EPS and spore coat synthesis, suggesting they exclusively function in LPS O-antigen synthesis.

MXAN_4623 and *_4622* have been suggested to form the *Wzm/Wzt* ABC transporter for translocation of O-antigen polysaccharide across the IM (Guo *et al.*, 1996). *A priori*, a mutant lacking the *Wzm/Wzt* ABC transporter would have been expected to accumulate O-antigen in the cytoplasm, as has been reported for *E. coli* lacking the ABC transporters for O8- and O9a-antigen translocation (Cuthbertson *et al.*, 2005) and for *Klebsiella pneumoniae* lacking the ABC transporter for O2a-antigen translocation (Kos *et al.*, 2009). However, whole cell extracts from mutants lacking *Wzm_{Mx}* (here), containing a loss-of-function point mutation in *wzm_{Mx}* (Guo *et al.*, 1996) or lacking *Wzm_{Mx}*, *Wzt_{Mx}* and the glycosyltransferase *WbgA* (Bowden and Kaplan, 1998), do not detectably accumulate O-antigen polymers by immunoblot analysis. Upon complementation with *wzm_{Mx}⁺*, O-antigen chains longer than in the WT were observed (Fig. 2A–C). We speculate that this may be due to an altered accumulation level of *Wzm_{Mx}* in the

complementation strain which could result in an imbalance between O-antigen translocation and chain length control (see below).

Heterologous expression in *E. coli* and *S. enterica* serovar Typhimurium indicated that *WbaP_{Mx}* can functionally replace *WbaP_{Se}*, which transfers Gal-1-P to Und-P in *S. enterica* serovar Typhimurium, but not *WcaJ_{Ec}*, which transfers Glc-1-P to Und-P in *E. coli*. The structure of the *M. xanthus* LPS core oligosaccharide has been successfully determined and the O-antigen repeat unit has been determined as the 1 → 6 linked disaccharide α -D-Glcp-(1 → 4)- α -GalpNAc, in which a fraction of the GalNAc residues are methylated (Maclean *et al.*, 2007). However, the linkage between the core and O-antigen was not established. Since the *M. xanthus* O-antigen is assembled by the *Wzm/Wzt* pathway, we propose the Und-PP-Gal product arising from the *WbaP_{Mx}* activity provides Gal as the priming sugar for the assembly of the O-antigen (Fig. 6), in a similar fashion as GlcNAc in the *E. coli* *Wzm/Wzt*-dependent O8 and O9 systems, in which the priming sugar is not part of the repeat (Greenfield and Whitfield, 2012). In our proposed model, *WbaP_{Mx}* catalyzes the priming step of *M. xanthus* O-antigen synthesis. Then, an additional glycosyltransferase attaches α -D-Glcp, and a second glycosyltransferase would extend the O-antigen by alternatively adding α -GalpNAc and α -D-Glcp residues in successive cycles of catalysis. *WbgA* (*MXAN_4621*; Fig. 6), which has been implicated in O-antigen synthesis, contains three distinct glycosyltransferase domains, as described for glycosyltransferases involved in O-antigen synthesis in the ABC transporter pathway (Greenfield *et al.*, 2012a; 2012b). We, therefore, propose that *WbgB* (*MXAN_4619*), which is required for O-antigen synthesis, is responsible for the addition of α -D-Glcp onto the priming Gal residue of Und-PP-Gal, and the polymer is extended by *WbgA* (*MXAN_4621*) (Fig. 6). We also propose that the predicted methyltransferase *SgmR* (*MXAN_4620*), which has been implicated in T4P-dependent motility (Youderian and Hartzell, 2006), terminates the growing chain by methylation of α -GalpNAc, consistent with the chemical analysis of O-antigen (Maclean *et al.*, 2007). The completed O-antigen chain is transported by *Wzm_{Mx}/Wzt_{Mx}* across the IM in a process that may involve recognition of the terminal modification by the C-terminal domain in *Wzt_{Mx}* as described for the *E. coli* *Wzm/Wzt*-dependent O8 and O9a systems (Greenfield and Whitfield, 2012). Although this model is consistent with the available evidence, confirmation of this pathway requires further research. Ultimately, the O-antigen is ligated to lipid A-core by *WaaL_{Mx}* and LPS molecules transported to the OM by the proposed *Lpt* pathway (Fig. 6).

The lack of O-antigen accumulation in the cytosol of the *wzm_{Mx}* *M. xanthus* mutant compared to *E. coli/K. pneumoniae wzm/wzt* mutants suggests that O-antigen synthesis

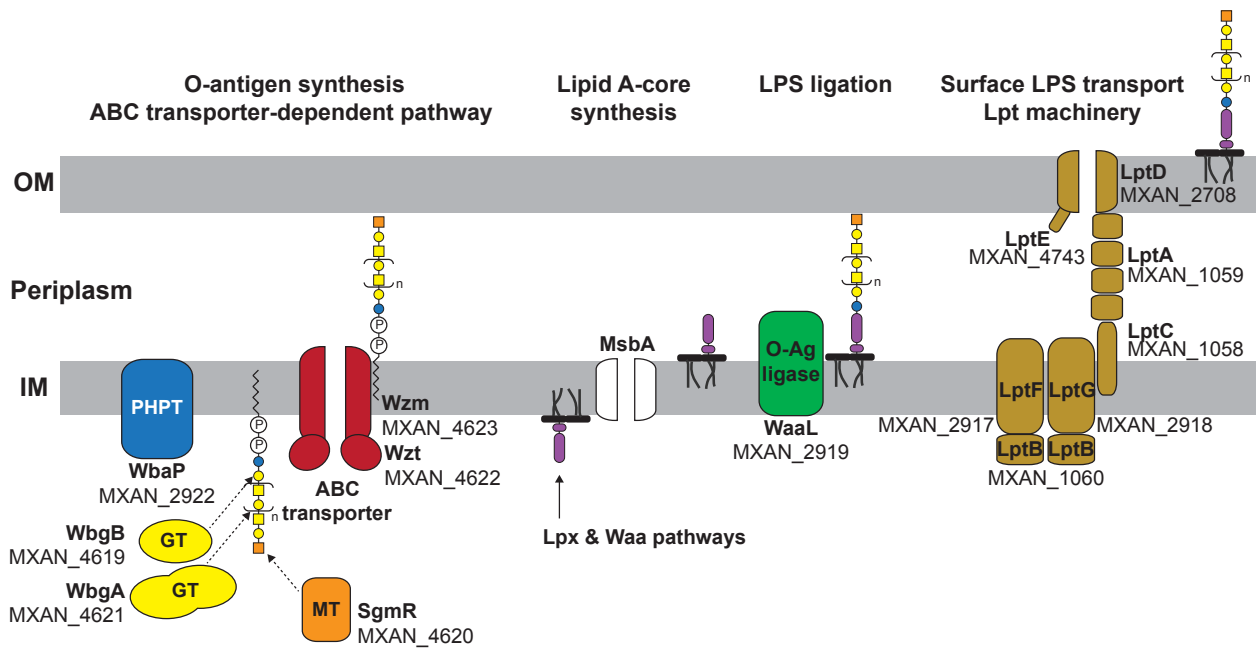


Fig. 6. Model of LPS biosynthesis in *M. xanthus*. In the O-antigen Gal (blue circle), Glu (yellow circle), GaINAc (yellow square) and methylated GaINAc (orange square) are indicated. Stippled lines indicate that the site of action of WbgA, WbgB and SgmR are hypothetical and remains to be determined experimentally. The Lpx and Waa pathways are responsible for synthesis of lipid A-Kdo₂ and core respectively (Raetz and Whitfield, 2002; Whitfield and Trent, 2014). None of these pathways have been described in detail in *M. xanthus*. See text in Discussion for details.

could be differently regulated in *M. xanthus*. Furthermore, the Δwzm_{Mx} mutant does not have the same dramatic growth defects and abnormal cell morphologies as those found in *E. coli* O8- and O9a-antigen ABC transporter mutants (Cuthbertson *et al.*, 2005). Although it is possible that second site suppressors preventing O-antigen synthesis in the Δwzm_{Mx} mutant could arise, this interpretation does not agree with the complementation experiment in which O-antigen synthesis is restored. An alternative explanation could be that accumulation of unprocessed (untransported) O-antigen may allosterically inhibit WbaP_{Mx} activity, shutting down O-antigen synthesis. It is possible that this inhibition involves the WbaP_{Mx} large cytoplasmic loop next to the C-terminal catalytic site. This region in Cps2E, the PHPT homolog of *Streptococcus pneumoniae*, has been implicated in regulation of polysaccharide synthesis and modulation of polysaccharide length by suppressing transferase activity *in vivo* and *in vitro* (Xayarath and Yother, 2007; James *et al.*, 2013).

Loss of WbaP_{Mx} or WaaL_{Mx} function had marginal effects on the cell length that were not fully restored in the complementation strains. Several non-mutually exclusive scenarios may explain these effects. In one scenario, the altered OM in the mutants together with accumulation of O-antigen in the periplasm in the case of the $\Delta waaL_{Mx}$ mutant could give rise to these defects. Alternatively, mutants with a defect in O-antigen and LPS synthesis can cause sequestration of Und-P resulting in

altered peptidoglycan synthesis and, consequently, cell length defects (Burrows and Lam, 1999; Valvano, 2008; Jorgenson and Young, 2016). In cells lacking WbaP_{Mx}, Und-P is not expected to be titrated because the step that consumes Und-P is blocked. Therefore, we consider this scenario unlikely in this mutant. By contrast, the level of accumulation of unligated O-antigen in cells lacking WaaL_{Mx} is similar to that of LPS O-antigen in WT (Fig. 2B). Therefore, Und-P might become limiting in $\Delta waaL_{Mx}$ cells. Accordingly, an *E. coli* mutant that lacks the O-antigen ligase also has morphological defects including an increased cell length and this effect is counteracted by deletion of *wecA*, which encodes the PNPT that initiates biosynthesis of O-antigen (Jorgenson and Young, 2016). The partial complementation of the cell length defect in the $\Delta waaL_{Mx}$ and $\Delta wbaP_{Mx}$ mutants may be caused by altered accumulation levels of WbaP_{Mx} and WaaL_{Mx} in the complementation strains compared to WT.

In contrast to the $\Delta waaL_{Mx}$ and $\Delta wbaP_{Mx}$ mutants, lack of Wzm_{Mx} caused significant pleiotropic effects such as reduced EPS accumulation, formation of significantly elongated cells, and elongated spores upon chemical induction. Three lines of evidence support that Wzm_{Mx} is not directly involved in translocation of EPS, spore coat or peptidoglycan precursors to the periplasm. First, the *eps* locus, which encodes the genes for EPS synthesis and export (Lu *et al.*, 2005), encodes homologs of the Wzx/Wzy pathway. Second, the *exo* locus involved in spore

coat formation encodes a Wzz homolog that is required for spore coat formation and, therefore, spore coat synthesis has been suggested to depend on a Wzx/Wzy pathway (Holkenbrink *et al.*, 2014). Third, MXAN_3558 encodes a homolog of the lipid II MurJ flippase, also a member of the Wzx flippase family. Therefore, we speculate that the sporulation defect upon chemical induction is a consequence of the increased cell length of growing cells. How then may lack of Wzm_{Mx} cause defects in EPS and peptidoglycan synthesis? One possibility is that the Δwzm_{Mx} mutant synthesizes short O-antigens that are not detected by the MAbs against O-antigen and which are not transported across the IM (due to lack of Wzm_{Mx}) and, therefore, not ligated to lipid A-core. In this case, synthesis of the short O-antigen chains could cause sequestration of Und-P as reported for other systems with a defect in O-antigen transport and synthesis and, therefore, reduced EPS and peptidoglycan synthesis (Burrows and Lam, 1999; Valvano, 2008; Jorgenson and Young, 2016). To test the idea that Und-P is sequestered in the Δwzm_{Mx} mutant, we tried to generate a $\Delta wbaP_{Mx} \Delta wzm_{Mx}$ double mutant; however, for reasons that we do not understand, we were unable to obtain this mutant. Another possibility is that the Δwzm_{Mx} mutant has accumulated mutations causing an effect on peptidoglycan synthesis. Supporting this scenario, ectopic expression of *wzm_{Mx}* in the Δwzm_{Mx} mutant largely complemented the defect in O-antigen synthesis and fully complemented the EPS synthesis defect. However, the cell morphology and sporulation defects were not complemented. Undoubtedly, more research is needed to clarify the mechanisms causing lack of O-antigen synthesis as well as reduced EPS and peptidoglycan synthesis and morphology defects in the Δwzm_{Mx} mutant.

Because previous experiments to determine the importance of LPS O-antigen for *M. xanthus* motility provided different results, we readdressed this question. We specifically used the mutant lacking WbaP_{Mx} because the $\Delta wbaP_{Mx}$ mutation only has a minor pleiotropic effect on cell length and does not accumulate intermediates in O-antigen synthesis. We observed that LPS is conditionally required for T4P-dependent motility: $\Delta wbaP_{Mx}$ cells that moved by means of T4P had a motility defect on 0.5% of agar, but not on a polystyrene surface covered with methylcellulose. In agreement with the observation that the triple *wzm_{Mx} wzt_{Mx} wbgA* mutant accumulated PilA and T4P (Bowden and Kaplan, 1998), the $\Delta wbaP_{Mx}$ mutant also accumulated PilA and T4P, albeit at slightly higher levels than WT. On polystyrene surfaces with methylcellulose, mutants lacking EPS show restored T4P-dependent motility, and polystyrene was suggested to serve as an anchor for T4P adhesion (Hu *et al.*, 2011). How polystyrene/methylcellulose restores the motility defect of the $\Delta wbaP_{Mx}$ mutant remains to be clarified because this mutant accumulates WT levels of EPS. We also observed that LPS is important for gliding motility

on 1.5% of agar. Gliding motility depends on the Agl/Glt machinery. Moreover, gliding cells deposit a slime trail. The function and composition of slime are unknown; however, slime may promote the adhesion of cells to the substratum and may contain polysaccharides and OM vesicles (Ducret *et al.*, 2012; 2013; Gloag *et al.*, 2016). We conclude that LPS is (conditionally) important for both motility systems. We speculate that the different results previously reported regarding the involvement of LPS O-antigen in motility can be explained by its conditional importance for T4P-dependent motility and the pleiotropic effects of certain mutations that affect LPS O-antigen synthesis.

Mutants with a defect in LPS synthesis have been suggested to have defects in development (Fink and Zissler, 1989b; Bowden and Kaplan, 1998; Yang *et al.*, 2000). However, in those experiments, neither the accumulation of EPS nor cell length was reported. We re-evaluated the connection between LPS O-antigen and development using the $\Delta wbaP_{Mx}$ mutant and observed that lack of WbaP_{Mx} caused a defect in aggregation and sporulation, in agreement with previous reports. Because $\Delta wbaP_{Mx}$ cells sporulate in response to chemical induction with glycerol, we suggest that the defect in sporulation during starvation-induced development is a consequence of the aggregation defect. Mutants affected in motility have developmental defects (Hodgkin and Kaiser, 1979). Therefore, it remains possible that the developmental defects caused by lack of O-antigen are indirect effects of the motility defects caused by lack of O-antigen.

In summary, we report that mutants blocked in different steps in LPS synthesis have very different phenotypes. With the detailed characterization of these mutants, the tools are now available to analyze in detail the function of LPS O-antigen in motility and development.

Experimental procedures

Strains and cell growth

All *M. xanthus* strains are derivatives of the wild-type DK1622 (Kaiser, 1979). Strains, plasmids and oligonucleotides used in this work are listed in Tables 1, 2, and S2 respectively. *M. xanthus* was grown at 32°C in 1% CTT (1% (w/v) Bacto Casitone, 10 mM Tris-HCl [pH 8.0], 1 mM K₂HPO₄/KH₂PO₄ [pH 7.6] and 8 mM MgSO₄) liquid medium or on 1.5% of agar supplemented with 1% of CTT and kanamycin (50 µg ml⁻¹) or oxytetracycline (10 µg ml⁻¹), as appropriate (Hodgkin and Kaiser, 1977). In-frame deletions were generated as described (Shi *et al.*, 2008), and plasmids for complementation experiments were integrated in a single copy by site specific recombination into the Mx8 *attB* site. In-frame deletions and plasmid integrations were verified by PCR. Plasmids were propagated in *E. coli* Mach1 and DH5α.

E. coli and *S. enterica* serovar Typhimurium strains were grown at 37°C in Luria-Bertani (LB) medium (10 mg tryptone ml⁻¹, 5 mg yeast extract ml⁻¹; 5 mg NaCl ml⁻¹) supplemented,

Table 1. Strains used in this work.

Strain	Genotype	References
<i>M. xanthus</i>		
DK1622	WT	Kaiser (1979)
DK10410	$\Delta pilA$	Wu and Kaiser (1997)
SA5923	$\Delta aglQ$	Jakobczak <i>et al.</i> (2015)
SW501	$diffE::Km^r$	Yang <i>et al.</i> (1998)
SA7439	$\Delta waaL_{Mx}$ ($\Delta MXAN_2919$)	This study
SA7440	Δwzm_{Mx} ($\Delta MXAN_4623$)	This study
SA7450	$\Delta wbaP_{Mx}$ ($\Delta MXAN_2922$)	This study
SA7495	$\Delta exoE$ ($\Delta MXAN_3229$)	This study
SA7468	$\Delta wzm_{Mx} attB::pJJ9$ ($P_{nat} wzm_{Mx}$)	This study
SA7471	$\Delta wbaP_{Mx} attB::pJJ7$ ($P_{nat} wbaP_{Mx}$)	This study
SA7476	$\Delta waaL_{Mx} attB::pJJ11$ ($P_{nat} waaL_{Mx}$)	This study
<i>E. coli</i>		
DH5 α	F ⁻ $\phi 80lacZ\Delta M15 endA recA hsdR(r_K^- m_K^-)$ <i>nupG thi glnV deoR gyrA relA1</i> $\Delta(lacZYA-argF)U169$	Lab stock
Mach1	$\Delta recA1398 endA1 tonA \phi 80\Delta lacM15 \Delta lacX74 hsdR(r_K^- m_K^+)$	Invitrogen
XBF1	W3110, $\Delta wcaJ::aph, Km^r$	Patel <i>et al.</i> (2012)
<i>Salmonella</i>		
LT2	WT, <i>S. enterica</i> serovar Typhimurium	S. Maloy
MSS2	LT2, $\Delta wbaP::cat Cm^r$	Saldías <i>et al.</i> (2008)

Table 2. Plasmids used in this work.

Plasmid	Description	References
pBJ114	$Km^r galK$	Julien <i>et al.</i> (2000)
pSWU30	Tet^r	Wu and Kaiser (1997)
pBADNTF	pBAD24 for N-terminal FLAG fusion and with arabinose inducible promoter, Amp^r	Marolda <i>et al.</i> (2004)
pLA3	pBADNTF, <i>wcaJ</i> , Amp^r	Furlong <i>et al.</i> (2015)
pSM13	pUC18, <i>wbaP</i> from <i>S. enterica</i> Ty2 containing a 1 bp deletion at position 583 and a 2 bp deletion at position 645. This causes a frame shift at WbaP I194 and frame restoration at Y215, Amp^r	Saldías <i>et al.</i> (2008)
pJD132	pBluescript SK ⁻ , <i>wbaP</i> and flanking sequences from <i>E. coli</i> O9:K30, Amp^r	Schäffer <i>et al.</i> (2002)
pWQ499	pKV102 containing <i>rcsAK30</i> , Tet^r	C. Whitfield
pMP062	pBJ114, in-frame deletion construct for <i>waaL_{Mx}</i> (<i>MXAN_2919</i>) Km^r	This study
pMP065	pBJ114, in-frame deletion construct for <i>wzm_{Mx}</i> (<i>MXAN_4623</i>) Km^r	This study
pMP071	pBJ114, in-frame deletion construct for <i>wbaP_{Mx}</i> (<i>MXAN_2922</i>) Km^r	This study
pMP099	pBJ114, in-frame deletion construct for <i>exoE</i> (<i>MXAN_3229</i>) Km^r	This study
pMP139	pBADNTF, <i>wbaP_{Mx}</i> (<i>MXAN_2922</i>) Amp^r	This study
pJJ7	pSWU30, P_{nat} - <i>wbaP_{Mx}</i> (<i>MXAN_2922</i>) Tet^r	This study
pJJ9	pSWU30, P_{nat} - <i>wzm_{Mx}</i> (<i>MXAN_4623</i>) Tet^r	This study
pJJ11	pSWU30, P_{nat} - <i>waaL_{Mx}</i> (<i>MXAN_2919</i>) Tet^r	This study

when required, with ampicillin, tetracycline, kanamycin or chloramphenicol at final concentrations of 100, 20, 40 and 30 $\mu\text{g ml}^{-1}$ respectively. Plasmids for heterologous complementation were introduced into MSS2 and XBF1 strains (Table 1) by electroporation (Dower *et al.*, 1988).

Motility assays

For population-based motility assays, exponentially growing cultures of *M. xanthus* were harvested (6000 g, room

temperature (RT)) and resuspended in 1% CTT to a calculated density of 7×10^9 cells ml^{-1} . 5 μl aliquots of cell suspensions were spotted on 0.5% and 1.5% agar supplemented with 0.5% CTT and incubated at 32°C. Cells were visualized after 24 h using a M205FA Stereomicroscope (Leica) and imaged using a Hamamatsu ORCA-flash V2 Digital CMOS camera (Hamamatsu Photonics). Gliding and T4P-dependent motility were quantified by determining the increase in colony diameter over three technical replicates. To quantify the movement of single cells, cultures were imaged using a DMi8 Inverted microscope and DFC9000 GT camera (Leica). For

the visualization of single cells moving by T4P-dependent motility, exponentially growing cultures were diluted to 3×10^8 and 5 μl cell suspension were placed in a 24-well polystyrene plate (Falcon) and incubated 10 min in the dark at RT. Then, 500 μl of 1% methylcellulose in MMC buffer (10 mM MOPS, 4 mM MgSO_4 , 2 mM CaCl_2 , pH 7.6) were added and cells incubated for 30 min in the dark at RT. Cells were imaged for 10 min with 10 s intervals. To visualize individual cells moving by gliding motility, exponentially growing cultures were diluted to 3×10^8 and 5 μl were spotted on 1.5% of agar plates supplemented with 0.5% of CTT and immediately covered by a cover slide. Cells were incubated 4 h at 32°C and then visualized for 10 min with 20 s intervals at 32°C. Pictures were analyzed using Metamorph® v 7.5 (Molecular Devices) and ImageJ (Schindelin *et al.*, 2012).

Cell length and width determination

About 5 μl aliquots of exponentially growing cell suspensions were spotted on 1.5% of agar supplemented with 0.2% of CTT, immediately covered with a cover slide and imaged as indicated above. Images were analyzed with Outfi (Paintdakhi *et al.*, 2016) and Matlab R2018a (The MathWorks) to determine the cell length. Violin plots were prepared using Matlab R2018a and the script violin.m (Hoffmann, 2015).

Development

Exponentially growing *M. xanthus* cultures were harvested (6000 g at RT), and resuspended in MC7 buffer (10 mM MOPS pH 7.0, 1 mM CaCl_2) to a calculated density of 7×10^9 cells ml^{-1} . 10 μl aliquots of cells were placed on TPM agar (10 mM Tris-HCl pH 7.6, 1 mM $\text{K}_2\text{HPO}_4/\text{KH}_2\text{PO}_4$ pH 7.6, 8 mM MgSO_4). Cells were visualized at the indicated time points using a M205FA Stereomicroscope (Leica) and imaged using a Hamamatsu ORCA-flash V2 Digital CMOS camera (Hamamatsu Photonics). After 120 h, cells were collected and incubated at 50°C for 2 h, and then sonicated with 30 pulses, pulse 50% and amplitude 75% with UP200St sonifier and microtip (Hielscher). Sporulation levels were determined as the number of sonication- and heat-resistant spores relative to WT using a Helber bacterial counting chamber (Hawksley, UK).

Chemically induced sporulation

Sporulation in response to 0.5 M of glycerol was performed as described (Müller *et al.*, 2010) with a slightly modified protocol. Briefly, cells were cultivated in 20 ml of CTT medium, at a cell density of 3×10^8 cells ml^{-1} , glycerol was added to a final concentration of 0.5 M. At 0, 4 and 24 h after glycerol addition, cell morphology was observed by placing 5 μl of cells on a 1.5% of agar pad supplemented with TPM (10 mM Tris-HCl pH 7.6, 1 mM $\text{K}_2\text{HPO}_4/\text{KH}_2\text{PO}_4$ pH 7.6, 8 mM MgSO_4); cells were immediately covered with a coverslip and imaged with DMi6000B microscope and a Hamamatsu Flash 4.0 Camera (Leica). To determine the resistance to heat and sonication of spores formed, cells from 5 ml of the culture after 24 h

incubation were harvested by centrifugation at 4150 g at RT, resuspended in 1 ml of sterile water, incubated at 50°C for 2 h, and then sonicated as described. 5 μl of the treated samples were placed on a 1.5% of agar pad supplemented with TPM, covered with a coverslip and imaged. To quantify sporulation efficiency, 5 μl of the treated samples were counted using a Helber bacterial counting chamber (Hawksley, UK). Image processing and data analysis were performed using Metamorph® v 7.5 (Molecular Devices).

Detection of EPS accumulation

EPS accumulation was detected using a slightly modified protocol from (Skotnicka *et al.*, 2015). Cells were grown in CTT medium to a density of 7×10^8 cells ml^{-1} , harvested by centrifugation (6000 g at RT) and resuspended in 1% CTT to a calculated density of 7×10^9 cells ml^{-1} . About 20 μl aliquots of the cell suspensions were placed on 0.5% of agar plates supplemented with 0.5% of CTT and 40 $\mu\text{g ml}^{-1}$ Congo red. Plates were incubated at 32°C and documented at 24 h.

LPS detection by immunoblot

M. xanthus cells growing exponentially in 1% CTT were harvested by centrifugation (6000 g, RT) and resuspended to a calculated density of 7×10^8 cells ml^{-1} by addition of SDS buffer (0.1 M DTT, 2% SDS, 10% glycerol, 5 mM EDTA, 60 mM Tris-HCl (pH 6.8) and bromophenol blue) to generate whole cell lysates. 15 μl were loaded and separated by SDS-PAGE on a 14% and 10% gel to detect the O-antigen and core respectively. LPS, O-antigen and lipid A-core and proteins were transferred to a nitrocellulose membrane. Immunoblots were performed as described (Sambrook and Russell, 2001) using MAb783 against O-antigen (dilution: 1:2000), MAb2254 against lipid A-core (dilution: 1:2000) (Fink and Zissler, 1989a) and polyclonal rabbit α -PilC antibodies (dilution: 1:2000) (Bulyha *et al.*, 2009) together with horseradish peroxidase-conjugated sheep α -mouse immunoglobulin G (dilution: 1:2000) (GE Healthcare) and horseradish peroxidase-conjugated goat α -rabbit immunoglobulin G (dilution: 1:15,000) (Sigma) as secondary antibody. Blots were developed using Luminata Forte chemiluminescence reagent (Millipore) on a LAS-4000 imager (Fujifilm). For detection of *Salmonella* O-antigen, immunoblotting was carried out with rabbit *Salmonella* O antiserum group B (Difco, Beckton Dickinson ref. number 229481) (dilution: 1:500) together with IRDye 800CW goat α -rabbit immunoglobulin G (dilution: 1:10,000) (LI-COR) as secondary antibody and detected with a LI-COR Odyssey infrared imaging system.

LPS purification and detection

LPS was purified from *M. xanthus* strains and detected as described (Davis and Goldberg, 2012) with some modifications. Briefly, 10 ml of overnight *M. xanthus* cultures grown in 1% of CTT were harvested by centrifugation (4150 g, RT) and resuspended in 200 μl of LPS/SDS buffer (2% β -mercaptoethanol, 2% SDS, 10% glycerol in 0.05 M Tris-HCl (pH

6.8) and bromphenol blue). The cell suspension was boiled for 15 min, and then incubated for 15 min at RT. Then, 5 μ l of DNaseI (10 mg ml⁻¹) (Roche) and 10 μ l of RNase (5 mg ml⁻¹) (Epicenter) were added, and samples incubated at 37°C for 30 min. 10 μ l of Proteinase K (10 mg ml⁻¹) (Epicenter) were added and samples incubated 3 h at 59°C. To extract LPS, 200 μ l of ice-cold water saturated phenol were added, samples vortexed and incubated 15 min at 65°C. After addition of 1 ml of diethyl ether, samples were centrifuged for 10 min (16,000 g, RT). Extraction with phenol was repeated until the samples did not appear cloudy. Fifteen μ l (1:1; extracted sample: SDS buffer) samples containing the same number of cells were loaded per lane on an Any kD™ Mini-PROTEAN® Gel (Bio-Rad) and separated by SDS-PAGE. Gels were stained with Pro-Q Emerald 300 Lipopolysaccharide Gel Stain Kit (Invitrogen) as described (Marolda *et al.*, 2006). Briefly, gels were fixed overnight with 50 ml fixing solution (60% methanol, 10% acetic acid), and washed twice with 50 ml of 3% acetic acid for 20 min. After incubation with 25 ml of Oxidizing Solution containing periodate, gels were washed three times with 3% acetic acid for 20 min each. Gels were stained with Stain solution containing Pro-Q Emerald 300 in the dark for 2 h and then washed twice for 20 min in the dark with 3% of acetic acid. Stained LPS was detected and imaged using GelStick Imager (Intas).

For complementation experiments with *S. enterica* serovar Typhimurium, LPS was extracted and visualized by silver staining as described (Marolda *et al.*, 2006). Briefly, bacteria were grown at 37°C overnight on LB plates supplemented with antibiotics and 0.2% arabinose, when needed. Biomass was collected from each plate, resuspended in 5 ml PBS, pH 7.2 and the OD_{600nm} adjusted to 4. 1 ml of the normalized suspension was transferred to a microcentrifuge tube and centrifuged at 10,000 g for 2 min. To lyse cells, pellets were resuspended in 150 μ l of lysis buffer (2% (w/v) SDS, 4% β -mercaptoethanol and 0.5 M of Tris-HCl pH 6.8), and boiled for 10 min. Then, 10 μ l of Proteinase K (10 mg ml⁻¹) was added and samples were incubated at 60°C for 2 h. To remove proteins, 150 μ l of 90% phenol solution (90% phenol, 0.1% β -mercaptoethanol and 0.2% 8-hydroxyquinoline) was added and extracts incubated at 70°C for 15 min. Samples were centrifuged at 10,000 g for 10 min. Finally, 50 μ l of the clear aqueous phase was transferred to a clean microcentrifuge tube and loading buffer was added. Eight microliter of LPS samples were separated on 14% of acrylamide gel using a Tricine-SDS buffer system and gel was silver-stained as described previously (Marolda *et al.*, 2006).

Detection of colanic acid biosynthesis in *E. coli* Δ wcaJ

Plasmids expressing full length _{FLAG}WcaJ_{Ec} (pLA3), _{FLAG}WbaP_{Mx} (pMP139) and the control vector (pBADNTF) were introduced into XBF1/pWQ499. Transformed strains were grown on LB plates with antibiotics and with or without 0.2% (w/v) arabinose at 37°C overnight. Incubation was extended to 24–48 h at RT to observe mucoidity (Furlong *et al.*, 2015).

Western blotting

E. coli and *S. enterica* strains containing arabinose-inducible plasmids and FLAG-fusion proteins were grown

overnight in 5 ml LB supplemented with needed antibiotics. The next day, cultures were diluted 1:100 in 20 ml of the same media and incubated until an OD_{600nm} of 0.5–0.7 at which point arabinose was added to a final concentration of 0.2% (w/v). Samples were incubated for 3 h under the same conditions. Cultures were centrifuged at 1000 g for 10 min at 4°C. Bacterial pellets were resuspended in 10 ml of 50 mM Tris-HCl pH 8, with protease inhibitor cocktail (Roche) and lysed at 12,000 PSI with a cell disruptor (Constant Systems, Kennesaw, GA). Cell debris was pelleted at 10,000 g for 15 min at 4°C. Total membranes were isolated by centrifugation in microcentrifuge tubes at 42,220 g for 1 h at 4°C and resuspended in 50 μ l of 50 mM Tris-HCl pH 8. Protein concentration was determined by the Bradford protein assay (Bio-Rad) and 10 μ g of each membrane preparation was separated by 15% SDS-PAGE. Proteins were transferred to nitrocellulose membrane by Trans-Blot Turbo Transfer System (Bio-Rad) and blocking overnight in Blocker™ Casein in TBS (Thermo Fisher Scientific). The primary antibody, α -FLAG M2 monoclonal antibody (Sigma), was diluted 1:10,000 in TBS pH 7.5 (20 mM Tris-HCl, 150 mM NaCl) and incubated for 2 h. Membrane was washed for 1 h with TTBS (TBS supplemented with 0.1% Tween 20 (Sigma)), changing the washing solution each 15 min. Secondary antibody, IRDye 800CW Goat α -Mouse IgG (H + L), 0.5 mg (LI-COR) was diluted 1:10,000 in TBS and applied to the membrane for 30 min. Membrane was washed for 1 h with TTBS (changing the washing solution each 15 min) and developed using LI-COR Odyssey infrared imaging system. Precision Plus Protein™ Kaleidoscope™ Prestained Protein Standards (Bio-Rad) were used as protein mass standards.

T4P shear off assay

T4P were sheared from cells that had been grown for 3 days on 1.5% agar plates supplemented with 1% of CTT at 32°C as described except that precipitation of sheared T4P was done using TCA as described (Koontz, 2014) and analyzed by immunoblotting with α -PilA antibodies as described previously (Wu and Kaiser, 1997). Blots were developed using Luminata Forte chemiluminescence reagent (Millipore) on a LAS-4000 imager (Fujifilm). PilA levels were quantified using ImageJ (Schindelin *et al.*, 2012) based on two biological replicates.

Bioinformatics

UniProt (The-UniProt-Consortium, 2019) and KEGG (Kanehisa and Goto, 2000) databases were used to assign functions to proteins encoded by LPS gene clusters I and II (Fig. 1A; Table S1). The Carbohydrate Active Enzymes (CAZy) database (<http://www.cazy.org/>) (Lombard *et al.*, 2014), Pfam v31.0 and v32.0 (pfam.xfam.org) (Finn *et al.*, 2016) and the Conserved Domain tool from NCBI (Marchler-Bauer *et al.*, 2017) were used to identify protein domains. Membrane topology was assessed by TMHMM v2.0 (Sonnhammer *et al.*, 1998) and DAS (Cserző *et al.*, 1997) and two-dimensional topology was graphically shown using TOPO2 (Johns). BlastP (Boratyn *et al.*, 2013) and the KEGG

database were used to identify Lpt homologs in *M. xanthus*. *E. coli* and *S. enterica* proteins used for comparison with *M. xanthus* proteins are listed in Table S3. Clustal Omega (Chojnacki *et al.*, 2017) was used to align protein sequences.

Statistics

Statistical analyses were performed using SigmaPlot v14. All data sets were tested for a normal distribution using a Shapiro–Wilk test. For all data sets without a normal distribution, the Mann–Whitney test was applied to test for significant differences.

Acknowledgements

We thank Heidi Kaplan for providing the monoclonal antibody MA783 and Natividad Ruiz and Johann Heider for helpful discussions. This work was supported by Deutsche Forschungsgemeinschaft (DFG, German Research Council) within the framework of the SFB987 ‘Microbial Diversity in Environmental Signal Response’ as well as by the Max Planck Society.

Conflict of interest

The authors declare no conflict of interest.

Data availability statement

The data that support the findings of this study are available from the corresponding author upon request.

References

- Antunes, L.C.S., Poppleton, D., Klingl, A., Criscuolo, A., Dupuy, B., Brochier-Armanet, C., *et al.* (2016) Phylogenomic analysis supports the ancestral presence of LPS-outer membranes in the Firmicutes. *eLife*, **5**, e14589.
- Arnold, J.W. and Shimkets, L.J. (1988) Cell surface properties correlated with cohesion in *Myxococcus xanthus*. *Journal of Bacteriology*, **170**, 5771–5777.
- Berleman, J.E. and Kirby, J.R. (2009) Deciphering the hunting strategy of a bacterial wolfpack. *FEMS Microbiology Reviews*, **33**, 942–957.
- Boratyn, G.M., Camacho, C., Cooper, P.S., Coulouris, G., Fong, A., Ma, N., *et al.* (2013) BLAST: a more efficient report with usability improvements. *Nucleic Acids Research*, **41**, W29–W33.
- Bowden, M.G. and Kaplan, H.B. (1998) The *Myxococcus xanthus* lipopolysaccharide O-antigen is required for social motility and multicellular development. *Molecular Microbiology*, **30**, 275–284.
- Bulyha, I., Schmidt, C., Lenz, P., Jakovljevic, V., Höne, A., Maier, B., *et al.* (2009) Regulation of the type IV pili molecular machine by dynamic localization of two motor proteins. *Molecular Microbiology*, **74**, 691–706.
- Burrows, L.L. and Lam, J.S. (1999) Effect of *wzx* (*rfbX*) mutations on A-band and B-band lipopolysaccharide biosynthesis in *Pseudomonas aeruginosa* O5. *Journal of Bacteriology*, **181**, 973–980.
- Cao, P., Dey, A., Vassallo, C.N. and Wall, D. (2015) How myxobacteria cooperate. *Journal of Molecular Biology*, **427**, 3709–3721.
- Chojnacki, S., Cowley, A., Lee, J., Foix, A. and Lopez, R. (2017) Programmatic access to bioinformatics tools from EMBL-EBI update: 2017. *Nucleic Acids Research*, **45**, W550–W553.
- Clarke, B.R., Cuthbertson, L. and Whitfield, C. (2004) Nonreducing terminal modifications determine the chain length of polymannose O antigens of *Escherichia coli* and couple chain termination to polymer export via an ATP-binding cassette transporter. *Journal of Biological Chemistry*, **279**, 35709–35718.
- Cserző, M., Wallin, E., Simon, I., von Heijne, G. and Elofsson, A. (1997) Prediction of transmembrane alpha-helices in prokaryotic membrane proteins: the dense alignment surface method. *Protein Engineering*, **10**, 673–676.
- Cuthbertson, L., Powers, J. and Whitfield, C. (2005) The C-terminal domain of the nucleotide-binding domain protein Wzt determines substrate specificity in the ATP-binding cassette transporter for the lipopolysaccharide O-antigens in *Escherichia coli* serotypes O8 and O9a. *Journal of Biological Chemistry*, **280**, 30310–30319.
- Cuthbertson, L., Kimber, M.S. and Whitfield, C. (2007) Substrate binding by a bacterial ABC transporter involved in polysaccharide export. *Proceedings of the National Academy of Sciences of the United States of America*, **104**, 19529–19534.
- Davis, M.R. and Goldberg, J.B. (2012) Purification and visualization of lipopolysaccharide from Gram-negative bacteria by hot aqueous-phenol extraction. *Journal of Visualized Experiments*, **63**, e3916.
- Dower, W.J., Miller, J.F. and Ragsdale, C.W. (1988) High efficiency transformation of *E. coli* by high voltage electroporation. *Nucleic Acids Research*, **16**, 6127–6145.
- Ducret, A., Valignat, M.P., Mouhamar, F., Mignot, T. and Theodoly, O. (2012) Wet-surface-enhanced ellipsometric contrast microscopy identifies slime as a major adhesion factor during bacterial surface motility. *Proceedings of the National Academy of Sciences of the United States of America*, **109**, 10036–10041.
- Ducret, A., Fleuchot, B., Bergam, P. and Mignot, T. (2013) Direct live imaging of cell–cell protein transfer by transient outer membrane fusion in *Myxococcus xanthus*. *eLife*, **2**, e00868.
- Dworkin, M. and Gibson, S.M. (1964) A system for studying microbial morphogenesis: rapid formation of microcysts in *Myxococcus xanthus*. *Science*, **146**, 243–244.
- Faure, L.M., Fiche, J.-B., Espinosa, L., Ducret, A., Anantharaman, V., Luciano, J., *et al.* (2016) The mechanism of force transmission at bacterial focal adhesion complexes. *Nature*, **539**, 530–535.
- Fink, J.M. and Zissler, J.F. (1989a) Characterization of lipopolysaccharide from *Myxococcus xanthus* by use of monoclonal antibodies. *Journal of Bacteriology*, **171**, 2028–2032.
- Fink, J.M. and Zissler, J.F. (1989b) Defects in motility and development of *Myxococcus xanthus* lipopolysaccharide mutants. *Journal of Bacteriology*, **171**, 2042–2048.

- Finn, R.D., Coghill, P., Eberhardt, R.Y., Eddy, S.R., Mistry, J., Mitchell, A.L., *et al.* (2016) The Pfam protein families database: towards a more sustainable future. *Nucleic Acids Research*, **44**, D279–D285.
- Furlong, S.E., Ford, A., Albarnez-Rodriguez, L. and Valvano, M.A. (2015) Topological analysis of the *Escherichia coli* WcaJ protein reveals a new conserved configuration for the polyisoprenyl-phosphate hexose-1-phosphate transferase family. *Scientific Reports*, **5**, 9178.
- Gill, J.S. and Dworkin, M. (1986) Cell surface antigens during submerged development of *Myxococcus xanthus* examined with monoclonal antibodies. *Journal of Bacteriology*, **168**, 505–511.
- Gloag, E.S., Turnbull, L., Javed, M.A., Wang, H., Gee, M.L., Wade, S.A. and Whitchurch, C.B. (2016) Stigmergy co-ordinates multicellular collective behaviours during *Myxococcus xanthus* surface migration. *Scientific Reports*, **6**, 26005.
- Gong, Y., Zhang, Z., Liu, Y., Zhou, X.-W., Anwar, M.N., Li, Z.-S., *et al.* (2018) A nuclease-toxin and immunity system for kin discrimination in *Myxococcus xanthus*. *Environmental Microbiology*, **20**, 2552–2567.
- Greenfield, L.K. and Whitfield, C. (2012) Synthesis of lipopolysaccharide O-antigens by ABC transporter-dependent pathways. *Carbohydrate Research*, **356**, 12–24.
- Greenfield, L.K., Richards, M.R., Li, J., Wakarchuk, W.W., Lowary, T.L. and Whitfield, C. (2012a) Biosynthesis of the polymannose lipopolysaccharide O-antigens from *Escherichia coli* serotypes O8 and O9a requires a unique combination of single- and multiple-active site mannosyltransferases. *Journal of Biological Chemistry*, **287**, 35078–35091.
- Greenfield, L.K., Richards, M.R., Vinogradov, E., Wakarchuk, W.W., Lowary, T.L. and Whitfield, C. (2012b) Domain organization of the polymerizing mannosyltransferases involved in synthesis of the *Escherichia coli* O8 and O9a lipopolysaccharide O-antigens. *Journal of Biological Chemistry*, **287**, 38135–38149.
- Guo, D., Bowden, M.G., Pershad, R. and Kaplan, H.B. (1996) The *Myxococcus xanthus* *rfbABC* operon encodes an ATP-binding cassette transporter homolog required for O-antigen biosynthesis and multicellular development. *Journal of Bacteriology*, **178**, 1631–1639.
- Hodgkin, J. and Kaiser, D. (1977) Cell-to-cell stimulation of movement in nonmotile mutants of *Myxococcus*. *Proceedings of the National Academy of Sciences of the United States of America*, **74**, 2938–2942.
- Hodgkin, J. and Kaiser, D. (1979) Genetics of gliding motility in *Myxococcus xanthus* (Myxobacteriales) – two gene systems control movement. *Molecular and General Genetics*, **171**, 177–191.
- Hoffmann, H. (2015) violin.m – Simple Violin Plot Using Matlab Default Kernel Density Estimation. Katzenburgweg 5, Germany: INRES (University of Bonn).
- Holkenbrink, C., Hoiczky, E., Kahnt, J. and Higgs, P.I. (2014) Synthesis and assembly of a novel glycan layer in *Myxococcus xanthus* spores. *Journal of Biological Chemistry*, **289**, 32364–32378.
- Hu, W., Hossain, M., Lux, R., Wang, J., Yang, Z., Li, Y., *et al.* (2011) Exopolysaccharide-independent social motility of *Myxococcus xanthus*. *PLoS ONE*, **6**, e16102.
- Inouye, M., Inouye, S. and Zusman, D.R. (1979a) Biosynthesis and self-assembly of protein S, a development specific protein of *Myxococcus xanthus*. *Proceedings of the National Academy of Sciences of the United States of America*, **76**, 209–213.
- Inouye, M., Inouye, S. and Zusman, D.R. (1979b) Gene expression during development of *Myxococcus xanthus*: pattern of protein synthesis. *Developmental Biology*, **68**, 579–591.
- Islam, S.T., Taylor, V.L., Qi, M. and Lam, J.S. (2010) Membrane topology mapping of the O-antigen flip-pase (Wzx), polymerase (Wzy), and ligase (WaaL) from *Pseudomonas aeruginosa* PAO1 reveals novel domain architectures. *mBio*, **1**, e00189–00110.
- Jakobczak, B., Keilberg, D., Wuichet, K. and Søgaard-Andersen, L. (2015) Contact- and protein transfer-dependent stimulation of assembly of the gliding motility machinery in *Myxococcus xanthus*. *PLoS Genetics*, **11**, e1005341.
- James, D.B.A., Gupta, K., Hauser, J.R. and Yother, J. (2013) Biochemical activities of *Streptococcus pneumoniae* serotype 2 capsular glycosyltransferases and significance of suppressor mutations affecting the initiating glycosyltransferase Cps2E. *Journal of Bacteriology*, **195**, 5469–5478.
- Johns, S.J. TOPO2, Transmembrane protein display software, <http://www.sacs.ucsf.edu/TOPO2/>
- Jorgenson, M.A. and Young, K.D. (2016) Interrupting biosynthesis of O Antigen or the lipopolysaccharide core produces morphological defects in *Escherichia coli* by sequestering undecaprenyl phosphate. *Journal of Bacteriology*, **198**, 3070–3079.
- Julien, B., Kaiser, A.D. and Garza, A. (2000) Spatial control of cell differentiation in *Myxococcus xanthus*. *Proceedings of the National Academy of Sciences of the United States of America*, **97**, 9098–9103.
- Kaiser, D. (1979) Social gliding is correlated with the presence of pili in *Myxococcus xanthus*. *Proceedings of the National Academy of Sciences of the United States of America*, **76**, 5952–5956.
- Kalynych, S., Morona, R. and Cygler, M. (2014) Progress in understanding the assembly process of bacterial O-antigen. *FEMS Microbiology Reviews*, **38**, 1048–1065.
- Kanehisa, M. and Goto, S. (2000) KEGG: kyoto encyclopedia of genes and genomes. *Nucleic Acids Research*, **28**, 27–30.
- Kim, S.K. and Kaiser, D. (1990a) C-factor: a cell-cell signaling protein required for fruiting body morphogenesis of *M. xanthus*. *Cell*, **61**, 19–26.
- Kim, S.K. and Kaiser, D. (1990b) Cell alignment required in differentiation of *Myxococcus xanthus*. *Science*, **249**, 926–928.
- Konovalova, A., Petters, T. and Søgaard-Andersen, L. (2010) Extracellular biology of *Myxococcus xanthus*. *FEMS Microbiology Reviews*, **34**, 89–106.
- Koontz, L. (2014) TCA precipitation. *Methods in Enzymology*, **541**, 3–10.
- Kos, V., Cuthbertson, L. and Whitfield, C. (2009) The *Klebsiella pneumoniae* O2a antigen defines a second mechanism for O antigen ATP-binding cassette transporters. *Journal of Biological Chemistry*, **284**, 2947–2956.
- Kottel, R.H., Bacon, K., Clutter, D. and White, D. (1975) Coats from *Myxococcus xanthus*: characterization and

- synthesis during myxospore differentiation. *Journal of Bacteriology*, **124**, 550–557.
- Li, Y., Sun, H., Ma, X., Lu, A., Lux, R., Zusman, D., et al. (2003) Extracellular polysaccharides mediate pilus retraction during social motility of *Myxococcus xanthus*. *Proceedings of the National Academy of Sciences of the United States of America*, **100**, 5443–5448.
- Licking, E., Gorski, L. and Kaiser, D. (2000) A common step for changing cell shape in fruiting body and starvation-independent sporulation in *Myxococcus xanthus*. *Journal of Bacteriology*, **182**, 3553–3558.
- Lombard, V., Golaconda Ramulu, H., Drula, E., Coutinho, P.M. and Henrissat, B. (2014) The Carbohydrate-active enzymes database (CAZY) in 2013. *Nucleic Acids Research*, **42**, D490–D495.
- Lu, A., Cho, K., Black, W.P., Duan, X.Y., Lux, R., Yang, Z., et al. (2005) Exopolysaccharide biosynthesis genes required for social motility in *Myxococcus xanthus*. *Molecular Microbiology*, **55**, 206–220.
- Lukose, V., Walvoort, M.T. and Imperiali, B. (2017) Bacterial phosphoglycosyl transferases: initiators of glycan biosynthesis at the membrane interface. *Glycobiology*, **27**, 820–833.
- Macleán, L., Perry, M.B., Nossova, L., Kaplan, H. and Vinogradov, E. (2007) The structure of the carbohydrate backbone of the LPS from *Myxococcus xanthus* strain DK1622. *Carbohydrate Research*, **342**, 2474–2480.
- Manat, G., El Ghachi, M., Auger, R., Baouche, K., Olatunji, S., Kerff, F., et al. (2015) Membrane topology and biochemical characterization of the *Escherichia coli* BacA undecaprenyl-pyrophosphate phosphatase. *PLoS ONE*, **10**, e0142870.
- Marchler-Bauer, A., Bo, Y., Han, L., He, J., Lanczycki, C.J., Lu, S., et al. (2017) CDD/SPARCLE: functional classification of proteins via subfamily domain architectures. *Nucleic Acids Research*, **45**, D200–D203.
- Marolda, C.L., Vicarioli, J. and Valvano, M.A. (2004) Wzx proteins involved in biosynthesis of O antigen function in association with the first sugar of the O-specific lipopolysaccharide subunit. *Microbiology*, **150**, 4095–4105.
- Marolda, C.L., Lahiry, P., Vines, E., Saldias, S. and Valvano, M.A. (2006) Micromethods for the characterization of lipid A-core and O-antigen lipopolysaccharide. *Methods in Molecular Biology*, **347**, 237–252.
- McCleary, W.R., Esmón, B. and Zusman, D.R. (1991) *Myxococcus xanthus* protein C is a major spore surface protein. *Journal of Bacteriology*, **173**, 2141–2145.
- Müller, F.D., Treuner-Lange, A., Heider, J., Huntley, S.M. and Higgs, P.I. (2010) Global transcriptome analysis of spore formation in *Myxococcus xanthus* reveals a locus necessary for cell differentiation. *BMC Genomics*, **11**, 264.
- Müller, F.D., Schink, C.W., Hoiczky, E., Cserti, E. and Higgs, P.I. (2012) Spore formation in *Myxococcus xanthus* is tied to cytoskeleton functions and polysaccharide spore coat deposition. *Molecular Microbiology*, **83**, 486–505.
- Nan, B., Bandaria, J.N., Moghtaderi, A., Sun, I.-H., Yildiz, A. and Zusman, D.R. (2013) Flagella stator homologs function as motors for myxobacterial gliding motility by moving in helical trajectories. *Proceedings of the National Academy of Sciences of the United States of America*, **110**, E1508–E1513.
- Nudleman, E., Wall, D. and Kaiser, D. (2005) Cell-to-cell transfer of bacterial outer membrane lipoproteins. *Science*, **309**, 125–127.
- Nudleman, E., Wall, D. and Kaiser, D. (2006) Polar assembly of the type IV pilus secretin in *Myxococcus xanthus*. *Molecular Microbiology*, **60**, 16–29.
- Okuda, S., Sherman, D.J., Silhavy, T.J., Ruiz, N. and Kahne, D. (2016) Lipopolysaccharide transport and assembly at the outer membrane: the PEZ model. *Nature Reviews Microbiology*, **14**, 337–345.
- Otani, M., Kozuka, S., Xu, C., Umezawa, C., Sano, K. and Inouye, S. (1998) Protein W, a spore-specific protein in *Myxococcus xanthus*, formation of a large electron-dense particle in a spore. *Molecular Microbiology*, **30**, 57–66.
- Paintdakhi, A., Parry, B., Campos, M., Irnov, I., Elf, J., Surovtsev, I., et al. (2016) Oufiti: an integrated software package for high-accuracy, high-throughput quantitative microscopy analysis. *Molecular Microbiology*, **99**, 767–777.
- Pan, Y., Ruan, X., Valvano, M.A. and Konermann, L. (2012) Validation of membrane protein topology models by oxidative labeling and mass spectrometry. *Journal of The American Society for Mass Spectrometry*, **23**, 889–898.
- Patel, K.B., Furlong, S.E. and Valvano, M.A. (2010) Functional analysis of the C-terminal domain of the WbaP protein that mediates initiation of O antigen synthesis in *Salmonella enterica*. *Glycobiology*, **20**, 1389–1401.
- Patel, K.B., Toh, E., Fernandez, X.B., Hanuszkiewicz, A., Hardy, G.G., Brun, Y.V., et al. (2012) Functional characterization of UDP-glucose:undecaprenyl-phosphate glucose-1-phosphate transferases of *Escherichia coli* and *Caulobacter crescentus*. *Journal of Bacteriology*, **194**, 2646–2657.
- Pathak, D.T., Wei, X., Bucuvalas, A., Haft, D.H., Gerloff, D.L. and Wall, D. (2012) Cell contact-dependent outer membrane exchange in *Myxobacteria*: genetic determinants and mechanism. *PLoS Genetics*, **8**, e1002626.
- Perez, J.M., McGarry, M.A., Marolda, C.L. and Valvano, M.A. (2008) Functional analysis of the large periplasmic loop of the *Escherichia coli* K-12 WaaL O-antigen ligase. *Molecular Microbiology*, **70**, 1424–1440.
- Raetz, C.R. and Whitfield, C. (2002) Lipopolysaccharide endotoxins. *Annual Review of Biochemistry*, **71**, 635–700.
- Reeves, P.R., Hobbs, M., Valvano, M.A., Skurnik, M., Whitfield, C., Coplin, D., et al. (1996) Bacterial polysaccharide synthesis and gene nomenclature. *Trends in Microbiology*, **4**, 495–503.
- Ruan, X., Loyola, D.E., Marolda, C.L., Perez-Donoso, J.M. and Valvano, M.A. (2012) The WaaL O-antigen lipopolysaccharide ligase has features in common with metal ion-independent inverting glycosyltransferases. *Glycobiology*, **22**, 288–299.
- Ruan, X., Monjaras Feria, J., Hamad, M. and Valvano, M.A. (2018) *Escherichia coli* and *Pseudomonas aeruginosa* lipopolysaccharide O-antigen ligases share similar membrane topology and biochemical properties. *Molecular Microbiology*, **110**, 95–113.
- Ruiz, N., Kahne, D. and Silhavy, T.J. (2009) Transport of lipopolysaccharide across the cell envelope: the long road of discovery. *Nature Reviews Microbiology*, **7**, 677–683.

- Saldías, M.S., Patel, K., Marolda, C.L., Bittner, M., Contreras, I. and Valvano, M.A. (2008) Distinct functional domains of the *Salmonella enterica* WbaP transferase that is involved in the initiation reaction for synthesis of the O antigen subunit. *Microbiology*, **154**, 440–453.
- Sambrook, J. and Russell, D.W. (2001) *Molecular Cloning: A Laboratory Manual*. Cold Spring Harbor, NY: Cold Spring Harbor Laboratory Press.
- Schäffer, C., Wugeditsch, T., Messner, P. and Whitfield, C. (2002) Functional expression of enterobacterial O-polysaccharide biosynthesis enzymes in *Bacillus subtilis*. *Applied and Environment Microbiology*, **68**, 4722–4730.
- Schild, S., Lamprecht, A.K. and Reidl, J. (2005) Molecular and functional characterization of O antigen transfer in *Vibrio cholerae*. *Journal of Biological Chemistry*, **280**, 25936–25947.
- Schindelin, J., Arganda-Carreras, I., Frise, E., Kaynig, V., Longair, M., Pietzsch, T., et al. (2012) Fiji: an open-source platform for biological-image analysis. *Nature Methods*, **9**, 676–682.
- Schumacher, D. and Søgaard-Andersen, L. (2017) Regulation of cell polarity in motility and cell division in *Myxococcus xanthus*. *Annual Review of Microbiology*, **71**, 61–78.
- Shi, W. and Zusman, D.R. (1993) The two motility systems of *Myxococcus xanthus* show different selective advantages on various surfaces. *Proceedings of the National Academy of Sciences of the United States of America*, **90**, 3378–3382.
- Shi, X., Wegener-Feldbrugge, S., Huntley, S., Hamann, N., Hedderich, R. and Søgaard-Andersen, L. (2008) Bioinformatics and experimental analysis of proteins of two-component systems in *Myxococcus xanthus*. *Journal of Bacteriology*, **190**, 613–624.
- Shimkets, L.J. (1986) Role of cell cohesion in *Myxococcus xanthus* fruiting body formation. *Journal of Bacteriology*, **166**, 842–848.
- Skotnicka, D., Petters, T., Heering, J., Hoppert, M., Kaever, V. and Søgaard-Andersen, L. (2015) c-di-GMP regulates type IV pili-dependent-motility in *Myxococcus xanthus*. *Journal of Bacteriology*, **198**, 77–90.
- Sonnhammer, E.L., von Heijne, G. and Krogh, A. (1998) A hidden Markov model for predicting transmembrane helices in protein sequences. *Proceedings of International Conference on Intelligent Systems for Molecular Biology*, **6**, 175–182.
- Steiner, K., Novotny, R., Patel, K., Vinogradov, E., Whitfield, C., Valvano, M.A., et al. (2007) Functional characterization of the initiation enzyme of S-layer glycoprotein glycan biosynthesis in *Geobacillus stearothermophilus* NRS 2004/3a. *Journal of Bacteriology*, **189**, 2590–2598.
- Sun, H., Zusman, D.R. and Shi, W. (2000) Type IV pilus of *Myxococcus xanthus* is a motility apparatus controlled by the *frz* chemosensory system. *Current Biology*, **10**, 1143–1146.
- Sun, M., Wartel, M., Cascales, E., Shaevitz, J.W. and Mignot, T. (2011) Motor-driven intracellular transport powers bacterial gliding motility. *Proceedings of the National Academy of Sciences of the United States of America*, **108**, 7559–7564.
- Tatar, L.D., Marolda, C.L., Polischuk, A.N., van Leeuwen, D. and Valvano, M.A. (2007) An *Escherichia coli* undecaprenyl-pyrophosphate phosphatase implicated in undecaprenyl phosphate recycling. *Microbiology*, **153**, 2518–2529.
- The-UniProt-Consortium. (2019) UniProt: a worldwide hub of protein knowledge. *Nucleic Acids Research*, **47**, D506–D515.
- Troselj, V., Treuner-Lange, A., Søgaard-Andersen, L. and Wall, D. (2018) Physiological heterogeneity triggers sibling conflict mediated by the type VI secretion system in an aggregative multicellular bacterium. *mBio*, **9**, e01645–01617.
- Valvano, M.A. (2008) Undecaprenyl phosphate recycling comes out of age. *Molecular Microbiology*, **67**, 232–235.
- Valvano, M.A. (2011) Common themes in glycoconjugate assembly using the biogenesis of O-antigen lipopolysaccharide as a model system. *Biochemistry (Mosc)*, **76**, 729–735.
- Vassallo, C., Pathak, D.T., Cao, P., Zuckerman, D.M., Hoiczkyk, E. and Wall, D. (2015) Cell rejuvenation and social behaviors promoted by LPS exchange in myxobacteria. *Proceedings of the National Academy of Sciences of the United States of America*, **112**, E2939–E2946.
- Vassallo, C.N., Cao, P., Conklin, A., Finkelstein, H., Hayes, C.S. and Wall, D. (2017) Infectious polymorphic toxins delivered by outer membrane exchange discriminate kin in myxobacteria. *eLife*, **6**, e29397.
- Wang, L., Liu, D. and Reeves, P.R. (1996) C-terminal half of *Salmonella enterica* WbaP (RfbP) is the galactosyl-1-phosphate transferase domain catalyzing the first step of O-antigen synthesis. *Journal of Bacteriology*, **178**, 2598–2604.
- Wei, X., Pathak, D.T. and Wall, D. (2011) Heterologous protein transfer within structured myxobacteria biofilms. *Molecular Microbiology*, **81**, 315–326.
- Whitfield, C. and Trent, M.S. (2014) Biosynthesis and export of bacterial lipopolysaccharides. *Annual Review of Biochemistry*, **83**, 99–128.
- Wu, S.S. and Kaiser, D. (1996) Markerless deletions of *pil* genes in *Myxococcus xanthus* generated by counterselection with the *Bacillus subtilis* *sacB* gene. *Journal of Bacteriology*, **178**, 5817–5821.
- Wu, S.S. and Kaiser, D. (1997) Regulation of expression of the *pilA* gene in *Myxococcus xanthus*. *Journal of Bacteriology*, **179**, 7748–7758.
- Xayarath, B. and Yother, J. (2007) Mutations blocking side chain assembly, polymerization, or transport of a Wzy-dependent *Streptococcus pneumoniae* capsule are lethal in the absence of suppressor mutations and can affect polymer transfer to the cell wall. *Journal of Bacteriology*, **189**, 3369–3381.
- Yang, Z., Geng, Y., Xu, D., Kaplan, H.B. and Shi, W. (1998) A new set of chemotaxis homologues is essential for *Myxococcus xanthus* social motility. *Molecular Microbiology*, **30**, 1123–1130.
- Yang, Z., Guo, D., Bowden, M.G., Sun, H., Tong, L., Li, Z., et al. (2000) The *Myxococcus xanthus* *wbgB* gene encodes a glycosyltransferase homologue required for

- lipopolysaccharide O-antigen biosynthesis. *Archives of Microbiology*, **174**, 399–405.
- Youderian, P. and Hartzell, P.L. (2006) Transposon insertions of magellan-4 that impair social gliding motility in *Myxococcus xanthus*. *Genetics*, **172**, 1397–1410.
- Yu, R. and Kaiser, D. (2007) Gliding motility and polarized slime secretion. *Molecular Microbiology*, **63**, 454–467.
- Zhang, Y., Ducret, A., Shaevitz, J. and Mignot, T. (2012) From individual cell motility to collective behaviors:

insights from a prokaryote, *Myxococcus xanthus*. *FEMS Microbiology Reviews*, **36**, 149–164.

Supporting Information

Additional supporting information may be found online in the Supporting Information section at the end of the article.

3.1.1 Supplementary material

Supplementary Figures & Legends

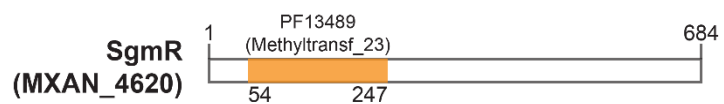


Figure S1. Bioinformatic analysis of SgmR (MXAN_4620). Methyltransferase domain is indicated.

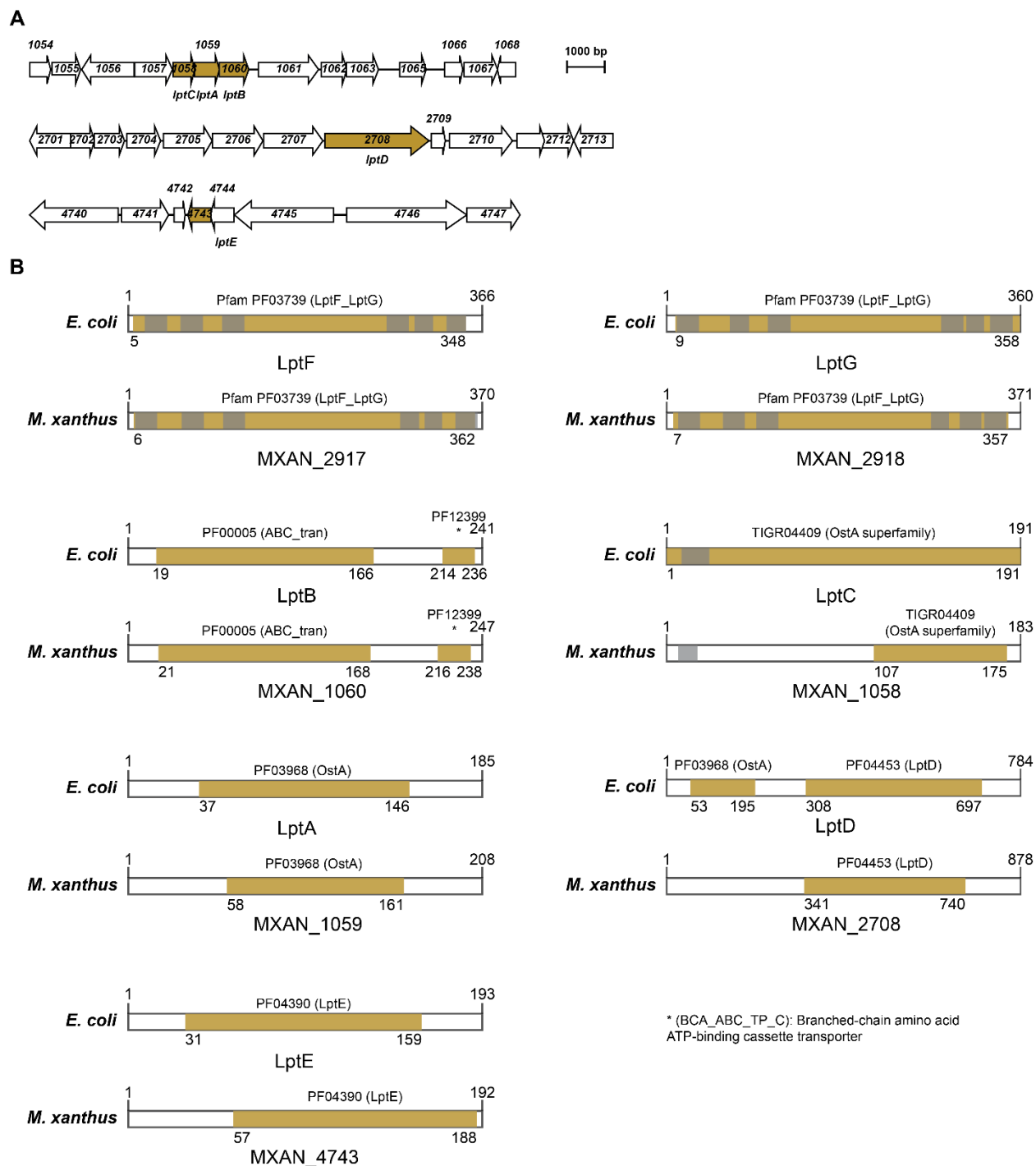


Figure S2. Bioinformatic analysis of Lpt homologs in *M. xanthus*. (A) *lpt* genes in *M. xanthus*. *lpt* genes are drawn to scale by brown arrows with gene name and MXAN number indicated. (B) Domain and TMH characterization of *M. xanthus* Lpt homologs in comparison to Lpt proteins of *E. coli*. Domains (brown) and TMHs (grey) are indicated. Using KEGG orthology, we identified LptF_{Mx} (MXAN_2917) and LptG_{Mx} (MXAN_2918) candidates encoded in LPS cluster I (Fig. 1A). Similar to the *E. coli* proteins, LptF_{Mx} and LptG_{Mx} are predicted to have six TMH and a large periplasmic domain (Pfam domain PF03739) (Okuda *et al.*, 2016, Ruiz *et al.*, 2009). An LptB_{Mx} (MXAN_1060) candidate was

identified by BlastP. Similar to LptB_{Ec} (Okuda *et al.*, 2016), LptB_{Mx} contains the domain characteristic of the ATPase subunit of ABC transporters (Pfam domain 00005), as well as a conserved C-terminal domain (Pfam domain 12399). LptC, LptA and LptD candidates were identified using KEGG orthology. Analysis of LptC_{Ec} shows one TMH and an OstA superfamily domain (TIGR04409), which we also identified in the C-terminal region of LptC_{Mx} (MXAN_1058). Similarly to LptA_{Ec}, LptA_{Mx} (MXAN_1059) contains a single OstA-like domain (Pfam PF03968). LptD_{Mx} (MXAN_2708) contains the LPS transport system D domain (Pfam PF04453), as is the case for LptD_{Ec}. LptE was identified based on searches for proteins with an LptE domain using the KEGG database. LptE_{Mx} (MXAN_4743) contains a single LptE domain (Pfam 04390), as in LptE_{Ec}.

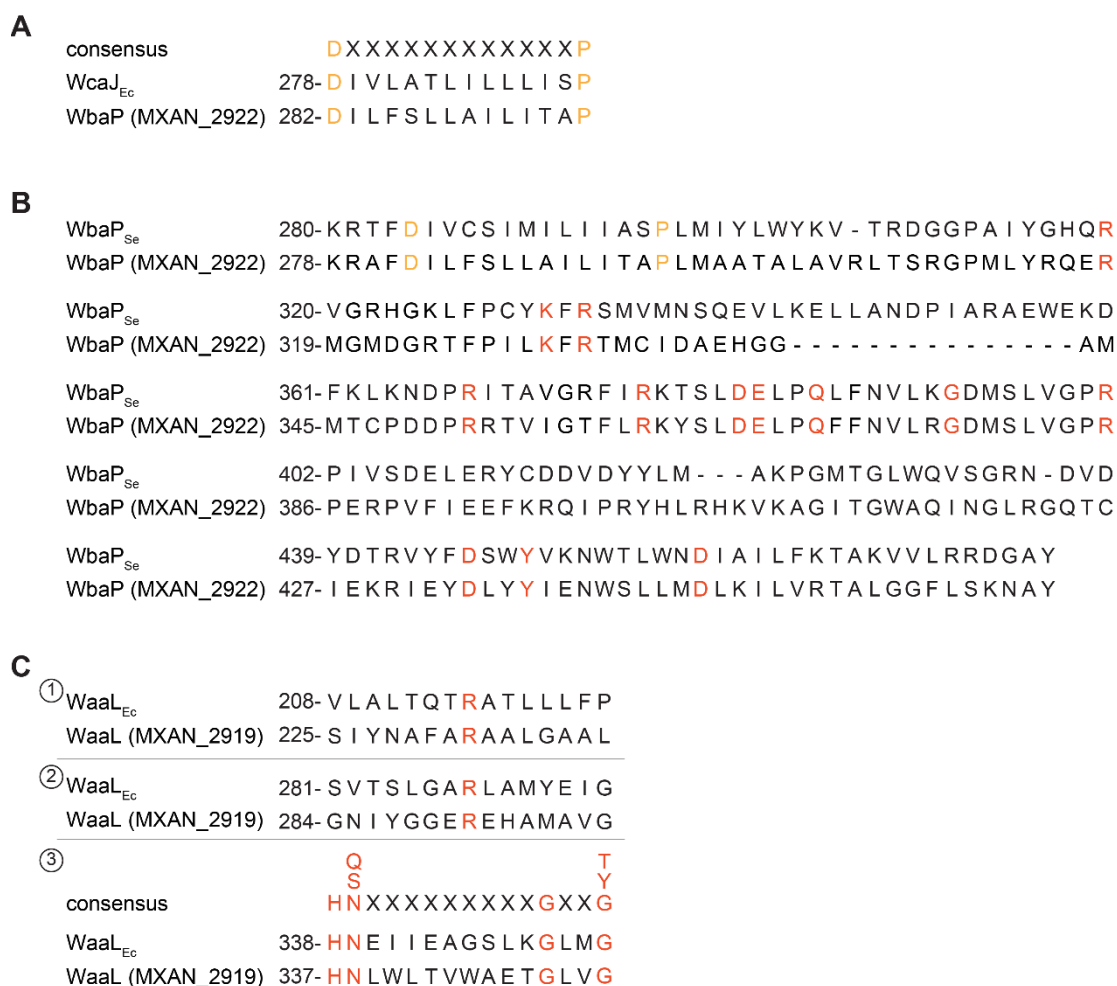


Figure S3. Sequence analysis of WbaP_{Mx} (MXAN_2922) and WaaL_{Mx} (MXAN_2919). (A) Sequence alignment of the region in WbaP_{Mx} (MXAN_2922) and WcaJ_{Ec} that contains the conserved Pro residue (orange) in the motif DX₁₂P as well as the conserved Asp residue (orange). (B) Sequence alignment of the C-terminal region of WbaP_{Mx} (MXAN_2922) and WbaP_{Se}. Conserved amino acids essential for catalytic activity are marked in red. (C) Sequence alignment of the three regions in WaaL_{Mx} (MXAN_2919) and WaaL_{Ec} containing conserved amino acids essential for catalytic activity (red).

Supplementary Experimental Procedures

Plasmid construction. All oligonucleotides used are listed in Table S2. All constructed plasmids were verified by DNA sequencing. Plasmid pMP062 (in-frame deletion of *MXAN_2919*): up- and downstream fragments were amplified using genomic DNA from *M. xanthus* DK1622 as a template and primer pairs 2919_A/2919_B and 2919_C/2919_D, respectively, as described in (Shi *et al.*, 2008). To generate the AD fragment, an overlapping PCR was performed using the AB and CD fragments as a DNA template and the primer pair 2919_A/2919_D. The AD fragment was digested with KpnI/XbaI and cloned into pBJ114.

Plasmids pMP065, pMP071 and pMP099 were generated in a similar way, as follows.

Plasmid pMP065 (in-frame deletion of *wzm*): up- and downstream fragments were amplified using genomic DNA from *M. xanthus* DK1622 as a template and the primer pair *wzm_A/wzm_B* and *wzm_C/wzm_D*, respectively. To generate the AD fragment, an overlapping PCR was performed using the AB and CD fragments as a DNA template and the primer pair *wzm_A/wzm_D*. The AD fragment was digested with KpnI/XbaI and cloned into pBJ114.

Plasmid pMP071 (in-frame deletion of *MXAN_2922*): up- and downstream fragments were amplified using genomic DNA from *M. xanthus* DK1622 as a template and the primers 2922_A/2922_B and 2922_C/2922_D respectively. To generate the AD fragment, an overlapping PCR using the AB and CD fragments as a DNA template and the primer pair 2922_A/2922_D was performed. The AD fragment was digested with KpnI/XbaI and cloned into pBJ114.

Plasmid pMP099 (in-frame deletion of *MXAN_2922*): up- and downstream fragments were amplified using genomic DNA from *M. xanthus* DK1622 as a template and the primers *exoE_A/exoE_B* and *exoE_C/ exoE_D* respectively. To generate the AD fragment, an overlapping PCR using the AB and CD fragments as a DNA template and the primer pair *exoE_A/ exoE_D* was performed. The AD fragment was digested with KpnI/XbaI and cloned into pBJ114.

Plasmid pJJ7 (expression of P_{nat} *MXAN_2922* from the *attB* site): P_{nat} *MXAN_2922* was amplified with the primer combination 2922_Pnat_300bp_fw/ 2922_rev and genomic DNA from *M. xanthus* DK1622 as a template. The fragment was digested with KpnI/XbaI and cloned into pSWU30.

pJJ9 (expression of P_{nat} *wzm* from the *attB* site): P_{nat} *wzm* was amplified with the primer combination *wzm_Pnat_202bp_fw/ wzm_rev* and genomic DNA from *M. xanthus* DK1622 as a template. The fragment was digested with KpnI/XbaI and cloned into pSWU30.

pJJ11 (expression of P_{nat} *MXAN_2919* from the *attB* site): the promoter region of *MXAN_2919* and *MXAN_2919* were separately amplified with 2914_Promoter_201bp_fw/2914_Promoter_rev and 2919_fw/2919_rev respectively by using genomic DNA from *M. xanthus* DK1622 as a template. An overlapping PCR with both fragments as a DNA template and the primer pair 2914_Promoter_201bp_fw/2919_rev gave the P_{nat} *MXAN_2919* fragment that was digested with KpnI/HindIII and cloned into pSWU30.

pMP139 (expression of *MXAN_2922* under the control of an arabinose promoter): *MXAN_2922* was amplified with the primer combination 2922_fw/ 2922_rev2 and genomic DNA from *M. xanthus* DK1622 as a template. The fragment was digested with XbaI/HindIII and cloned into pBADNTF.

Table S1. Analysis of LPS gene cluster I and II

Locus tag MXAN	Gene name (new gene name)	(Putative) function of encoded protein	Reference
4606		Carbohydrate-binding protein	
4607		Hypothetical protein	
4608		Hypothetical protein	
4609		Drug resistance transporter, EmrB/QacA family	
4610	<i>rbcC</i>	dTDP-4-dehydrorhamnose 3,5-epimerase	
4611	<i>rbcA</i>	Glucose-1-phosphate thymidyltransferase	
4612		dTDP-4-dehydrorhamnose reductase	
4613	<i>sgmP, rbcB</i>	dTDP-glucose 4,6-dehydratase	(Youderian & Hartzell, 2006)
4614		Glycosyltransferase	
4615		Hypothetical protein	
4616	<i>sgmQ, pglF</i>	Glycosyltransferase	(Youderian & Hartzell, 2006, Yu & Kaiser, 2007)
4617		Glycosyltransferase	
4618		Putative membrane protein	
4619	<i>wbgB</i>	Glycosyltransferase	(Yang <i>et al.</i> , 2000a)
4620	<i>sgmR</i>	Methyltransferase domain containing protein	(Youderian & Hartzell, 2006)
4621	<i>wbgA</i>	Glycosyltransferase	(Guo <i>et al.</i> , 1996, Bowden & Kaplan, 1998)
4622	<i>wzt</i>	O-antigen ABC transporter	(Guo <i>et al.</i> , 1996, Bowden & Kaplan, 1998)
4623	<i>wzm</i>	O-antigen ABC transporter	(Guo <i>et al.</i> , 1996, Bowden & Kaplan, 1998)
4624		tRNA-Gly	
2913	<i>asgB</i>	DNA-binding protein	(Kuspa & Kaiser, 1989, Plamann <i>et al.</i> , 1994)
2914	<i>purH</i>	Phosphoribosyl-amino-imidazole-carboxamide formyltransferase	
2915		Hypothetical protein	
2916	<i>purD</i>	Phosphoribosylamine-glycine ligase	
2917	<i>lptF</i>	LPS export system permease protein	(Vassallo <i>et al.</i> , 2015)
2918	<i>lptG</i>	LPS export system permease protein	(Vassallo <i>et al.</i> , 2015)
2919	<i>pglJ, wzyC (waaL)</i>	Wzy_C domain containing protein New annotation: O-antigen ligase	(Yu & Kaiser, 2007, Vassallo <i>et al.</i> , 2015)
2920		Glycotransferase	
2921	<i>sgmJ, pglB</i>	Mannosyl-transferase	(Youderian & Hartzell, 2006, Yu & Kaiser, 2007)
2922	<i>sgmK</i>	Bacterial sugar transferase	(Youderian & Hartzell, 2006)

	<i>(wbaP)</i>	New annotation: polyisoprenyl-phosphate hexose-1-phosphate	
2923	<i>agmQ</i>	Peptidase	(Youderian <i>et al.</i> , 2003)

Table S2. Oligonucleotides used in this work¹

Primer name	Sequence 5'-3'	Brief description
2922_A (KpnI)	ATCGGGTACCGGATGCGTCGCTTCCGGCGC	For Δ MXAN_2922
2922_B	GCCGCCAGGTAGAAACGCTGGAGACG	For Δ MXAN_2922
2922_C	CGTTTCTACCTGGGCGGCTTCTGTGC	For Δ MXAN_2922
2922_D (XbaI)	ATCGTCTAGACACCGGTGACACGTGGCTGC	For Δ MXAN_2922
2922_E	CTGCCCGAAAATATTCGCTT	For Δ MXAN_2922
2922_F	AACACCACCAATCACACCAT	For Δ MXAN_2922
2922_G	GAGGGGATACCTCCCTGGAC	For Δ MXAN_2922
2922_H	CTTCAGGTCCATCAGCAGCG	For Δ MXAN_2922
2922_Pnat_300bp_fw (KpnI)	ATCGGGTACCTGATCAAAGTGCCATTCTTCGAG	For complementation fw
2922_rev (XbaI)	ATCGTCTAGATCAGTAGGCGTTCTTCGACA	For complementation rv
2922_fw + 1nt (XbaI)	ATCGTCTAGAGGTGTTTCAGTCGTCTCCAGCG	For protein expression under an arabinose inducible promoter.
2922_rev2 (HindIII)	ATCGAAGCTTTTCAGTAGGCGTTCTTCGACA	For protein expression under an arabinose inducible promoter.
2919_A (KpnI)	ATCGGGTACCACGTGTCCGTCTTCACGGTG	For Δ MXAN_2919
2919_B	CATCTCCAGGGACACGGTTCATGAG	For Δ MXAN_2919
2919_C	ACCGTGTCCCTGGAGATGGAAGGCGCG	For Δ MXAN_2919
2919_D (XbaI)	ATCGTCTAGAGAACGGTACGAGCTGCCAGC	For Δ MXAN_2919
2919_E	CTTCCTCCGGGGCGGCAGCG	For Δ MXAN_2919
2919_F	ACCCAGGCCGAGGCCGCGC	For Δ MXAN_2919
2919_G	CGCTGGACCTGCGCTGGCGC	For Δ MXAN_2919
2919_H	TCACTGCCCTCGCACAGCCC	For Δ MXAN_2919
2914_Promoter_201bp_fw (KpnI)	ATCGGGTACCTGAACCCGCGAGCGCATCCGCCA	For complementation, promoter fw
2914_Promoter_rev	CGCGGACACGTGTGGCCTCGGTGTGC	For complementation, promoter rv
2919_fw	GGCCACACGTGTCCGCGCTCATGGGA	For complementation fw
2919_rev (HindIII)	ATCGAAGCTTTTAGGGCGTGGGCCCGGGCG	For complementation rv
wzm_A (KpnI)	ATCGGGTACCTGCTCGTCTACCTGTCTGGT	For Δ wzm
wzm_B	GCGGCGGGACTGATACAGTTCACGGAC	For Δ wzm
wzm_C	CTGTATCAGTCCCGCCGGAAGAGTTC	For Δ wzm
wzm_D (XbaI)	ATCGTCTAGAGACGCTTGAAGTCCATCATC	For Δ wzm
wzm_E	CTACAACCTGGTGGGCCAGG	For Δ wzm
wzm_F	CCAGGACGATGGTCTTCCCC	For Δ wzm
wzm_G	CGGGGCTTGCTCATCAGCCT	For Δ wzm
wzm_H	GATGGACGAGGCCGCCACA	For Δ wzm

wzm_Pnat_202bp_fw (KpnI)	ATCGGGTACCTGAAATTGAGGCCCTCTGGGAAG	For complementation fw
wzm_rev (XbaI)	ATCGTCTAGATCAGATGGACTCCGCGAACT	For complementation rv
exoE_A (KpnI)	ATATGGTACCATGCGCAACAAGATGGGCCT	For Δ exoE
exoE_B	GAGAAGCACAAAATAATGGTGAAAAAC	For Δ exoE
exoE_C	CATTATTTTGTGCTTCTCGGTCGTGGG	For Δ exoE
exoE_D (XbaI)	ATATTCTAGAGCACCGCTTCCATGAAGTCA	For Δ exoE
exoE_E	GGGCGGCGTGGCGGCCATGC	For Δ exoE
exoE_F	GCGCCCAGCAGCTCCCCGGA	For Δ exoE
exoE_G	GTTCTTCCTCGCCGAGAGTT	For Δ exoE
exoE_H	CACGGTGTGGAAGATGATTC	For Δ exoE

¹ Underlined sequences indicate restriction sites.

Table S3. *E. coli* and *S. enterica* proteins used for bioinformatics analyses

Protein	Organism	Accession number
Wzm-O8	<i>Escherichia coli</i>	WP_073533836.1
Wzt-O8	<i>Escherichia coli</i>	WP_057108493.1
WcaJ	<i>Escherichia coli</i> str. K-12 substr. MG1655	NP_416551.1
WaaL	<i>Escherichia coli</i> str. K-12 substr. MG1655	NP_418079.1
WbaP	<i>Salmonella enterica</i> subsp. enterica serovar Typhimurium str. LT2	NP_461027.1
LptA	<i>Escherichia coli</i> str. K-12 substr. MG1655	NP_417667.1
LptB	<i>Escherichia coli</i> str. K-12 substr. MG1655	NP_417668.1
LptC	<i>Escherichia coli</i> str. K-12 substr. MG1655	NP_417666.1
LptD	<i>Escherichia coli</i> str. K-12 substr. MG1655	NP_414596.1
LptE	<i>Escherichia coli</i> str. K-12 substr. MG1655	NP_415174.1
LptF	<i>Escherichia coli</i> str. K-12 substr. MG1655	NP_418682.1
LptG	<i>Escherichia coli</i> str. K-12 substr. MG1655	NP_418683.4

3.2 Identification of the Wzx flippase, Wzy polymerase and sugar-modifying enzymes for spore coat polysaccharide biosynthesis in *Myxococcus xanthus*

Pérez-Burgos, M., García-Romero, I., Valvano, M.A., & Søggaard-Andersen, L.

This chapter contains our advances in the identification of the spore coat polysaccharide biosynthesis components (Pérez-Burgos *et al.*, 2020). The article was reused with permission of the publisher. This part of the thesis is written in a manuscript style and was accepted in Molecular Microbiology in 2020. I contributed to this work by designing, performing and analyzing experiments, preparing the figures and the manuscript.

Specifically, I carried out all the experiments and analysis shown in Fig. 1-3, 4a-b, 5, 6, S1-S3 and S5. Heterologous experiments shown in Figs.4c-g and S4 were carried out by Dr. Inmaculada García Romero at the Wellcome-Wolfson Institute for Experimental Medicine (Queen's University Belfast) and I generated the plasmid expressing the *M. xanthus* PHPT homolog used for the heterologous experiments.

RESEARCH ARTICLE

Identification of the Wzx flippase, Wzy polymerase and sugar-modifying enzymes for spore coat polysaccharide biosynthesis in *Myxococcus xanthus*

María Pérez-Burgos¹ | Inmaculada García-Romero² | Miguel A. Valvano ² | Lotte Søgaaard Andersen ¹

¹Department of Ecophysiology, Max Planck Institute for Terrestrial Microbiology, Marburg, Germany

²Wellcome-Wolfson Institute for Experimental Medicine, Queen's University Belfast, Belfast, UK

Correspondence

Lotte Søgaaard-Andersen, Department of Ecophysiology, Max Planck Institute for Terrestrial Microbiology, Karl-von-Frisch Str. 10, Marburg 35043, Germany.
Email: sogaaard@mpi-marburg.mpg.de

Funding information

Deutsche Forschungsgemeinschaft, Grant/Award Number: SFB987 "Microbial Diversity in Environmental Signal Response; Max-Planck-Gesellschaft

Abstract

The rod-shaped cells of *Myxococcus xanthus*, a Gram-negative deltaproteobacterium, differentiate to environmentally resistant spores upon starvation or chemical stress. The environmental resistance depends on a spore coat polysaccharide that is synthesised by the ExoA-I proteins, some of which are part of a Wzx/Wzy-dependent pathway for polysaccharide synthesis and export; however, key components of this pathway have remained unidentified. Here, we identify and characterise two additional loci encoding proteins with homology to enzymes involved in polysaccharide synthesis and export, as well as sugar modification and show that six of the proteins encoded by these loci are essential for the formation of environmentally resistant spores. Our data support that MXAN_3260, renamed ExoM and MXAN_3026, renamed ExoJ, are the Wzx flippase and Wzy polymerase, respectively, responsible for translocation and polymerisation of the repeat unit of the spore coat polysaccharide. Moreover, we provide evidence that three glycosyltransferases (MXAN_3027/ExoK, MXAN_3262/ExoO and MXAN_3263/ExoP) and a polysaccharide deacetylase (MXAN_3259/ExoL) are important for formation of the intact spore coat, while ExoE is the polyisoprenyl-phosphate hexose-1-phosphate transferase responsible for initiating repeat unit synthesis, likely by transferring *N*-acetylgalactosamine-1-P to undecaprenyl-phosphate. Together, our data generate a more complete model of the Exo pathway for spore coat polysaccharide biosynthesis and export.

KEYWORDS

development, Exo, Nfs, O-antigen, polysaccharide, sporulation

1 | INTRODUCTION

Bacteria have evolved different strategies that enable their survival in response to environmental changes. Often these strategies

include alterations in gene expression, motility behaviour and/or metabolism without evident changes in cell morphology. However, as an alternative strategy, some bacteria undergo cellular differentiation resulting in the formation of cell types with altered

This is an open access article under the terms of the Creative Commons Attribution License, which permits use, distribution and reproduction in any medium, provided the original work is properly cited.

© 2020 The Authors. Molecular Microbiology published by John Wiley & Sons Ltd

morphology and novel characteristics. The best-studied examples of environmentally induced bacterial differentiation include spore formation in three phylogenetically widely separated species *Bacillus subtilis* (Tan & Ramamurthi, 2014), *Streptomyces coelicolor* (Flärdh & Buttner, 2009) and *Myxococcus xanthus* (Konovalova, Petters, & Søggaard-Andersen, 2010). While the spore formation process varies among these three species, the resulting spores have in common that they have a spore coat that confers resistance to environmental stress.

In *B. subtilis*, sporulation is initiated in response to starvation and depends on an unusual cell division event in which the division septum is placed asymmetrically close to a cell pole, resulting in the formation of a large mother cell and a smaller forespore. Next, the mother cell engulfs the forespore and lysis of the mother cell finally releases the mature spore (Tan & Ramamurthi, 2014). The spore envelope, partly generated by the mother cell and partly by the forespore, consists of a multilayered structure comprising from inside to outside: the cytoplasmic membrane, peptidoglycan (PG), an outer membrane, which is originally the cytoplasmic membrane of the mother cell and a proteinaceous coat (Driks & Eichenberger, 2016; McKenney, Driks, & Eichenberger, 2013). In response to nutrient depletion, *S. coelicolor* generate aerial hyphae, and here, multiple synchronous cell divisions give rise to the spores (Flärdh & Buttner, 2009; Sigle, Ladwig, Wohlleben, & Muth, 2015). The spore envelope of *S. coelicolor* is less well-studied but contains PG, a proteinaceous sheath made of chaplins and rodlins and spore wall teichoic acids (Flärdh & Buttner, 2009; Sigle et al., 2015). In the Gram-negative deltaproteobacterium *M. xanthus*, sporulation is also typically induced by starvation (Konovalova et al., 2010). However, in this bacterium, spores are formed independently of a cell division event and during the sporulation process, PG is replaced by a spore coat consisting mainly of polysaccharide. Here, we focus on the identification of proteins important for formation of the spore coat polysaccharide in *M. xanthus*.

In response to nutrient limitation, the rod-shaped cells of *M. xanthus* initiate a developmental programme resulting in the formation of multicellular spore-filled fruiting bodies (Konovalova et al., 2010). Fruiting bodies are formed as cells aggregate to form mounds during the first 24 hr of starvation. These mounds eventually convert into fruiting bodies as the rod-shaped cells that have accumulated inside the mounds begin to differentiate into spherical desiccation-, heat- and sonication-resistant spores. Spore morphogenesis occurs from ~24 hr and over the next 48 hr; in this process, the ~7 µm × ~0.5 µm rod-shaped cells are remodelled to become shorter and wider, ultimately forming spherical spores with a diameter of 1–2 µm (Dworkin & Gibson, 1964; Dworkin & Voelz, 1962). The PG cell wall is removed during this cellular remodelling process; in parallel, the spore coat is synthesised (Bui et al., 2009; Holkenbrink, Hoiczky, Kahnt, & Higgs, 2014; Müller, Schink, Hoiczky, Cserti, & Higgs, 2012). The spore coat consists of a thick layer of polysaccharide and several proteins outside of the outer membrane (OM) (Inouye, Inouye, & Zusman, 1979a; Leng, Zhu, Jin, & Mao, 2011; McCleary, Esmon, & Zusman, 1991). While

none of these proteins are essential for spore formation (Curtis, Atwood, Orlando, & Shimkets, 2007; Inouye, Inouye, & Zusman, 1979b; Komano, Furuichi, Teintze, Inouye, & Inouye, 1984; Lee et al., 2011; Leng et al., 2011), lack of the spore coat polysaccharide causes a sporulation defect (Holkenbrink et al., 2014; Müller et al., 2012). Because, only cells inside fruiting bodies differentiate to spores, starvation-dependent sporulation depends on the processes that are important for aggregation of cells into mounds including intracellular and intercellular signalling cascades, exopolysaccharide (EPS), lipopolysaccharide (LPS) and motility (Konovalova et al., 2010). Interestingly, spore formation can also occur independently of starvation, that is, in the presence of nutrients, in response to addition of glycerol (Dworkin & Gibson, 1964), other alcohols (e.g., isopropanol and ethylene glycol) (Sadler & Dworkin, 1966), dimethyl sulphoxide (Komano, Inouye, & Inouye, 1980) or β-lactams and D-amino acids (O'Connor & Zusman, 1997). Spore formation by this process, often referred to as chemically induced sporulation, occurs rapidly and synchronously within 4–8 hr; these spores are not identical to the spores formed in response to starvation since the spore coat polysaccharide is thinner and several proteins that are present in starvation-induced spores are absent (Downard & Zusman, 1985; Inouye et al., 1979a, 1979b; Komano et al., 1980; McCleary et al., 1991; Müller et al., 2012; Otani et al., 1998). However, the morphogenesis process associated with chemically induced sporulation involves a similar cellular remodelling process as for starvation-induced spores; the composition of the spore coat polysaccharide appears to be similar in both (Kottel, Bacon, Clutter, & White, 1975; Sutherland & Mackenzie, 1977) and formation of the spore coat polysaccharide is essential for formation of both types of spores (Licking, Gorski, & Kaiser, 2000; Müller et al., 2012).

Synthesis of the *M. xanthus* spore coat polysaccharide involves the ExoA-I proteins and the NfsA-H/AgIQRS systems (Holkenbrink et al., 2014; Licking et al., 2000; Müller et al., 2012; Ueki & Inouye, 2005; Wartel et al., 2013). The ExoA-I proteins, encoded by the *exoA-I* locus, were suggested to be components of an incomplete Wzx/Wzy-dependent pathway for polysaccharide synthesis and export (Table S1 and Figure 1a) (Holkenbrink et al., 2014; Müller et al., 2012; Schmid et al., 2015; Valvano, 2011, Valvano, Furlong, & Patel, 2011). The NfsA-H machinery, encoded by the *nfsA-H* locus, localise to the cell envelope (Holkenbrink et al., 2014) and is thought to be powered by the AgIQRS proteins in a proton motive force-dependent manner (Wartel et al., 2013). While these proteins are important for sporulation, they are not required for spore coat polysaccharide synthesis and export, but rather, function to modify the ExoA-I-produced polysaccharide to generate the rigid, stress-bearing spore coat (Holkenbrink et al., 2014; Müller et al., 2012; Wartel et al., 2013). This modification involves an alteration in spore coat polysaccharide chain length by an unknown mechanism (Holkenbrink et al., 2014).

In Wzx/Wzy pathways, the individual repeat units of the polysaccharide chain are synthesised in the cytoplasm on the lipid carrier undecaprenyl-phosphate (Und-P) in a process that is primed

by a polyisoprenyl-phosphate hexose-1-phosphate transferase (PHPT) or a polyisoprenyl-phosphate *N*-acetylhexosamine-1-phosphate transferase (PNPT). Next, specific glycosyltransferases (GTs) transfer the additional sugar building blocks from nucleotide-sugar donors to the Und-PP-sugar primer molecule to generate the Und-PP-repeat unit, which can be further modified by additional enzymes. Individual repeat units are transported across the inner membrane (IM) by the Wzx flippase, assembled into the

polysaccharide by the Wzy polymerase together with a polysaccharide co-polymerase (PCP) protein and transported across the OM by a Wza OM polysaccharide export (OPX) protein (Valvano et al., 2011). In the Exo pathway (Figure 1a), ExoE is a predicted PHPT responsible for priming synthesis of individual repeat units (Holkenbrink et al., 2014). The integral membrane protein ExoC together with the cytoplasmic ExoD tyrosine kinase form part of a bipartite Wzc protein of the PCP-2 family, in which ExoD (formerly

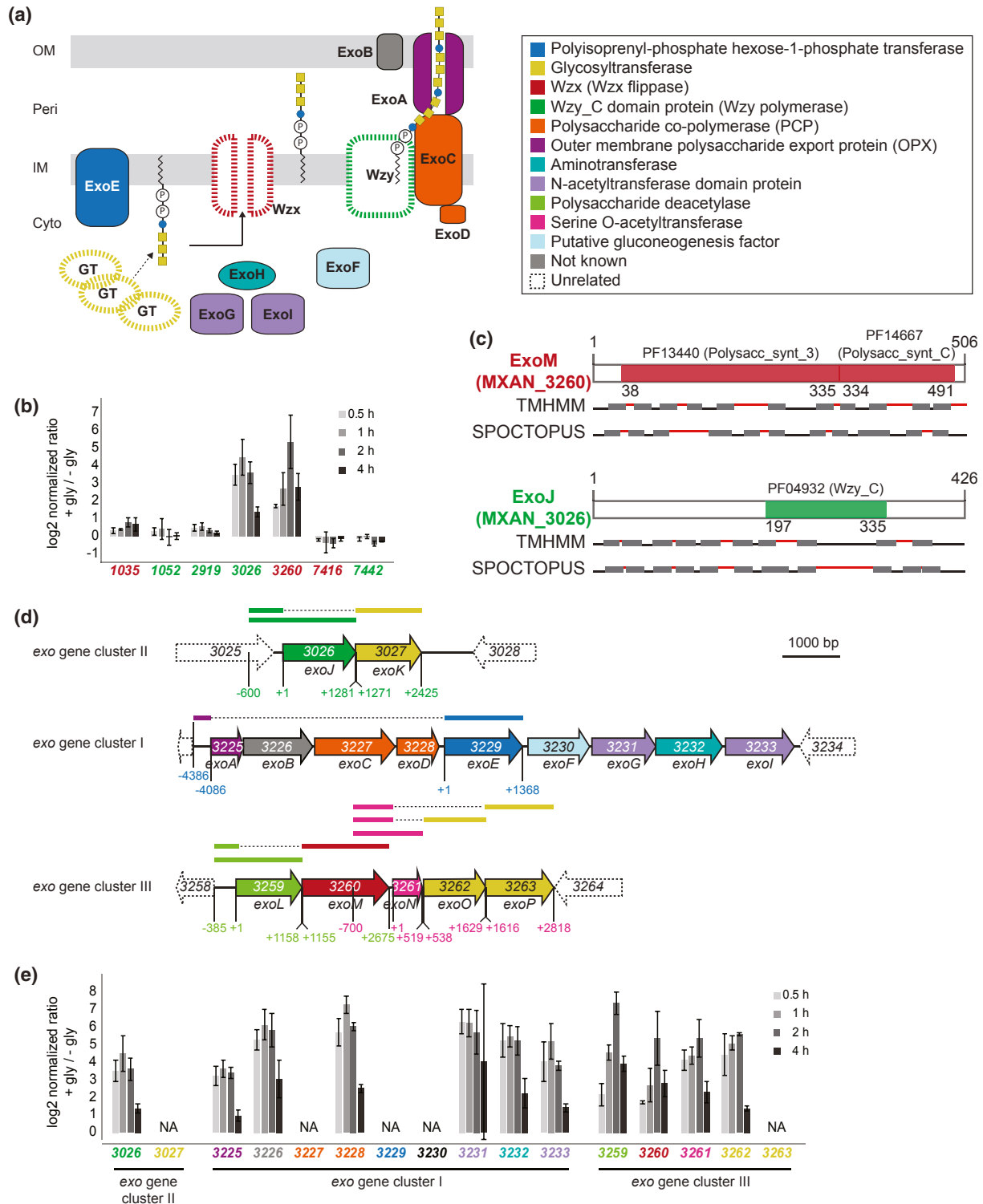


FIGURE 1 Model and expression analysis of gene clusters involved in spore coat polysaccharide synthesis. (a) Current model for spore coat polysaccharide synthesis in *M. xanthus* (see text). Proteins indicated in stippled lines have not been identified. Note that the number of GTs is unknown. Right panel, the colour code indicates predicted functions and is used throughout all figures. (b,e) Transcription pattern of indicated genes in response to chemical induction of sporulation with 0.5 M glycerol (+gly) based on data from (Müller et al., 2010) and shown as log₂-fold change compared to cells in the absence of glycerol (-gly). Note that the expression pattern of the genes in the *exo I* gene cluster were previously published (Müller et al., 2012, 2010) and are included for comparison. (c) Domain and TMH prediction of ExoM (MXAN_3260) and ExoJ (MXAN_3026), where domains are indicated in red and green, respectively. Grey rectangles indicate TMHs, red and black lines indicate periplasmic and cytoplasmic regions, respectively. Numbers indicate domain borders. (d) *exo* gene cluster I, II and III. Genes are drawn to scale and MXAN number and gene name are indicated (see also Table S1). Gene orientation is indicated by the direction of arrows. Note that the *exoJ-K*, *exoL-M* and *exoN-P* genes are likely in operons. The *exoA-I* genes form an operon (Müller et al., 2012). Gene coordinates are relative to the first nucleotide of the first gene in an operon and are indicated by the same gene colour, except for *exoE*, for which coordinates are indicated relative to its first nucleotide. DNA fragments comprising promoter and structural gene used in complementation experiments are indicated by a line above the corresponding region/s

BtkA (Kimura, Yamashita, Mori, Kitajima, & Takegawa, 2011)) is thought to participate in regulating ExoC activity (Holkenbrink et al., 2014; Kimura et al., 2011). ExoA (formerly FdgA [Ueki & Inouye, 2005]) is a homolog of Wza OPX proteins (Holkenbrink et al., 2014). ExoG and ExoI are *N*-acetyltransferase homologs that could be involved in modifying sugars before or after incorporation into the Und-PP-repeat units before export; ExoH is homologous to aminotransferases, ExoF is a putative gluconeogenesis factor and ExoB is an OM β -barrel protein of unknown function (Holkenbrink et al., 2014). All Exo proteins except for ExoF are essential for sporulation and synthesis of an intact spore coat polysaccharide (Holkenbrink et al., 2014; Licking et al., 2000; Ueki & Inouye, 2005). Generally, Wzc proteins of the PCP-2 family are components of Wzx/Wzy-dependent pathways for polysaccharide synthesis and export (Morona, Purins, Tocilj, Matte, & Cygler, 2009) supporting the notion that the ExoA-I proteins are part of a Wzx/Wzy pathway. Notably, such an Exo pathway is incomplete and lacks several key enzymes including the GTs that add sugars from nucleotide-sugar donors to the Und-PP-sugar primer molecule, the Wzx flippase and the Wzy polymerase (Figure 1a).

Here, we report the identification of two additional gene clusters encoding seven proteins that have homology to enzymes involved in polysaccharide synthesis and/or modification, and show that they are essential for sporulation and by implication for synthesis of the spore coat polysaccharide. We identify MXAN_3260 as the Wzx flippase (renamed ExoM) and MXAN_3026 (renamed to ExoJ) as the Wzy polymerase. We also identify five additional proteins important for spore coat polysaccharide synthesis including three GTs and determine the nucleotide sugar specificity of the ExoE priming enzyme, thus, generating a more complete model of the Exo pathway for spore coat polysaccharide biosynthesis.

2 | RESULTS

2.1 | Identification of two loci encoding a Wzx flippase, a Wzy polymerase and other proteins involved in polysaccharide synthesis

To identify missing components for spore coat polysaccharide biosynthesis, we used a two-pronged strategy. First, as polysaccharide

biosynthesis genes are often clustered (Rehm, 2010), we searched for homologs of the missing components in the *M. xanthus* genome. Because, the genome encodes at least 66 GTs, we specifically searched for Wzx flippase and Wzy polymerase homologs (see Section 4). A domain search suggested that the *M. xanthus* genome encodes three Wzx flippase homologs (MXAN_1035, MXAN_3260 and MXAN_7416) and four Wzy_C domain proteins (MXAN_1052, MXAN_2919, MXAN_3026 and MXAN_7442). Second, because expression of the *exoA-I* and *nfsA-H* genes is induced in response to starvation and chemical induction of sporulation (Giglio, Zhu, Klunder, Kummer, & Garza, 2015; Kimura et al., 2011; Licking et al., 2000; Müller, Treuner-Lange, Heider, Huntley, & Higgs, 2010; Ueki & Inouye, 2005; Wartel et al., 2013), we identified those candidate genes whose transcription pattern was similar to that of the *exoA-I* and *nfsA-H* genes during chemically induced sporulation using published data (Müller et al., 2010). Among the seven candidate genes, only the genes for the Wzx homolog MXAN_3260 and the Wzy_C domain protein MXAN_3026 were upregulated (Figure 1b) suggesting these two proteins could be the missing Wzx flippase and Wzy polymerase, respectively, for spore coat polysaccharide synthesis. Further, mutation of MXAN_1035 was previously reported to only slightly affect spore formation (Holkenbrink et al., 2014), while MXAN_1052 is in the same polysaccharide biosynthesis gene cluster as MXAN_1035, and therefore, likely also not involved in spore coat synthesis. MXAN_7416 and MXAN_7442 are part of the *eps* locus, which is important for EPS synthesis (Lu et al., 2005). Finally, MXAN_2919 is the WaaL O-antigen ligase involved in LPS synthesis (Pérez-Burgos, García-Romero, Jung, Valvano, & Søgaard-Andersen, 2019). Therefore, we investigated the Wzx flippase homolog MXAN_3260 and the Wzy polymerase homolog MXAN_3026 for a potential role in spore coat polysaccharide synthesis.

Sequences of Wzx flippases and Wzy polymerases are not well conserved, but both are membrane proteins with a high number of transmembrane helices (TMHs) (Hug & Feldman, 2011; Raetz & Whitfield, 2002). Sequence analysis of MXAN_3260 revealed a PF13440 (Polysacc_synt_3) domain (Figure 1c), similar to the LPS O-antigen Wzx flippase of *Yersinia similis* serotype O:9 (Beczala et al., 2015) and a PF14667 (Polysacc_synt_C) domain. The protein had also 11 or 12 predicted TMHs according to TMHMM and SPOCTOPUS, respectively (Figure 1c), as found in other flippases (Valvano, 2011). The Wzy polymerase candidate MXAN_3026

contains a PF04932 (Wzy_C) domain (Figure 1c), which is also found in O-antigen ligases, Wzy polymerases and O-linked oligosaccharyltransferases (Hug & Feldman, 2011; Schild, Lamprecht, & Reidl, 2005) and multiple TMHs whose topology depended on the prediction programme used (Figure 1c).

MXAN_3260 and MXAN_3026 are encoded by genes in two distinct gene clusters that we renamed to *exo* gene cluster III and II, while we renamed the *exoA-I* gene cluster to Exo gene cluster I (Figure 1d). Analysis of the genetic neighbourhood of MXAN_3260 and MXAN_3026 (Figure 1d; Table S1) showed that MXAN_3262, MXAN_3263 and MXAN_3027 are putative GTs, each containing a single GT4 domain according to the CAZy database. MXAN_3259 is a polysaccharide deacetylase homolog while MXAN_3261 is a serine O-acetyltransferase homolog. In the three *exo* gene clusters, all genes for which published microarray data are available are upregulated during chemically induced sporulation with 0.5 M glycerol (Figure 1e) (Müller et al., 2010). As discussed in details below, *exo* gene cluster I and III make up one cluster in *Vulgatibacter incomptus* and all three clusters are present as one cluster in Anaeromyxobacteraceae supporting that the gene products of the three clusters may function together.

As shown below, the genes of *exo* gene cluster II and III are important for sporulation and our data support that the encoded proteins form part of the same machinery. For simplicity and to facilitate identification of the genes throughout this study, we renamed MXAN_3026, MXAN_3027 and MXAN_3259-MXAN_3263 to ExoJ-P following the Exo nomenclature (Holkenbrink et al., 2014; Müller et al., 2012) (Figure 1d).

2.2 | ExoJ-ExoP are important for chemically induced sporulation

To determine the importance of the seven *exoJ-P* genes in sporulation, we generated in-frame deletion mutations in each of the genes separately and determined their importance for sporulation using chemical induction (Figure 2a,b). After addition of glycerol to a final concentration of 0.5 M, wild-type (WT) cells rounded up during the first 4 hr and had turned into phase-bright resistant spores by 24 hr. Cells of the ΔexoE mutant, which cannot produce spore coat polysaccharide (Holkenbrink et al., 2014), served as a negative control. As previously described (Holkenbrink et al., 2014), ΔexoE cells initially shortened becoming ovoid by 4 hr; by 24 hr, most ΔexoE cells had reverted to a non-phase-bright rod-shape while a few remained non-phase-bright ovoid-shaped or were branched and non-phase-bright. ΔexoE cells were not resistant to heat and sonic treatment.

The ΔexoM and ΔexoJ mutants formed large round cells by 4 hr; by 24 hr, many cells had reverted to rod-shape, however, a significant fraction were ovoid, branched or formed large spheres; cells of these two mutants were neither phase-bright nor resistant to heat and sonic treatment. The ΔexoK , ΔexoO and ΔexoP mutants had cell morphologies and sporulation defects similar to those of the ΔexoM and ΔexoJ mutants. By 4 hr, ΔexoL cells were ovoid; by 24 hr, many of these cells had reverted to rod-shape, however, a significant fraction

were ovoid and a few were branched or had turned into large spheres. None of these cells were phase-bright or resistant to heat and sonic treatment. Finally, the ΔexoN mutant formed phase-bright spores that were resistant to heat and sonic treatment but at a two-fold reduced level compared to WT; moreover, a significant fraction of cells at 24 hr were non-phase-bright rod-shaped or ovoid while a small fraction were branched or formed large spheres. Sporulation of all eight in-frame deletion mutants was restored by ectopic expression of the corresponding full-length gene under the control of the native promoter (P_{nat}) on a plasmid integrated in a single copy at the Mx8 *attB* site (Figures 1d and 2).

We conclude that all seven ExoJ-P proteins, except ExoN, are essential for chemically induced sporulation. These data agree with the idea that ExoM is the Wzx flippase, ExoJ the Wzy polymerase, ExoK/O/P GTs and ExoL a polysaccharide deacetylase essential for synthesis of an intact spore coat polysaccharide and are also consistent with a previous report that an insertional mutation in *exoJ* caused a sporulation defect (Müller et al., 2012). Of note, cells lacking ExoE, which are blocked in the initiation of repeat unit synthesis because they lack the PHPT for spore coat polysaccharide synthesis, mostly reverted from ovoid at 4 hr to rod-shaped at 24 hr while the remaining mutants, which would be impaired in spore coat polysaccharide synthesis at later steps, formed morphologically highly abnormal cells (ovoid-shaped, branched or large spheres) by 24 hr (Figure 2b) (see Section 3).

2.3 | Loss of ExoE and ExoJ-ExoP neither affects EPS and LPS synthesis, cell morphology nor motility

In addition to the spore coat polysaccharide, *M. xanthus* synthesises two additional polysaccharides, that is, EPS and LPS, both of which are important for fruiting body formation. Because, blocking synthesis of one glycan polymer can affect synthesis of other polymers including PG by sequestration of Und-P through accumulation of Und-PP intermediates (Burrows & Lam, 1999; Jorgenson, Kannan, Laubacher, & Young, 2016; Jorgenson & Young, 2016; Ranjit & Young, 2016; Valvano, 2008), we determined whether lack of Exo proteins interferes with EPS, LPS or PG synthesis during growth.

EPS synthesis was tested using nutrient-rich agar supplemented with Congo red. As a result of binding of the dye to EPS, WT colonies acquired a red colour while the negative control, a ΩdifE mutant (Yang, Geng, Xu, Kaplan, & Shi, 1998), did not (Figure 3a). All *exo* mutants tested accumulated EPS at WT level. LPS was extracted from cell extracts from growing cells and detected by Emerald green staining. For WT as well as all tested *exo* mutants, a fast running lipid A-core band and polymeric LPS O-antigen bands were detected while only the lipid A-core band was detected in the ΔwbaP negative control strain, which is impaired in O-antigen synthesis (Pérez-Burgos et al., 2019) (Figure 3b). Because, interference with PG synthesis causes the formation of abnormally shaped cells including filamentous cells in the presence of nutrients (Schumacher et al., 2017; Treuner-Lange et al., 2013, 2015), we used cell morphology as a proxy for PG synthesis to test whether lack of the Exo proteins

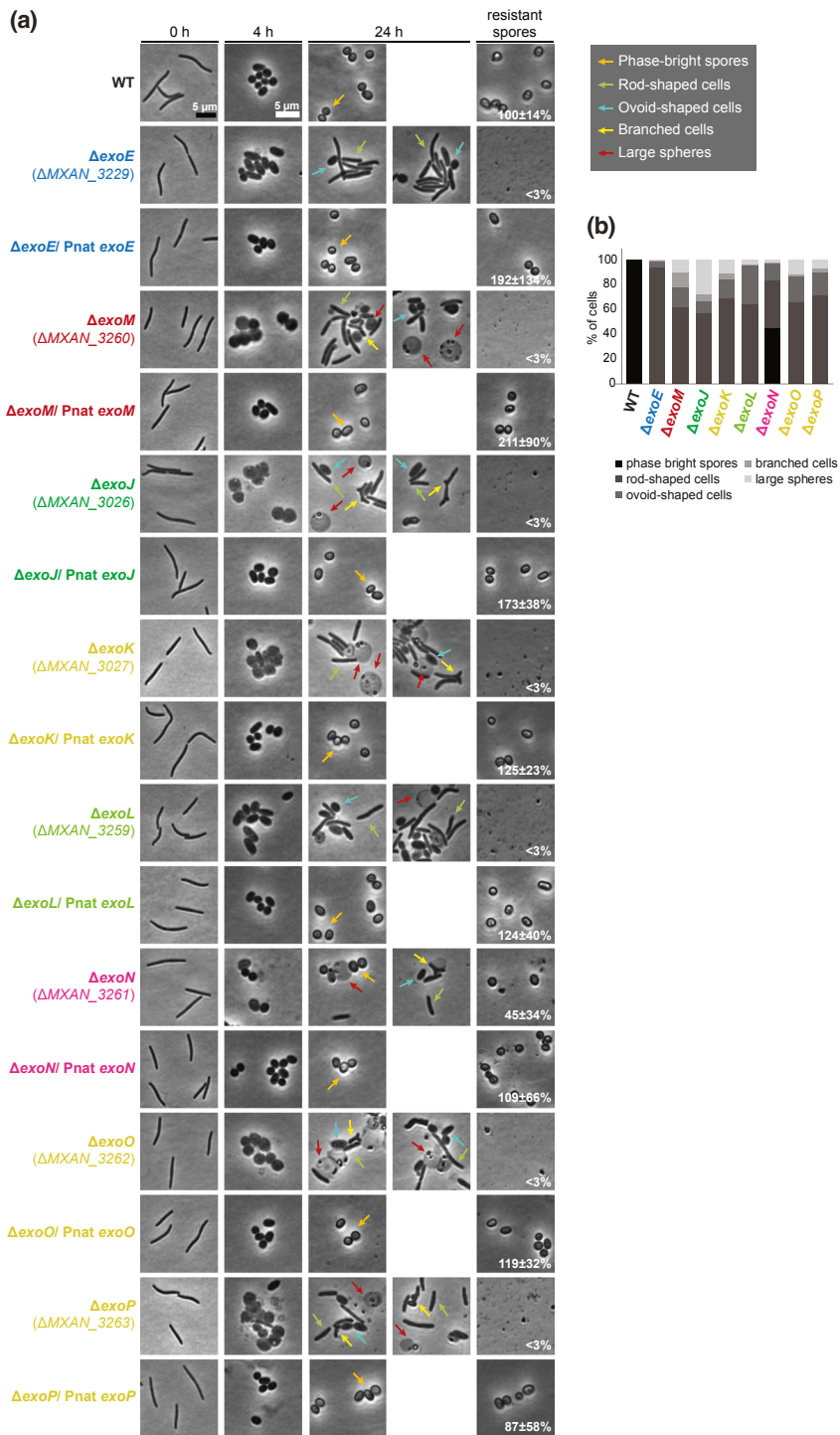


FIGURE 2 Chemically induced sporulation in Δ exo mutants. (a) Sporulation was induced by addition of glycerol to a final concentration of 0.5 M. At 0, 4 and 24 hr, cell morphology was observed by phase contrast microscopy. In images labelled resistant spores, cells were exposed to sonic and heat treatment before microscopy. Sporulation frequency after sonic and heat treatment is indicated as the mean \pm SD from three biological experiments relative to WT. P_{nat} is short for the native promoter and is used throughout the study. Scale bars, 5 μ m. (b) Quantification of cell morphology at 24 hr before sonic and heat treatment relative to WT (100%); $n = 300$ combined from three biological replicates

interferes with PG synthesis during growth. Lack of the tested components of the Exo machinery did not affect cell morphology (Figure 2 (0 hr) and 3c), with the exception of Δ exoL cells, which were marginally but significantly ($p = .029$) shorter than WT. Therefore, loss of spore coat polysaccharide synthesis does not interfere with EPS, LPS or PG synthesis during growth in agreement with the observation that *exo* gene expression is induced during sporulation. Moreover, these observations support that the Exo machinery is dedicated to spore coat synthesis and that the EPS, LPS and PG machineries function independently of the Exo proteins during growth.

M. xanthus possesses two distinct motility systems that are important for fruiting body formation; one of them depends on type IV pili (T4P) and the other one depends on the Agl/Glt gliding motility complexes (Schumacher & Søgaard-Andersen, 2017; Zhang, Ducret, Shaevitz, & Mignot, 2012). EPS and LPS are important for motility (Lu et al., 2005; Pérez-Burgos et al., 2019). On 0.5% agar, which favours T4P-dependent motility, WT displayed the flares characteristic of this type of motility; by contrast, the negative control Δ *pilA* strain, which lacks the major pilin of T4P (Wu & Kaiser, 1996), did not. On 1.5% agar, which favours gliding motility, single cells were

FIGURE 3 EPS and LPS synthesis, and cell length determination in the *Δexo* mutants. (a) Determination of EPS accumulation. 20 μl of cell suspensions at 7×10^9 cells/ml were spotted on 0.5% agar supplemented with 0.5% CTT and Congo red and incubated at 32°C for 24 hr. The *ΩdifE* mutant served as a negative control. (b) Detection of LPS O-antigen. Extracted LPS samples from the same number of cells were separated by SDS-PAGE and visualised using Pro-Q Emerald 300. The *ΔwbaP* mutant served as a negative control. (c) Cell length determination. Cell length distribution is shown in a violin plot. Each violin indicates the probability density of the data at different cell lengths. Mean and median values are represented by a continuous and dashed line, respectively. For each strain, mean cell length \pm standard deviation is indicated; $n = 800$ combined from four biological replicates. Samples were compared using a Mann-Whitney test, * indicates p value $< .05$ and ns, not significant

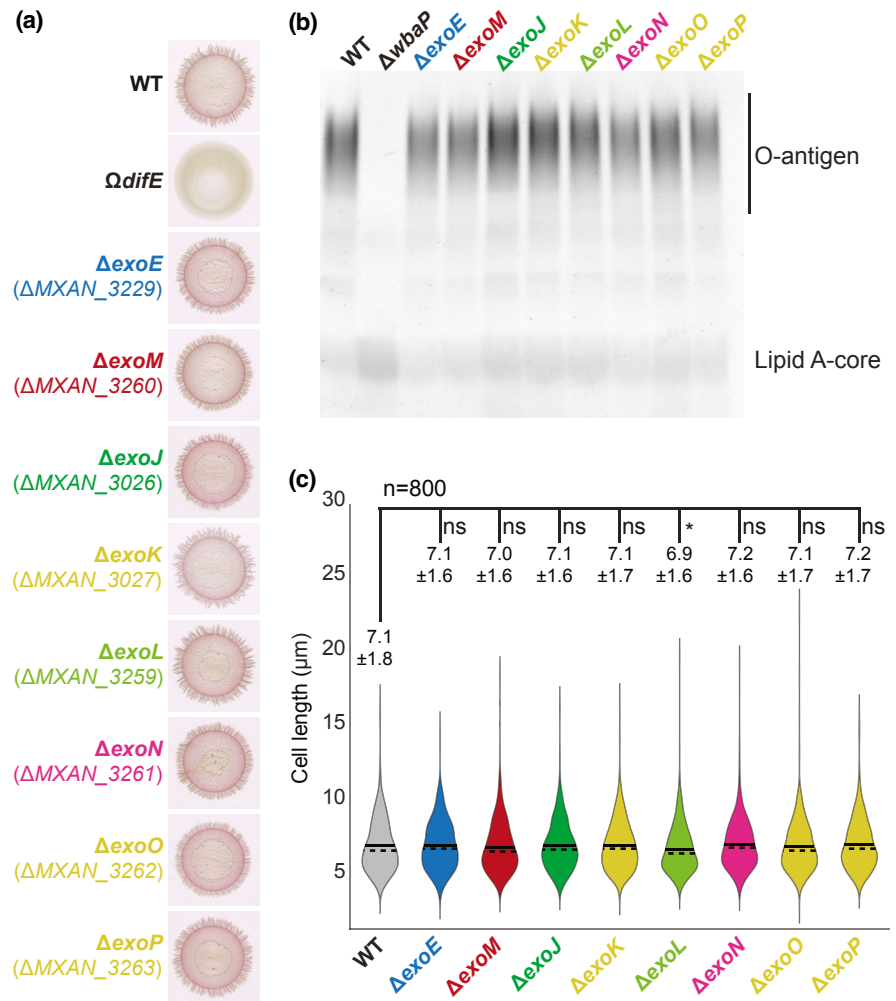


TABLE 1 Motility and starvation-induced sporulation phenotypes of the *exo* mutants

Strain genotype	T4P-dependent motility	Gliding motility	Sporulation on TPM agar ^a	Sporulation in submerged culture ^a
WT	+	+	100 \pm 50%	100 \pm 40%
<i>ΔexoE</i>	+	+	<3% (143 \pm 59%)	<3% (89 \pm 17%)
<i>ΔexoM</i>	+	+	<3% (185 \pm 39%)	<3% (115 \pm 33%)
<i>ΔexoJ</i>	+	+	<3% (118 \pm 33%)	<3% (91 \pm 33%)
<i>ΔexoK</i>	+	+	<3% (108 \pm 38%)	<3% (82 \pm 26%)
<i>ΔexoL</i>	+	+	<3% (97 \pm 27%)	<3% (64 \pm 13%)
<i>ΔexoN</i>	+	+	54 \pm 12% (69 \pm 30%)	39 \pm 26% (45 \pm 10%)
<i>ΔexoO</i>	+	+	<3% (68 \pm 18%)	<3% (71 \pm 29%)
<i>ΔexoP</i>	+	+	<3% (106 \pm 70%)	<3% (114 \pm 42%)

^aSporulation efficiency after heat and sonic treatment is indicated as the mean \pm SD from three biological replicates relative to WT. Numbers in brackets indicate sporulation levels in the complementation strains.

observed at the colony edge of WT, while the *ΔaglQ* mutant, which lacks an essential component of the gliding machinery motor (Nan et al., 2013; Sun, Wartel, Cascales, Shaevitz, & Mignot, 2011), had a smooth edge. By contrast, all tested *exo* mutants were indistinguishable from WT (Figure S1; Table 1). Together, these results indicate that loss of the Exo machinery does not interfere with motility during growth.

2.4 | ExoJ-M and ExoO-P are important for starvation-induced sporulation

Having shown that the Exo proteins are neither important for EPS, LPS or PG biosynthesis nor for motility during growth, we asked whether the *exo* mutants are able to generate starvation-induced spores during fruiting body formation. Previous analyses showed

that ΔexoA , ΔexoC , ΔexoD and ΔexoJ mutants are generally able to form fruiting bodies but have a reduced sporulation efficiency (Kimura et al., 2011; Licking et al., 2000; Müller et al., 2012; Ueki & Inouye, 2005). Because, these experiments were performed under different conditions, we tested the developmental proficiency of eight *exo* mutants on TPM 1.5% agar and under submerged conditions.

Similar to WT, all eight *exo* mutants had aggregated to form fruiting bodies by 24 hr under both conditions (Figure S2). However, all *exo* mutants with the exception of the ΔexoN mutant had a strong sporulation defect (Figure S2; Table 1). Importantly, the sporulation defects were partially or completely complemented by ectopic expression of the relevant full-length gene from the native promoter (Figures 1d and S2; Table 1). Because, the sporulation defects of the *exo* mutants during chemically induced sporulation were fully complemented, we speculate that the partial complementation observed for some of the *exo* mutants is caused by insufficient expression of the relevant gene during starvation. As in the case of chemically induced sporulation, we conclude that ExoJ-P proteins, with the exception of ExoN, are essential for starvation-induced sporulation and by implication in formation of an intact spore coat.

2.5 | ExoE has GalNAc-1-P transferase activity

ExoE was suggested to be the PHPT homolog that initiates repeat unit biosynthesis for spore coat polysaccharide biosynthesis (Holkenbrink et al., 2014); however, it is unknown which sugar ExoE transfers to Und-P. Similarly to the *Escherichia coli* WcaJ_{Ec} , which transfers Glc-1-P to Und-P and the *Salmonella enterica* WbaP_{Se} , which transfers Gal-1-P to Und-P (Furlong, Ford, Albarnez-Rodriguez, & Valvano, 2015; Saldías et al., 2008), ExoE contains a PF02397 (Bacterial Sugar Transferase) domain in the C-terminus and five putative transmembrane domains (Figure 4a). By contrast, PNPTs including the *E. coli* WecA_{Ec} , which transfers GlcNAc-1-P to Und-P, contain a PF00953 (Glycosyl transferase family 4) domain (Figure 4a) (Lehrman, 1994). In WcaJ_{Ec} , the fifth TMH forms a helix-break-helix structure and does not fully span the IM resulting in the cytoplasmic localisation of the C-terminal catalytic domain. This depends on the residue P291 that forms part of a DX_{12}P motif highly conserved among PHPTs (Furlong et al., 2015). ExoE also carries the DX_{12}P motif and contains all the other conserved essential residues important for catalytic activity that have been identified in the C-terminal catalytic domain of WbaP_{Se} (Patel, Furlong, & Valvano, 2010) (Figures 4b and S3). Thus, ExoE is a PHPT with a predicted topology similar to that described for WcaJ_{Ec} and WbaP_{Se} .

Compositional analysis of the spore coat polysaccharide showed that it is composed of 1-3-, 1-4-linked GalNAc, 1-4-linked Glc (GalNAc:Glc ratio 17:1) and glycine (Holkenbrink et al., 2014). These findings suggest that ExoE could use either UDP-Glc or UDP-GalNAc as a substrate. To test the activity of ExoE, we performed heterologous expression experiments in *E. coli* and *S. enterica*. To this end, we generated the plasmids pMP158 and pMP147, which encode native,

untagged ExoE and a FLAG-tagged ExoE variant ($_{\text{FLAG}}\text{ExoE}$), respectively, from an arabinose-inducible promoter in plasmid pBAD24. We used native ExoE to test for ExoE activity and $_{\text{FLAG}}\text{ExoE}$ to test for protein accumulation using immunoblotting.

To determine whether ExoE can use UDP-Glc, we carried out heterologous complementation experiments in a $\Delta\text{wcaJ}_{\text{Ec}}$ *E. coli* strain, which lacks the ability to produce colanic acid as previously reported (Patel et al., 2012; Pérez-Burgos et al., 2019). For this experiment, native ExoE was synthesised in the $\Delta\text{wcaJ}_{\text{Ec}}$ strain also containing pWQ499, which encodes the RcsA regulator that increases the production of colanic acid (Furlong et al., 2015). Cells growing in the absence and presence of arabinose were examined for a glossy and mucoid colony phenotype characteristic of colanic acid capsule production (Figure 4c). Only cells containing the $_{\text{FLAG}}\text{WcaJ}_{\text{Ec}}$ -encoding plasmid pLA3 exhibited the distinct mucoid phenotype representing colanic acid production, whereas the strain synthesising native ExoE or containing the pBAD24 vector control did not display this phenotype. As shown in Figure S4a, $_{\text{FLAG}}\text{ExoE}$ accumulated although at a slightly lower level than $_{\text{FLAG}}\text{WcaJ}_{\text{Ec}}$. Together, these results indicate ExoE is not a Glc-1-P transferase.

PHPT proteins were initially described as hexose-1-phosphate transferases while PNPTs are considered *N*-acetylhexosamine-1-phosphate transferases; however, there are several examples of proteins of the PHPT family with specificities for *N*-acetylated nucleotide sugars (Chamot-Rooke et al., 2007; Glover, Weerapana, Chen, & Imperiali, 2006; Merino et al., 2011; Power et al., 2000). Because, ExoE did not transfer Glc-1-P, we next investigated whether ExoE could transfer GalNAc-1-P. To this end, we performed heterologous expression experiments in *E. coli* in which we first tested for transfer of GlcNAc-1-P and subsequently for transfer of GalNAc-1-P. GlcNAc-1-P transferase activity can be tested using the *E. coli* strain MV501, which has a transposon insertion in wecA_{Ec} . As described, WecA_{Ec} is a PNPT that uses UDP-GlcNAc for initiating synthesis of O7 polysaccharide antigen (Alexander & Valvano, 1994). Native ExoE in MV501 did not restore O7 polysaccharide synthesis (Figure 4d). In immunoblot experiments, we observed that $_{\text{FLAG}}\text{ExoE}$ accumulated in MV501, especially in an oligomeric form, although at a low level (Figure S4b). By contrast, pMAV11 carrying the wecA_{Ec} gene complemented the defect in O-antigen synthesis. These observations suggest that ExoE is not a GlcNAc-1-P transferase.

E. coli lacks the Gne epimerase, which interconverts UDP-GlcNAc and UDP-GalNAc. Previously, Merino et al. (Merino et al., 2011) demonstrated that the *Aeromonas hydrophila* PHPT homolog WecP_{Ah} in the presence of a plasmid encoding the Gne homolog from *A. hydrophila* modified the MV501 lipid A-core. This modification is consistent with formation of an O7 repeat containing GalNAc. This modified lipid A-core likely only contains one O7 repeat because the addition of GalNAc to the repeat may interfere with O7 polymerisation (Merino et al., 2011). Similar to Merino et al., we observed formation of this GalNAc containing O7 repeat in MV501 in the presence of plasmids encoding $_{\text{FLAG}}\text{WecP}_{\text{Ah}}$ (pSEF88) and the *A. hydrophila* Gne homolog (pGEMT-Gne $_{\text{Ah}}$) (Figure 4e). More importantly, co-expression of ExoE and Gne $_{\text{Ah}}$ in

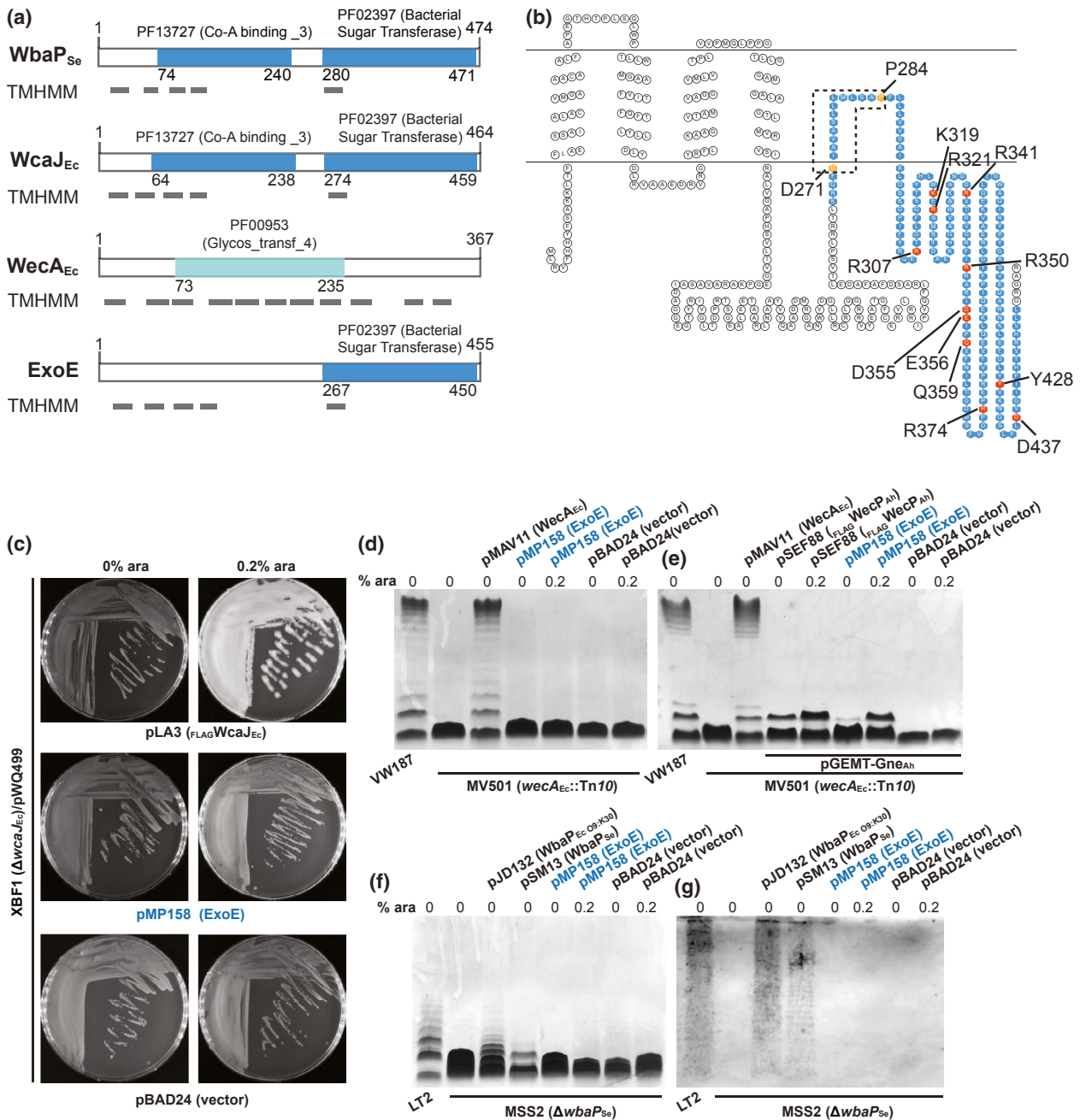


FIGURE 4 ExoE has GalNAc-1-P transferase activity. (a) Domain and TMH prediction for WbaP_{Se}, WcaJ_{Ec}, WecA_{Ec} and ExoE. Grey rectangles indicate TMH. Numbers indicate domain borders. (b) Topology predictions for ExoE. The catalytic PF02397 domain is indicated in blue and conserved amino acids important for structure or activity are marked with orange and red, respectively. The amino acid sequence alignment of ExoE with WbaP_{Se} is shown in Figure S3. (c–g) Heterologous complementation experiments to characterise ExoE specificity. (c) *E. coli* XBF1 ($\Delta wcaJ_{Ec}$) containing pWQ499 (*rcaA*⁺) was transformed with the indicated plasmids and plated on LB agar in the absence or presence of 0.2% arabinose (ara) to induce gene expression. Cells were incubated for 24 hr at 37°C, and then, 24 hr at room temperature before scoring the mucoid phenotype. (d,e) Silver-stained polyacrylamide gels of LPS extracted from the *E. coli* *wecA::Tn10* mutant strain MV501 carrying the indicated plasmids. In (e), MV501 also contained the plasmid pGEMT-Gne, which encodes the UDP-GlcNAc/UDP-GalNAc epimerase Gne_{Ah}. VW187 is the parental *wecA*⁺ strain. Arabinose was added as indicated. (f) Silver-stained polyacrylamide gel and (g) immunoblot with rabbit *Salmonella* group B O-antigen antiserum of LPS extracted from *S. enterica* LT2 (WT) and the MSS2 $\Delta wbaP_{Se}$ mutant carrying the indicated plasmids. Arabinose was added as indicated

MV501 resulted in a lipid A-core modified band similar to that observed with co-expression of FLAG WecP_{Ah} and Gne_{Ah} (Figure 4e). This result supports that ExoE can transfer GalNAc-1-P to Und-P in *E. coli*.

Finally, we investigated the specificity of ExoE for UDP-Gal, in this case using the *S. enterica* $\Delta wbaP_{Se}$ mutant MSS2 that is blocked in the first step in O-antigen synthesis. ExoE did not restore O-antigen synthesis in MSS2 despite the FLAG-tagged variant of the

protein accumulating (Figures 4f,g and S4a). By contrast, the control plasmids pJD132 and pSM13, which encode WbaP_{Ec O9:K30} of *E. coli* and WbaP_{Se} of *S. enterica*, respectively, both restored O-antigen synthesis (Figure 4f,g). Collectively, the heterologous expression experiments support that ExoE has specificity for UDP-GalNAc but lacks specificity for UDP-Glc, UDP-GlcNAc and UDP-Gal. These data, together with the observation that the spore coat polysaccharide contains Glc and GalNAc, suggest that ExoE is a GalNAc-1-P transferase forming Und-PP-GalNAc and that GalNAc is likely the first sugar added to Und-P during the biosynthesis of the spore coat polysaccharide repeat.

2.6 | The *exo* and *nfs* gene clusters co-occur only in a subset of sporulating Myxococcales

Because, the majority of the members of the order Myxococcales can sporulate (Reichenbach, 1999), we hypothesised that the Exo and Nfs machineries for formation of the rigid spore coat would be conserved in Myxococcales. We, therefore, searched for orthologs of each Exo and Nfs protein in Myxococcales with fully sequenced genomes using a reciprocal best BlastP hit method (Section 4).

Within the suborder Cystobacterineae, all individual components of the Exo machinery are conserved in *F. Myxococcaceae*, *F. Archangiaceae* and *F. Vulgatibacteraceae*, while there is somewhat less conservation, especially of cluster III, in the *Anaeromyxobacteraceae* (Figure 5a). By contrast, in the suborders *Nannocystineae* and *Sorangineae*, Exo orthologs were largely missing. Interestingly, in the small genomes of *V. incomptus* and *Anaeromyxobacteraceae* that only have approximately half the size of other myxobacterial genomes (Figure 5a, right), *exo* gene cluster I and III are organised in one cluster (*V. incomptus*), while all three clusters are present in one in *Anaeromyxobacteraceae* (Figures 5a and S5a), lending further support to the idea that these proteins function in the same pathway. The taxonomic distribution of the *exo* genes supports an evolutionary scenario in which the last common ancestor of the Cystobacterineae acquired the *exo* gene cluster, and then, over time gene organisation diversified. Alternatively, a common ancestor of the myxobacteria contained the *exo* gene cluster and the *exo* genes were lost in ancestors of the *Nannocystineae* or *Sorangineae*.

The NfsA-H proteins are paralogs of the GltA-H proteins that are important for gliding motility (Agrebi, Wartel, Brochier-Armanet, & Mignot, 2015; Wartel et al., 2013). While NfsA-H are encoded in one gene cluster, GltA-H are encoded in two gene clusters in the *M. xanthus* genome (Figure 5a,b). In agreement with previous analyses (Agrebi et al., 2015; Luciano et al., 2011), in which conservation of GltA-H/NfsA-H homologs were studied without distinguishing between the two machineries, orthologs of the GltA-H proteins are widely conserved in Myxococcales although with less conservation in the *Nannocystineae* and *Sorangineae*. Moreover, the two *glt* gene clusters are in close proximity outside of the *F. Myxococcaceae*, *F. Archangiaceae* and *F. Vulgatibacteraceae* (Figures 5a and S5b) as

previously described for *Anaeromyxobacter* (Luciano et al., 2011). By contrast, our analysis shows that orthologs of NfsA-H are exclusively found in the *F. Myxococcaceae*, *F. Archangiaceae* and *F. Vulgatibacteraceae*. The taxonomic distribution of the *glt* and *nfs* gene clusters suggests that the primitive *gltA-H* genes were present in the last common ancestor of the Myxococcales and that the *nfs* cluster results from a duplication event of the ancestral *gltA-H* gene cluster shortly after the divergence of the *Anaeromyxobacteraceae* from the remaining Cystobacterineae. This agrees with a previous suggestion (Agrebi et al., 2015; Luciano et al., 2011), except that our analysis clearly supports that the primitive Glt proteins are ancestral to the Nfs proteins.

Also, our analysis shows that the *exo* and *nfs* genes co-occur in the Cystobacterineae except in the *Anaeromyxobacteraceae*. Interestingly, except for *V. incomptus*, for which no fruiting body formation and sporulation were observed (Yamamoto, Muramatsu, & Nagai, 2014), all the species containing both the *exo* and *nfs* gene clusters have been reported to form phase-bright spores. By contrast, *Haliangium ochraceum*, *Minicystis rosea*, *Sorangium cellulorum* and *Chondromyces crocatus* also form spores despite they generally lack the Exo and Nfs machineries. These observations suggest that sporulation occurs by a different mechanism in the sporulating Cystobacterineae compared to sporulating *Nannocystineae* and *Sorangineae*. Consistently, *Sorangineae* spores have been reported to be less phase-bright than the *M. xanthus* spores and rod-shaped (Garcia & Müller, 2014b) and *M. rosea* spores are phase-dark and rod-shaped (Garcia, Gemperlein, & Müller, 2014).

3 | DISCUSSION

Cells of *M. xanthus* generate at least three different polysaccharidic cell surface structures, namely LPS, EPS and the spore coat polysaccharide. Here, we focused on identifying the proteins that would function together with the ExoA-I proteins in spore coat polysaccharide biosynthesis and export.

Using bioinformatics and gene co-expression analyses, we identified two loci that encode proteins important for sporulation. One of them, named the *exo* gene cluster II, encodes a homolog of Wzy polymerases (ExoJ, MXAN_3026) and a predicted GT (ExoK, MXAN_3027), while the other, *exo* gene cluster III, encodes a predicted polysaccharide deacetylase (ExoL, MXAN_3259), a Wzx flippase (ExoM, MXAN_3260), a serine O-acetyltransferases (ExoN, MXAN_3261) and two GTs (ExoO, MXAN_3262 and ExoP, MXAN_3263). All seven proteins with the exception of ExoN, which is only partially required, are essential for sporulation, and therefore, predicted to function in formation of the intact spore coat polysaccharide. Based on these findings, we propose a revised model for spore coat polysaccharide biosynthesis (Figure 6).

The *M. xanthus* spore coat polysaccharide is composed of 1-3-, 1-4-linked GalNAc, 1-4-linked Glc and glycine (Holkenbrink et al., 2014) and with the latter proposed to form glycine bridges between polysaccharide chains (Holkenbrink et al., 2014). The spore coat

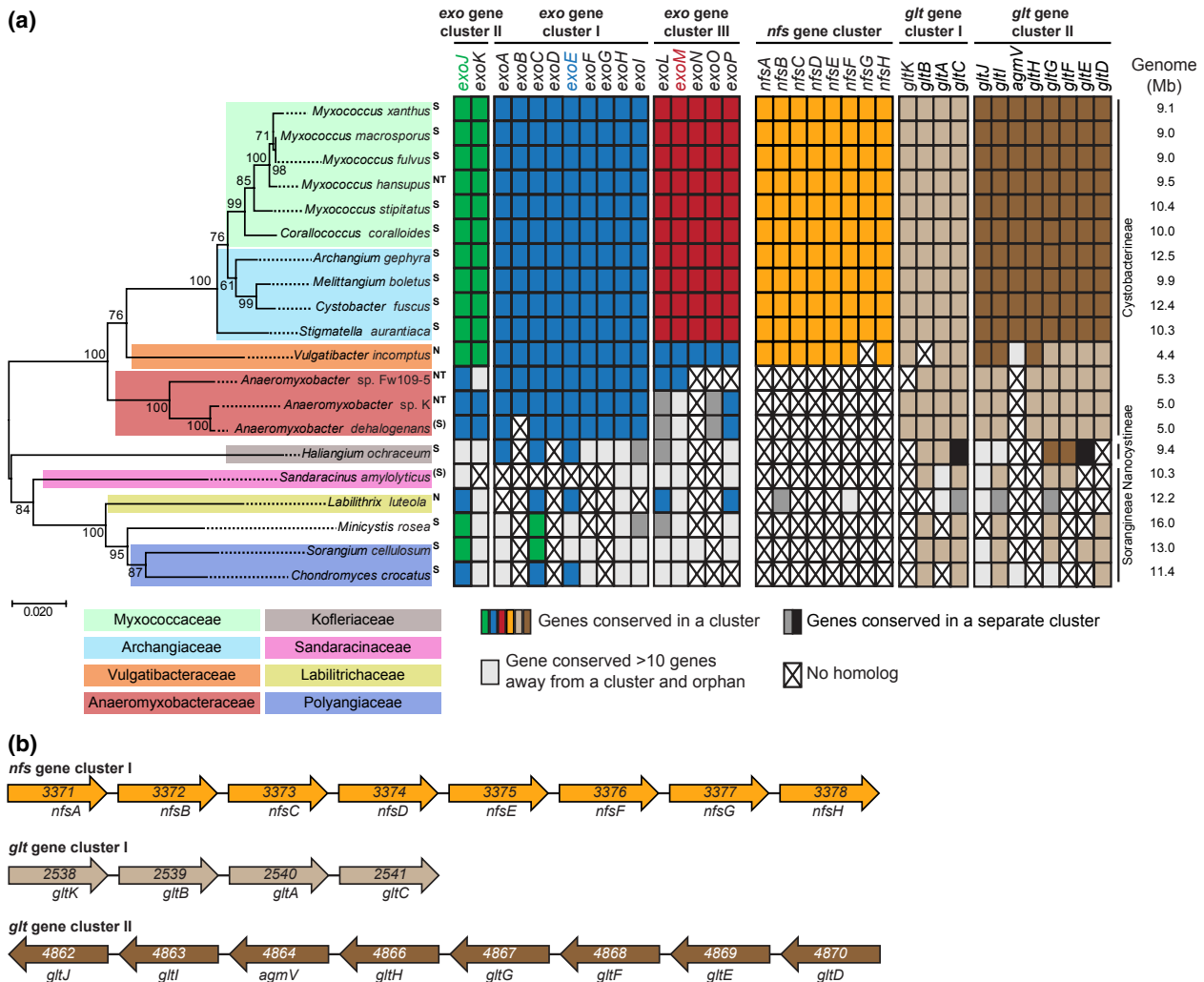


FIGURE 5 Analysis of *exo*, *nfs* and *glt* gene occurrence and organisation in myxobacteria. (a) Taxonomic distribution, co-occurrence and synteny of the *exo*, *nfs* and *glt* genes in Myxococcales. Left, 16S rRNA tree of Myxococcales with fully sequenced genomes. Family and suborder classification are indicated. Genome size is indicated on the right. Used strains are listed in Table S2. S, species that form spores; (S), tested for sporulation but with ambiguous results; NT, sporulation not tested; N, sporulation tested and not observed (dos Santos et al., 2014; Fudou, Jojima, Iizuka, & Yamanaka, 2002; Garcia et al., 2014; Garcia & Müller, 2014a, 2014b; Mohr, Garcia, Gerth, Irschik, & Müller, 2012; Sanford, Cole, & Tiedje, 2002; Yamamoto et al., 2014). For the *exo*, *nfs* and *glt* gene clusters, a reciprocal best BlastP hit method was used to identify orthologs. Generally, the *exo* gene clusters are marked in green (cluster II), blue (cluster I) and red (cluster III) and the *nfs* and *glt* gene clusters in orange (*nfs*), light brown (*glt* cluster I) and dark brown (*glt* cluster II). To evaluate gene proximity and cluster conservation, 10 genes were considered as the maximum distance for a gene to be in a cluster. Genes found in the same cluster are marked with the same colour. If two or three gene clusters are within a distance of <10 genes, all genes are marked in the same colour (e.g., two of the *exo* clusters in *V. incompitus*, all three *exo* clusters in Anaeromyxobacteraceae and the *glt* clusters in Anaeromyxobacteraceae, Nannocystineae and Sorangineae). Light grey indicates a conserved gene that is found somewhere else on the genome (>10 genes away from a cluster); dark grey and black indicate conservation of the marked genes but in a separate cluster; a cross indicates no homolog found. Note that the *nfsB* gene in *L. luteola* DSM 27648 is found in close proximity to the *gltC*, *gIG* and *gltI* genes and is most likely a *gltB* homolog. (b) *nfs* and *glt* gene clusters in *M. xanthus*. Genes are not drawn to scale, MXAN number or gene name are indicated and gene orientation is indicated by arrows. The tree in A was prepared in MEGA7 (Kumar, Stecher, & Tamura, 2016) using the Neighbour-Joining method (Saitou & Nei, 1987). Bootstrap values (500 replicates) are shown next to the branches (Felsenstein, 1985)

polysaccharide is also acetylated (Filer, White, Kindler, & Rosenberg, 1977b; Holkenbrink et al., 2014). However, the precise structure of the spore coat polysaccharide is unknown. The data of Holkenbrink et al. (Holkenbrink et al., 2014), together with our results, suggest a model in which ExoE is the PHPT homolog responsible for the first step in repeat unit synthesis by catalysing the transfer of a sugar-1-P donor to Und-P (Holkenbrink et al., 2014). Here, we demonstrate

that ExoE is functionally similar to WecP_{Ah}, a GalNAC-1-P transferase from *A. hydrophila* (Merino et al., 2011) in heterologous expression experiments in *E. coli*, suggesting that GalNAC is the first sugar of the spore coat repeat unit. Alternatively, because, several of the Exo proteins are sugar-modifying enzymes, it is also possible that ExoE has affinity for GalNAC in *E. coli* but incorporates a modified GalNAC as the first sugar in the repeat unit in *M. xanthus*. Subsequently, we

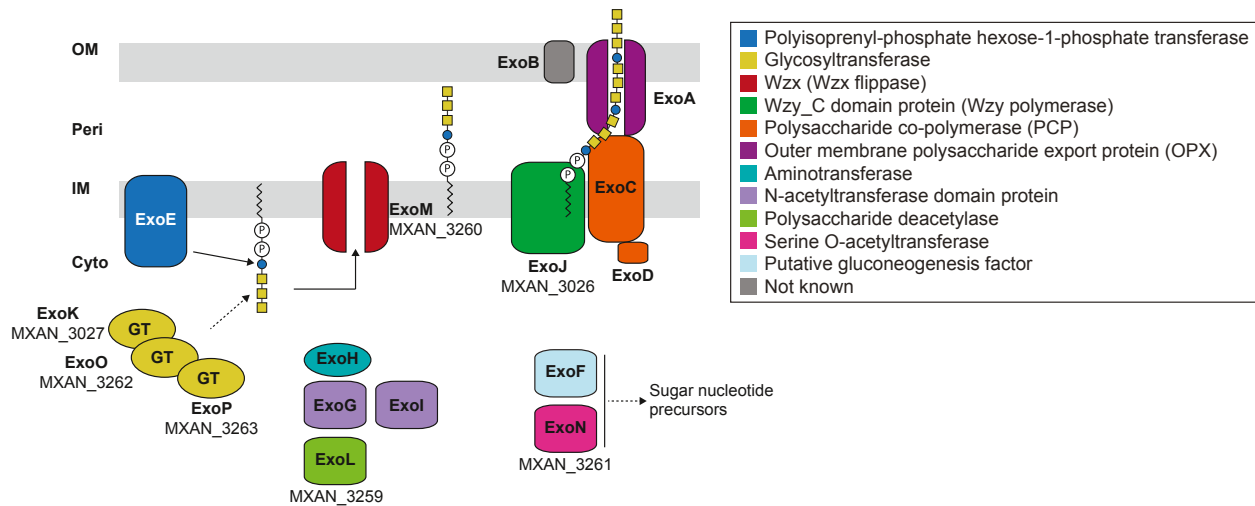


FIGURE 6 Model of spore coat polysaccharide biosynthesis in *M. xanthus*. Colour code indicates predicted functions. Stippled lines indicate that the site of action is hypothetical and remains to be determined experimentally. See Section 3 for details. ExoE adds the first sugar of the repeat unit (blue), which is likely GalNAc, followed by addition of monosaccharides (Glc and GalNAc) by the GTs (yellow)

predict that the GTs ExoK, ExoO and ExoP transfer sugar building blocks to the repeat unit, which is likely a tetrasaccharide. The *N*-acetyltransferase homologs ExoG and ExoI, the aminotransferase homolog ExoH and the polysaccharide deacetylase homolog ExoL presumably modify sugars before or after incorporation into the repeat unit.

Based on the composition of the spore coat polysaccharide (Holkenbrink et al., 2014), we suggest that the GTs ExoK, ExoO and ExoP incorporate GalNAc and Glc into the repeat unit. Acetylation of the spore coat polysaccharide may involve the ExoG and ExoI *N*-acetyltransferases (but see also below). ExoL is the first identified potential polysaccharide deacetylase implicated in *M. xanthus* spore coat synthesis. Interestingly, phase-bright spores were not detected in the *exoG* and *exoI* mutants (Holkenbrink et al., 2014); similarly, the *exoL* mutant did not form phase-bright spores (here) suggesting that proper acetylation of the spore coat polysaccharide is important for its synthesis, stability and/or function. However, it is unknown which residue is modified by ExoG, ExoI and ExoL, and whether these proteins function on the same or independent targets. In *Caulobacter crescentus*, the polysaccharide deacetylase HfsH and the *N*-acetyltransferase HfsK affect acetylation of the holdfast polysaccharide; in the absence of any of these two proteins there is a defect in adhesive and cohesive properties of the holdfast polysaccharide without affecting its synthesis (Sprecher et al., 2017; Wan, Brown, Elliott, & Brun, 2013).

ExoH is predicted to be a pyridoxal phosphate-dependent (PLP) aminotransferase with a DegT/DnrJ/EryC1/StrS family domain (PF01041), which generally catalyses the transfer of an amino group from an amino acid to an amino acceptor (John, 1995). Similarly to the aminotransferase ArnB that transfers an amino group to arabinose in *S. enterica* (Noland et al., 2002) or the PLP aminotransferase PseC from *Helicobacter pylori*, which transfers an amino group to a sugar moiety prior to acetylation by PseH (Ud-Din, Liu, & Roujeinikova, 2015), we suggest that ExoH may add an amino group

to monosaccharides before their incorporation into the repeat unit or modify sugar(s) in the repeat unit.

The glycine in the spore coat polysaccharide was proposed to form glycine bridges between polysaccharide chains (Holkenbrink et al., 2014). Holkenbrink et al. also suggested that glycine is added to the spore coat polysaccharide in the cytoplasm. Interestingly, a structure-based search with HHPred revealed that the closest homolog of the *N*-acetyltransferases ExoG and ExoI is FemX from *Staphylococcus aureus*, that is, for ExoG and ExoI, the probabilities of homology to FemX is 100% with an E-value of $1.9e-31$ and 100% with an E-value of $4.1e-30$. The Fem proteins belong to GCN5-related *N*-acetyltransferases (GNAT) that generally transfer acetylated molecules to an amino acceptor of different target molecules including sugars (Favrot, Blanchard, & Vergnolle, 2016; Reith & Mayer, 2011; Ud-Din et al., 2015). In *S. aureus*, the FemA/B/X proteins add five glycine residues to the lysine in the stem peptide of the lipid II PG precursor using glycylyl-charged tRNA molecules as substrates (Favrot et al., 2016). The pentaglycine modification crosslinks PG glycan chains (Favrot et al., 2016). Therefore, it is tempting to speculate that one or both of ExoG and ExoI rather than being involved in acetylation of the spore coat repeat unit could be involved in glycine addition to amino group(s) in the repeat unit. In this context, we speculate that the amino group added by ExoH could serve as an acceptor for glycine transfer. This is also consistent with the absence of glycine modified sugars after acid hydrolysis of the spore coat polysaccharide (Holkenbrink et al., 2014). Amino acid modified sugars, in this case with serine, have also been identified in the K40 capsular polysaccharide of *E. coli* O8 and the modification demonstrated to be essential for the polymerisation of the capsular repeat unit (Amor, Yethon, Monteiro, & Whitfield, 1999).

Two Exo proteins are important, but not essential, for formation of phase-bright spores and by implication spore coat synthesis: ExoF (Holkenbrink et al., 2014) and ExoN (here). ExoN is a putative serine O-acetyltransferase, which are commonly involved in the first step

of cysteine synthesis from serine. *M. xanthus* utilises amino acids and lipids as carbon and energy sources and does not grow on carbohydrates because it lacks required catabolic enzymes (Dworkin, 1962; Hemphill & Zahler, 1968; Watson & Dworkin, 1968). During glycerol-induced sporulation, genes for large portions of the tricarboxylic acid cycle are downregulated, whereas genes for the glyoxylate shunt and gluconeogenesis are upregulated (Müller et al., 2010), for example, the activity of at least six enzymes putatively involved in synthesis of the major spore coat component UDP-GalNAc increases in response to glycerol addition prior to shortening of cells (Filer, Kindler, & Rosenberg, 1977a). Given these metabolic changes, we speculate that ExoN may contribute to synthesis of monosaccharides or other metabolites important for spore coat polysaccharide synthesis, and therefore, without ExoN, cells may lack this precursor(s). The *M. xanthus* genome encodes two additional serine O-acetyltransferase homologs (MXAN_1572 and MXAN_7449), which may function redundantly with ExoN, and therefore, the Δ exoN mutant is still able to form some phase-bright spores. Similarly, the partially dispensable ExoF, which is a putative gluconeogenesis factor, has been suggested to be important for biosynthesis of activated sugar precursors (Holkenbrink et al., 2014).

After the repeat unit has been synthesised on the cytoplasmic side of the IM, translocation occurs via the Wzx flippase homolog ExoM. In the periplasm, the Wzy polymerase ExoJ elongates the chain with the help/control of the Wzc homolog formed by the integral membrane protein ExoC and the cytoplasmic ExoD tyrosine kinase, which could regulate ExoC activity (Kimura et al., 2011). Subsequently, the polysaccharide chain is transported to the cell surface via the Wza OPX homolog ExoA. The Nfs machinery modifies the Exo-generated polysaccharide by an unknown mechanism to generate shorter polysaccharide chains and the rigid polysaccharide spore coat. How, where and when the Nfs proteins do this is not known.

Disruption of the synthesis of one polysaccharide can have pleiotropic effects on the synthesis of other polysaccharidic molecules. It was previously shown that *M. xanthus* cells lacking the PHPT WbaP for LPS O-antigen synthesise EPS and spore coat and has a normal cell morphology; similarly, mutants that do not synthesise EPS, synthesise LPS and the spore coat polysaccharide (Holkenbrink et al., 2014; Lu et al., 2005; Pérez-Burgos et al., 2019). Here, we show that during growth mutants that are unable to synthesise the spore coat polysaccharide synthesise WT levels of LPS and EPS and have a normal cell morphology in the absence of glycerol. Together, these observations suggest the existence of dedicated biosynthesis machineries for LPS, EPS and spore coat polysaccharide synthesis.

A fascinating aspect of the sporulation process in *M. xanthus* is that the PG is degraded during spore morphogenesis (Bui et al., 2009). It has been suggested that the spore coat protects cells from bursting due to intracellular turgor in the absence of PG (Bui et al., 2009; Müller et al., 2012). Therefore, we predict that the removal of PG must be closely coordinated with synthesis of the spore coat polysaccharide. Previous research on chemical induction of

sporulation in the *exoA-I* mutants showed that mutant cells initiate the sporulation process with cell shortening and widening. However, at a certain point the sporulation process is aborted and cells regain rod-shape even in the continued presence of glycerol. Of note, after abortion of the sporulation process, many cells display severe morphological defects including branching, formation of spiral-shaped cells and formation of large spherical cells (Holkenbrink et al., 2014; Müller et al., 2012). Here, we observed similar morphological defects in mutants impaired in spore coat polysaccharide synthesis after chemical induction of sporulation. Interestingly, cells lacking the PHPT ExoE have less severe shape defects after 4 and 24 hr of glycerol-induction than mutants lacking enzymes suggested to act downstream of the priming step. These observations have two implications. First, we speculate that the abortion of the sporulation process in the *exo* mutants (as opposed to cell lysis due to lack of PG as well as spore coat) is caused by a coupling between spore coat polysaccharide synthesis and the PG removal process. Therefore, in the absence of proper spore coat polysaccharide synthesis, PG would not be completely removed and cells regain rod-shape through de novo synthesis of PG. Because, the Exo proteins are not important for PG synthesis during growth, we speculate that the coupling between spore coat polysaccharide synthesis and the PG removal process is regulatory rather than involving shared proteins. Second, we speculate that in the absence of ExoE PHPT activity, Und-P is not sequestered in intermediates for spore coat polysaccharide biosynthesis, and therefore, PG can be resynthesised. By contrast, in the Δ exoJ-M, O-P mutants (here) and the previously described Δ exoA-D, G-I (Holkenbrink et al., 2014) mutants, Und-P would be sequestered in intermediates for spore coat polysaccharide, thus, titrating Und-P away from PG metabolism resulting in more cells with an abnormal shape. A future goal will be to understand how spore coat polysaccharide synthesis and PG removal are coordinated.

Our analysis of the taxonomic distribution of the *exo* and *nfs* gene clusters lend support to the notion that the spore coat could be synthesised by a different mechanism in sporulating Cystobacterineae compared to sporulating Nannocystineae and Sorangineae. Based on a comparison of gene content in four fruiting body and sporulating Myxococcales (*M. xanthus*, *Stigmatella aurantiaca*, *H. ochraceum*, *S. cellulosum*), we previously reported that key developmental regulators in *M. xanthus* are not widely conserved outside the Cystobacterineae (Huntley et al., 2011). This finding also suggests that the genetic programmes for fruiting body formation and sporulation in *M. xanthus* and *S. aurantiaca* are highly similar but significantly different from the genetic programme directing fruiting body formation in *S. cellulosum* and *H. ochraceum* (Huntley et al., 2011). The distribution of the *exo* and *nfs* genes supports this scenario also at the level of the spore coat formation. Thus, it remains an open question whether fruiting body formation including sporulation in the Myxococcales is the result of convergent evolution or divergent evolution from a shared primordial genetic programme (Huntley et al., 2011).

4 | EXPERIMENTAL PROCEDURES

4.1 | Strains and cell growth

M. xanthus cells were grown in 1% CTT (1% (w/v) Bacto Casitone, 10 mM of Tris-HCl pH 8.0, 1 mM of K_2HPO_4/KH_2PO_4 pH 7.6 and 8 mM of $MgSO_4$) liquid medium or on 1.5% agar supplemented with 1% CTT at 32°C (Hodgkin & Kaiser, 1977). Oxytetracycline and kanamycin were used at final concentrations of 10 µg/ml and 50 µg/ml, respectively. All *M. xanthus* strains are derivatives of the WT strain DK1622 (Kaiser, 1979). *M. xanthus* strains and plasmids used in this work are listed in Tables 2 and 3, respectively. In-frame deletions were generated as described previously

(Shi et al., 2008) and plasmids for complementation experiments were integrated in a single copy by site-specific recombination into the Mx8 *attB* site. All in-frame deletions and plasmid integrations were verified by PCR. Plasmids were propagated in *E. coli* Mach1 and DH5α.

E. coli and *S. enterica* serovar Typhimurium strains were grown in Luria-Bertani medium (LB) (10 mg of tryptone ml⁻¹, 5 mg of yeast extract/ml; 5 mg of NaCl/ml) at 37°C. When required, medium was supplemented with ampicillin, tetracycline, kanamycin or chloramphenicol at final concentrations of 100, 20, 40 and 30 µg/ml, respectively. Electroporation was used to introduce plasmids for heterologous complementation into MSS2, XBF1 and MV501 strains (Dower, Miller, & Ragsdale, 1988).

TABLE 2 Strains used in this work

Strain	Genotype	Reference
<i>M. xanthus</i>		
DK1622	Wildtype	(Kaiser, 1979)
DK10410	Δ <i>pilA</i>	(Wu & Kaiser, 1997)
SA5923	Δ <i>aglQ</i>	(Jakobczak, Keilberg, Wuichet, & Søgaard-Andersen, 2015)
SW501	<i>difE::Km^r</i>	(Yang et al., 1998)
SA7450	Δ <i>wbaP</i>	(Pérez-Burgos et al., 2019)
SA7495	Δ <i>exoE</i>	(Pérez-Burgos et al., 2019)
SA8534	Δ <i>exoE attB::pMP136 (P_{nat} exoE)</i>	This study
SA7455	ΔMXAN_3026	This study
SA7489	ΔMXAN_3026 <i>attB::pJJ18 (P_{nat} MXAN_3026)</i>	This study
SA8507	ΔMXAN_3260	This study
SA8502	ΔMXAN_3260 <i>attB::pJJ18 (P_{nat} MXAN_3260)</i>	This study
SA8516	ΔMXAN_3027	This study
SA8523	ΔMXAN_3027 <i>attB::pMP125 (P_{nat} MXAN_3027)</i>	This study
SA8519	ΔMXAN_3259	This study
SA8522	ΔMXAN_3259 <i>attB::pMP126 (P_{nat} MXAN_3259)</i>	This study
SA8527	ΔMXAN_3261	This study
SA8528	ΔMXAN_3261 <i>attB::pMP133 (P_{nat} MXAN_3261)</i>	This study
SA8547	ΔMXAN_3262	This study
SA8548	ΔMXAN_3262 <i>attB::pMP134 (P_{nat} MXAN_3262)</i>	This study
SA8517	ΔMXAN_3263	This study
SA8531	ΔMXAN_3263 <i>attB::pMP135 (P_{nat} MXAN_3263)</i>	This study
<i>E. coli</i>		
DH5α	F ⁻ φ80 <i>lacZ</i> ΔM15 <i>endA recA hsdR(r_K⁻ m_K⁻) nupG thi glnV deoR gyrA relA1 Δ(lacZYA-argF)U169</i>	Lab stock
Mach1	Δ <i>recA1398 endA1 tonA</i> φ80Δ <i>lacM15 ΔlacX74 hsdR(r_K⁻ m_K⁺)</i>	Invitrogen
XBF1	W3110, Δ <i>wcaJ::aph</i> , Km ^r	(Patel et al., 2012)
VW187	O7:K1, clinical isolate	(Valvano & Crosa, 1984)
MV501	VW187, <i>wecA::Tn10 Tc^r</i>	(Alexander & Valvano, 1994)
<i>Salmonella</i>		
LT2	WT, <i>S. enterica</i> serovar Typhimurium	S. Maloy
MSS2	LT2, Δ <i>wbaP::cat</i> Cm ^r	(Saldías et al., 2008)

TABLE 3 Plasmids used in this work

Plasmid	Description	Reference
pBJ114	Km ^r <i>galK</i>	(Julien, Kaiser, & Garza, 2000)
pSWU30	Tet ^r	(Wu & Kaiser, 1997)
pBAD24	Cloning vector with arabinose-inducible promoter, Amp ^r	(Guzman, Belin, Carson, & Beckwith, 1995)
pBADNTF	pBAD24 for N-terminal FLAG fusion, Amp ^r	(Marolda, Vicarioli, & Valvano, 2004)
pLA3	pBADNTF, <i>wcaJ</i> , Amp ^r	(Furlong et al., 2015)
pSM13	pUC18, <i>wbaP</i> from <i>S. enterica</i> Ty2 containing a 1 bp deletion at position 583 and a 2 bp deletion at position 645. This causes a frame shift at <i>WbaP</i> I194 and frame restoration at Y215, Amp ^r	(Saldías et al., 2008)
pJD132	pBluescript SK, <i>wbaP</i> and flanking sequences from <i>E. coli</i> O9:K30, Amp ^r	(Schäffer, Wugeditsch, Messner, & Whitfield, 2002)
pWQ499	pKV102 containing <i>rscAK30</i> , Tet ^r	C. Whitfield
pMAV11	pACYC184, containing <i>rfe</i> , Cm ^r	(Alexander & Valvano, 1994)
pSEF88	pBAD24 expressing _{FLAG} WecP from <i>Aeromonas hydrophila</i> AH-3, Amp ^r	S. Furlong
pGEMT-Gne	pGEMT encoding <i>gne</i> from <i>Aeromonas hydrophila</i> AH-3, Amp ^r	(Canals et al., 2006)
pJJ5	pBJ114, in-frame deletion construct for <i>MXAN_3026</i> Km ^r	This work
pJJ18	pSWU30, P _{nat} <i>MXAN_3026</i> Tet ^r	This work
pMP113	pBJ114, in-frame deletion construct for <i>MXAN_3260</i> Km ^r	This work
pMP118	pSWU30, P _{nat} <i>MXAN_3260</i> Tet ^r	This work
pMP120	pBJ114, in-frame deletion construct for <i>MXAN_3027</i> Km ^r	This work
pMP121	pBJ114, in-frame deletion construct for <i>MXAN_3259</i> Km ^r	This work
pMP123	pBJ114, in-frame deletion construct for <i>MXAN_3263</i> Km ^r	This work
pMP125	pSWU30, P _{nat} <i>MXAN_3027</i> Tet ^r	This work
pMP126	pSWU30, P _{nat} <i>MXAN_3259</i> Tet ^r	This work
pMP131	pBJ114, in-frame deletion construct for <i>MXAN_3261</i> Km ^r	This work
pMP133	pSWU30, P _{nat} <i>MXAN_3261</i> Tet ^r	This work
pMP134	pSWU30, P _{nat} <i>MXAN_3262</i> Tet ^r	This work
pMP135	pSWU30, P _{nat} <i>MXAN_3263</i> Tet ^r	This work
pMP136	pSWU30, P _{nat} <i>exoE</i> Tet ^r	This work
pMP144	pBJ114, in-frame deletion construct for N-terminal <i>MXAN_3262</i> Km ^r	This work
pMP147	pBADNTF, <i>exoE</i> Amp ^r	This work
pMP158	pBAD24, <i>exoE</i> Amp ^r	This work

4.2 | Motility assays

Exponentially growing cultures of *M. xanthus* were harvested (6,000 g, room temperature (RT)) and resuspended in 1% CTT to a calculated density of 7×10^9 cells/ml. About 5 μ l aliquots of cell suspensions were spotted on 0.5% and 1.5% agar supplemented with 0.5% CTT and incubated at 32°C. Cells were visualised after 24 hr using a M205FA Stereomicroscope (Leica) and imaged using a Hamamatsu ORCA-flash V2 Digital CMOS camera (Hamamatsu Photonics). Pictures were analysed using Metamorph® v 7.5 (Molecular Devices).

4.3 | Glycerol-induced sporulation assay

Assay was performed as described (Müller et al., 2010) with a slightly modified protocol. Briefly, cells were cultivated in 10 ml of CTT and induced at a density of 3×10^8 cells/ml with glycerol to a final

concentration of 0.5 M. At 0, 4 and 24 hr cell morphology was observed by placing 5 μ l of cells on a thin 1.5% agar TPM pad on a slide, immediately covered with a coverslip and imaged. To determine the efficiency of glycerol-induced sporulation, 5 ml of the culture were harvested (10 min, 4,150 g, RT) after 24 hr induction, resuspended in 1 ml of sterile water, incubated at 50°C for 2 hr, and then, sonicated with 30 pulses, pulse 50%, amplitude 75% with a UP200St sonifier and microtip (Hielscher). About 5 μ l of the treated samples were placed on a glass slide, covered with a coverslip and imaged. Sporulation levels were determined as the number of sonication- and heat-resistant spores relative to WT using a Helber bacterial counting chamber (Hawksley, UK).

4.4 | Development

Exponentially growing *M. xanthus* cultures were harvested (3 min, 6,000 g at RT) and resuspended in MC7 buffer (10 mM of MOPS pH

7.0, 1 mM of CaCl₂) to a calculated density of 7×10^9 cells/ml. About 10 μ l of aliquots of cells were placed on TPM agar (10 mM of Tris-HCl pH 7.6, 1 mM of K₂HPO₄/KH₂PO₄ pH 7.6, 8 mM of MgSO₄), while for development in submerged culture, 50 μ l of aliquots were mixed with 350 μ l of MC7 buffer and placed in a 24-well polystyrene plate (Falcon). Cells were visualised at the indicated time points using a M205FA Stereomicroscope (Leica) and imaged using a Hamamatsu ORCA-flash V2 Digital CMOS camera (Hamamatsu Photonics) and a DMi8 Inverted microscope and DFC9000 GT camera (Leica). After 120 hr, cells were collected and incubated at 50°C for 2 hr, and then, sonicated as described for chemically induced spores. Sporulation levels were determined as the number of sonication- and heat-resistant spores relative to WT using a Helber bacterial counting chamber (Hawksley, UK).

4.5 | Detection of EPS accumulation

EPS accumulation was detected as in (Pérez-Burgos et al., 2019). Briefly, exponentially growing cells were harvested, and resuspended in 1% CTT to a calculated density of 7×10^9 cells/ml. About 20 μ l aliquots of cell suspensions were placed on 0.5% CTT 0.5% agar supplemented with 40 μ g/ml Congo red. The plates were incubated at 32°C and documented at 24 hr.

4.6 | LPS extraction and detection

LPS was extracted from *M. xanthus* and visualised by Emerald staining as previously described (Pérez-Burgos et al., 2019). LPS from *S. enterica* and *E. coli* was extracted and visualised by silver staining as previously described (Marolda, Lahiry, Vines, Saldias, & Valvano, 2006; Pérez-Burgos et al., 2019). For *S. enterica*, O-antigen was detected by immunoblot using rabbit *Salmonella* O antiserum group B (Difco, Beckton Dickinson ref. number 229481) (1:500) and the secondary antibody IRDye 800CW goat α -rabbit immunoglobulin G (1:10,000) (LI-COR) (Pérez-Burgos et al., 2019).

4.7 | Cell length determination

About 5 μ l aliquots of exponentially growing cultures were spotted on 1.5% agar supplemented with 0.2% CTT, immediately covered with a cover slide, imaged using a DMi8 Inverted microscope and DFC9000 GT camera (Leica) and cell length determined and visualised as described (Pérez-Burgos et al., 2019).

4.8 | Detection of colanic acid biosynthesis

E. coli strains were grown at 37°C overnight on LB plates with antibiotics plus 0.2% (w/v) arabinose, when needed, to induce protein synthesis. Incubation was prolonged to 24–48 hr at RT to visualise the mucoid phenotype (Furlong et al., 2015).

4.9 | Immunoblot analysis

Total cell extracts were prepared and FLAG-tagged proteins detected by immunoblot analysis as previously described using α -FLAG M2 monoclonal antibody (Sigma) (1:10,000) and a secondary antibody, IRDye 800CW Goat α -Mouse IgG (H + L), 0.5 mg (LI-COR) (1:10,000) (Pérez-Burgos et al., 2019).

4.10 | Bioinformatics

The KEGG SSDB (Sequence Similarity DataBase) (Kanehisa & Goto, 2000) database was used to identify Wzx homologs (PF01943-Polysacc_synt and PF13440-Polysacc_synt_3) and Wzy_C (PF04932) domain containing proteins. KEGG SSDB was also used to identify homologs of Exo, Nfs and Glt proteins in other Myxococcales using a reciprocal best BlastP hit method. UniProt (The UniProt Consortium, 2019) and the KEGG databases were used to assign functions to proteins (Figure 1d; Table S1). SMART (smart.embl-heidelberg.de) (Letunic, Doerks, & Bork, 2015) and the Carbohydrate Active Enzymes (CAZy) database (<http://www.cazy.org/>) (Lombard, Golaconda Ramulu, Drula, Coutinho, & Henrissat, 2014) were used to identify protein domains. Membrane topology was assessed by TMHMM v2.0 (Sonnhammer, Heijne, & Krogh, 1998) and SPOCTOPUS (Viklund, Bernsel, Skwark, & Elofsson, 2008). Structure-based searches with HHPred were done using the <https://toolkit.tuebingen.mpg.de/> (Zimmermann et al., 2018). Clustal Omega (Chojnacki, Cowley, Lee, Foix, & Lopez, 2017) was used to align protein sequences.

4.11 | Statistics

Statistical analyses were performed using SigmaPlot v14. All data sets were tested for a normal distribution using a Shapiro-Wilk test. For all data sets without a normal distribution, the Mann-Whitney test was applied to test for significant differences.

ACKNOWLEDGEMENTS

The authors thank Jana Jung for constructing SA7455 and SA7489, Sarah Furlong for the gift of pSEF88, Marco Herfurth for the help and discussions with the gene co-occurrence studies and Dobromir Szadkowski for providing the script and guidance with the Matlab analysis. This work was supported by Deutsche Forschungsgemeinschaft (DFG, German Research Council) within the framework of the SFB987 'Microbial Diversity in Environmental Signal Response' as well as by the Max Planck Society.

CONFLICT OF INTEREST

The authors declare no conflict of interest.

DATA AVAILABILITY STATEMENT

The data that support the findings of this study are available from the corresponding author upon request.

ORCID

Miguel A. Valvano  <https://orcid.org/0000-0001-8229-3641>

Lotte Søgaard Andersen  <https://orcid.org/0000-0002-0674-0013>

REFERENCES

- Agrebi, R., Wartel, M., Brochier-Armanet, C., & Mignot, T. (2015). An evolutionary link between capsular biogenesis and surface motility in bacteria. *Nature Reviews Microbiology*, *13*, 318–326. <https://doi.org/10.1038/nrmicro3431>
- Alexander, D. C., & Valvano, M. A. (1994). Role of the *rfe* gene in the biosynthesis of the *Escherichia coli* O7-specific lipopolysaccharide and other O-specific polysaccharides containing N-acetylglucosamine. *Journal of Bacteriology*, *176*, 7079–7084. <https://doi.org/10.1128/JB.176.22.7079-7084.1994>
- Amor, P. A., Yethon, J. A., Monteiro, M. A., & Whitfield, C. (1999). Assembly of the K40 antigen in *Escherichia coli*: Identification of a novel enzyme responsible for addition of L-serine residues to the glycan backbone and its requirement for K40 polymerization. *Journal of Bacteriology*, *181*, 772–780. <https://doi.org/10.1128/JB.181.3.772-780.1999>
- Beccafà, A., Ovchinnikova, O. G., Datta, N., Mattinen, L., Knapska, K., Radziejewska-Lebrecht, J., ... Skurnik, M. (2015). Structure and genetic basis of *Yersinia similis* serotype O:9 O-specific polysaccharide. *Innate Immunity*, *21*, 3–16.
- Bui, N. K., Gray, J., Schwarz, H., Schumann, P., Blanot, D., & Vollmer, W. (2009). The peptidoglycan sacculus of *Myxococcus xanthus* has unusual structural features and is degraded during glycerol-induced myxospore development. *Journal of Bacteriology*, *191*, 494–505. <https://doi.org/10.1128/JB.00608-08>
- Burrows, L. L., & Lam, J. S. (1999). Effect of *wzx* (*rfbX*) mutations on A-band and B-band lipopolysaccharide biosynthesis in *Pseudomonas aeruginosa* O5. *Journal of Bacteriology*, *181*, 973–980. <https://doi.org/10.1128/JB.181.3.973-980.1999>
- Canals, R., Jimenez, N., Vilches, S., Regue, M., Merino, S., & Tomas, J. M. (2006). The UDP N-acetylgalactosamine 4-epimerase gene is essential for mesophilic *Aeromonas hydrophila* serotype O34 virulence. *Infection and Immunity*, *74*, 537–548. <https://doi.org/10.1128/IAI.74.1.537-548.2006>
- Chamot-Rooke, J., Rousseau, B., Lanternier, F., Mikaty, G., Mairey, E., Malosse, C., ... Dumenil, G. (2007). Alternative *Neisseria* spp. type IV pilin glycosylation with a glyceramido acetamido trideoxyhexose residue. *Proceedings of the National Academy of Sciences of the United States of America*, *104*, 14783–14788. <https://doi.org/10.1073/pnas.0705335104>
- Chojnacki, S., Cowley, A., Lee, J., Foix, A., & Lopez, R. (2017). Programmatic access to bioinformatics tools from EMBL-EBI update: 2017. *Nucleic Acids Research*, *45*, W550–W553. <https://doi.org/10.1093/nar/gkx273>
- Curtis, P. D., Atwood, J. 3rd, Orlando, R., & Shimkets, L. J. (2007). Proteins associated with the *Myxococcus xanthus* extracellular matrix. *Journal of Bacteriology*, *189*, 7634–7642. <https://doi.org/10.1128/JB.01007-07>
- dos Santos, D. F. K., Kyaw, C. M., De Campos, T. A., Miller, R. N. G., Noronha, E. F., Bustamante, M. M. D. C., & Kruger, R. (2014). The family cystobacteraceae. In E. Rosenberg, E. F. DeLong, S. Lory, E. Stackebrandt, & F. Thompson (Eds.), *The prokaryotes: Deltaproteobacteria and epsilonproteobacteria* (pp. 19–40). Berlin, Germany: Springer, Berlin Heidelberg.
- Dower, W. J., Miller, J. F., & Ragsdale, C. W. (1988). High efficiency transformation of *E. coli* by high voltage electroporation. *Nucleic Acids Research*, *16*, 6127–6145. <https://doi.org/10.1093/nar/16.13.6127>
- Downard, J. S., & Zusman, D. R. (1985). Differential expression of protein S genes during *Myxococcus xanthus* development. *Journal of Bacteriology*, *161*, 1146–1155. <https://doi.org/10.1128/JB.161.3.1146-1155.1985>
- Driks, A., & Eichenberger, P. (2016). The spore coat. *Microbiology Spectrum*, *4*. <https://doi.org/10.1128/microbiolspec.TBS-0023-2016>
- Dworkin, M. (1962). Nutritional requirements for vegetative growth of *Myxococcus xanthus*. *Journal of Bacteriology*, *84*, 250–257. <https://doi.org/10.1128/JB.84.2.250-257.1962>
- Dworkin, M., & Gibson, S. M. (1964). A system for studying microbial morphogenesis: Rapid formation of microcysts in *Myxococcus xanthus*. *Science*, *146*, 243–244. <https://doi.org/10.1126/science.146.3641.243>
- Dworkin, M., & Voelz, H. (1962). The formation and germination of microcysts in *Myxococcus xanthus*. *Journal of General Microbiology*, *28*, 81–85. <https://doi.org/10.1099/00221287-28-1-81>
- Favrot, L., Blanchard, J. S., & Vergnolle, O. (2016). Bacterial GCN5-related N-acetyltransferases: From resistance to regulation. *Biochemistry*, *55*, 989–1002.
- Felsenstein, J. (1985). Confidence-limits on phylogenies—An approach using the bootstrap. *Evolution*, *39*, 783–791. <https://doi.org/10.1111/j.1558-5646.1985.tb00420.x>
- Filer, D., Kindler, S. H., & Rosenberg, E. (1977a). Myxospore coat synthesis in *Myxococcus xanthus*: Enzymes associated with uridine 5'-diphosphate-N-acetylgalactosamine formation during myxospore development. *Journal of Bacteriology*, *131*, 745–750. <https://doi.org/10.1128/JB.131.3.745-750.1977>
- Filer, D., White, D., Kindler, S. H., & Rosenberg, E. (1977b). Myxospore coat synthesis in *Myxococcus xanthus*: In vivo incorporation of acetate and glycine. *Journal of Bacteriology*, *131*, 751–758. <https://doi.org/10.1128/JB.131.3.751-758.1977>
- Flärdh, K., & Buttner, M. J. (2009). *Streptomyces* morphogenetics: Dissecting differentiation in a filamentous bacterium. *Nature Reviews Microbiology*, *7*, 36–49. <https://doi.org/10.1038/nrmicro1968>
- Fudou, R., Jojima, Y., Iizuka, T., & Yamanaka, S. (2002). *Haliangium ochraceum* gen. nov., sp. nov. and *Haliangium tepidum* sp. nov.: Novel moderately halophilic myxobacteria isolated from coastal saline environments. *Journal of General and Applied Microbiology*, *48*, 109–116. <https://doi.org/10.2323/jgam.48.109>
- Furlong, S. E., Ford, A., Albarnez-Rodriguez, L., & Valvano, M. A. (2015). Topological analysis of the *Escherichia coli* WcaJ protein reveals a new conserved configuration for the polyisoprenyl-phosphate hexose-1-phosphate transferase family. *Scientific Reports*, *5*, 9178. <https://doi.org/10.1038/srep09178>
- Garcia, R., Gemperlein, K., & Müller, R. (2014). *Minicystis rosea* gen. nov., sp. nov., a polyunsaturated fatty acid-rich and steroid-producing soil myxobacterium. *International Journal of Systematic and Evolutionary Microbiology*, *64*, 3733–3742. <https://doi.org/10.1099/ij.s.0.068270-0>
- Garcia, R., & Müller, R. (2014a). The family myxococcaceae. In E. Rosenberg, E. F. DeLong, S. Lory, E. Stackebrandt, & F. Thompson (Eds.), *The prokaryotes: Deltaproteobacteria and epsilonproteobacteria* (pp. 191–212). Berlin, Germany: Springer, Berlin Heidelberg.
- Garcia, R., & Müller, R. (2014b). The family polyangiaceae. In E. Rosenberg, E. F. DeLong, S. Lory, E. Stackebrandt, & F. Thompson (Eds.), *The prokaryotes: Deltaproteobacteria and epsilonproteobacteria* (pp. 247–279). Berlin, Germany: Springer, Berlin Heidelberg.
- Giglio, K. M., Zhu, C., Klunder, C., Kummer, S., & Garza, A. G. (2015). The enhancer binding protein Nla6 regulates developmental genes that are important for *Myxococcus xanthus* sporulation. *Journal of Bacteriology*, *197*, 1276–1287. <https://doi.org/10.1128/JB.02408-14>
- Glover, K. J., Weerapana, E., Chen, M. M., & Imperiali, B. (2006). Direct biochemical evidence for the utilization of UDP-bacillosamine by PglC, an essential glycosyl-1-phosphate transferase in the *Campylobacter jejuni* N-linked glycosylation pathway. *Biochemistry*, *45*, 5343–5350.

- Guzman, L. M., Belin, D., Carson, M. J., & Beckwith, J. (1995). Tight regulation, modulation, and high-level expression by vectors containing the arabinose PBAD promoter. *Journal of Bacteriology*, *177*, 4121–4130. <https://doi.org/10.1128/JB.177.14.4121-4130.1995>
- Hemphill, H. E., & Zahler, S. A. (1968). Nutrition of *Myxococcus xanthus* FBa and some of its auxotrophic mutants. *Journal of Bacteriology*, *95*, 1011–1017. <https://doi.org/10.1128/JB.95.3.1011-1017.1968>
- Hodgkin, J., & Kaiser, D. (1977). Cell-to-cell stimulation of movement in nonmotile mutants of *Myxococcus*. *Proceedings of the National Academy of Sciences of the United States of America*, *74*, 2938–2942. <https://doi.org/10.1073/pnas.74.7.2938>
- Holkenbrink, C., Hoiczky, E., Kahnt, J., & Higgs, P. I. (2014). Synthesis and assembly of a novel glycan layer in *Myxococcus xanthus* spores. *Journal of Biological Chemistry*, *289*, 32364–32378.
- Hug, I., & Feldman, M. F. (2011). Analogies and homologies in lipopolysaccharide and glycoprotein biosynthesis in bacteria. *Glycobiology*, *21*, 138–151. <https://doi.org/10.1093/glycob/cwq148>
- Huntley, S., Hamann, N., Wegener-Feldbrugge, S., Treuner-Lange, A., Kube, M., Reinhardt, R., ... Sogaard-Andersen, L. (2011). Comparative genomic analysis of fruiting body formation in Myxococcales. *Molecular Biology and Evolution*, *28*, 1083–1097. <https://doi.org/10.1093/molbev/msq292>
- Inouye, M., Inouye, S., & Zusman, D. R. (1979a). Biosynthesis and self-assembly of protein S, a development specific protein of *Myxococcus xanthus*. *Proceedings of the National Academy of Sciences of the United States of America*, *76*, 209–213. <https://doi.org/10.1073/pnas.76.1.209>
- Inouye, M., Inouye, S., & Zusman, D. R. (1979b). Gene expression during development of *Myxococcus xanthus*: Pattern of protein synthesis. *Developmental Biology*, *68*, 579–591. [https://doi.org/10.1016/0012-1606\(79\)90228-8](https://doi.org/10.1016/0012-1606(79)90228-8)
- Jakobczak, B., Keilberg, D., Wuichet, K., & Sogaard-Andersen, L. (2015). Contact- and protein transfer-dependent stimulation of assembly of the gliding motility machinery in *Myxococcus xanthus*. *PLoS Genetics*, *11*, e1005341. <https://doi.org/10.1371/journal.pgen.1005341>
- John, R. A. (1995). Pyridoxal phosphate-dependent enzymes. *Biochimica et Biophysica Acta*, *1248*, 81–96. [https://doi.org/10.1016/0167-4838\(95\)00025-P](https://doi.org/10.1016/0167-4838(95)00025-P)
- Jorgenson, M. A., Kannan, S., Laubacher, M. E., & Young, K. D. (2016). Dead-end intermediates in the enterobacterial common antigen pathway induce morphological defects in *Escherichia coli* by competing for undecaprenyl phosphate. *Molecular Microbiology*, *100*, 1–14.
- Jorgenson, M. A., & Young, K. D. (2016). Interrupting biosynthesis of O antigen or the lipopolysaccharide core produces morphological defects in *Escherichia coli* by sequestering undecaprenyl phosphate. *Journal of Bacteriology*, *198*, 3070–3079. <https://doi.org/10.1128/JB.00550-16>
- Julien, B., Kaiser, A. D., & Garza, A. (2000). Spatial control of cell differentiation in *Myxococcus xanthus*. *Proceedings of the National Academy of Sciences of the United States of America*, *97*, 9098–9103. <https://doi.org/10.1073/pnas.97.16.9098>
- Kaiser, D. (1979). Social gliding is correlated with the presence of pili in *Myxococcus xanthus*. *Proceedings of the National Academy of Sciences of the United States of America*, *76*, 5952–5956. <https://doi.org/10.1073/pnas.76.11.5952>
- Kanehisa, M., & Goto, S. (2000). KEGG: Kyoto encyclopedia of genes and genomes. *Nucleic Acids Research*, *28*, 27–30. <https://doi.org/10.1093/nar/28.1.27>
- Kimura, Y., Yamashita, S., Mori, Y., Kitajima, Y., & Takegawa, K. (2011). A *Myxococcus xanthus* bacterial tyrosine kinase, BtkA, is required for the formation of mature spores. *Journal of Bacteriology*, *193*, 5853–5857. <https://doi.org/10.1128/JB.05750-11>
- Komano, T., Furuichi, T., Teintze, M., Inouye, M., & Inouye, S. (1984). Effects of deletion of the gene for the development-specific protein S on differentiation in *Myxococcus xanthus*. *Journal of Bacteriology*, *158*, 1195–1197. <https://doi.org/10.1128/JB.158.3.1195-1197.1984>
- Komano, T., Inouye, S., & Inouye, M. (1980). Patterns of protein production in *Myxococcus xanthus* during spore formation induced by glycerol, dimethyl sulfoxide, and phenethyl alcohol. *Journal of Bacteriology*, *144*, 1076–1082. <https://doi.org/10.1128/JB.144.3.1076-1082.1980>
- Konvalova, A., Petters, T., & Sogaard-Andersen, L. (2010). Extracellular biology of *Myxococcus xanthus*. *FEMS Microbiology Reviews*, *34*, 89–106.
- Kottel, R. H., Bacon, K., Clutter, D., & White, D. (1975). Coats from *Myxococcus xanthus*: Characterization and synthesis during myxospore differentiation. *Journal of Bacteriology*, *124*, 550–557. <https://doi.org/10.1128/JB.124.1.550-557.1975>
- Kumar, S., Stecher, G., & Tamura, K. (2016). MEGA7: molecular evolutionary genetics analysis version 7.0 for bigger datasets. *Molecular Biology and Evolution*, *33*, 1870–1874. <https://doi.org/10.1093/molbev/msw054>
- Lee, B., Mann, P., Grover, V., Treuner-Lange, A., Kahnt, J., & Higgs, P. I. (2011). The *Myxococcus xanthus* spore cuticula protein C is a fragment of FibA, an extracellular metalloprotease produced exclusively in aggregated cells. *PLoS ONE*, *6*, e28968. <https://doi.org/10.1371/journal.pone.0028968>
- Lehrman, M. A. (1994). A family of UDP-GlcNAc/MurNAc: Polysiprenol-P GlcNAc/MurNAc-1-P transferases. *Glycobiology*, *4*, 768–771.
- Leng, X., Zhu, W., Jin, J., & Mao, X. (2011). Evidence that a chaperone-usher-like pathway of *Myxococcus xanthus* functions in spore coat formation. *Microbiology*, *157*, 1886–1896. <https://doi.org/10.1099/mic.0.047134-0>
- Letunic, I., Doerks, T., & Bork, P. (2015). SMART: Recent updates, new developments and status in 2015. *Nucleic Acids Research*, *43*, D257–D260. <https://doi.org/10.1093/nar/gku949>
- Licking, E., Gorski, L., & Kaiser, D. (2000). A common step for changing cell shape in fruiting body and starvation-independent sporulation in *Myxococcus xanthus*. *Journal of Bacteriology*, *182*, 3553–3558.
- Lombard, V., Golaconda Ramulu, H., Drula, E., Coutinho, P. M., & Henrissat, B. (2014). The carbohydrate-active enzymes database (CAZy) in 2013. *Nucleic Acids Research*, *42*, D490–D495. <https://doi.org/10.1093/nar/gkt1178>
- Lu, A., Cho, K., Black, W. P., Duan, X. Y., Lux, R., Yang, Z., ... Shi, W. (2005). Exopolysaccharide biosynthesis genes required for social motility in *Myxococcus xanthus*. *Molecular Microbiology*, *55*, 206–220. <https://doi.org/10.1111/j.1365-2958.2004.04369.x>
- Luciano, J., Agrebi, R., Le Gall, A. V., Wartel, M., Fiegna, F., Ducret, A., ... Mignot, T. (2011). Emergence and modular evolution of a novel motility machinery in bacteria. *PLoS Genetics*, *7*, e1002268. <https://doi.org/10.1371/journal.pgen.1002268>
- Marolda, C. L., Lahiry, P., Vines, E., Saldias, S., & Valvano, M. A. (2006). Micromethods for the characterization of lipid A-core and O-antigen lipopolysaccharide. *Methods in Molecular Biology*, *347*, 237–252.
- Marolda, C. L., Vicarioli, J., & Valvano, M. A. (2004). Wzx proteins involved in biosynthesis of O antigen function in association with the first sugar of the O-specific lipopolysaccharide subunit. *Microbiology*, *150*, 4095–4105. <https://doi.org/10.1099/mic.0.27456-0>
- McCleary, W. R., Esmon, B., & Zusman, D. R. (1991). *Myxococcus xanthus* protein C is a major spore surface protein. *Journal of Bacteriology*, *173*, 2141–2145. <https://doi.org/10.1128/JB.173.6.2141-2145.1991>
- McKenney, P. T., Driks, A., & Eichenberger, P. (2013). The *Bacillus subtilis* endospore: Assembly and functions of the multilayered coat. *Nature Reviews Microbiology*, *11*, 33–44. <https://doi.org/10.1038/nrmicr02921>
- Merino, S., Jimenez, N., Molero, R., Bouamama, L., Regue, M., & Tomas, J. M. (2011). A UDP-HexNAc:Polyprenol-P GalNAc-1-P transferase (WecP) representing a new subgroup of the enzyme family. *Journal of Bacteriology*, *193*, 1943–1952. <https://doi.org/10.1128/JB.01441-10>

- Mohr, K. I., Garcia, R. O., Gerth, K., Irschik, H., & Müller, R. (2012). *Sandaracinus amylolyticus* gen. nov., sp. nov., a starch-degrading soil myxobacterium, and description of *Sandaracinaceae* fam. nov. *International Journal of Systematic and Evolutionary Microbiology*, *62*, 1191–1198. <https://doi.org/10.1099/ijs.0.033696-0>
- Morona, R., Purins, L., Tocilj, A., Matte, A., & Cygler, M. (2009). Sequence-structure relationships in polysaccharide co-polymerase (PCP) proteins. *Trends in Biochemical Sciences*, *34*, 78–84. <https://doi.org/10.1016/j.tibs.2008.11.001>
- Müller, F. D., Schink, C. W., Hoiczky, E., Cserti, E., & Higgs, P. I. (2012). Spore formation in *Myxococcus xanthus* is tied to cytoskeleton functions and polysaccharide spore coat deposition. *Molecular Microbiology*, *83*, 486–505. <https://doi.org/10.1111/j.1365-2958.2011.07944.x>
- Müller, F. D., Treuner-Lange, A., Heider, J., Huntley, S. M., & Higgs, P. I. (2010). Global transcriptome analysis of spore formation in *Myxococcus xanthus* reveals a locus necessary for cell differentiation. *BMC Genomics*, *11*, 264. <https://doi.org/10.1186/1471-2164-11-264>
- Nan, B., Bandaria, J. N., Moghtaderi, A., Sun, I.-H., Yildiz, A., & Zusman, D. R. (2013). Flagella stator homologs function as motors for myxobacterial gliding motility by moving in helical trajectories. *Proceedings of the National Academy of Sciences of the United States of America*, *110*, E1508–E1513. <https://doi.org/10.1073/pnas.1219982110>
- Noland, B. W., Newman, J. M., Hendle, J., Badger, J., Christopher, J. A., Tresser, J., ... Buchanan, S. G. (2002). Structural studies of *Salmonella typhimurium* ArnB (PmrH) aminotransferase: A 4-amino-4-deoxy-L-arabinose lipopolysaccharide-modifying enzyme. *Structure*, *10*, 1569–1580. [https://doi.org/10.1016/S0969-2126\(02\)00879-1](https://doi.org/10.1016/S0969-2126(02)00879-1)
- O'Connor, K. A., & Zusman, D. R. (1997). Starvation-independent sporulation in *Myxococcus xanthus* involves the pathway for beta-lactamase induction and provides a mechanism for competitive cell survival. *Molecular Microbiology*, *24*, 839–850.
- Otani, M., Kozuka, S., Xu, C., Umezawa, C., Sano, K., & Inouye, S. (1998). Protein W, a spore-specific protein in *Myxococcus xanthus*, formation of a large electron-dense particle in a spore. *Molecular Microbiology*, *30*, 57–66.
- Patel, K. B., Furlong, S. E., & Valvano, M. A. (2010). Functional analysis of the C-terminal domain of the WbaP protein that mediates initiation of O antigen synthesis in *Salmonella enterica*. *Glycobiology*, *20*, 1389–1401. <https://doi.org/10.1093/glycob/cwq104>
- Patel, K. B., Toh, E., Fernandez, X. B., Hanuszkiewicz, A., Hardy, G. G., Brun, Y. V., ... Valvano, M. A. (2012). Functional characterization of UDP-glucose:Undecaprenyl-phosphate glucose-1-phosphate transferases of *Escherichia coli* and *Caulobacter crescentus*. *Journal of Bacteriology*, *194*, 2646–2657. <https://doi.org/10.1128/JB.06052-11>
- Pérez-Burgos, M., García-Romero, I., Jung, J., Valvano, M. A., & Søggaard-Andersen, L. (2019). Identification of the lipopolysaccharide O-antigen biosynthesis priming enzyme and the O-antigen ligase in *Myxococcus xanthus*: Critical role of LPS O-antigen in motility and development. *Molecular Microbiology*, *112*, 1178–1198.
- Power, P. M., Roddam, L. F., Dieckelmann, M., Srihanta, Y. N., Tan, Y. C., Berrington, A. W., & Jennings, M. P. (2000). Genetic characterization of pilin glycosylation in *Neisseria meningitidis*. *Microbiology*, *146*(Pt 4), 967–979.
- Raetz, C. R., & Whitfield, C. (2002). Lipopolysaccharide endotoxins. *Annual Review of Biochemistry*, *71*, 635–700. <https://doi.org/10.1146/annurev.biochem.71.110601.135414>
- Ranjit, D. K., & Young, K. D. (2016). Colanic acid intermediates prevent *de novo* shape recovery of *Escherichia coli* spheroplasts, calling into question biological roles previously attributed to colanic acid. *Journal of Bacteriology*, *198*, 1230–1240.
- Rehm, B. H. (2010). Bacterial polymers: Biosynthesis, modifications and applications. *Nature Reviews Microbiology*, *8*, 578–592. <https://doi.org/10.1038/nrmicro2354>
- Reichenbach, H. (1999). The ecology of the myxobacteria. *Environmental Microbiology*, *1*, 15–21. <https://doi.org/10.1046/j.1462-2920.1999.00016.x>
- Reith, J., & Mayer, C. (2011). Characterization of a glucosamine/glucosaminide N-acetyltransferase of *Clostridium acetobutylicum*. *Journal of Bacteriology*, *193*, 5393–5399. <https://doi.org/10.1128/JB.05519-11>
- Sadler, W., & Dworkin, M. (1966). Induction of cellular morphogenesis in *Myxococcus xanthus*. II. Macromolecular synthesis and mechanism of inducer action. *Journal of Bacteriology*, *91*, 1520–1525. <https://doi.org/10.1128/JB.91.4.1520-1525.1966>
- Saitou, N., & Nei, M. (1987). The neighbor-joining method—A new method for reconstructing phylogenetic trees. *Molecular Biology and Evolution*, *4*, 406–425.
- Saldías, M. S., Patel, K., Marolda, C. L., Bittner, M., Contreras, I., & Valvano, M. A. (2008). Distinct functional domains of the *Salmonella enterica* WbaP transferase that is involved in the initiation reaction for synthesis of the O antigen subunit. *Microbiology*, *154*, 440–453. <https://doi.org/10.1099/mic.0.2007/013136-0>
- Sanford, R. A., Cole, J. R., & Tiedje, J. M. (2002). Characterization and description of *Anaeromyxobacter dehalogenans* gen. nov., sp. nov., an aryl-halo-respiring facultative anaerobic myxobacterium. *Applied and Environment Microbiology*, *68*, 893–900. <https://doi.org/10.1128/AEM.68.2.893-900.2002>
- Schäffer, C., Wugeditsch, T., Messner, P., & Whitfield, C. (2002). Functional expression of enterobacterial O-polysaccharide biosynthesis enzymes in *Bacillus subtilis*. *Applied and Environment Microbiology*, *68*, 4722–4730. <https://doi.org/10.1128/AEM.68.10.4722-4730.2002>
- Schild, S., Lamprecht, A. K., & Reidl, J. (2005). Molecular and functional characterization of O antigen transfer in *Vibrio cholerae*. *Journal of Biological Chemistry*, *280*, 25936–25947.
- Schmid, J., Sieber, V., & Rehm, B. (2015). Bacterial exopolysaccharides: Biosynthesis pathways and engineering strategies. *Frontiers in Microbiology*, *6*, 496. <https://doi.org/10.3389/fmicb.2015.00496>
- Schumacher, D., Bergeler, S., Harms, A., Vonck, J., Huneke-Vogt, S., Frey, E., & Sogaard-Andersen, L. (2017). The PomXYZ proteins self-organize on the bacterial nucleoid to stimulate cell division. *Developmental Cell*, *41*, 299–314.e13. <https://doi.org/10.1016/j.devcel.2017.04.011>
- Schumacher, D., & Sogaard-Andersen, L. (2017). Regulation of cell polarity in motility and cell division in *Myxococcus xanthus*. *Annual Review of Microbiology*, *71*, 61–78.
- Shi, X., Wegener-Feldbrugge, S., Huntley, S., Hamann, N., Hedderich, R., & Sogaard-Andersen, L. (2008). Bioinformatics and experimental analysis of proteins of two-component systems in *Myxococcus xanthus*. *Journal of Bacteriology*, *190*, 613–624. <https://doi.org/10.1128/JB.01502-07>
- Sigle, S., Ladwig, N., Wohlleben, W., & Muth, G. (2015). Synthesis of the spore envelope in the developmental life cycle of *Streptomyces coelicolor*. *International Journal of Medical Microbiology*, *305*, 183–189. <https://doi.org/10.1016/j.ijmm.2014.12.014>
- Sonnhammer, E. L., von Heijne, G., & Krogh, A. (1998). A hidden Markov model for predicting transmembrane helices in protein sequences. *Proceedings of International Conference on Intelligent Systems for Molecular Biology*, *6*, 175–182.
- Sprecher, K. S., Hug, I., Nesper, J., Potthoff, E., Mahi, M. A., Sangermani, M., ... Jenal, U. (2017). Cohesive properties of the caulobacter *crescentus* holdfast adhesin are regulated by a novel c-di-GMP effector protein, *mBio*, *8*, e00294-17. <https://doi.org/10.1128/mBio.00294-17>
- Sun, M., Wartel, M., Cascales, E., Shaevitz, J. W., & Mignot, T. (2011). Motor-driven intracellular transport powers bacterial gliding motility. *Proceedings of the National Academy of Sciences of the United States of America*, *108*, 7559–7564. <https://doi.org/10.1073/pnas.1101101108>

- Sutherland, I. W., & Mackenzie, C. L. (1977). Glucan common to the microcyst walls of cyst-forming bacteria. *Journal of Bacteriology*, *129*, 599–605. <https://doi.org/10.1128/JB.129.2.599-605.1977>
- Tan, I. S., & Ramamurthi, K. S. (2014). Spore formation in *Bacillus subtilis*. *Environmental Microbiology Reports*, *6*, 212–225.
- The-UniProt-Consortium. (2019). UniProt: A worldwide hub of protein knowledge. *Nucleic Acids Research*, *47*, D506–D515.
- Treuner-Lange, A., Aguiluz, K., van der Does, C., Gomez-Santos, N., Harms, A., Schumacher, D., ... Sogaard-Andersen, L. (2013). PomZ, a ParA-like protein, regulates Z-ring formation and cell division in *Myxococcus xanthus*. *Molecular Microbiology*, *87*, 235–253.
- Treuner-Lange, A., Macia, E., Guzzo, M., Hot, E., Faure, L. M., Jakobczak, B., ... Mignot, T. (2015). The small G-protein MglA connects to the MreB actin cytoskeleton at bacterial focal adhesions. *Journal of Cell Biology*, *210*, 243–256. <https://doi.org/10.1083/jcb.201412047>
- Ud-Din, A. I., Liu, Y. C., & Roujeinikova, A. (2015). Crystal structure of *Helicobacter pylori* pseudaminic acid biosynthesis N-acetyltransferase PseH: Implications for substrate specificity and catalysis. *PLoS ONE*, *10*, e0115634. <https://doi.org/10.1371/journal.pone.0115634>
- Ueki, T., & Inouye, S. (2005). Identification of a gene involved in polysaccharide export as a transcription target of FruA, an essential factor for *Myxococcus xanthus* development. *Journal of Biological Chemistry*, *280*, 32279–32284.
- Valvano, M. A. (2008). Undecaprenyl phosphate recycling comes out of age. *Molecular Microbiology*, *67*, 232–235. <https://doi.org/10.1111/j.1365-2958.2007.06052.x>
- Valvano, M. A. (2011). Common themes in glycoconjugate assembly using the biogenesis of O-antigen lipopolysaccharide as a model system. *Biochemistry (Moscow)*, *76*, 729–735. <https://doi.org/10.1134/S0006297911070029>
- Valvano, M. A., & Crosa, J. H. (1984). Aerobactin iron transport genes commonly encoded by certain ColV plasmids occur in the chromosome of a human invasive strain of *Escherichia coli* K1. *Infection and Immunity*, *46*, 159–167. <https://doi.org/10.1128/IAI.46.1.159-167.1984>
- Valvano, M. A., Furlong, S. E., & Patel, K. B. (2011). Genetics, biosynthesis and assembly of O-antigen. In Y. A. Knirel & M. A. Valvano (Eds.), *Bacterial lipopolysaccharides: Structure, chemical synthesis, biogenesis and interaction with host cells* (pp. 275–310). Vienna, Austria: Springer Vienna.
- Viklund, H., Bernsel, A., Skwark, M., & Elofsson, A. (2008). SPOCTOPUS: A combined predictor of signal peptides and membrane protein topology. *Bioinformatics*, *24*, 2928–2929. <https://doi.org/10.1093/bioinformatics/btn550>
- Wan, Z., Brown, P. J., Elliott, E. N., & Brun, Y. V. (2013). The adhesive and cohesive properties of a bacterial polysaccharide adhesin are modulated by a deacetylase. *Molecular Microbiology*, *88*, 486–500. <https://doi.org/10.1111/mmi.12199>
- Wartel, M., Ducret, A., Thutupalli, S., Czerwinski, F., Le Gall, A. V., Mauriello, E. M., ... Mignot, T. (2013). A versatile class of cell surface directional motors gives rise to gliding motility and sporulation in *Myxococcus xanthus*. *PLoS Biology*, *11*, e1001728. <https://doi.org/10.1371/journal.pbio.1001728>
- Watson, B. F., & Dworkin, M. (1968). Comparative intermediary metabolism of vegetative cells and microcysts of *Myxococcus xanthus*. *Journal of Bacteriology*, *96*, 1465–1473.
- Wu, S. S., & Kaiser, D. (1996). Markerless deletions of *pil* genes in *Myxococcus xanthus* generated by counterselection with the *Bacillus subtilis* *sacB* gene. *Journal of Bacteriology*, *178*, 5817–5821. <https://doi.org/10.1128/JB.178.19.5817-5821.1996>
- Wu, S. S., & Kaiser, D. (1997). Regulation of expression of the *pilA* gene in *Myxococcus xanthus*. *Journal of Bacteriology*, *179*, 7748–7758. <https://doi.org/10.1128/JB.179.24.7748-7758.1997>
- Yamamoto, E., Muramatsu, H., & Nagai, K. (2014). *Vulгатibacter in-comptus* gen. nov., sp. nov. and *Labilithrix luteola* gen. nov., sp. nov., two myxobacteria isolated from soil in Yakushima Island, and the description of *Vulгатibacteraceae* fam. nov., *Labilithricaceae* fam. nov. and *Anaeromyxobacteraceae* fam. nov. *International Journal of Systematic and Evolutionary Microbiology*, *64*, 3360–3368. <https://doi.org/10.1099/ijs.0.063198-0>
- Yang, Z., Geng, Y., Xu, D., Kaplan, H. B., & Shi, W. (1998). A new set of chemotaxis homologues is essential for *Myxococcus xanthus* social motility. *Molecular Microbiology*, *30*, 1123–1130. <https://doi.org/10.1046/j.1365-2958.1998.01160.x>
- Zhang, Y., Ducret, A., Shaevitz, J., & Mignot, T. (2012). From individual cell motility to collective behaviors: Insights from a prokaryote, *Myxococcus xanthus*. *FEMS Microbiology Reviews*, *36*, 149–164.
- Zimmermann, L., Stephens, A., Nam, S.-Z., Rau, D., Kübler, J., Lozajic, M., ... Alva, V. (2018). A completely reimplemented MPI bioinformatics toolkit with a new HHpred server at its core. *Journal of Molecular Biology*, *430*, 2237–2243. <https://doi.org/10.1016/j.jmb.2017.12.007>

SUPPORTING INFORMATION

Additional Supporting Information may be found online in the Supporting Information section.

How to cite this article: Pérez-Burgos M, García-Romero I, Valvano MA, Søgaard Andersen L. Identification of the Wzx flippase, Wzy polymerase and sugar-modifying enzymes for spore coat polysaccharide biosynthesis in *Myxococcus xanthus*. *Mol Microbiol*. 2020;00:1–20. <https://doi.org/10.1111/mmi.14486>

3.2.1 Supplementary material

Supplementary Figures & Legends

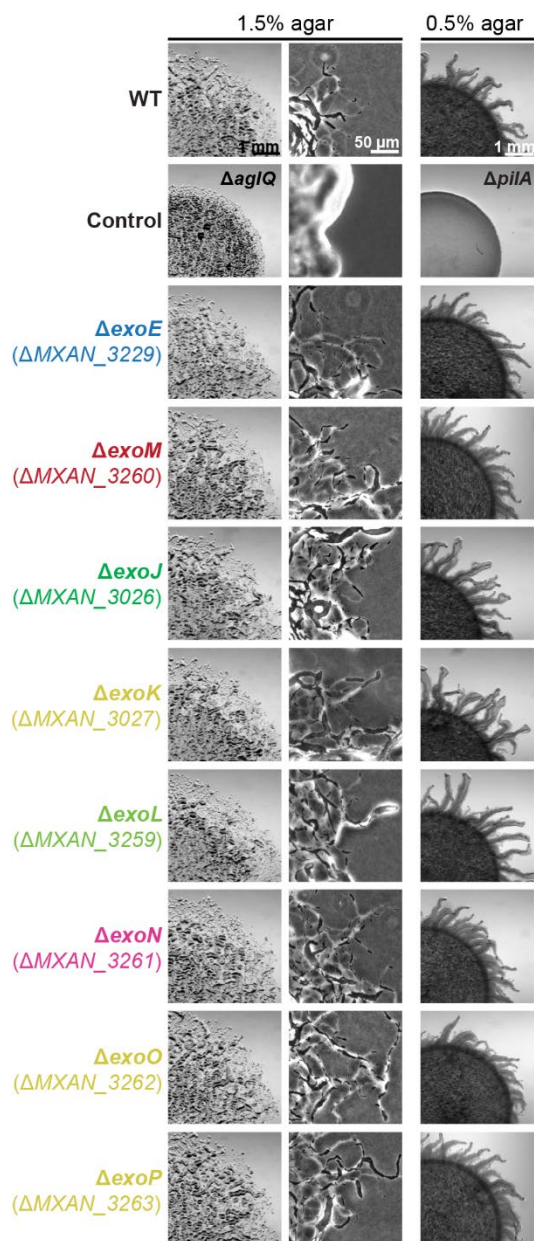


Figure S1. Colony-based motility assay of Δ exo mutants. T4P-dependent motility and gliding motility were analyzed on 0.5% and 1.5% agar, respectively. Images were recorded after 24 h. The Δ *pilA* mutant is deficient in T4P-dependent motility and the Δ *agIQ* mutant is deficient in gliding motility; these strains were used as negative controls. Scale bars: 1mm (left), 50 μ m (middle), 1mm (right).

Results

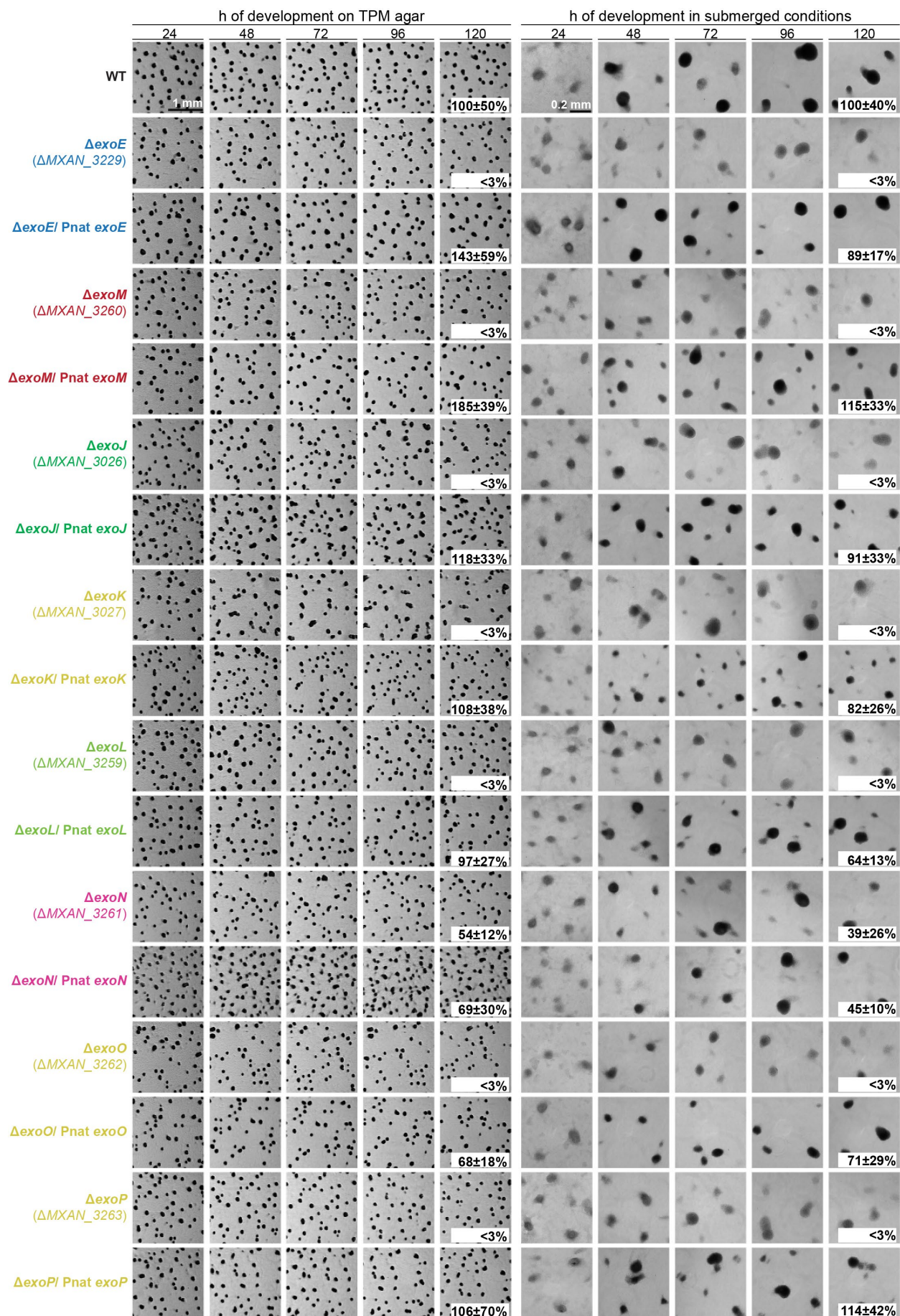


Figure S2. Development of Δ exo mutants. Cells on TPM agar and under submerged conditions were followed during development. Images were recorded at the indicated time points. Sporulation efficiency after heat and sonic treatment is indicated as the mean \pm standard deviation from three biological replicates relative to WT. Scale bars: 1mm (left), 200 μ m (right).

```

WbaPSe -MDNIDNKYN PQLCKIFLAI SDLIFFNLAL WFSLGCYVFI FDQVQRFIPQ DQ-----LDT RVITHFILSV VCVGWFWIRL 74
ExoESe MLRVFHHYFS AKKLTFFLAE SSAIALACVM GAAACAALFA PEGHTPLSQ LWPTLLWMGA AFVITFQFTL YLLDLYDLRV 80

WbaPSe RHYTYRKPWF YELKEIFRTI VIFAIFDLAL IAFTKWQFSR YVWVFCWTF A LILVPFFRAL TKHLLNKLGI WKKKTIILGS 154
ExoESe AAEDRVRGYR FLKAAGVTAM VAGGVMLVTP LVVP-MQLPP GTLLGGAMGA LAGTLMVRVS IRALVGAP-- --HSLVIVGE 155

WbaPSe GQNARGAYS A LQSEEMMGFD VIAFFD TDAS -DAEINMLPV IKDTEI IWDL NRTGDVHYIL AYEYTELEKT HFWLRELSKH 233
ExoESe GPKARAVASA IDAGGEGTYR IVGLTDPRTS GEALEETAAR LNAAYVVQAA DDMRGANWVD GLLRCRLQGR --RVYEATGF 233

WbaPSe HCRSVTVVPS FRGLPLYNTD MSFIFSHEVM LLRIQNNAK RSSRFLKRTF DIVCSIMILI IASPLMIYLW YKVTRDG-GP 312
ExoESe CERVLRRIP - - - -VQFLRA SDFAFAD E L T VSPLR - - - - - RTLKRGF DIVAVASLLLM LSA P F L L L V V V A I K L D S K G P 300

WbaPSe AIYGHQRVGR HGKLFPCYKF RSMVMNSQEV LKELLANDPI ARAWEKDFK LKNDRITAV GRFIRKTSLD ELPOLFNVLK 392
ExoESe IFYRQERTGL FGSTYHLWK RSMRTDAEKH G----- --AVWAK-- -ANDDRVTRV GRFIRRARID EIPQVFNILT 365

WbaPSe GDMSLVGPRP IVSDELERYC DDVDY---L MAKPGMTGLW QVS---GRND VDYDTRVYFD SWYVKNWTLW NDIAILFKTA 466
ExoESe GDMSFVGPRP ERPVFVEQLK EQIPFYGLRE AVKPGLTGWA QIRYPYGASV EDARNKLEFD LYVYKNGSLF LDVGIIFHTV 445

WbaPSe KVVLR RDGAY 476
ExoESe RHVLLGRGAR 455

```

Figure S3. Sequence alignment of ExoE and WbaP^{Se} showing the Pro and Asp (orange) residues in the motif DX₁₂P and the conserved amino acids essential for catalytic activity (red).

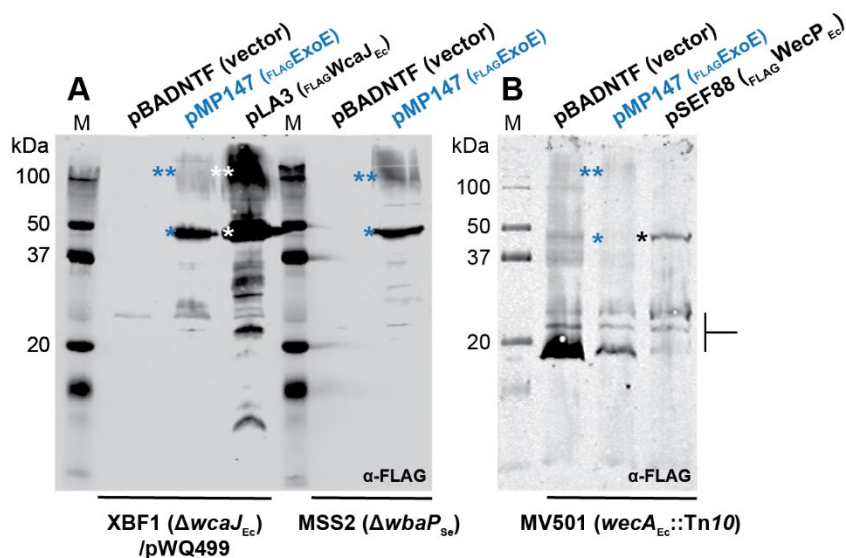


Figure S4. Immunoblot analysis of FLAG-ExoE accumulation in *E. coli* strains XBF1 (A, left) and MV501 (B), and *S. enterica* MSS2 (A, right). Bacteria were incubated with 0.2% arabinose to induce gene expression before lysis. * and ** indicate the position of monomeric and oligomeric forms of the relevant proteins. Cross reactive bands with apparent masses of 18-25 kDa with the α -FLAG monoclonal antibody that appear in lysates of MV501 (panel B) are indicated. M, molecular mass markers.

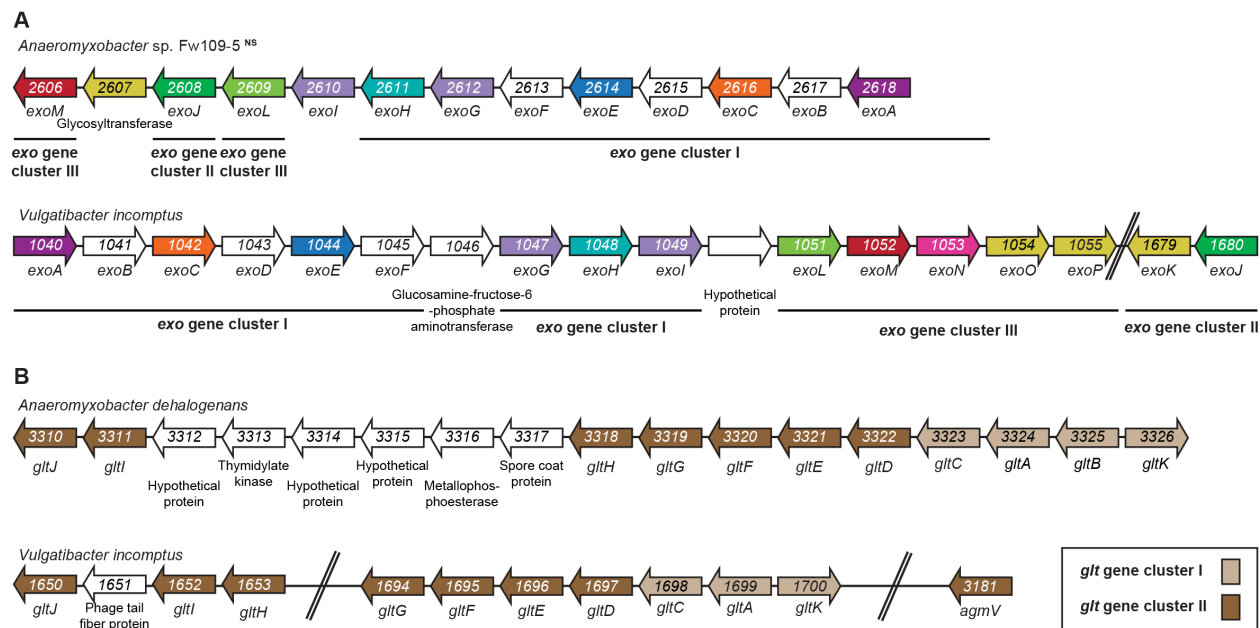


Figure S5. *exo* (A) and *glt* (B) gene organization in *Anaeromyxobacter* and *Vulgatibacter incomptus*. Genes are not drawn to scale.

Supplementary Experimental Procedures

Plasmid construction. All oligonucleotides used are listed in Table S3. All constructed plasmids were verified by DNA sequencing.

pJJ5 (for generation of in-frame deletion of *MXAN_3026/exoJ*): up- and downstream fragments were amplified from genomic DNA of DK1622 using the primer pairs 3026_A/3026_B and 3026_C/3026_D, respectively, as described in (Shi *et al.*, 2008). Subsequently, the AB and CD fragments were used as templates to perform an overlapping PCR with the primer pair 3262_A/3262_D to generate the AD fragment. The AD fragment was digested with KpnI/BamHI and cloned in pBJ114.

pJJ18 (expression of P_{nat} *MXAN_3026/exoJ* from the *attB* site): P_{nat} *MXAN_3026* was amplified with the primer combination 3026_Pnat forw/3026_Pnat/PpilA rev and genomic DNA from *M. xanthus* DK1622 as a template. The fragment was digested with EcoRI/HindIII and cloned into pSWU30.

pMP113 (for generation of in-frame deletion of *MXAN_3260/exoM*): up- and downstream fragments were amplified from genomic DNA of DK1622 using the primer pairs 3260_A2/3260_B and 3260_C/3260_D2, respectively. Subsequently, the AB and CD fragments were used as templates to perform an overlapping PCR with the primer pair 3260_A2/3260_D2 to generate the AD fragment. The AD fragment was digested with EcoRI/XbaI and cloned in pBJ114.

pMP118 (expression of P_{nat} *MXAN_3260/exoM* from the *attB* site): the promoter region of *MXAN_3260* and *MXAN_3260* were separately amplified with 3260_Pnat forw /3260_Pnat int.1 and 3260_Pnat int.2/3260_Pnat/PpilA rev respectively by using genomic DNA from *M. xanthus* DK1622 as a template. An overlapping PCR with both

fragments as a DNA template and the primer pair 3260_Pnat forw/3260_Pnat/PpilA rev gave the P_{nat} *MXAN_3260* fragment that was digested with EcoRI/HindIII and cloned into pSWU30.

pMP120 (for generation of in-frame deletion of *MXAN_3027/exoK*): up- and downstream fragments were amplified from genomic DNA of DK1622 using the primer pairs 3027_A/3027_B and 3027_C/3027_D, respectively. Subsequently, the AB and CD fragments were used as templates for overlapping PCR with the primer pair 3027_A/3027_D to generate the AD fragment. The AD fragment was digested with KpnI/XbaI and cloned in pBJ114.

pMP121 (for generation of in-frame deletion of *MXAN_3259/exoL*): up- and downstream fragments were amplified from genomic DNA of DK1622 using the primer pairs 3259_A/3259_B and 3259_C/3259_D, respectively. Subsequently, the AB and CD fragments were used as templates for overlapping PCR with the primer pair 3259_A/3259_D to generate the AD fragment. The AD fragment was digested with KpnI/XbaI and cloned in pBJ114.

pMP123 (for generation of in-frame deletion of *MXAN_3263/exoP*): up- and downstream fragments were amplified from genomic DNA of DK1622 using the primer pairs 3263_A/3263_B and 3263_C/3263_D, respectively. Subsequently, the AB and CD fragments were used as templates for overlapping PCR with the primer pair 3263_A/3263_D to generate the AD fragment. The AD fragment was digested with KpnI/XbaI and cloned in pBJ114.

pMP125 (expression of P_{nat} *MXAN_3027/exoK* from the *attB* site): the promoter region of *MXAN_3027* and *MXAN_3027* were separately amplified with 3026_Pnat forw/3026_Promoter rev and 3027_fw for Pnat /3027_rev respectively by using genomic DNA from *M. xanthus* DK1622 as a template. An overlapping PCR with both fragments as a DNA template and the primer pair 3026_Pnat forw2/3027_rev gave the P_{nat} *MXAN_3027* fragment that was digested with EcoRI/HindIII and cloned into pSWU30.

pMP126 (expression of P_{nat} *MXAN_3259/exoL* from the *attB* site): P_{nat} *MXAN_3259* was amplified with the primer combination 3260_Pnat forw/3259_rev and genomic DNA from *M. xanthus* DK1622 as a template. The fragment was digested with EcoRI/HindIII and cloned into pSWU30.

pMP131 (for generation of in-frame deletion of *MXAN_3261/exoN*): up- and downstream fragments were amplified from genomic DNA of DK1622 using the primer pairs 3261_A/3261_B and 3261_C/3261_D, respectively. Subsequently, the AB and CD fragments were used as templates for overlapping PCR with the primer pair 3261_A/3261_D to generate the AD fragment. The AD fragment was digested with EcoRI/HindIII and cloned in pBJ114.

pMP133 (expression of P_{nat} *MXAN_3261/exoN* from the *attB* site): P_{nat} *MXAN_3261* was amplified with the primer combination 3261_Pnat fw 3 700 up/3261_rev and genomic DNA from *M. xanthus* DK1622 as a template. The fragment was digested with EcoRI/HindIII and cloned into pSWU30.

pMP134 (expression of P_{nat} *MXAN_3262/exoO* from the *attB* site): the promoter region of *MXAN_3262* and *MXAN_3262* were separately amplified with 3261_Pnat fw 3 700 up/3261_Promoter rev 1 and 3262_fw for Pnat/3262_rev respectively by using genomic DNA from *M. xanthus* DK1622 as a template. An overlapping PCR with both fragments as a DNA template and the primer pair 3261_Pnat fw 3 700 up/3262_rev gave the P_{nat} *MXAN_3262* fragment that was digested with EcoRI/HindIII and cloned into pSWU30.

pMP135 (expression of P_{nat} *MXAN_3263/exoP* from the *attB* site): the promoter region of *MXAN_3263* and *MXAN_3263* were separately amplified with 3261_Pnat fw 3 700 up/3261_promoter rv for 3263 and 3261_promoter fw

for 3263/3263 rev respectively by using genomic DNA from *M. xanthus* DK1622 as a template. An overlapping PCR with both fragments as a DNA template and the primer pair 3261_Pnat fw 3 700 up/3263 rev gave the P_{nat} *MXAN_3263* fragment that was digested with EcoRI/HindIII and cloned into pSWU30.

pMP136 (expression of P_{nat} *MXAN_3229/exoE* from the *attB* site): the promoter region of *exoE* and *exoE* were separately amplified with 3225_Pnat forw 300/3229_promoter rev 3225 and 3229_prmt 3225 int fw/3229_rev respectively by using genomic DNA from *M. xanthus* DK1622 as a template. An overlapping PCR with both fragments as a DNA template and the primer pair 3229_prmt 3225 int fw /3229_rev gave the P_{nat} *exoE* fragment that was digested with EcoRI/HindIII and cloned into pSWU30.

pMP144 (for generation of in-frame deletion of *MXAN_3262/exoO*): up- and downstream fragments were amplified from genomic DNA of DK1622 using the primer pairs 3262_A/3262_B2 and 3262_C2/3262_D, respectively. Subsequently, the AB and CD fragments were used as templates for overlapping PCR with the primer pair 3262_A/3262_D to generate the AD fragment. The AD fragment was digested with EcoRI/XbaI and cloned in pBJ114.

pMP147 (plasmid for expression of *FlagMXAN_3229/exoE* under the control of an arabinose promoter): the *MXAN_3229* fragment was amplified with the primer pair 3229_fw + 1nt /3229_rev from genomic DNA of DK1622, digested with XbaI/HindIII and cloned into pBADNTF.

pMP158 (plasmid for expression of *MXAN_3229/exoE* under the control of an arabinose promoter): the *MXAN_3229* fragment was amplified with the primer pair 3229_fw_ATG_EcoRI/3229_rev from genomic DNA of DK1622, digested with EcoRI/HindIII and cloned into pBAD24. In this construct, the original GTG start codon has been replaced with an ATG start codon.

Table S1. Analysis of *exo* gene cluster I-III

Locus tag MXAN	Gene name	(Putative) function of encoded protein	Reference
3225	<i>exoA</i> (<i>fdgA</i>)	Polysaccharide biosynthesis/export	(Holkenbrink <i>et al.</i> , 2014, Ueki & Inouye, 2005)
3226	<i>exoB</i>	Hypothetical protein, OM protein	(Holkenbrink <i>et al.</i> , 2014)
3227	<i>exoC</i>	Chain length determinant protein	(Holkenbrink <i>et al.</i> , 2014)
3228	<i>exoD</i> (<i>btkA</i>)	Tyrosine kinase	(Holkenbrink <i>et al.</i> , 2014, Kimura <i>et al.</i> , 2011)
3229	<i>exoE</i>	Polyprenyl glycosylphosphotransferase New annotation: <i>Polyisoprenyl</i>-phosphate hexose-1-phosphate	(Holkenbrink <i>et al.</i> , 2014)
3230	<i>exoF</i>	Gluconeogenesis factor	(Holkenbrink <i>et al.</i> , 2014)
3231	<i>exoG</i>	<i>N</i> -acetyltransferase	(Holkenbrink <i>et al.</i> , 2014)
3232	<i>exoH</i>	3-Amino-5-hydroxybenzoic acid synthase family New annotation: Aminotransferase	(Holkenbrink <i>et al.</i> , 2014)

3233	<i>exoI</i>	N-acetyltransferase	(Holkenbrink <i>et al.</i> , 2014)
3026	<i>exoJ</i>	Wzy polymerase	(Müller <i>et al.</i> , 2012)
3027	<i>exoK</i>	Glycosyltransferase	Uniprot, KEGG
3259	<i>exoL</i>	Polysaccharide deacetylase family protein	Uniprot, KEGG
3260	<i>exoM</i>	Putative membrane protein New annotation: Wzx flippase	Uniprot, KEGG
3261	<i>exoN</i>	Serine O-acetyltransferase	Uniprot, KEGG
3262	<i>exoO</i>	Glycosyltransferase	Uniprot, KEGG
3263	<i>exoP</i>	Glycosyltransferase	Uniprot, KEGG

Table S2. Fully sequenced myxobacterial genomes used for the 16S RNA tree

Species and strain name
<i>Anaeromyxobacter dehalogenans</i> 2CP-C
<i>Anaeromyxobacter</i> sp. Fw109-5
<i>Anaeromyxobacter</i> sp. K
<i>Archangium gephyra</i> DSM 2261
<i>Chondromyces crocatus</i> Cm c5
<i>Corallocooccus coralloides</i> DSM 2259
<i>Cystobacter fuscus</i> DSM 52655
<i>Haliangium ochraceum</i> DSM 14365
<i>Labilithrix luteola</i> DSM 27648
<i>Melittangium boletus</i> DSM 14713SG
<i>Minicystis rosea</i> DSM 24000
<i>Myxococcus fulvus</i> HW-1FB, S
<i>Myxococcus hansupus</i> (<i>Myxococcus</i> sp. mixupus)
<i>Myxococcus macrosporus</i> DSM 14697
<i>Myxococcus stipitatus</i> DSM 14675
<i>Myxococcus xanthus</i> DK1622
<i>Sandaracinus amylolyticus</i> DSM 53668
<i>Sorangium cellulosum</i> So ce 56
<i>Stigmatella aurantiaca</i> DW4/3-1
<i>Vulgatibacter incomptus</i> DSM 27710

Table S3. Oligonucleotides used in this work¹

Primer name	Sequence 5'-3'	Brief description
3026_A	ATCGGGTACCGGCGCGAGCTGGCCGCCACC	For Δ MXAN_3026
3026_B	CCCCTCCCAGCGCTGCCCTGCTCTCC	For Δ MXAN_3026
3026_C	GGGCAGCGCTGGGAGGGGTCCGGACAT	For Δ MXAN_3026
3026_D	ATCGGGATCCGCGCAATTGGGCCAGCGCG	For Δ MXAN_3026
3026_E	CGCGTGGAAGGCGCGGAGCC	For Δ MXAN_3026
3026_F	GCCGGCGCGGACCATCTCCC	For Δ MXAN_3026
3026_G	TCTATGCGCTGACCGCTTTC	For Δ MXAN_3026
3026_H	GACCCCATTGCCTGTCCAAC	For Δ MXAN_3026
3026_Pnat forw	ATATGAATTCTGAGCGCTGCTGGCCCGCGCGGA	For complementation fw
3026_Pnat/PpilA rev	ATCGAAGCTTTCACGCCGCATGTCCGGACC	For complementation rev
3260_A2	CGCGGAATTCGCTACCGCGACGTCTACCGG	For Δ MXAN_3260
3260_B	TCGCAGCCCCGCGGCCGACGTGGAACC	For Δ MXAN_3260
3260_C	TCGGCCGCGGGGCTGCGAGCGCGAAGG	For Δ MXAN_3260
3260_D2	CGGCTCTAGAGTGGAGGGTGATGACCCGGG	For Δ MXAN_3260
3260_E2	CTTGTGCGTCGTCACGTTCG	For Δ MXAN_3260
3260_F2	GAGGTAGTCCGGCAGCAGTC	For Δ MXAN_3260
3260_G	CATCCCCTCGTGCTCGCCC	For Δ MXAN_3260
3260_H	CCCAGCTTCCGCTCCGGCGT	For Δ MXAN_3260
3260_Pnat forw	ATATGAATTCTGACGGCGGGCGTTCGTATCCG	For complementation, promoter fw
3260_Pnat int.1	tccgctcacGATGAGGATGCGCCTCCC	For complementation, promoter rev
3260_Pnat int.2	ATCCTCATCgtgagcggagggtccacg	For complementation fw
3260_Pnat/PpilA rev	ATCGAAGCTTctacccccccctcgcgctc	For complementation rev
3027_A	ATCGGGTACCCAAGAGCAGCGGCTGGCTGT	For Δ MXAN_3027
3027_B	GGCAATCCGGAGGGGCTCCTGCCCAT	For Δ MXAN_3027
3027_C	GAGCCCCTCCGGATTGCCCGGGGCGCG	For Δ MXAN_3027
3027_D	GCCGTCTAGACATCCGCCTGGGCCGGCAGC	For Δ MXAN_3027
3027_E	CTGGCGGTGGCCTTCGTGGC	For Δ MXAN_3027
3027_F	CCTCGCGGGACTGTCGTTGA	For Δ MXAN_3027
3027_G	CATTGGAGGGACCGAAGTGC	For Δ MXAN_3027
3027_H	CGTGCAGCGTGATGCCGGAA	For Δ MXAN_3027
3259_A	ATCGGGTACCGTTCTGGTGCGCGGTGAGG	For Δ MXAN_3259
3259_B	GGTCGTGGCAGACTGGGAGCGCCGATA	For Δ MXAN_3259
3259_C	TCCCAGTCTGCCACGACCATCCAGGAG	For Δ MXAN_3259
3259_D	ATCGTCTAGAGGGGAATGGCCAAGAGCATC	For Δ MXAN_3259
3259_E	CAGAAGCCGGGCCAGCACCG	For Δ MXAN_3259
3259_F	CCACCGGTACAGGTGCGCG	For Δ MXAN_3259

3259_G	ACCTTCCGCCGGCACCTCGA	For Δ MXAN_3259
3259_H	CGAAGCAGTCATCCAGCTGG	For Δ MXAN_3259
3263_A	ATCGGGTACCGCCCCGCGGAGAAGATCGACG	For Δ MXAN_3263
3263_B	CGCCATGAGCAGTGCCCTGCGCGCGAG	For Δ MXAN_3263
3263_C	AGGGCACTGCTCATGGCGGACGCAAG	For Δ MXAN_3263
3263_D	CGCGTCTAGAGAGGTGTACGTGCTGGCCGG	For Δ MXAN_3263
3263_E	GCGGTGAAGTCCGCGCTGGT	For Δ MXAN_3263
3263_F	CGGTGTGGCGCAGGGCCATG	For Δ MXAN_3263
3263_G	CGACTGGGATGGGGACCCGC	For Δ MXAN_3263
3263_H	CGAAGATGCGCTCGGCGCGC	For Δ MXAN_3263
3026_Promoter rev	ACGCCGCATTCACTCCACCTCCCGGCA	For complementation, promoter rev
3027_fw for Pnat	GTGGAGTGAATGCGGCGTGAGGAGGCG	For complementation fw
3027_rev	ATAGAAGCTTTCAGGCGTCCGCGCCCCGGG	For complementation rev
3259_rev	ATCGAAGCTTTCACGGAGCCTCCTGGATGG	For complementation rev
3261_A	ATAGGAATTCCCCGCGGTGCCCGTCTTCCG	For Δ MXAN_3261
3261_B	AGACGACGGGTAGAACGTCATCGCGTC	For Δ MXAN_3261
3261_C	ACGTTCTACCCGTCGTCTTCCAGGCTG	For Δ MXAN_3261
3261_D	ATCGAAGCTTATGGATGGTGCATGGAC	For Δ MXAN_3261
3261_E	GGGCGATGTTCCGGTGAGAAG	For Δ MXAN_3261
3261_F	AACATCAGCGCGCGCCCGTA	For Δ MXAN_3261
3261_G	AGGCTGAAGAAGCGGGGTGT	For Δ MXAN_3261
3261_H	ATCCGGGTCTGCCGGATGA	For Δ MXAN_3261
3261_Pnat fw 3 700 up	ATAGGAATTCTGACGTGAAGCGGCCGAAAGCT	For complementation, promoter fw
3261_rev	ATCGAAGCTTCTACTGGCGCAGCCTGGAAG	For complementation rev
3261_Promoter rev 1	CACGCGCATCACGCCTCCCAATCCCCT	For complementation, promoter rev
3262_fw for Pnat	GGAGGCGTGATGCGCGTGCTCCTCGTC	For complementation fw
3262_rev	AGCGAAGCTTTCACTGCGCCGCATGTCTCG	For complementation rev
3261_promoter rv for 3263	GCGCCGCATCACGCCTCCCAATCCCCT	For complementation, promoter rev
3261_promoter fw for 3263	GGAGGCGTGATGCGGCGCAGTGATGAG	For complementation fw
3263 rev	ATCGAAGCTTTCAGAGCGCCTTGCCGTCCG	For complementation rev
3225_Pnat forw 300	ATCGGAATTCTGAACGCGTGCCAGCCTCCAGCC	For complementation, promoter fw
3229_promoter rev 3225	GCGGAGCACCGTCAGCCCTCCCTCAA	For complementation, promoter rev
3229_prmt 3225 int fw	GGGCTGACGGTGCTCCGCGTTTTTCAC	For complementation fw

3229_rev	AGCGA <u>AAGCTT</u> CTACCGCGCCCCACGACCGA	For complementation rev
3229_fw + 1nt	ATCGT <u>CTAGAG</u> GGTGCTCCGCGTTTTTACCA	For protein expression under an arabinose inducible promoter.
3229_fw_ATG_EcoRI	ATAGGA <u>AATTCAT</u> GCTCCGCGTTTTTAC	For protein expression under an arabinose inducible promoter.
3262_A	ATCAGA <u>AATTCG</u> CGAAGGGCGGGGTAGCGCA	For Δ MXAN_3262
3262_B2	GCGGATGAAGTAATCCCCGACGAGGAG	For Δ MXAN_3262
3262_C2	GGGGATTACTTTCATCCGCGACGTCCGC	For Δ MXAN_3262
3262_D	ATCGT <u>CTAGAC</u> CGCACCAGCACCGTGCGCG	For Δ MXAN_3262
3262_E	AGCTTGATCGCGGGGCTGCG	For Δ MXAN_3262
3262_F	CGAAGTGGGTGAAGTCGGTG	For Δ MXAN_3262
3262_G	ACCAAGTGGCAACAACCCGAA	For Δ MXAN_3262
3262_H	ACATGCATGAGCCCTGCCGC	For Δ MXAN_3262

¹ Underlined sequences indicate restriction sites.

3.3 Identification of the exopolysaccharide biosynthesis pathway in *Myxococcus xanthus*

Pérez-Burgos, M., García-Romero, I., Jung, J., Schander, E., Valvano, M.A., & Søgaard-Andersen, L.

This chapter contains our advances in the identification of the EPS biosynthesis components and reevaluates the role of EPS in motility and development. The following text is part of a manuscript in preparation for submission. I contributed to this work by designing, performing and analyzing experiments, preparing the figures and the manuscript.

Specifically, I carried out all the experiments and analysis shown in Fig. 1-2, 3A-B, 4- 7, S1-S2 with the assistance of Jana Jung and Eugenia Schander. Heterologous experiments shown in Fig. 3C-E were carried out by Dr. Inmaculada García Romero at the Wellcome-Wolfson Institute for Experimental Medicine (Queen's University Belfast) and I generated the plasmid expressing the *M. xanthus* PHPT homolog used for the heterologous experiments.

3.3.1 Summary

The Gram-negative delta-proteobacterium *Myxococcus xanthus* is a model organism to study social behaviors in bacteria. EPS has been implicated with the regulation of social behaviors during growth and development. Here, we identify and characterize the EPS biosynthetic machinery through bioinformatics, genetics, heterologous expression, and biochemical experiments, and reexamined the role of EPS in *M. xanthus* social behaviors using mutants exclusively blocked in EPS synthesis. Our data support that EpsZ (MXAN_7415) is the polyisoprenyl-phosphate hexose-1-phosphate transferase responsible for initiation of EPS synthesis and we showed that EpsZ has Gal-1-P transferase activity. We also identified MXAN_7416 as the Wzx flippase and MXAN_7442 as the Wzy polymerase, which were renamed to Wzx_{EPS} and Wzy_{EPS} respectively, EpsV (MXAN_7421) as a Wzz chain length regulator and EpsY (MXAN_7417) as the outer membrane polysaccharide export (OPX) protein involved in EPS synthesis. Using in-frame deletion mutants, we revisited the role of EPS and demonstrate that it is important for T4P assembly and T4P-dependent motility and conditionally important for development. Additionally, we identified a novel polysaccharide biosynthesis gene cluster encoding homologs of a Wzx/Wzy-dependent pathway and an orphan gene encoding an OPX protein.

3.3.2 Introduction

Bacteria often exist in biofilms, which are surface-associated communities in which cells are embedded in a self-produced extracellular matrix (ECM) (Stoodley *et al.*, 2002). Typically, the ECM is composed of proteins, eDNA and exopolysaccharides (EPS) (Flemming *et al.*, 2016). EPS can serve several functions in a biofilm including structural roles, hydration, adhesion to substrates, cohesion between cells and protection against antibacterials, grazing and bacteriophages (Flemming *et al.*, 2007, Flemming & Wingender, 2010, Flemming *et al.*, 2016).

The Gram-negative delta-proteobacterium *Myxococcus xanthus* organizes into two morphologically distinct biofilms depending on the nutritional status of the cells. In the presence of nutrients, cells grow, divide and move across surfaces by means of two motility systems, type IV pili (T4P)-dependent motility and gliding motility, to generate EPS-embedded colonies in which cells at the colony edge spread outwards in a highly coordinated fashion (Schumacher & Søgaard-Andersen, 2017, Zhang *et al.*, 2012, Hu *et al.*, 2013). In the absence of nutrients, growth ceases and cells modify their motility behavior and begin to aggregate. The aggregation process culminates in the formation of mounds of cells inside which the rod-shaped cells differentiate into

spores leading to the formation of mature fruiting bodies (Konovalova *et al.*, 2010, Zhang *et al.*, 2012). EPS has been suggested to be important for fruiting body formation and makes up a substantial part of individual fruiting bodies (Lu *et al.*, 2005, Shimkets, 1986b, Lux *et al.*, 2004).

EPS in *M. xanthus* has been implicated in cell-cell cohesion (Arnold & Shimkets, 1988a), T4P-dependent motility by stimulating T4P retractions (Li *et al.*, 2003), regulation of motility by regulating the reversal frequency (Zhou & Nan, 2017), and fruiting body formation (Lu *et al.*, 2005, Shimkets, 1986b). However, precisely how EPS modulates these different processes remains unclear because many of the studies on EPS⁻ mutants were done using regulatory mutants that may have pleiotropic effects. Moreover, in some cases conflicting results were obtained for the function of EPS in a particular process, e.g. reversal frequency: While Zhou & Nan (Zhou & Nan, 2017) observed an increase in the reversal frequency of $\Delta epsZ$ cells on soft and hard agar, Berleman *et al.* (Berleman *et al.*, 2016) observed no changes in the reversal frequency of an *epsZ* mutant in comparison to WT; similarly, gliding cells of *sglK*, *difE*, *difA* or *difC* mutants showed either no effects (Yang *et al.*, 1998b, Yang *et al.*, 1998a) or a decrease (Shi *et al.*, 2000, Kearns *et al.*, 2000) in their reversal frequency.

The Dif chemosensory system is the most studied EPS regulatory pathway and the *dif* (previously *dsp* (Lancero *et al.*, 2002, Yang *et al.*, 2000b)) mutants have been used to assign most of the functions of EPS in *M. xanthus* (i.e. essential for T4P-dependent motility (Yang *et al.*, 1998b, Bellenger *et al.*, 2002), T4P-retraction (Li *et al.*, 2003), aggregation and fruiting body formation (Shimkets, 1986b, Arnold & Shimkets, 1988a, Yang *et al.*, 1998b, Bellenger *et al.*, 2002)). Additionally, the Dif proteins are implicated with phosphatidylethanolamine sensory transduction and regulation of the reversal frequency (Bonner *et al.*, 2005, Kearns *et al.*, 2000). To understand the function, and ultimately also the structure of EPS, we focused on the identification of proteins involved in the EPS biosynthesis pathway and reevaluated the role of EPS in the *M. xanthus* life cycle using mutants exclusively blocked in EPS synthesis.

Synthesis of surface polysaccharides (e.g. EPS and O-antigen lipopolysaccharide (LPS)) can occur via three different pathways: the Wzx/Wzy, ABC-transporter or the synthase dependent pathway (Schmid *et al.*, 2015). In the Wzx/Wzy and ABC-transporter dependent pathways, synthesis generally starts with the transfer of a sugar-1-P from uridine diphosphate (UDP) to an undecaprenyl phosphate (Und-P) molecule in the inner leaflet of the inner membrane (IM) to form an Und-PP-sugar molecule (Valvano *et al.*, 2011). The priming enzymes can be broadly classified in two groups: the polyisoprenyl-phosphate hexose-1-phosphate transferases (PHPTs) or the polyisoprenyl-phosphate *N*-acetylhexosamine-1-phosphate transferases (PNPTs) (Valvano,

2011). The polysaccharide chain is elongated by the action of specific glycosyltransferases (GTs) and this depends on the specific pathway. In the Wzx/Wzy-dependent pathway, GTs synthesize the repeat unit on the cytoplasmic side of the IM; each unit is then translocated across the IM by the Wzx flippase and polymerized by the Wzy polymerase into a longer chain. Chain length is generally controlled by the Wzz protein belonging to the polysaccharide co-polymerase (PCP) family resulting in the formation of molecules with a range of lengths (Reid & Szymanski, 2010, Morona *et al.*, 2000). By contrast, in the ABC-transporter dependent pathway, the full-length polysaccharide chain is synthesized on the cytoplasmic side of the IM, and is then translocated across the IM by an ABC transporter (Cuthbertson *et al.*, 2010). In the synthase dependent pathway, synthesis and transport take place simultaneously by a multifunctional synthase protein complex that spans the complete cell envelope (Whitney & Howell, 2013). In all three systems, the polysaccharide molecule reaches the cell surface by translocation through an outer membrane (OM) polysaccharide export (OPX) protein or a β -barrel protein in the case of the synthase-dependent pathway (Schmid *et al.*, 2015, Whitney & Howell, 2013).

The *eps* locus in *M. xanthus* was identified by transposon mutagenesis and several *eps* genes have been shown to be important for EPS biosynthesis (Lu *et al.*, 2005). Here, we re-annotated the *eps* locus and searched this locus as well as the remaining *M. xanthus* genome for homologs of proteins involved in polysaccharide biosynthesis and export. We report that the *eps* locus encodes a complete Wzx/Wzy-dependent pathway for EPS synthesis and export. Moreover, we identify a novel polysaccharide biosynthesis gene cluster, which together with an orphan gene encoding an OPX protein also encode a complete Wzx/Wzy-dependent pathway for EPS synthesis and export. Generally, only mutations in the *eps* locus resulted in EPS biosynthesis defects. We identify EpsZ (MXAN_7415) as the PHPT responsible for initiation of EPS biosynthesis and show that it has Galactose-1-phosphate (Gal-1-P) transferase activity, suggesting that the starting sugar of the EPS repeat unit is likely galactose. We identify MXAN_7416 as the Wzx flippase, MXAN_7442 as the Wzy polymerase, which we renamed Wzx_{EPS} and Wzy_{EPS}, respectively, EpsV (MXAN_7421) as a Wzz chain length regulator and EpsY (MXAN_7417) as the OPX protein involved in EPS export. In-frame deletions in the corresponding genes not only result in EPS synthesis defects but also in adhesion defects, and a defect in T4P-dependent motility. Moreover, we find that EPS is conditionally important for development.

3.3.3 Results

Identification of homologs of proteins of the Wzx/Wzy-dependent pathway important for EPS biosynthesis and export

In order to identify the EPS biosynthesis and export machinery, we searched the *M. xanthus* genome for homologs (see *Experimental Procedures*) of the membrane components of the three biosynthesis pathways (Fig. S1). We identified homologs potentially belonging to the Wzx/Wzy and the ABC-transporter pathways but no homologs of a synthase-dependent pathway. Several of these homologs were previously shown to be important for O-antigen synthesis or spore coat polysaccharide biosynthesis: WbaP_{Mx} (MXAN_2922), WaaL_{Mx} (MXAN_2919), Wzm_{Mx} (MXAN_4623) and Wzt_{Mx} (MXAN_4622) are important for LPS biosynthesis (Pérez-Burgos *et al.*, 2019), and ExoA-ExoP are involved in spore coat polysaccharide synthesis (Holkenbrink *et al.*, 2014, Müller *et al.*, 2012, Pérez-Burgos *et al.*, 2020) (Fig. S1). Importantly, none of these proteins are directly involved in with EPS biosynthesis and export (Pérez-Burgos *et al.*, 2019, Pérez-Burgos *et al.*, 2020). Note that the MraY homolog (MXAN_5607), which belongs to the PNPT family and is involved in PG synthesis, was not considered here.

Importantly, we found that the reannotated *eps* locus previously identified by transposon mutagenesis (Lu *et al.*, 2005) encodes all the proteins for a Wzx/Wzy-dependent pathway (Fig. 1A, Table S1): a PHPT (EpsZ/MXAN_7415), GTs (EpsU/MXAN_7422, EpsH/MXAN_7441, EpsE/MXAN_7445, EpsD/MXAN_7448, EpsA/MXAN_7451), a Wzx flippase (MXAN_7416), a Wzy polymerase (MXAN_7442, previously SgnF (Youderian & Hartzell, 2006)), a Wzz chain length regulator (EpsV/MXAN_7421) belonging to the PCP-1 family (Morona *et al.*, 2009) and an OPX protein (EpsY/MXAN_7417). Additionally, we identified a second locus encoding homologs of the Wzx/Wzy pathway (Fig. 1B, Table S2): a PNPT (MXAN_1043), GTs (MXAN_1026, MXAN_1027, MXAN_1029, MXAN_1030, MXAN_1031, MXAN_1032, MXAN_1036, MXAN_1037, MXAN_1042), a Wzx flippase (MXAN_1035), a Wzy polymerase (MXAN_1052), a Wzc chain length regulator (MXAN_1025 or BtkB (Kimura *et al.*, 2012)) of the PCP-2 family; and an orphan gene encoding an OPX protein (MXAN_1915) (Fig. 1C, Table S2).

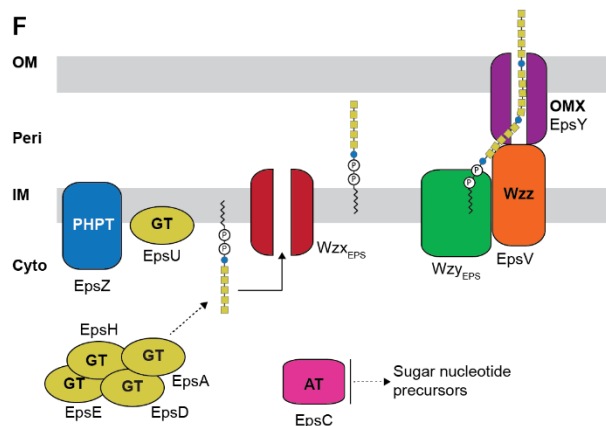
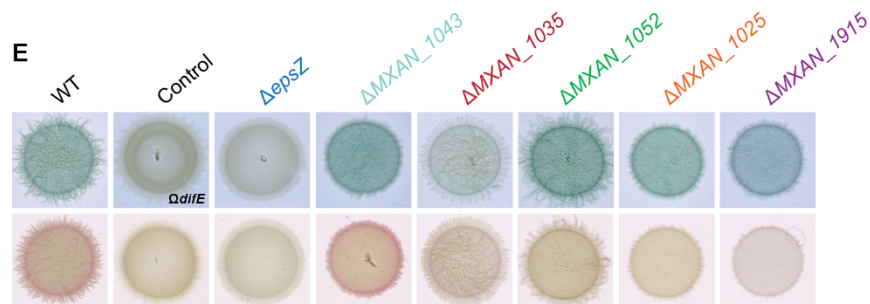
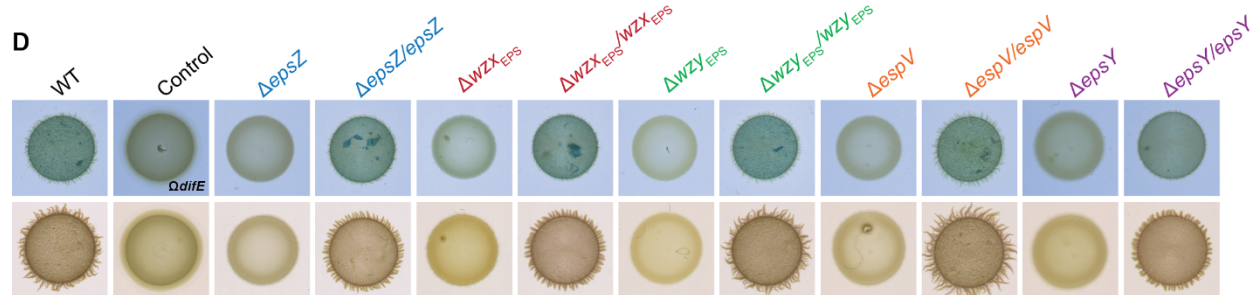
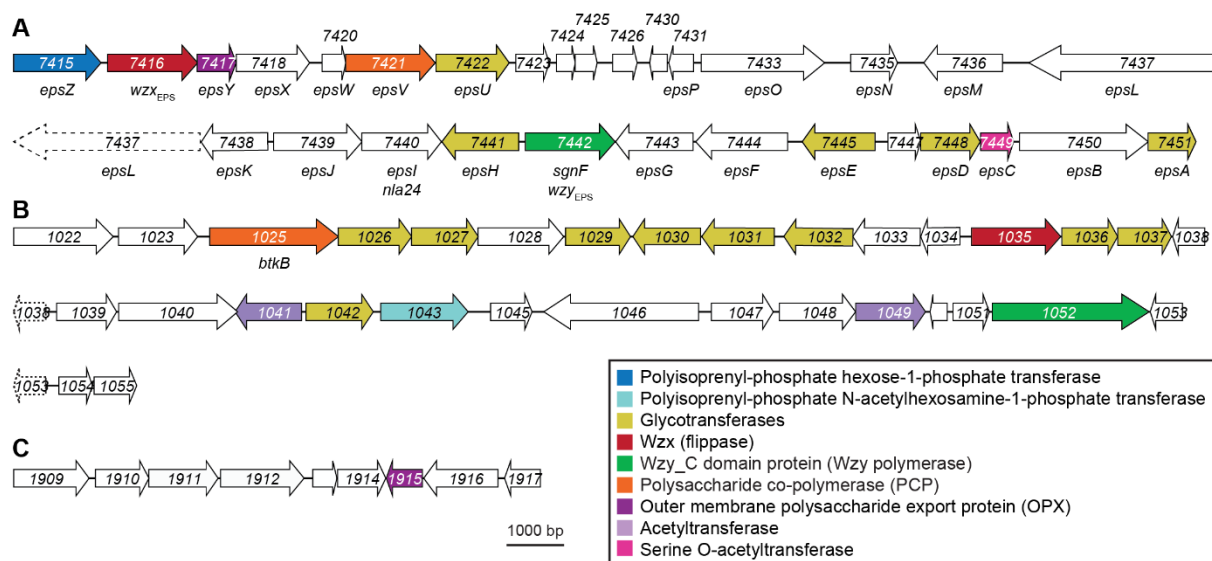


Figure 1. (A-C) Polysaccharide biosynthesis loci (see text). Genes are drawn to scale and MXAN number or gene name indicated (Table S1 and S2). The color code indicates predicted functions and is used throughout all figures. (D-E) Determination of EPS accumulation. 20 μ l aliquots of cell suspensions at 7×10^9 cells ml^{-1} were spotted on 0.5% agar supplemented with 0.5% CTT and Congo red or Trypan blue and incubated at 32°C for 24 h. The $\Omega difE$ mutant served as a negative control. (F) EPS biosynthesis model. See text for details.

In order to test for the importance of genes of the *eps* locus and the “second” locus for EPS synthesis, we generated ten in-frame deletion mutants of the membrane components and used plate-based colorimetric assays with either Congo red or Trypan blue to assess EPS biosynthesis and export. As a negative control, we used the $\Omega difE$ mutant, which has a defect in EPS synthesis (Yang *et al.*, 1998b). All mutations in the *eps* locus completely abolished EPS synthesis (Fig. 1D-E) in agreement with (Lu *et al.*, 2005). Importantly, the EPS synthesis defects of the *eps* mutants was complemented by the ectopic expression of the relevant full-length gene from a plasmid integrated in a single copy at the *Mx8 attB* site (Fig. 1D). By contrast, in the “second locus” only the $\Delta MXAN_1035$ mutant, lacking a *Wzx* flippase homolog (Fig. 1B, E, Fig. S1), caused a decrease in EPS accumulation. Based on several arguments, we do not think that *MXAN_1035* is directly involved in EPS synthesis but rather that the $\Delta MXAN_1035$ mutation results in titration of Und-P. First, blocking translocation of a specific sugar unit across the IM can cause sequestration of Und-P and pleiotropic effects on the synthesis of other sugars (Jorgenson & Young, 2016, Jorgenson *et al.*, 2016). Second, enzymes of the same polysaccharide biosynthesis and export pathway are typically encoded in the same locus (Rehm, 2010); however, the three other mutations in the “second locus” did not have an effect on EPS biosynthesis. Third, mutation of *MXAN_7416*, which encodes a *Wzx* flippase homolog in the *eps* locus, completely blocked EPS synthesis supporting that *MXAN_7416* is the flippase involved in EPS biosynthesis. Fourth, the $\Delta MXAN_1035$ mutation also causes a reduction in glycerol-induced sporulation likely by interfering with spore coat polysaccharide biosynthesis (Holkenbrink *et al.*, 2014); however, *MXAN_3260* (ExoM) was recently shown to be the flippase important for spore coat polysaccharide synthesis (Pérez-Burgos *et al.*, 2020). Thus, it is unlikely that *MXAN_1035* forms part of the EPS biosynthesis machinery. Altogether, our results suggest that the *eps* locus encodes homologs of the *Wzx/Wzy*-dependent pathway involved in EPS biosynthesis (Fig. 1F). Therefore, we renamed *MXAN_7416* and *MXAN_7442* to *WZX_{EPS}* and *WZY_{EPS}*.

Lack of components of the EPS machinery does not affect spore coat polysaccharide, LPS synthesis or cell morphology

In addition to EPS, *M. xanthus* synthesizes O-antigen LPS (Fink & Zissler, 1989a) and a spore coat polysaccharide (Kottel *et al.*, 1975). Because blocking synthesis of one glycan polymer can

affect synthesis of a second one including PG by sequestration of Und-P through accumulation of Und-PP intermediates (Valvano, 2008, Burrows & Lam, 1999, Jorgenson & Young, 2016, Jorgenson *et al.*, 2016, Ranjit & Young, 2016), we determined whether lack of the EPS biosynthetic proteins affects LPS, spore coat polysaccharide or PG synthesis.

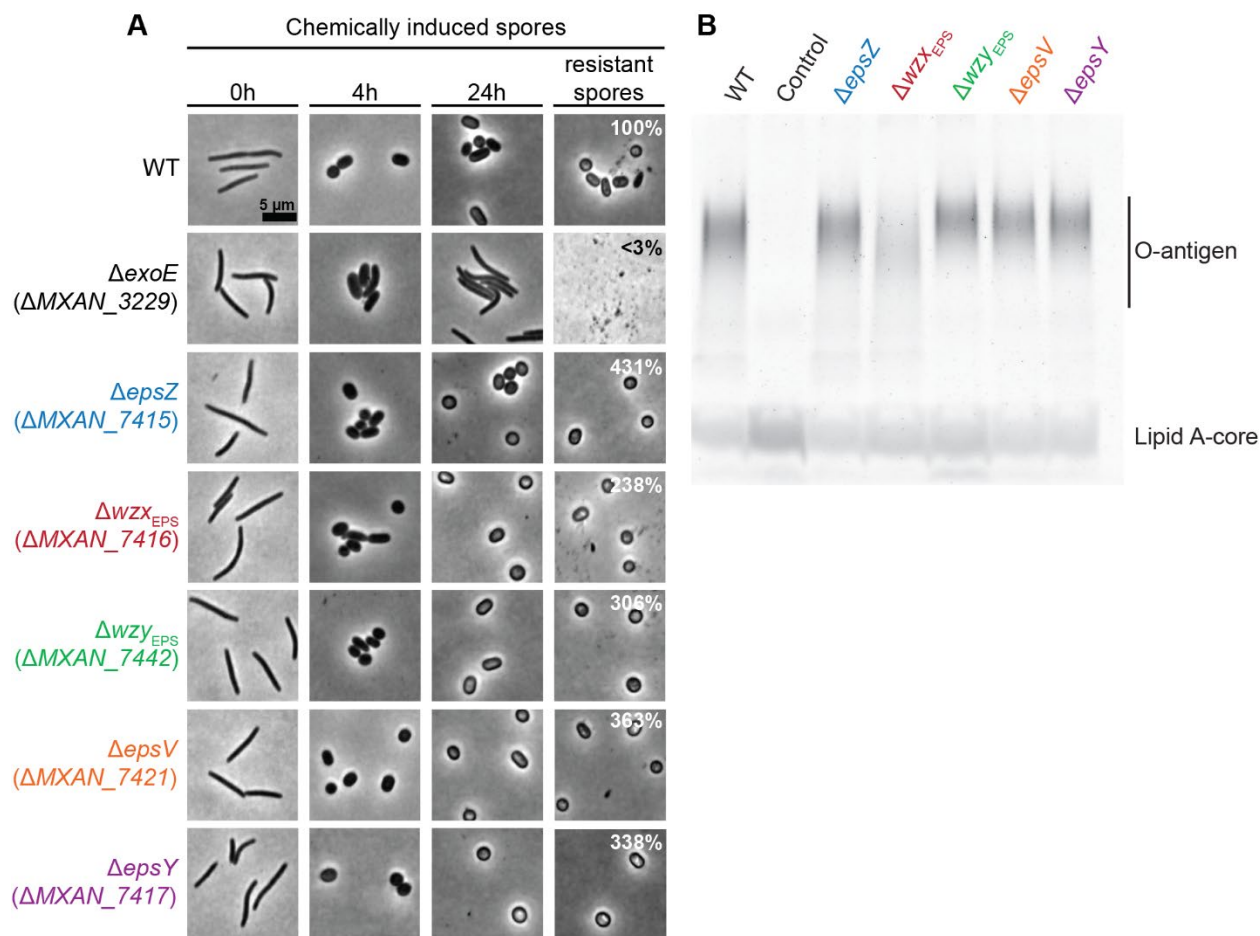


Figure 2. Phenotypic characterization of the Δ eps mutants. (A) Chemically induced sporulation. Sporulation was induced by addition of glycerol to a final concentration of 0.5 M. At 0, 4 and 24 h after induction cell morphology was documented. In images labelled resistant spores, cells were exposed to sonic and heat treatment before microscopy. Sporulation frequency after sonic and heat treatment is indicated as the mean of three technical replicates relative to WT. Scale bars, 5 μ m. (B) Extracted LPS from the same number of cells was separated by SDS-PAGE and detected with Pro-Q Emerald 300.

Synthesis of the spore coat polysaccharide is essential for sporulation in *M. xanthus* (Licking *et al.*, 2000, Müller *et al.*, 2012). In order to evaluate if the *eps* mutants synthesized spore coat polysaccharide, we analyzed sporulation independently of starvation. To this end, we profited from an assay in which sporulation is rapidly and synchronously induced by the addition of 0.5 M glycerol at a high concentration to cells growing in nutrient-rich broth (Dworkin & Gibson, 1964).

In response to the addition of glycerol, cells of WT and all *eps* five in-frame deletion mutants tested rounded up during the first 4 h and had turned into phase-bright resistant spores by 24 h (Fig. 2A). Cells of the ΔexoE mutant, which lacks the PHPT for initiating spore coat polysaccharide biosynthesis was used as a negative control (Holkenbrink *et al.*, 2014, Pérez-Burgos *et al.*, 2020), remained rod-shaped and did not form spherical, phase-bright spores. We conclude that EPS is not required for sporulation in agreement with the previous observation that a mutation in the *dif* locus does not affect glycerol-induced sporulation (Shimkets, 1986b). Interestingly, the sporulation efficiency of the *eps* mutants was increased (Fig. 2A). Because the chemically-induced spores of WT adhered to the shaking flasks and each other forming large aggregates, the *eps* spores did not suggesting that this lack of adhesion and aggregation (see below) facilitated the harvest of the spores rather than the *eps* mutations causing an increase in the overall sporulation efficiency.

Interference with PG synthesis during growth causes morphological defects (Treuner-Lange *et al.*, 2015, Treuner-Lange *et al.*, 2013, Schumacher *et al.*, 2017). Therefore we used cell morphology as a proxy for PG synthesis to test whether lack of the EPS biosynthetic proteins interferes with PG synthesis during growth. Because, cell morphology of the *eps* mutants was similar than for WT, we conclude that PG synthesis was not affected in the *eps* mutants (Fig.2A (0 h)).

LPS in total cell extracts were detected by Emerald staining and the ΔwbaP mutant, which lacks the PHPT for O-antigen biosynthesis and is impaired in O-antigen synthesis, served as a negative control (Pérez-Burgos *et al.*, 2019). For WT as well as all tested *eps* mutants, a fast running lipid-A core band and polymeric LPS O-antigen bands were detected (Fig. 2B), while only the lipid-A core band was detected in the ΔwbaP mutant. Overall, we conclude that lack of the EPS biosynthetic proteins does not interfere with spore coat polysaccharide, PG synthesis or LPS synthesis.

MXAN 7415 has Gal-1-P transferase activity

EpsZ is the predicted PHPT of the EPS biosynthesis pathway. Supporting that EpsZ is a PHPT, we identified a PF13727 (CoA_binding_3) domain, a C-terminal a PF02397 (Bac_transf) domain and five transmembrane regions (Fig. 3A), similarly to WcaJ_{Ec} from *E. coli* and WbaP_{Se} from *S. enterica* (Saldías *et al.*, 2008, Furlong *et al.*, 2015, Pérez-Burgos *et al.*, 2020). The fifth TMH of WcaJ does not fully span the IM and this results on the cytoplasmic localization of the C-terminal catalytic domain. This depends on the residue P291 that arranges a helix-break-helix in the structure and forms part of a DX₁₂P motif conserved among PHPTs (Furlong *et al.*, 2015).

Because EpsZ contains the DX₁₂P motif and all the conserved essential residues important for catalytic activity that have been identified in the C-terminal catalytic region of WbaP (Patel *et al.*, 2010) (Fig. 3B, Fig S2), we suggest that EpsZ is a PHPT with a topology similar to the one of WcaJ.

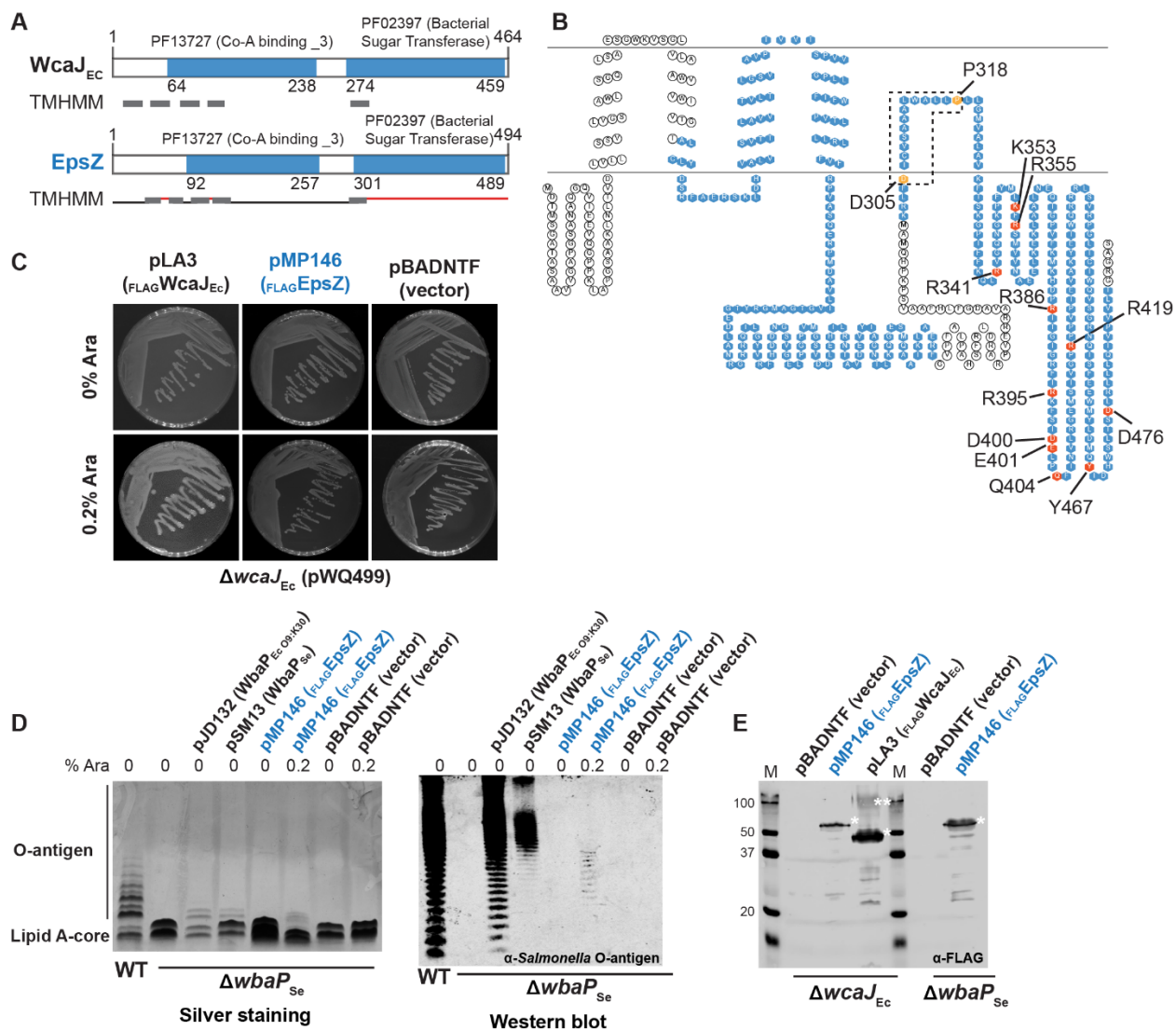


Figure 3. PHPT activity of MXAN_7415. (A) Domain and TMH prediction of MXAN_7415 and WcaJ. Grey rectangles indicate TMH. Numbers indicate domain borders. (B) Topology predictions for MXAN_7415. Domains are indicated in blue and conserved amino acids important for structure or activity of the protein are marked with orange and red, respectively. Sequence alignment of MXAN_7415 with WbaP, is shown in Fig. S2. (C-E) Complementation of O-antigen and colanic acid synthesis in *S. enterica* LT2 ($\Delta wbaP$) and *E. coli* K-12 W3110 ($\Delta wcaJ$) mutants respectively, by plasmids encoding the indicated PHPT proteins. (C) $\Delta wcaJ_{Ec}$ mutant XBF1 containing pWQ499 (RcsA⁺) and the indicated complementing plasmids or vector control on LB plates was incubated overnight at 37°C with 10 μ g ml⁻¹ tetracycline (to maintain pWQ499) and with or without arabinose (Ara) to induce gene expression. Incubation was extended to 24-48 h at room temperature to further increase colanic polysaccharide synthesis. (D) Complementation

of $\Delta wbaP$ mutant in *S. enterica* Typhimurium LT2 containing the indicated plasmids. LPS samples were extracted, separated by electrophoresis on SDS–14% polyacrylamide gels and silver stained (left panel) or examined by immunoblotting using rabbit *Salmonella* O antiserum group B (right panel). Each lane corresponds to LPS extracted from 10^8 cells. Cultures included addition of arabinose as indicated. (E) Immunoblot using α -FLAG monoclonal antibody to confirm expression of $_{FLAG}MXAN_7415$ and $_{FLAG}WcaJ$ in the $\Delta wcaJ$ mutant, and the expression of $_{FLAG}MXAN_7415$ in *S. enterica*. Note that WbaP expressed from pSM13 was not tested since it is not fused to a FLAG tag. * and ** denote the monomeric and oligomeric forms of the PHPT proteins, usually present under the gel conditions required to ensure their visualization.

PHPTs generally utilize UDP-galactose (UDP-Gal) or UDP-glucose (UDP-Glc) as substrates (Lukose *et al.*, 2017, Valvano, 2011). Therefore, following the same strategy as previously reported (Patel *et al.*, 2012, Pérez-Burgos *et al.*, 2019, Pérez-Burgos *et al.*, 2020), we tested whether EpsZ could functionally replace $WcaJ_{Ec}$ or $WbaP_{Se}$, which catalyse the transfer of Glc-1-P and Gal-1-P to Und-P, respectively. Therefore, *epsZ* was cloned into pBADNTF resulting in plasmid pMP146, which encodes EpsZ with an N-terminal FLAG-tag ($_{FLAG}EpsZ$) to facilitate detection by immunoblot and under the control of an arabinose inducible promoter.

$WcaJ_{Ec}$ initiates colanic acid biosynthesis, which provides a strong glossy and mucoid phenotype in $wcaJ_{Ec}^+$ cells containing the plasmid pWQ499, which encodes the positive regulator RcsA (Furlong *et al.*, 2015). An *E. coli* $\Delta wcaJ_{Ec}$ (pWQ499) mutant can be complemented with the plasmid pLA3, which encodes $_{FLAG}WcaJ_{Ec}$ under the control of the arabinose inducible promoter, in the presence of arabinose (Fig. 3C). By contrast, no complementation was observed with expression of $_{FLAG}EpsZ$ or the empty pBADNTF vector in the presence of arabinose (Fig. 3C), suggesting that EpsZ does not have Glc-1-P transferase activity.

$WbaP_{Se}$ initiates O-antigen synthesis in *S. enterica* and the O-antigen synthesis defect of a $\Delta wbaP_{Se}$ mutant can be partially corrected by complementation with the plasmid pJD132, which encodes the *E. coli* O9:K30 $WbaP_{Se}$ homolog ($WbaP_{Ec\ O9:K30}$), and with the plasmid pSM13, which encodes $WbaP_{Se}$ (Saldías *et al.*, 2008) (Fig. 3D, left panel). The differences in the O-antigen profile between the different complementation strains are likely due to different processing of the O-antigen as previously reported (Saldías *et al.*, 2008). Interestingly, expression of $_{FLAG}EpsZ$ in the $\Delta wbaP_{Se}$ mutant in the presence of arabinose resulted in a change of the LPS profile (Fig. 3D, left panel), while the empty pBADNTF vector did not affect the LPS profile. We validated these results by using *Salmonella* O-antigen rabbit antibodies (Fig. 3D, right panel).

To confirm the expression of $_{FLAG}EpsZ$ in the *E. coli* and *S. enterica* strains when grown in the presence of arabinose, we performed immunoblots using α -FLAG antibodies (Fig. 3E). EpsZ accumulated in both strains predominantly in a monomeric form. By contrast, $_{FLAG}WcaJ_{Ec}$ showed

the characteristic oligomeric and monomeric bands as previously reported for PHPTs (Saldías *et al.*, 2008). We conclude from these experiments that WbaP_{Mx} transfers Gal-1-P onto Und-P and it lacks specificity for UDP-Glc.

EPS is important for agglutination

Cell-cell cohesion has been suggested to depend on EPS (Shimkets, 1986b, Dana & Shimkets, 1993, Arnold & Shimkets, 1988a), but also on T4P (Wu & Kaiser, 1997, Shimkets, 1986a). However, mutations in genes encoding core components of the T4P machinery, which abolish T4P formation (Friedrich *et al.*, 2014, Bulyha *et al.*, 2009, Wu & Kaiser, 1995, Wu *et al.*, 1997, Nudleman *et al.*, 2006, Siewering *et al.*, 2014), also cause a reduction in EPS (Fig. 4A). In contrast, mutants lacking components of the T4P machinery that still assembled T4P also synthesized EPS; e.g the hyperpiliated $\Delta pilT$ mutant accumulated increased levels of EPS (Fig. 4A) (Black *et al.*, 2006, Wallace *et al.*, 2014, Dana & Shimkets, 1993, Bretl *et al.*, 2016, Wu *et al.*, 1997, Shimkets, 1986a, Black *et al.*, 2017, Kaiser, 1979). We therefore suggest that the cell-cell cohesion defect of Δpil mutants may be caused by lack of EPS (see Discussion).

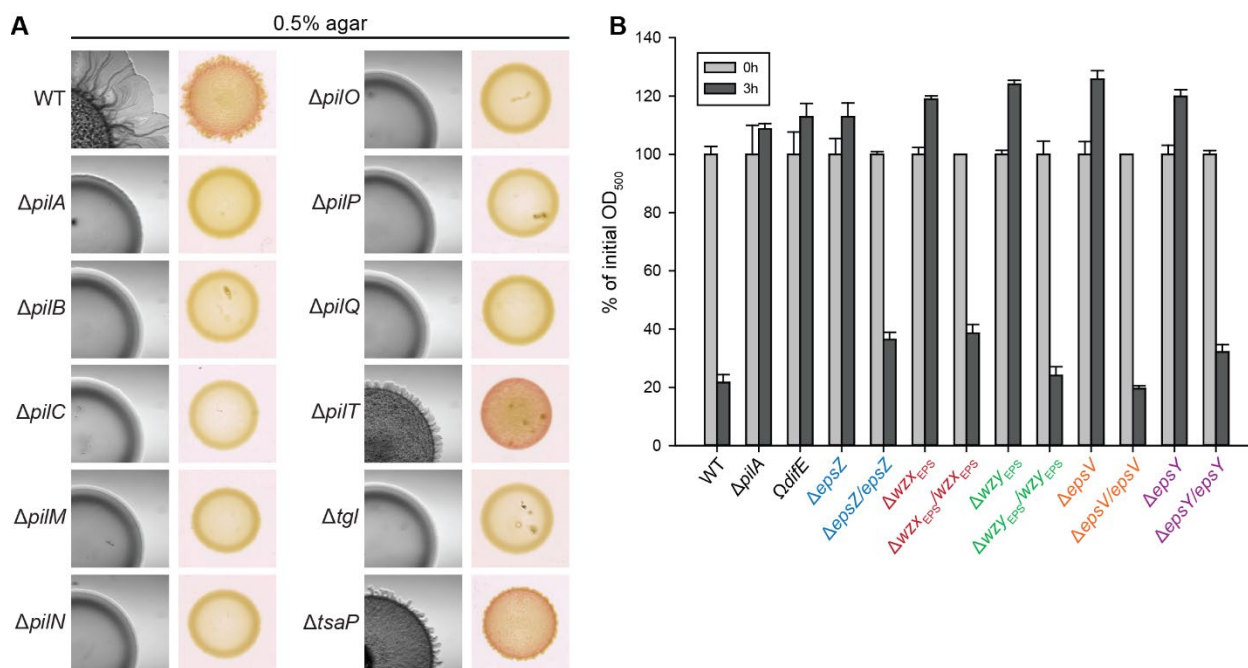


Figure 4. (A) Colony-based motility assay and EPS accumulation. 5 and 20 μ l aliquots of cell suspensions at 7×10^9 cells/ml were spotted on 0.5% agar and on 0.5% agar supplemented with 0.5% CTT and Congo red respectively. Plates were incubated at 32°C for 24 h. (B) Cell agglutination assay. 1 ml of exponentially growing cells were transferred to a cuvette. Agglutination was monitored by measuring the decrease in absorbance at 550 nm at 0 and 3 h relative to the initial absorbance for each strain. The graph shows data from three technical replicates of one representative experiment.

In order to evaluate whether the Δeps mutants are affected in cell-cell cohesion, we transferred exponentially growing cells to a cuvette and measured the change in cell density over time. WT cells agglutinated and sedimented during the course of the experiment, causing a decrease in the absorbance (Fig. 4B). The $\Omega difE$ mutant was used as a negative control and did not agglutinate over time. None of the five *eps* in-frame deletion strains agglutinated (Fig. 4B). Similarly, a $\Delta pilA$ strain, lacking the major pilin, did not agglutinate in agreement with (Velicer & Yu, 2003). The agglutination defects of the five *eps* mutants were complemented in the complementation strains (Fig. 4B).

EPS is important for T4P formation

EPS has been implicated with *M. xanthus* T4P-dependent motility on multiple occasions. Here, we reevaluate the motility phenotype using the five *eps* mutants. To analyze the effect of the *eps* mutation on T4P-dependent and gliding motility, cells were spotted on 0.5 and 1.5% agar, respectively (Shi & Zusman, 1993). On 0.5% agar, WT cells formed the long flares characteristic of T4P-dependent motility whereas on 1.5% agar, WT displayed single cells at the colony edge. $\Delta pilA$ lacks the major pilin subunit and does not assemble T4P (Wu & Kaiser, 1997) while $\Delta aglQ$ lacks a component of the gliding machinery (Sun *et al.*, 2011, Nan *et al.*, 2013) and both were used as negative controls for T4P-dependent and gliding motility, respectively. We additionally included the $\Omega difE$ mutant in the study to compare it with the Δeps mutants. As expected, lack of components of the EPS biosynthetic machinery caused a T4P-dependent motility defect (Fig. 5A). However, colony morphology of the Δeps mutants was different from that of the $\Omega difE$ mutant.

Because we observed formation of a halo in the $\Omega difE$ mutant (Fig. 5A), differently than described by Yang *et al.* (Yang *et al.*, 1998b) and suggesting that cells were still able to move by T4P-dependent motility, we generated an in-frame deletion mutant. The $\Delta difE$ strain phenotype was identical to the $\Omega difE$ strain and the motility defects could be complemented when ectopically expressing full-length *difE* on a plasmid integrated in a single copy at the Mx8 *attB* site (Fig. 5A). Additionally, the movement of single cells on 1.5 % agar was generally not impaired in mutants lacking Eps proteins (Fig. 5A). However, the total colony expansion was reduced as in the case of the $\Delta pilA$ mutant. Both motility systems work synergistically, and while T4P-dependent motility and gliding motility are enhanced on 0.5 or 1.5 % agar respectively, a mutation in any of the motility system has a slight impact on the other (Kaiser & Crosby, 1983, Burchard, 1974, Zhou & Nan, 2017, Guzzo *et al.*, 2009). Since a $\Delta pilA$ mutant is affected in EPS synthesis, it is not clear if the slight defect in gliding results from lack of EPS and/or from the defect in T4P-dependent motility.

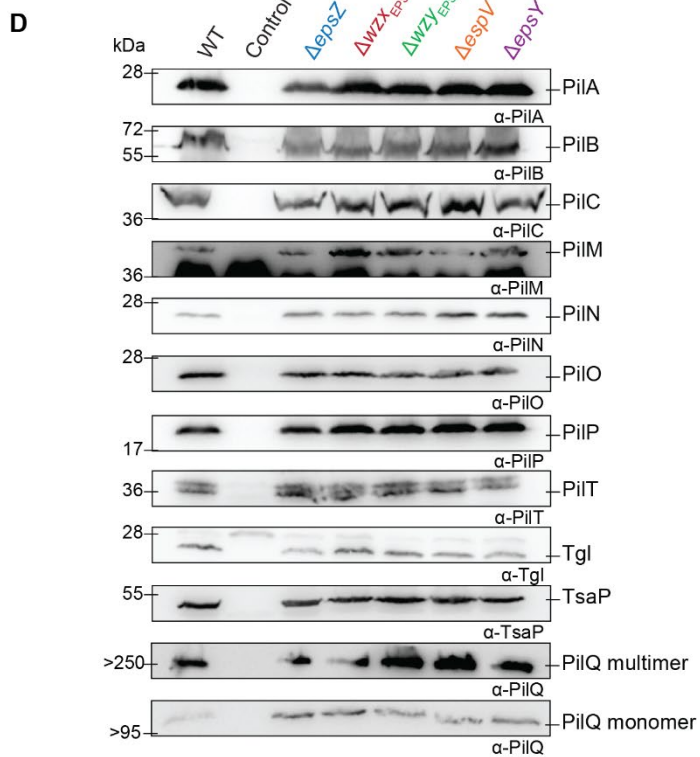
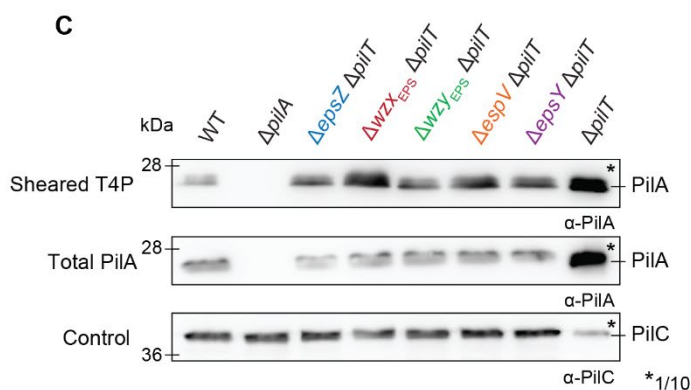
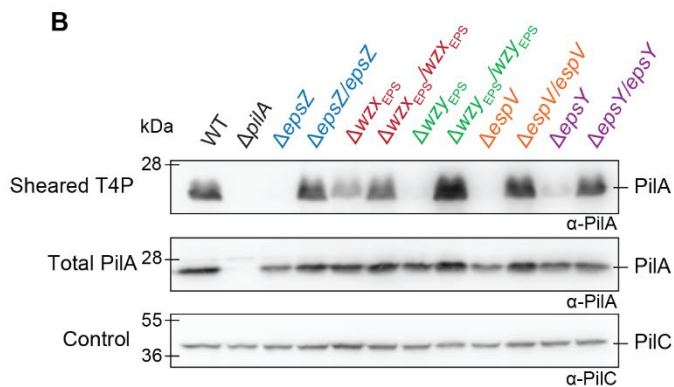
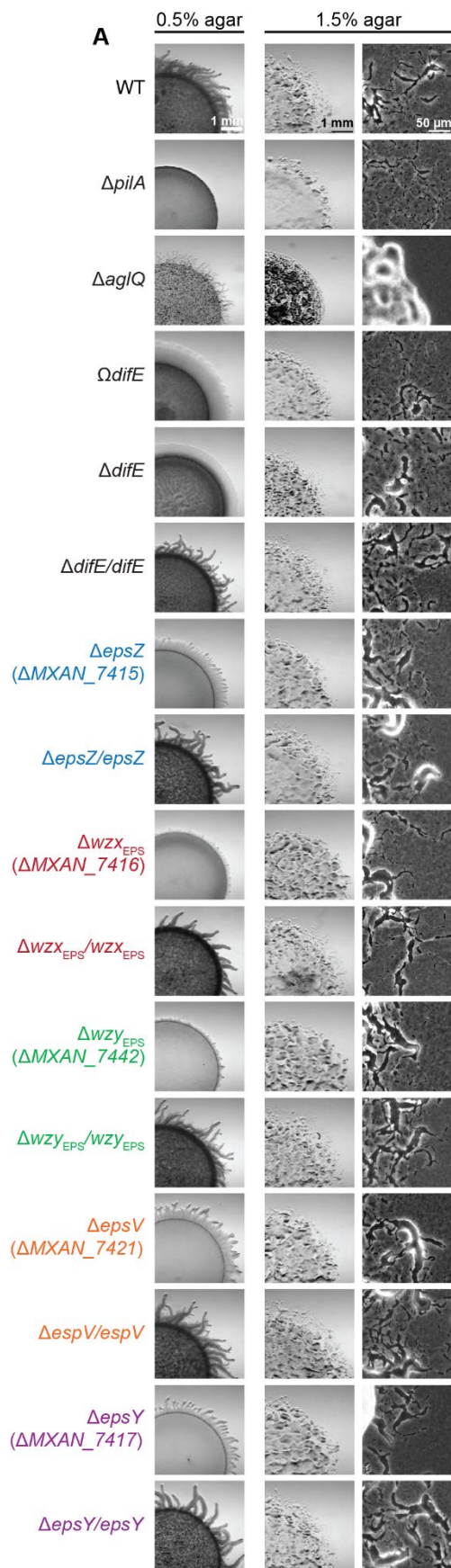


Figure 5. Motility studies of the Δeps mutants. (A) Colony-based motility assay of Δeps mutants. T4P-dependent motility and gliding motility were tested on 0.5% and 1.5% agar respectively. Images were recorded after 24 h. (B-C) T4P shear off assay. Immunoblot detection of the major pilin PilA in sheared T4P (top) and in total cell extract (middle), where the same number of cells grown on 1% CTT 1.5% agar plates was loaded per lane. The top and middle blots were probed against PilA (23.4 kDa). The middle blot was stripped and probed against PilC (45.2 kDa), as a loading control. (D) Immunoblot detection of proteins of the T4P machinery using anti-PilA, -B, -C, -M, -N, -O, -P, -Q, -T, Tgl and TsaP. The same number of cells coming from exponentially growing liquid cultures was loaded per lane. As a negative control, cells containing a single in-frame deletion mutation in each correspondent gene were used.

Next, using a shear-off assay followed by immunoblotting, we analyzed whether the Δeps mutants cause hyperpiliation as observed for the $\Omega difE$ mutant (Li et al., 2003). Surprisingly, the T4P level was reduced in all five eps mutants tested (Fig. 5B). Given that the low T4P level can result from a lower assembly or higher pili retraction, we deleted the $pilT$ gene encoding the major retraction ATPase (Jakovljevic et al., 2008) and repeated the assay. For all strains tested, the $eps pilT$ strains still assembled T4P, but at a significantly lower level than the $\Delta pilT$ strain (Fig. 5C). Thus, lack of EPS and/or the EPS biosynthetic machinery affects T4P assembly. However we cannot exclude that EPS influences T4P retraction.

To determine whether the reduced T4P formation resulted from a lower protein concentration of one of the Pil proteins, we determined whether any of the eps mutations caused reduced accumulation of the 10 core proteins of the T4P machine. All 10 components of the pilus machinery were detected at WT levels in the eps mutants (Fig. 5D).

Development

EPS is a major component of the *M. xanthus* fruiting body (Lux et al., 2004) and has also been implicated in completion of the developmental program (Shimkets, 1986b, Yang et al., 1998a) Here, we reevaluate the role of EPS in development using the five Δeps mutants.

On TPM agar and in submerged culture, WT cells had aggregated to form darkened mounds at 24 h of starvation, $\Omega difE$ and $\Delta difE$ strains did not aggregate (Fig. 6) in agreement with previous studies (Yang et al., 1998b, Shimkets, 1986b). The defect of the $\Delta difE$ mutant was complemented when full-length $difE$ was ectopically expressed from a plasmid integrated in a single copy at the Mx8 $attB$ site. By contrast, on TPM agar the Δeps mutants showed a delay in aggregation but eventually formed bigger and less compact fruiting bodies (Fig. 6). Importantly, the Δeps mutants sporulated with an efficiency similar to that of WT. In submerged conditions, however, the Δeps mutants formed no aggregates as expected from the adhesion and agglutination defects. Development of the five Δeps mutants was restored by ectopic expression of the corresponding full-length gene on a plasmid integrated in a single copy at the Mx8 $attB$ site (Fig. 6).

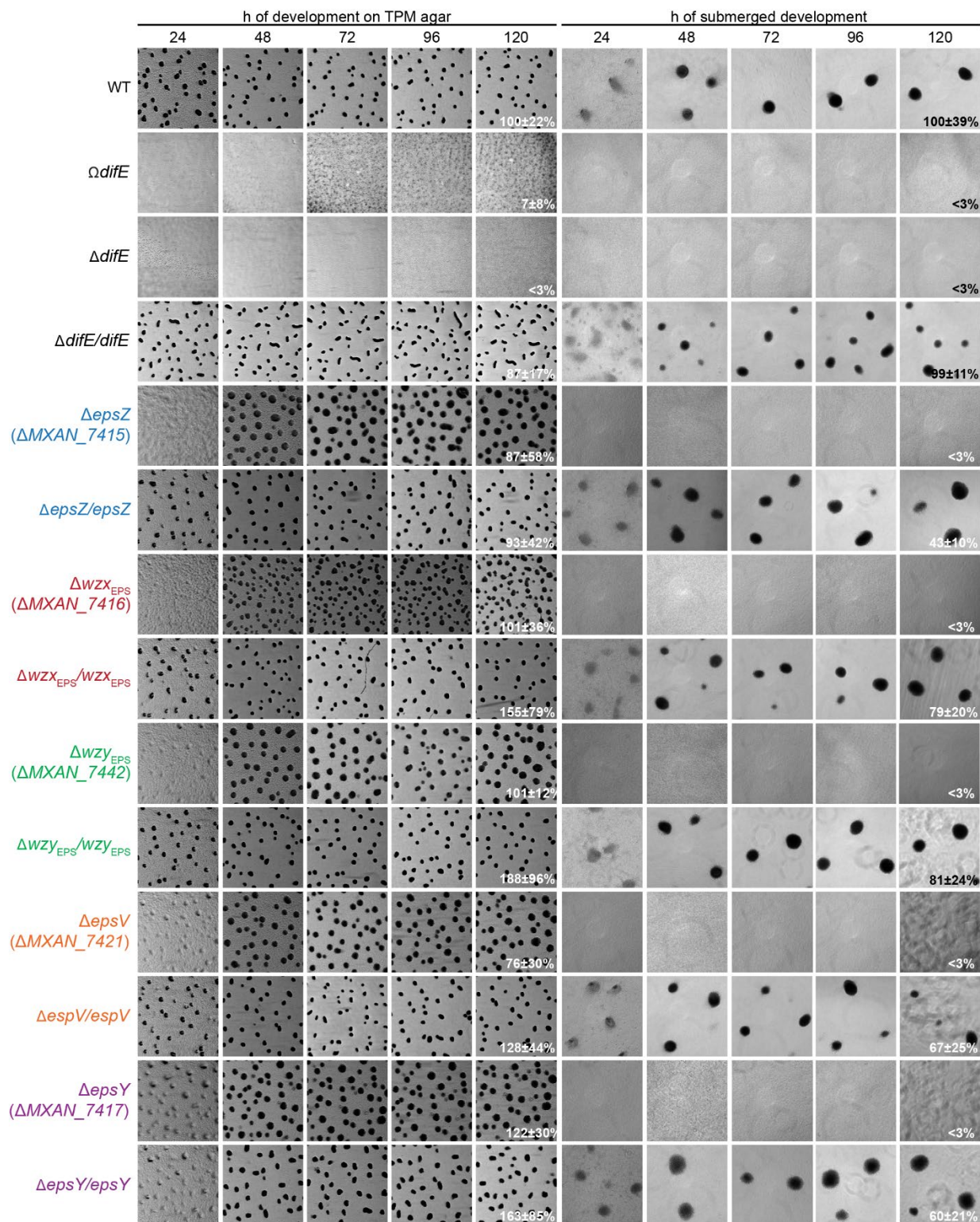


Figure 6. Development assay. Cells on TPM agar and under submerged conditions were followed during development. Images were recorded at the indicated time points. Sporulation efficiency after heat and sonic treatment is indicated as the mean \pm standard deviation from at least two biological replicates relative to WT. Scale bars: 1mm (left), 200 μ m (right).

The *eps* locus co-occur only in a subset of myxobacteria

Because EPS is important for development (Shimkets, 1986b) and the majority of the members of the order Myxococcales forms spore-filled fruiting bodies (Reichenbach, 1999), we hypothesized that the EPS machinery would be conserved in the Myxococcales. We therefore searched for orthologs of the proteins encoded by the *eps* locus in Myxococcales with fully sequenced genomes using a reciprocal best BlastP hit method as in (Pérez-Burgos *et al.*, 2020).

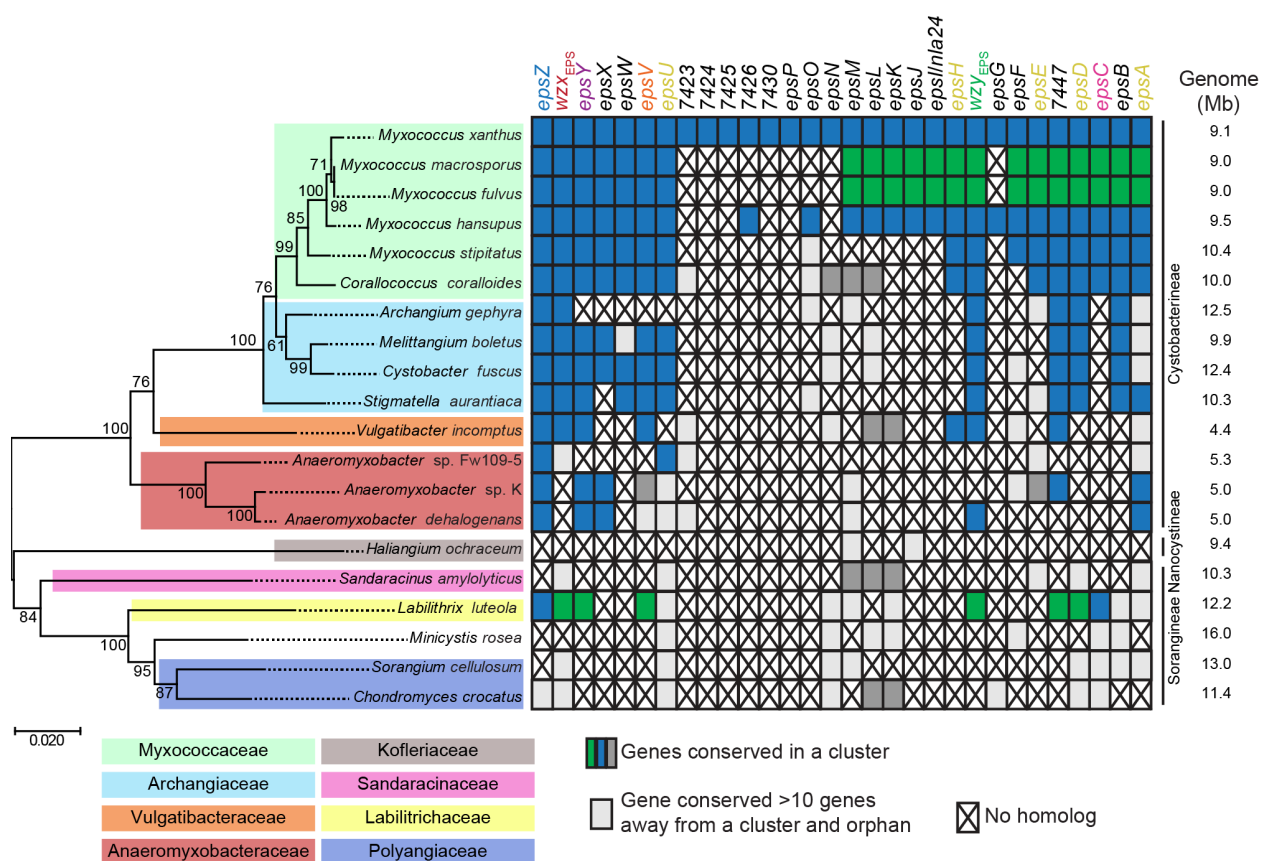


Figure 7. Taxonomic distribution and synteny of the *eps* gene organization in myxobacteria. A reciprocal best BlastP hit method was used to identify orthologs. 16S rRNA tree of Myxococcales with fully sequenced genomes (left). Genome size, family and suborder classification are indicated (right). To evaluate gene proximity and cluster conservation, 10 genes were considered as the maximum distance for a gene to be in a cluster. Genes found in the same cluster (within a distance of <10 genes) are marked with the same color (i.e. blue, green and dark grey). Light grey indicates a conserved gene that is found somewhere else on the genome (>10 genes away from a cluster); a cross indicates no homolog found.

Interestingly, the core components of the machinery (Fig. 1F) seem to be conserved in a cluster especially in Cystobacterineae (Fig. 7), but less conserved in the rest of the myxobacteria. The *eps* gene cluster contains genes that are not essential for EPS synthesis (Lu *et al.*, 2005) (e.g. metal transporters) (Table S1). This region (i.e. *MXAN_7423-MXAN_7440*) is not highly

conserved in myxobacteria supporting that they likely function independently of the EPS biosynthesis pathway. Similarly, the *eps* locus of *Myxococcus macrosporus* and *Myxococcus fulvus* also contains a non-conserved genetic region that is homologous for the two organisms.

3.3.4 Discussion

M. xanthus colonies are embedded in EPS and while its structure is not known, EPS contains at least GlcNAc, Glc and Gal while results of other monosaccharides vary depending on the analysis (Behmlander & Dworkin, 1994, Li *et al.*, 2003, Sutherland & Thomson, 1975). Here, we focused on elucidating key steps of EPS biosynthesis and export, and determining and reevaluating the functional consequences of EPS loss.

Using bioinformatics, we identified components of a Wzx/Wzy pathway encoded by the *eps* locus that is important for EPS synthesis (Lu *et al.*, 2005). Our results support a model in which the synthesis of the EPS repeat unit is initiated by the PHPT homolog EpsZ (MXAN_7415) (Fig. 1F). Here, we demonstrate through heterologous expression experiments that EpsZ is functionally similar to the Gal-1-P transferase WbaP_{Se}, suggesting that Gal is the first sugar of the EPS repeat unit. Different GTs (i.e. EpsU/MXAN_7422, EpsH/MXAN_7441, EpsE/MXAN_7445 and EpsD/MXAN_7448) add monosaccharides to build the repeat unit, which is translocated through the IM by the Wzx_{EPS} flippase (MXAN_7416). The repeat unit is polymerized by the Wzy_{EPS} polymerase (MXAN_7442) with the help of the Wzz protein EpsV (MXAN_7421) into the EPS polysaccharide. In the last step, the EPS polymer is transported to the surface through the OPX protein EpsY (MXAN_7417). Moreover, the EPS machinery is exclusively dedicated to EPS biosynthesis and since it is not conserved in all the fruiting myxobacteria, we suggest that other polysaccharides may overtake the role of EPS.

Additionally, we have identified two new polysaccharide biosynthesis loci that are not directly implicated with EPS, LPS or spore coat polysaccharide biosynthesis; MXAN_1025-MXAN_1052 encode proteins some of them homologous to the Wzx/Wzy-dependent pathway and an orphan gene (MXAN_1915) encoding an OPX protein. Cells moving by gliding motility deposit a slime trail whose composition and function are unknown; however it may promote the adhesion of cells to the substratum, and it contains polysaccharides and OM vesicles (Gloag *et al.*, 2016, Ducret *et al.*, 2012, Ducret *et al.*, 2013). A future goal will be to understand if MXAN_1025-MXAN_1052 and MXAN_1915 are involved in slime polysaccharide biosynthesis.

Because the majority of the studies evaluating the role of EPS had been performed using regulatory mutants instead of mutants exclusively blocked in EPS synthesis, we decided to reevaluate the impact of EPS on the social behaviors of *M. xanthus*. We show that the defects caused by mutations in components of the EPS machinery are several folds. The *eps* mutants show a defect in EPS synthesis and agglutination in agreement with (Lu *et al.*, 2005, Arnold &

Shimkets, 1988a). Cell-cell cohesion had initially been suggested to depend on EPS (Shimkets, 1986b, Dana & Shimkets, 1993, Arnold & Shimkets, 1988a) and on T4P (Wu & Kaiser, 1997, Shimkets, 1986a). Based on several observations, we propose that influence of T4P on cell agglutination is likely caused by an indirect effect on EPS synthesis in agreement with (Hu *et al.*, 2012b). First, EPS synthesis is regulated by T4P formation. Second, a *stk* mutation in cells lacking core components of the T4P machinery (e.g. PilQ) that are blocked in T4P assembly, recovered the ability to synthesize EPS and agglutinate, suggesting that agglutination can occur independently of T4P. Third, cells containing a mutation in *pilA* showed recovery of cell cohesion and EPS accumulation through evolution (Velicer & Yu, 2003). Fourth, $\Delta difA$ cells lack EPS and do not aggregate (Yang *et al.*, 2000b) despite they assemble pili (Yang *et al.*, 2000b, Li *et al.*, 2003) that are functional (Hu *et al.*, 2011). Therefore, we suggest that cell agglutination and adhesion to the surfaces depends mainly on EPS.

Moreover, EPS has been implicated with *M. xanthus* T4P-dependent motility in multiple occasions. However, because different regulatory mutants were used, there are many controversial results on how this regulation occurs. Here, we show that EPS, or alternatively components of the EPS machinery, is important for T4P formation and *vice versa*. The T4P machinery functions upstream of the Dif pathway in the regulation of EPS synthesis (Black *et al.*, 2006, Dana & Shimkets, 1993, Black *et al.*, 2009). However, how this regulation occurs is not known. Additionally, we show that EPS is conditionally important for development. While aggregation in submerged cultures of the Δeps mutants was completely blocked likely through the agglutination defect, the Δeps mutants were able to develop and sporulate on solid surfaces.

Importantly, the *dif* mutants lacking EPS behaved differently than the Δeps mutants at both stages of the *M. xanthus* life cycle: $\Omega difE$ and $\Delta difE$ show a different colony morphology during growth on soft surfaces and they do not form aggregates in response to lack of nutrients in agreement with (Shimkets, 1986b, Arnold & Shimkets, 1988a, Yang *et al.*, 1998b, Bellenger *et al.*, 2002). Thus, we suggest that the Dif pathway is involved in regulation of additional physiological processes apart from EPS synthesis.

3.4.5 Acknowledgement

The authors thank Dorota Skotnicka for construction of SA5649 as well as A. Treuner-Lange for construction of pMAT150. This work was supported by Deutsche Forschungsgemeinschaft (DFG, German Research Council) within the framework of the SFB987 “Microbial Diversity in Environmental Signal Response” as well as by the Max Planck Society.

3.3.6 Experimental procedures

Strains and cell growth. All *M. xanthus* strains are derivatives of the wild type DK1622 (Kaiser, 1979). Strains, plasmids and oligonucleotides used in this work are listed in Table 1, Table 2, and Table S3, respectively. *M. xanthus* was grown at 32°C in 1% CTT (1% (w/v) Bacto Casitone, 10 mM Tris-HCl pH 8.0, 1 mM K₂HPO₄/KH₂PO₄ pH 7.6 and 8 mM MgSO₄) liquid medium or on 1.5% agar supplemented with 1% CTT and kanamycin (50 µg ml⁻¹) or oxytetracycline (10 µg ml⁻¹), as appropriate (Hodgkin & Kaiser, 1977). In-frame deletions were generated as described (Shi *et al.*, 2008), and plasmids for complementation experiments were integrated in a single copy by site specific recombination into the Mx8 *attB* site. In-frame deletions and plasmid integrations were verified by PCR. Plasmids were propagated in *E. coli* Mach1 and DH5α.

E. coli and *S. enterica* serovar Typhimurium strains were grown at 37°C in Luria-Bertani (LB) medium (10 mg tryptone ml⁻¹, 5 mg yeast extract ml⁻¹; 5 mg NaCl ml⁻¹) supplemented, when required, with ampicillin, tetracycline, kanamycin or chloramphenicol at final concentrations of 100, 20, 40 and 30 µg ml⁻¹, respectively. Plasmids for heterologous complementation were introduced into MSS2 and XBF1 strains (Table 1) by electroporation (Dower *et al.*, 1988).

Table 1. Strains used in this work

Strain	Genotype	Reference
<i>M. xanthus</i>		
DK1622	WT	(Kaiser, 1979)
DK8615	$\Delta pilQ$	(Wall <i>et al.</i> , 1999)
DK10405	Δtgl	(Rodriguez-Soto & Kaiser, 1997, Wall <i>et al.</i> , 1998)
DK10409	$\Delta pilT$	(Jakovljevic <i>et al.</i> , 2008, Wu <i>et al.</i> , 1997)
DK10410	$\Delta pilA$	(Wu <i>et al.</i> , 1997)
DK10416	$\Delta pilB$	(Jakovljevic <i>et al.</i> , 2008, Wu <i>et al.</i> , 1997)
DK10417	$\Delta pilC$	(Wu <i>et al.</i> , 1997)
SW501	<i>difE::Km^r</i>	(Yang <i>et al.</i> , 1998b)
SA3001	$\Delta pilO$	(Friedrich <i>et al.</i> , 2014)
SA3002	$\Delta pilM$	(Bulyha <i>et al.</i> , 2009)
SA3005	$\Delta pilP$	(Friedrich <i>et al.</i> , 2014)
SA3044	$\Delta pilN$	(Friedrich <i>et al.</i> , 2014)
SA5923	$\Delta aglQ$	(Jakobczak <i>et al.</i> , 2015)
SA6011	$\Delta tsaP$	(Siewering <i>et al.</i> , 2014)
SA7450	$\Delta wbaP_{Mx}$	(Pérez-Burgos <i>et al.</i> , 2019)
SA7495	$\Delta exoE$	(Pérez-Burgos <i>et al.</i> , 2019)

SA5649	$\Delta difE$	This study.
SA7400	$\Delta MXAN_7415$	This study.
SA7405	$\Delta MXAN_7416$	This study.
SA7406	$\Delta MXAN_7421$	This study.
SA7407	$\Delta MXAN_7442$	This study.
SA7408	$\Delta MXAN_7417$	This study.
SA7410	$\Delta MXAN_7416 attB::pMP024 (P_{nat} MXAN_7416)$	This study.
SA7411	$\Delta MXAN_7415 attB::pMP021 (P_{nat} MXAN_7415)$	This study.
SA7412	$\Delta MXAN_7417 attB::pMP030 (P_{pilA} MXAN_7417)$	This study.
SA7413	$\Delta MXAN_7421 attB::pMP032 (P_{pilA} MXAN_7421)$	This study.
SA7427	$\Delta MXAN_7416 \Delta pilT$	This study.
SA7433	$\Delta MXAN_7415 \Delta pilT$	This study.
SA7435	$\Delta MXAN_7442 \Delta pilT$	This study.
SA7444	$\Delta MXAN_7417 \Delta pilT$	This study.
SA7445	$\Delta MXAN_7421 \Delta pilT$	This study.
SA7451	$\Delta MXAN_1025$	This study.
SA7452	$\Delta MXAN_1035$	This study.
SA7456	$\Delta MXAN_1052$	This study.
SA7454	$\Delta MXAN_1915$	This study.
SA7477	$\Delta MXAN_7442 attB::pMP091 (P_{nat} MXAN_7442)$	This study.
SA8515	$\Delta MXAN_1043$	This study.
SA8538	$\Delta difE attB::pMP137 (P_{pilA} difE)$	This study.
<i>E. coli</i>		
DH5 α	F ⁻ $\phi 80/lacZ\Delta M15 endA recA hsdR(r_{K^-} m_{K^-}) nupG thi glnV deoR gyrA relA1 \Delta(lacZYA-argF)U169$	Lab stock
Mach1	$\Delta recA1398 endA1 tonA \Phi 80\Delta lacM15 \Delta lacX74 hsdR(r_{K^-} m_{K^+})$	Invitrogen
XBF1	W3110, $\Delta wcaJ::aph, Km^r$	(Patel <i>et al.</i> , 2012)
<i>Salmonella</i>		
LT2	WT, <i>S. enterica</i> serovar Typhimurium	S. Maloy
MSS2	LT2, $\Delta wbaP::cat Cm^r$	(Saldías <i>et al.</i> , 2008)

Table 2. Plasmids used in this work

Plasmid	Description	Reference
pBJ114	Km ^r <i>galK</i>	(Julien <i>et al.</i> , 2000)
pSWU30	Tet ^r	(Wu & Kaiser, 1997)
pSW105	Km ^r , PpilA	(Jakovljevic <i>et al.</i> , 2008)
pBADNTF	pBAD24 for N-terminal FLAG fusion and with arabinose inducible promoter, Amp ^r	(Marolda <i>et al.</i> , 2004)
pLA3	pBADNTF, <i>wcaJ</i> , Amp ^r	(Furlong <i>et al.</i> , 2015)
pSM13	pUC18, <i>wbaP</i> from <i>S. enterica</i> Ty2 containing a 1 bp deletion at position 583 and a 2 bp deletion at position 645. This causes a frame shift at WbaP I194 and frame restoration at Y215, Amp ^r	(Saldías <i>et al.</i> , 2008)

pJD132	pBluescript SK, <i>wbaP</i> and flanking sequences from <i>E. coli</i> O9:K30, Amp ^r	(Schäffer <i>et al.</i> , 2002)
pWQ499	pKV102 containing <i>rcsAK30</i> , Tet ^r	C. Whitfield
pMAT150	pBJ114, in-frame deletion construct for <i>pilT</i> Km ^r	Anke Treuner-Lange
pDJS102	pBJ114, in-frame deletion construct for <i>difE</i> Km ^r	Dorota Skotnicka
pMP001	pBJ114, in-frame deletion construct for <i>MXAN_7415</i> Km ^r	This study.
pMP012	pBJ114, in-frame deletion construct for <i>MXAN_7421</i> Km ^r	This study.
pMP015	pBJ114, in-frame deletion construct for <i>MXAN_7442</i> Km ^r	This study.
pMP016	pBJ114, in-frame deletion construct for <i>MXAN_7416</i> Km ^r	This study.
pMP018	pBJ114, in-frame deletion construct for <i>MXAN_7417</i> Km ^r	This study.
pMP021	pSWU30, P _{nat} <i>MXAN_7415</i> Tet ^r	This study.
pMP024	pSWU30, P _{nat} <i>MXAN_7416</i> Tet ^r	This study.
pMP030	pSW105, <i>MXAN_7417</i> Km ^r	This study.
pMP032	pSW105, <i>MXAN_7421</i> Km ^r	This study.
pMP091	pSWU30, P _{nat} <i>MXAN_7442</i> Tet ^r	This study.
pMP124	pBJ114, in-frame deletion construct for <i>MXAN_1043</i> Km ^r	This study.
pMP137	pSW105, <i>difE</i> Km ^r	This study.
pMP146	pBADNTE, <i>MXAN_7415</i> Amp ^r	This study.
pJJ1	pBJ114, in-frame deletion construct for <i>MXAN_1035</i> Km ^r	This study.
pJJ2	pBJ114, in-frame deletion construct for <i>MXAN_1025</i> Km ^r	This study.
pJJ3	pBJ114, in-frame deletion construct for <i>MXAN_1052</i> Km ^r	This study.
pJJ4	pBJ114, in-frame deletion construct for <i>MXAN_1915</i> Km ^r	This study.

Cell agglutination assay. Cell agglutination was performed as described previously (Wu *et al.*, 1997) with a slightly modified protocol. Briefly, 1 ml of exponentially growing cells in 1% CTT was transferred to a cuvette and cell density was measured at the indicated time points.

Motility assays. Exponentially growing cultures of *M. xanthus* were harvested (6000 g, room temperature (RT)) and resuspended in 1% CTT to a calculated density of 7×10^9 cells ml⁻¹. 5 µl aliquots of cell suspensions were spotted on 0.5% and 1.5% agar supplemented with 0.5% CTT. The plates were incubated at 32°C for 24 h and cells were visualized using a M205FA Stereomicroscope (Leica) and imaged using a Hamamatsu ORCA-flash V2 Digital CMOS camera (Hamamatsu Photonics). Pictures were analyzed using Metamorph® v 7.5 (Molecular Devices).

Development. Exponentially growing *M. xanthus* cultures were harvested (3 min, 6000 g at RT), and resuspended in MC7 buffer (10 mM MOPS pH 7.0, 1 mM CaCl₂) to a calculated density of 7×10^9 cells ml⁻¹. 10 µl aliquots of cells were placed on TPM agar (10 mM Tris-HCl pH 7.6, 1 mM K₂HPO₄/KH₂PO₄ pH 7.6, 8 mM MgSO₄), and 50 µl aliquots were mixed with 350 µl of MC7 buffer and placed in a 24-well polystyrene plate (Falcon) for development in submerged culture. Cells

were visualized at the indicated time points using a M205FA Stereomicroscope (Leica) and imaged using a Hamamatsu ORCA-flash V2 Digital CMOS camera (Hamamatsu Photonics), and a DMI8 Inverted microscope and DFC9000 GT camera (Leica). Images were analyzed as previously described. After 120 h, cells were collected and incubated at 50°C for 2 h, and then sonicated with 30 pulses, pulse 50%, amplitude 75% with a UP200St sonifier and microtip (Hielscher). Sporulation levels were determined as the number of sonication- and heat-resistant spores relative to WT using a Helber bacterial counting chamber (Hawksley, UK).

Glycerol-induced sporulation assay. Sporulation in response to 0.5 M glycerol was performed as described (Müller *et al.*, 2010) with a slightly modified protocol. Briefly, cells were cultivated in 10 ml of CTT medium, at a cell density of 3×10^8 cells ml⁻¹, glycerol was added to a final concentration of 0.5 M. At 0, 4 and 24 h after glycerol addition, cell morphology was observed by placing 5 µl of cells on a 1.5% agar TPM pad on a slide. Cells were immediately covered with a coverslip and imaged with DMI6000B microscope and a Hamamatsu Flash 4.0 Camera (Leica). To determine the resistance to heat and sonication of spores formed, cells from 5 ml of the culture after 24 h incubation were harvested (10 min, 4150 g, RT), resuspended in 1 ml sterile water, incubated at 50°C for 2 h, and then sonicated as described. 5 µl of the treated samples were placed on a 1.5 % agar TPM pad on a slide, covered with a coverslip and imaged. Sporulation efficiency was quantified as indicated and image processing and data analysis was performed as previously described.

Detection of EPS accumulation. Exponentially growing cells were harvested, (3 min, 6000 g at RT), and resuspended in 1% CTT to a calculated density of 7×10^9 cells ml⁻¹. 20 µl aliquots of the cell suspensions were placed on 0.5% agar plates supplemented with 0.5% CTT and 10 or 20 µg ml⁻¹ of Trypan blue or Congo red respectively. Plates were incubated at 32°C and documented at 24 h.

LPS extraction and detection. LPS was extracted from *M. xanthus* and visualized by Emerald staining as previously described (Pérez-Burgos *et al.*, 2019). LPS from *S. enterica* and *E. coli* was extracted and visualized by silver staining as previously described (Marolda *et al.*, 2006, Pérez-Burgos *et al.*, 2019). For *S. enterica*, O-antigen was detected by immunoblot using rabbit *Salmonella* O antiserum group B (Difco, Beckton Dickinson ref. number 229481) (1:500) and the secondary antibody IRDye 800CW goat α-rabbit immunoglobulin G (1:10000) (LI-COR) (Pérez-Burgos *et al.*, 2019).

Detection of colanic acid biosynthesis. *E. coli* $\Delta wcaJ$ strains were grown on LB plates with antibiotics and with or without 0.2 % (w/v) arabinose at 37°C overnight. Incubation was extended to 24-48 h at RT to visualize the mucoid phenotype (Furlong et al 2015).

Immunoblot analysis. Immunoblots were carried out as described (Sambrook & Russell, 2001). For *M. xanthus* immunoblots, rabbit polyclonal α -PilA (dilution: 1:2000), α -PilB (dilution: 1:2000) (Jakovljevic et al., 2008), α -PilC (dilution: 1:2000) (Bulyha et al., 2009), α -PilM (dilution: 1:3000) (Bulyha et al., 2009), α -PilN (dilution: 1:2000) (Friedrich et al., 2014), α -PilO (dilution: 1:2000) (Friedrich et al., 2014), α -PilP (dilution: 1:2000) (Friedrich et al., 2014), α -PilT (dilution: 1:3000) (Jakovljevic et al., 2008), α -Tgl (dilution: 1:2000) (Friedrich et al., 2014), α -TsaP (dilution: 1:2000) (Siewering et al., 2014), α -PilQ (dilution: 1:5000) (Bulyha et al., 2009) were used together with a horseradish-conjugated goat anti-rabbit immunoglobulin G (Sigma) as secondary antibody. Blots were developed using Luminata crescendo Western HRP Substrate (Millipore) on a LAS-4000 imager (Fujifilm).

For *E. coli* and *S. enterica* strains, total cell extracts were prepared and FLAG-tagged proteins detected by immunoblot analysis as previously described using α -FLAG M2 monoclonal antibody (Sigma) (1:10000) and a secondary antibody, IRDye 800CW Goat α -Mouse IgG (H+L), 0.5 mg (LI-COR) (1:10000) (Pérez-Burgos et al., 2019).

T4P shear off assay. T4P were sheared from cells that had been grown for three days on 1.5% agar plates supplemented with 1% CTT at 32°C as described, except that precipitation of sheared T4P was done using TCA as described (Koontz, 2014), and analyzed by immunoblotting with α -PilA antibodies as described previously (Wu & Kaiser, 1997). Blots were developed as indicated.

Bioinformatics. The KEGG SSDB (Sequence Similarity DataBase) (Kanehisa & Goto, 2000) database was used to identify homologs of PHPT (PF02397- Bacterial Sugar Transferase), PNPT (PF00953- Glycosyl transferase family 4) (Lehrman, 1994), Wzx (PF01943- Polysacc_synt and PF13440- Polysacc_synt_3), Wzy_C (PF04932- Wzy_C), PCP (PF02706- Wzz) and OPX (PF02563- Poly_export) as in (Pérez-Burgos et al., 2020, Beczała et al., 2015). For the ABC-transporter dependent pathway we used (PF01061- ABC2_membrane) for the permease and, (PF00005- ABC_tran) and (PF14524- Wzt_C) for the ATPase as in (Pérez-Burgos et al., 2019) together with an analysis of the genetic neighborhood to search for glycan related proteins. BlastP was used to identify homologs of the synthase dependent pathway using previously identified components (Whitney & Howell, 2013). KEGG SSDB was also used to identify EPS homolog proteins in other Myxococcales using a reciprocal best BlastP hit method. UniProt (The-UniProt-

Consortium, 2019), KEGG (Kanehisa & Goto, 2000) and the Carbohydrate Active Enzymes (CAZy) (<http://www.cazy.org/>) (Lombard *et al.*, 2014) databases were used to assign functions to proteins (Fig. 1A-C,F; Table S1 and S2). SMART (smart.embl-heidelberg.de) (Letunic *et al.*, 2015) and Pfam v31.0 and v32.0 (pfam.xfam.org) (Finn *et al.*, 2016) were used to identify protein domains. Membrane topology was assessed by TMHMM v2.0 (Sonnhammer *et al.*, 1998) and two-dimensional topology was graphically shown using TOPO2 (Johns). Clustal Omega (Chojnacki *et al.*, 2017) was used to align protein sequences. The phylogenetic tree was prepared as in (Pérez-Burgos *et al.*, 2020) in MEGA7 (Kumar *et al.*, 2016) using the Neighbor-Joining method (Saitou & Nei, 1987). Bootstrap values (500 replicates) are shown next to the branches (Felsenstein, 1985).

3.3.7 Supplementary material

Supplementary Figures & Legends

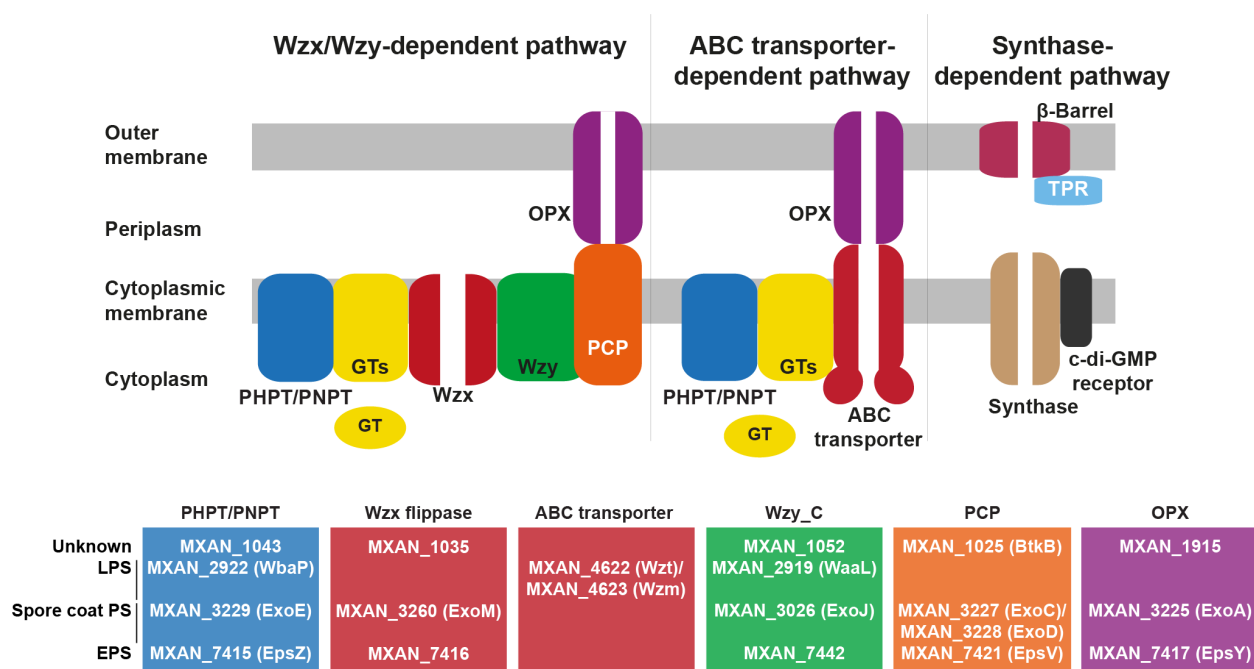


Figure S1. Bioinformatics-based identification of polysaccharide biosynthesis homolog proteins belonging to the Wzx/Wzy and the ABC transporter dependent pathways.

```

WbaPse  -----  - - - - MDN IDNK  YNPQLCK IFL  A ISDL IFFNL  ALWFS LGCVY  F IFDQVQRFI  PQDQLDTRVI  57
EpsZ   MDTMSGATAS  AAVVGAPGSA  NAQQQVIEEV  QGPPKLAGPS  AAKLNLTVDL  VLLSSVLVGS  AWLSGQLSAE  SGWKVSGLVL  80

WbaPse  THF ILSVVCV  GWFWIRLRHY  TYRKPFWYEL  KEIFRTIVIF  AIFDLALIAF  TKWQFSRYVW  VFCWTFALIL  VPPFRALTKH  137
EpsZ   AAWVVWIVTG  TALCLYDSRF  AERSKLDHVA  LVSVTTLAVV  TVLTLGSAV  PTVVTSPPVG  PLLFIWFPVT  LLLRLFVFRP  160

WbaPse  LLNKLGIWKK  KTIILGSGQN  ARGAYSALQS  EEMMGFDVIA  FFDTDASDAE  INMLP - - VIK  DTEIIWDLNR  - - TGDVHYIL  213
EpsZ   VASQE - - RP  MDAVLIVGTG  AMGRYTGEDL  ANRRRQILG  YVRFHDDNGS  VGELPGPVMG  SVDDLEHILR  NTAVDEVYIA  237

WbaPse  AYEYTELEKT  HFWLRELSKH  HCRSVTVVPS  FRGLPLYNTD  MSFIFSHVEVM  LLRIQNNLAK  RSSRFLKRTF  D IVCSIMILI  293
EpsZ   GNTLKQGESH  QAAIKLAERF  GVPFALPAHS  FRLDRARPVE  RRAVADGFLH  FAAVS - - PK  PHQMAMKRLF  D ICVSAAALW  314

WbaPse  IASPLMIYLW  YKVTRDG-GP  AIYGHORVGR  HGKLFPCYKF  RSMVMNSQEV  LKELLANDPI  ARAWEKDFK  LKNDRITAV  372
EpsZ   ALLPLLMGVA  LAVKFTSKGP  IFFKQLRVGQ  NGKPFYMLKF  RSMVVAEEL  KEKLAALN - -  - - EQTGPVFK  MKHDPITGI  390

WbaPse  GRFIRKTSLD  ELPQLFNVLK  GDMSLVGPRP  IVSDELERYC  DDVDYLLMAK  PGMTGLWQVS  GRNDVDYDTR  VYFDSWYVKN  452
EpsZ   GRFIRKFSID  ELPQFINVLR  GEMSLVGRPR  PVPTEVAKYE  TWQRRRLSVR  PGLTCIWQVS  GRNQISFEFW  MYLDMQYIDH  470

WbaPse  WTLWNDAAIL  FKTAKVVLRR  DGAY  476
EpsZ   WSLTSDLRLL  LQTVPVVLTG  RGAS  494

```

Figure S2. Sequence alignment of EpsZ (MXAN_715) and WbaP^{se} showing the Pro and Asp (orange) residues in the motif DX₁₂P and the conserved amino acids essential for catalytic activity (red).

Supplementary Experimental Procedures

Plasmid construction. All oligonucleotides used are listed in Table S3. All constructed plasmids were verified by DNA sequencing.

pMP001 (for generation of in-frame deletion of *MXAN_7415*): up- and downstream fragments were amplified from genomic DNA of DK1622 using the primer pairs 7415_A/7415_B and 7415_C/7415_D respectively, as described in (Shi *et al.*, 2008). Subsequently, the AB and CD fragments were used as templates to perform an overlapping PCR with the primer pair 7415_A/7415_D to generate the AD fragment. The AD fragment was digested with KpnI/XbaI and cloned in pBJ114.

pMP012 (for generation of in-frame deletion of *MXAN_7421*): up- and downstream fragments were amplified from genomic DNA of DK1622 using the primer pairs 7421_A/7421_B and 7421_C/7421_D respectively. Subsequently, the AB and CD fragments were used as templates to perform an overlapping PCR with the primer pair 7421_A/7421_D to generate the AD fragment. The AD fragment was digested with KpnI/XbaI and cloned in pBJ114.

pMP015 (for generation of in-frame deletion of *MXAN_7442*): up- and downstream fragments were amplified from genomic DNA of DK1622 using the primer pairs 7442_A/7442_B and 7442_C/7442_D respectively. Subsequently, the AB and CD fragments were used as templates to perform an overlapping PCR with the primer pair 7442_A/7442_D to generate the AD fragment. The AD fragment was digested with KpnI/XbaI and cloned in pBJ114.

pMP016 (for generation of in-frame deletion of *MXAN_7416*): up- and downstream fragments were amplified from genomic DNA of DK1622 using the primer pairs 7416_A/7416_B and 7416_C/7416_D respectively. Subsequently, the AB and CD fragments were used as templates to perform an overlapping PCR with the primer pair 7416_A/7416_D to generate the AD fragment. The AD fragment was digested with KpnI/XbaI and cloned in pBJ114.

pMP018 (for generation of in-frame deletion of *MXAN_7417*): up- and downstream fragments were amplified from genomic DNA of DK1622 using the primer pairs 7417_A/7417_B and 7417_C/7417_D respectively. Subsequently, the AB and CD fragments were used as templates to perform an overlapping PCR with the primer pair 7417_A/7417_D to generate the AD fragment. The AD fragment was digested with EcoRI/XbaI and cloned in pBJ114.

pMP021 (expression of P_{nat} *MXAN_7415* from the *attB* site): P_{nat} *MXAN_7415* was amplified with the primer combination 7415_Pnat900 forw2/7415_Pnat rev and genomic DNA from *M. xanthus* DK1622 as a template. The fragment was digested with KpnI and XbaI, cloned into pSWU30 and sequenced.

pMP024 (expression of P_{nat} *MXAN_7416* from the *attB* site): P_{nat} *MXAN_7416* was amplified with the primer combination 7416_Pnat forw2/7416_Pnat rev and genomic DNA from *M. xanthus* DK1622 as a template. The fragment was digested with HindIII and XbaI, cloned into pSWU30 and sequenced.

pMP030 (expression of P_{pilA} *MXAN_7417* from the *attB* site): *MXAN_7417* was amplified with the primer combination 7417_PpilA forw/7417_PpilA rev and genomic DNA from *M. xanthus* DK1622 as a template. The fragment was digested with XbaI and HindIII, cloned into pSW105 and sequenced.

pMP032 (expression of P_{pilA} *MXAN_7421* from the *attB* site): *MXAN_7421* was amplified with the primer combination 7421_PpilA forw/7421_PpilA rev and genomic DNA from *M. xanthus* DK1622 as a template. The fragment was digested with XbaI and HindIII, cloned into pSW105 and sequenced.

pMP036 (for generation of in-frame deletion of *MXAN_7420*): up- and downstream fragments were amplified from genomic DNA of DK1622 using the primer pairs 7420_A/7420_B and 7420_C/7420_D respectively. Subsequently, the AB and CD fragments were used as templates to perform an overlapping PCR with the primer pair 7420_A/7420_D to generate the AD fragment. The AD fragment was digested with KpnI/XbaI and cloned in pBJ114.

pMP091 (expression of P_{nat} *MXAN_7442* from the *attB* site): P_{nat} *MXAN_7442* was amplified with the primer combination 7442_Pnat 600 up /7442_Pnat rev and genomic DNA from *M. xanthus* DK1622 as a template. The fragment was digested with HindIII and XbaI, cloned into pSWU30 and sequenced.

pMP098 (for generation of in-frame deletion of *fibA*): up- and downstream fragments were amplified from genomic DNA of DK1622 using the primer pairs 6106_A/6106_B and 6106_C/6106_D respectively. Subsequently, the AB and CD fragments were used as templates to perform an overlapping PCR with the primer pair 6106_A/6106_D to generate the AD fragment. The AD fragment was digested with KpnI/XbaI and cloned in pBJ114.

pMP124 (for generation of in-frame deletion of *MXAN_1043*): up- and downstream fragments were amplified from genomic DNA of DK1622 using the primer pairs 1043_A/1043_B and 1043_C/1043_D respectively. Subsequently, the AB and CD fragments were used as templates to perform an overlapping PCR with the primer pair 1043_A/1043_D to generate the AD fragment. The AD fragment was digested with EcoRI/HindIII and cloned in pBJ114.

pMP137 (expression of P_{pilA} *difE* from the *attB* site): *MXAN_7420* was amplified with the primer combination *difE_PpilA* forw/*difE* rev and genomic DNA from *M. xanthus* DK1622 as a template. The fragment was digested with XbaI and HindIII, cloned into pSW105 and sequenced.

pMP145 (expression of P_{pilA} *MXAN_7420* from the *attB* site): *MXAN_7420* was amplified with the primer combination 7420_PpilA fw/7420_PpilA rev and genomic DNA from *M. xanthus* DK1622 as a template. The fragment was digested with XbaI and HindIII, cloned into pSW105 and sequenced.

pMP146 (expression of *MXAN_7415* under the control of an arabinose promoter): *MXAN_7415* was amplified with the primer combination 7415 fw +1/ 7415 rev new (*pilA*) and genomic DNA from *M. xanthus* DK1622 as a template. The fragment was digested with XbaI and HindIII, cloned into pBADNTF and sequenced.

pJJ1 (for generation of in-frame deletion of *MXAN_1035*): up- and downstream fragments were amplified from genomic DNA of DK1622 using the primer pairs 1035_A/1035_B and 1035_C/1035_D respectively. Subsequently, the AB and CD fragments were used as templates to perform an overlapping PCR with the primer pair 1035_A/1035_D to generate the AD fragment. The AD fragment was digested with KpnI/XbaI and cloned in pBJ114.

pJJ2 (for generation of in-frame deletion of *MXAN_1025*): up- and downstream fragments were amplified from genomic DNA of DK1622 using the primer pairs 1025_A/1025_B and 1025_C/1025_D respectively. Subsequently, the AB and CD fragments were used as templates to perform an overlapping PCR with the primer pair 1025_A/1025_D to generate the AD fragment. The AD fragment was digested with KpnI/XbaI and cloned in pBJ114.

pJJ3 (for generation of in-frame deletion of *MXAN_1052*): up- and downstream fragments were amplified from genomic DNA of DK1622 using the primer pairs 1025_A/1025_B and 1052_C/1052_D respectively. Subsequently, the AB and CD fragments were used as templates to perform an overlapping PCR with the primer pair 1052_A/1052_D to generate the AD fragment. The AD fragment was digested with KpnI/BamHI and cloned in pBJ114.

pJJ4 (for generation of in-frame deletion of *MXAN_1915*): up- and downstream fragments were amplified from genomic DNA of DK1622 using the primer pairs 1915_A/1915_B and 1915_C/1915_D respectively. Subsequently, the AB and CD fragments were used as templates to perform an overlapping PCR with the primer pair 1915_A/1915_D to generate the AD fragment. The AD fragment was digested with KpnI/XbaI and cloned in pBJ114.

pMAT150 (for generation of in-frame deletion of *pilT*): up- and downstream fragments were amplified from genomic DNA of DK10409 ($\Delta pilT$) using the primer pairs pilT-A EcoRI/ pilT-D HindIII. The AD fragment was digested with EcoRI/HindIII and cloned in pBJ114.

pDJS102 (for generation of in-frame deletion of *diffE*): up- and downstream fragments were amplified from genomic DNA of DK1622 using the primer pairs 6692_A/6692_B and 6692_C/6692_D respectively. Subsequently, the AB and CD fragments were used as templates to perform an overlapping PCR with the primer pair 6692_A/6692_D to generate the AD fragment. The AD fragment was digested with EcoRI/XbaI and cloned in pBJ114.

Table S1. Analysis of the *eps* locus

Locus tag MXAN	Gene name	(Putative) function of encoded protein	Reference ¹
7415	<i>epsZ</i>	Polyprenyl glycosylphosphotransferase New annotation: polyisoprenyl-phosphate hexose-1-phosphate transferase	(Berleman <i>et al.</i> , 2016)
7416	wzx _{EPS}	Wzx flippase	(Holkenbrink <i>et al.</i> , 2014)
7417	<i>epsY</i>	Polysaccharide biosynthesis/export protein New annotation: OPX protein	Uniprot, KEGG
7418	<i>epsX</i>	Hypothetical protein	
7420	<i>epsW</i>	Response regulator	(Black <i>et al.</i> , 2015)
7421	<i>epsV</i>	Chain length determinant protein New annotation: Wzz protein	Uniprot, KEGG
7422	<i>epsU</i>	Glycosyltransferase	
7423		Hypothetical protein	
7424		Hypothetical protein	
7425		Hypothetical protein	
7426		Hypothetical protein	
7430		Transposase orfB, IS5 family	Uniprot, KEGG
7431	<i>epsP</i>	Transposase orfA, IS5 family	
7433	<i>epsO</i>	von Willebrand factor type A domain protein, Ca-activated chloride channel homolog	
7435	<i>epsN</i>	Hydrolase	
7436	<i>epsM</i>	Outer membrane efflux protein, cobalt-zinc-cadmium efflux system	
7437	<i>epsL</i>	Heavy metal efflux pump, CzcA family, cobalt-zinc-cadmium resistance protein	Uniprot, KEGG
7438	<i>epsK</i>	putative cobalt-zinc-cadmium resistance protein	Uniprot, KEGG
7439	<i>epsJ</i>	Sensor histidine kinase	
7440	<i>epsI</i> <i>nla24</i>	Sigma-54 dependent DNA-binding response regulator	(Lancero <i>et al.</i> , 2004)
7441	<i>epsH</i>	Glycosyltransferase	
7442	<i>sgnF</i> , wzy _{EPS}	Putative membrane protein, Wzy_C domain New annotation: Wzy polymerase	(Youderian <i>et al.</i> , 2003)
7443	<i>epsG</i>	Magnesium transporter	
7444	<i>epsF</i>	Response regulator/sensory box histidine kinase	

7445	<i>epsE</i>	Glycosyltransferase	
7447		Hypothetical protein	Uniprot, KEGG
7448	<i>epsD</i>	Glycosyltransferase	
7449	<i>epsC</i>	Serine O-acetyltransferase	
7450	<i>epsB</i>	Glycosyl hydrolase	Uniprot, KEGG
7451	<i>epsA</i>	Glycosyltransferase	Uniprot, KEGG

¹Based on (Lu *et al.*, 2005) unless indicated otherwise.

Table S2. Analysis of the *MXAN_1025-MXAN_1052* and *MXAN_1915* loci

Locus tag MXAN	Gene name	(Putative) function of encoded protein	Reference ¹
1022		Putative membrane protein	
1023		Putative pristinamycin I synthase 3	
1025		Bacterial tyrosine kinase, Capsular exopolysaccharide family protein New annotation: Wzc	(Kimura <i>et al.</i> , 2012)
1026		Glycosyltransferase	
1027		Glycosyltransferase	
1028		Putative membrane protein	
1029		Glycosyltransferase	
1030		Glycosyltransferase	
1031		Glycosyltransferase	
1032		Glycosyltransferase	
1033		Glyco_trans_4-like_N domain-containing protein	
1034		Conserved domain protein	
1035		Putative membrane protein, PST family New annotation: Wzx flippase	
1036		Glycosyltransferase	
1037		Glycosyltransferase	
1038		Hypothetical protein	
1039	<i>glkA</i>	Glucokinase	
1040		Sulfatase family protein	
1041		Acyltransferase family protein	
1042		Glycosyltransferase	
1043		Glycosyltransferase New annotation: polyisoprenyl-phosphate N-acetylhexosamine-1-phosphate transferase	
1045		Hypothetical protein	
1046		FG-GAP repeat/HVR domain protein	
1047		Hypothetical protein	
1048		UDP-glucose 6-dehydrogenase	
1049		Acyltransferase family protein	
1050		Hypothetical protein	
1051		Hypothetical protein	
1052		O-antigen polymerase family protein New annotation: Wzy polymerase	

1053		tRNA_edit domain-containing protein	
1054		Hypothetical protein	
1055		Hypothetical protein	
1914	<i>suhB</i>	Inositol-1-monophosphatase	
1915		Polysaccharide biosynthesis/export protein New annotation: OPX protein	
1916		Hypothetical protein	
1917		Hypothetical protein	

¹Based on Uniprot and KEGG, unless indicated otherwise.

Table S3. Oligonucleotides used in this work¹

Primer name	Sequence 5'-3'	Brief description
7415_A	ATCGGGTACCGTGGTCTCGCCGTCAGTGG	For Δ MXAN_7415
7415_B	CACCGGCACCGGGGCCAGCTTGGGCGG	For Δ MXAN_7415
7415_C	CTGGCCCCGGTGCCGGTGGTCTCACG	For Δ MXAN_7415
7415_D	ATCGTCTAGACCCCCGCCACACCAGCTT	For Δ MXAN_7415
7415_E	ACCTCCTGGCCGCCATGAG	For Δ MXAN_7415
7415_F	CTTACCGCCTCGGACGCCA	For Δ MXAN_7415
7415_G	CATCTTCTGGCCGGTGACGC	For Δ MXAN_7415
7415_H	GCATGTAGAAGGGCTTGCCG	For Δ MXAN_7415
7415_Pnat900 forw2	ATCGGGTACCTGAGCCTTCTCGACGTGGAGCG	For complementation fw
7415_Pnat rev	ATCGTCTAGACTAGCTGGCGCCGCGGCCCG	For complementation rev
7415 fw +1	ATCGTCTAGAGGTGGACACGATGAGCGGCGC	For protein expression under an arabinose inducible promoter fw.
7415 rev new	ATCGAAGCTTCTAGCTGGCGCCGCGGCCCG	For protein expression under an arabinose inducible promoter rev.
7416_A	ATCGGGTACCGCAGCTTCGCGTGGGGCAGA	For Δ MXAN_7416
7416_B	TTCGGGCGCTTGGAGCCCGTTGCGCAC	For Δ MXAN_7416
7416_C	GGGCTCCAAGCGCCGAAGCCGCGCCC	For Δ MXAN_7416
7416_D	ATCGTCTAGAGCGCCCTCGGCGTGGATGA	For Δ MXAN_7416
7416_E	TGAAGTTCACCTCCAAGGGC	For Δ MXAN_7416
7416_F	TCCACCACCACACGTACC	For Δ MXAN_7416
7416_G	CGAGGTGCGCCAGCTCGTCT	For Δ MXAN_7416
7416_H	CCCATCAGCCCCACCCACAG	For Δ MXAN_7416
7416_Pnat forw2	ATCGAAGCTTTGACAAGCCTCCAGGCAACCCAA	For complementation fw
7416_Pnat rev	ATCGTCTAGATCACGGGGTGGGCGCGGCTT	For complementation rev
7417_A	ATCGGAATTCGATGATGCTCATCGTCTGG	For Δ MXAN_7417
7417_B	GTCACCGGGGCGGTGCGTGGACGGCAT	For Δ MXAN_7417
7417_C	ACGCACCGCCCCGGTGACGTGGTGGTG	For Δ MXAN_7417
7417_D	ATCGTCTAGAGCCGCTGATGGAGAAGCCGC	For Δ MXAN_7417
7417_E	GCGCCGCTCGCTGGAGGGCA	For Δ MXAN_7417
7417_F	CGCGGGCGGGCCCGTCCAGG	For Δ MXAN_7417
7417_G	CGTCCCTGGCGCTCGTTCCG	For Δ MXAN_7417
7417_H	CGCAGGCGGAAGGTGGGCGC	For Δ MXAN_7417

7417_PpilA forw	ATCGTCTAGAGTGAGGAGAGTTCCACCGCT	For complementation fw
7417_PpilA rev	ATCGAAGCTTTTATTCCACCACCACCACGT	For complementation rev
7421_A	ATCGGGTACCCCTGCCAGCCAAGGCGGCG	For Δ MXAN_7421
7421_B	CGCCAGCACGGGAGCCCCGGGCGCGGG	For Δ MXAN_7421
7421_C	GGGGCTCCCGTGCTGGCGGAGCTGGAG	For Δ MXAN_7421
7421_D	ATCGTCTAGAGCCAGGACGCCGTGGGGTTC	For Δ MXAN_7421
7421_E	CGTGCGGCAAACCTGGTATTC	For Δ MXAN_7421
7421_F	AGGGCAATGGTCATCAGCCG	For Δ MXAN_7421
7421_G	GAGCGCCCGGAGACGAACGC	For Δ MXAN_7421
7421_H	CGCGAAGATGCCCATGCCGA	For Δ MXAN_7421
7421_PpilA forw	ATCGTCTAGAGTGACGGTCCCCGCGCCCGG	For complementation fw
7421_PpilA rev	ATCGAAGCTTTCAGCGCCGCTCCAGCTCCG	For complementation rev
7442_A	ATCGGGTACCGGGCAGACCGCCATTGAGCG	For Δ MXAN_7421
7442_B	GGAGGATGGGGCCAACGCGACCACGGG	For Δ MXAN_7421
7442_C	GCGTTGGCCCCATCCTCCGCGCGAAC	For Δ MXAN_7421
7442_D	ATCGTCTAGACCAGAAGGTGGGTGGCACGG	For Δ MXAN_7421
7442_E	CCACTCCTTCTCCCGCCGCC	For Δ MXAN_7421
7442_F	ATCGTCAGCGTGGTGCAGGC	For Δ MXAN_7421
7442_G	CGTGGGGGTGGTGTGGGTCA	For Δ MXAN_7421
7442_H	CCTCGTTGGGGTAGGTGATG	For Δ MXAN_7421
7442_Pnat 600 up	ATCGAAGCTTTGAGCCCTTGGGCCAGGGCAGAC	For complementation fw
7442_Pnat rev	ATCGTCTAGATCAGCGCGGGTTTCGCGGCGG	For complementation rev
1025_A	ATAGGGTACCGTGACGGAGCGCAGCGCCTC	For Δ MXAN_1025
1025_B	ATCCTTGGAGGCCGGGTCGAAACCGGT	For Δ MXAN_1025
1025_C	GACCCGGCCTCCAAGGATGGGGTGGCG	For Δ MXAN_1025
1025_D	ACTGTCTAGAAGTAGACGAGCCGCCCCACC	For Δ MXAN_1025
1025_E	CTGCGCGGCCAGCTTACCA	For Δ MXAN_1025
1025_F	ACCCGGCGCAGGGCCTGTAG	For Δ MXAN_1025
1025_G	GACGCGGTGGCGCTGGTCCA	For Δ MXAN_1025
1025_H	ACGAAGAGGCCGGGCACCTC	For Δ MXAN_1025
1035_A	ATCGGGTACCAGCCGGAGCGGTGCACCTGG	For Δ MXAN_1035
1035_B	CGCCGAGTGGCTTCGGGCGCTGGGGT	For Δ MXAN_1035
1035_C	CCCGAAGCCACTCCGGCGAGTCCGGCG	For Δ MXAN_1035
1035_D	ATCGTCTAGACTTCCAGGCCCGCACGCACC	For Δ MXAN_1035
1035_E	GCTTCCAGCCGCTCATGCCG	For Δ MXAN_1035
1035_F	TAATCACCGCCTCCGGGCAG	For Δ MXAN_1035
1035_G	GCGGCCTCCCTGGGCGTGTT	For Δ MXAN_1035
1035_H	AGCGCCTGCGCCACCACACC	For Δ MXAN_1035
1043_A	ATCGGAATTCATGCCGAAGGCGTGCCTT	For Δ MXAN_1043
1043_B	CAGGCGTCCGAAGAAGGCGACCAGAAG	For Δ MXAN_1043
1043_C	GCCTTCTTCGGACGCCTGGTTCGCGATG	For Δ MXAN_1043
1043_D	ATCGAAGCTTCCCTCCAGCGCCTCGCCCCA	For Δ MXAN_1043
1043_E	CGCGGAGATGGTGGCCGTGC	For Δ MXAN_1043
1043_F	CGTCTCCGCCCGCGCCAGCA	For Δ MXAN_1043
1043_G	TGGGGATGGCTGGACCAGGC	For Δ MXAN_1043
1043_H	TGTTGGCGAAGTTCAGCGCC	For Δ MXAN_1043
1052_A	ATCGGGTACCTTGATGGAGCAGTCGCACAG	For Δ MXAN_1052
1052_B	CTCGCCATCAGAGGCACTGCGGGAAGC	For Δ MXAN_1052

1052_C	AGTGCCTCTGATGGCGAGGCTCGGGAC	For Δ MXAN_1052
1052_D	ATCGGGATCCCTCGAACCCCTGTACGGCGC	For Δ MXAN_1052
1052_E	GCGAAGGCACAGCTCCTTCT	For Δ MXAN_1052
1052_F	GGATGAAGACGGGAGAGCGC	For Δ MXAN_1052
1052_G	GCTCGTCGTGGTGTGTCCGC	For Δ MXAN_1052
1052_H	CGAAGAACGCATCCGCGCCA	For Δ MXAN_1052
1915_A	ATCGGGTACCGCTTCTGCCGAAGACGGCG	For Δ MXAN_1915
1915_B	CACGAAGACGGTGAGGGCGGCGCGGAA	For Δ MXAN_1915
1915_C	GCCCTCACCGTCTTCGTGCCGGAGAGC	For Δ MXAN_1915
1915_D	ATCGTCTAGACAGGGCACCGACAGCCTGCG	For Δ MXAN_1915
1915_E	GACTACGGCAACCTGCGAGT	For Δ MXAN_1915
1915_F	CCCCGACCACGCCATCCTCG	For Δ MXAN_1915
1915_G	TGACGCTGCCCCGCTGCTTC	For Δ MXAN_1915
1915_H	TCGCCGGGCTGGAGCATGAA	For Δ MXAN_1915
6692_A	ATCGGAATTCAGGCTGGGTGGCCTGGGAGT	For Δ difE
6692_B	CGGCACGTTCGAGGTAGCGGGACATGTC	For Δ difE
6692_C	CGCTACCTCGACGTGCCGAGGTTACTG	For Δ difE
6692_D	ATCGTCTAGACAGCAGGTCGCGGATGCTGT	For Δ difE
6692_E	ACGGCGCCAGGAAAGATGAC	For Δ difE
6692_F	TTTCAGCGCCTTCTCATCCA	For Δ difE
6692_G	AAGGTGACGGCGCTGAAGCC	For Δ difE
6692_H	CCAGCGCTGGGCCAGCGTTT	For Δ difE
difE_PpilA_forw	ATACTCTAGAATGACGATGGACATGTCCCG	For complementation fw
difE_rev	ATCGAAGCTTTCACGCGGACAGTAACCTCG	For complementation rev
pilT-A_EcoRI	GCGCGAATTCGCGACTTCGAGACGGCGG	For Δ pilT
pilT-D_HindIII	GCGCAAGCTTGAGCTTCTCGTTCTTCTCC	For Δ pilT
pilT_E	CTCCGCCAGGACCCGGACATC	For Δ pilT
pilT_F	TATCGAGGCACTGCACCA	For Δ pilT
pilT_G	CTTGAAGACGGCGCCGCTGA	For Δ pilT
pilT_H	CGCGCTGATTCACGAGGCAG	For Δ pilT

¹ Underlined sequences indicate restriction sites.

3.4 Regulation by the diguanylate cyclase DmxA and c-di-GMP in *M. xanthus*

3.4.1 Results

Introduction to DmxA and its genetic context

DmxA (diguanylate cyclase from *Myxococcus xanthus* A) is a predicted integral membrane protein with a C-terminal GGEEF domain (Fig. 1A) that has enzymatic activity and binds c-di-GMP *in vitro* (Skotnicka *et al.*, 2015). Previous inactivation of DmxA showed an increased level of c-di-GMP and EPS accumulation, faster agglutination and reduced T4P-dependent motility (Skotnicka *et al.*, 2015).

dmxA forms a putative operon with *ftsB* (MXAN_3704) (Fig. 1B), which encodes the divisome FtsB (or DivIC) homolog (Du & Lutkenhaus, 2017, Goley *et al.*, 2011). While *dmxA* and *ftsB* are conserved among myxobacteria, they are only found in close proximity in the suborders Cystobacterineae and Nannocystineae (Fig. 1C). Other genes in close proximity to *dmxA* encode proteins involved in iron homeostasis or binding. MXAN_3702 is a ferric uptake regulator (FUR) homolog. Ferric uptake regulators are DNA-binding repressors that maintain iron homeostasis by binding to the upstream region of genes important for iron uptake and inhibiting its transcription when the level of iron inside the cell is high (Andrews *et al.*, 2003). MXAN_3703 is a thioredoxin family protein homolog, which participate in redox reactions inside the cell. Similarly, MXAN_3706 is an oxidoreductase homolog containing a cytochrome C domain.

To determine if *dmxA* and *ftsB* are co-transcribed, we attempted to PCR amplify the intragenic region between the genes using cDNA from growing cells. As a positive control, genomic DNA was used, and as a negative control, cDNA sample in which the reverse transcriptase was omitted was used as template. We additionally PCR amplified a region inside each of the genes to confirm transcription of the individual genes. The PCR products (Fig. 1D) confirmed that *dmxA* and *ftsB* form an operon.

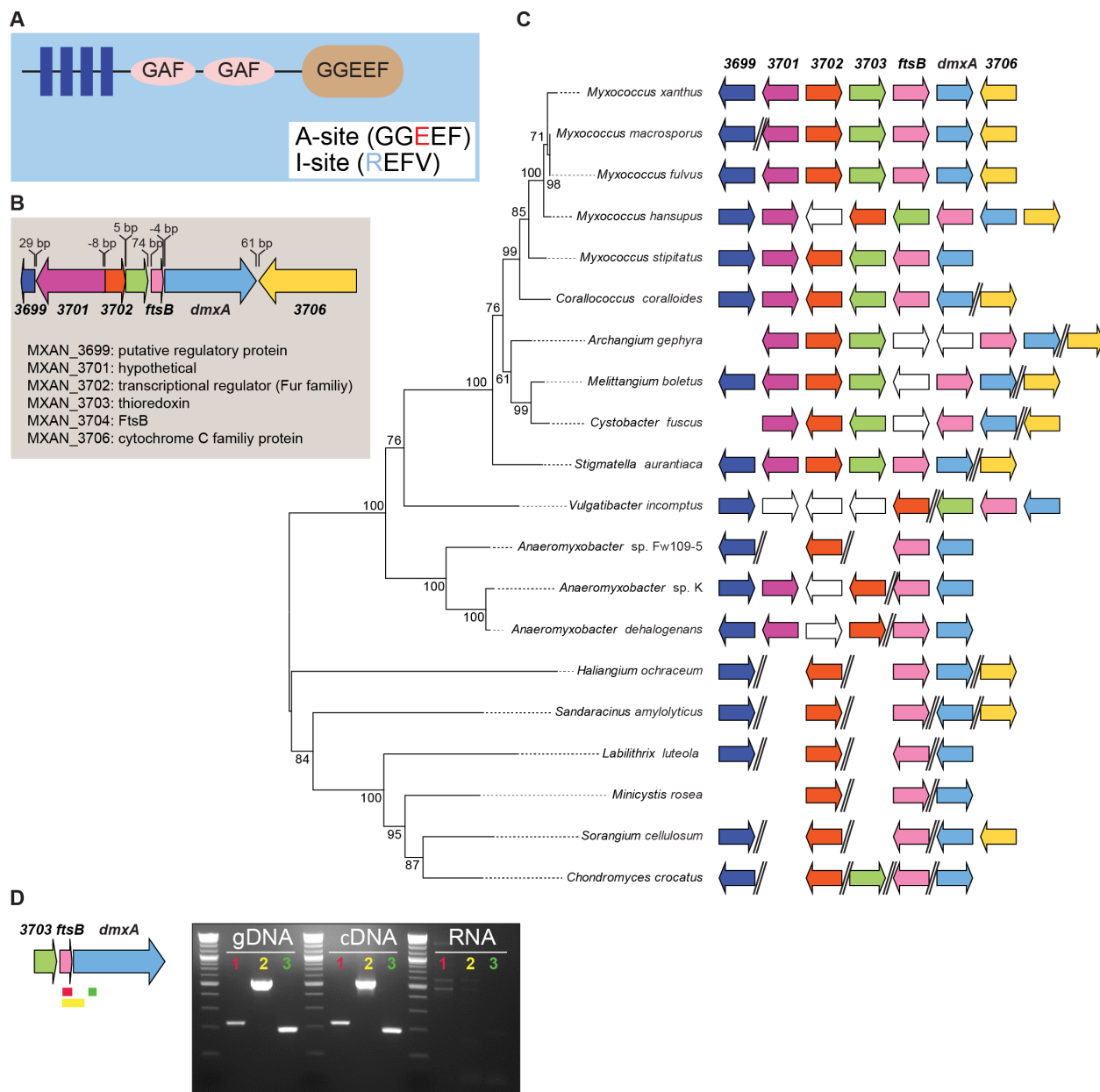


Figure 1. (A) Domain and transmembrane helix (TMH) prediction of DmxA. (B) Genetic neighborhood of *dmxA*. Genes are drawn to scale and *MXAN* number or gene name indicated. (C) Conservation of *dmxA* and its genetic neighborhood in other Myxococcales. Double slashes indicate no close proximity between the genes. (D) Operon mapping. Red, yellow and green lines represent the regions amplified by PCR during operon mapping.

Lack of DmxA shows a defect in motility, which is specific to DmxA

Previous work on DmxA function was assessed by using a strain containing an insertion in *dmxA*. For this study, a clean in-frame deletion strain was constructed.

To analyze the motility of the $\Delta dmxA$ strain, cells were spotted on 0.5% and 1.5% agar, which are favorable for gliding motility and T4P-dependent motility, respectively (Shi & Zusman, 1993). On 0.5% agar, WT cells move in groups and display long flares, while on 1.5% the WT colony edge displays contains single cells. $\Delta pilA$ and $\Delta aglQ$ are defective in T4P-dependent and gliding motility respectively, and were used as negative controls (Sun *et al.*, 2011, Nan *et al.*, 2013, Wu & Kaiser, 1996). $\Delta dmxA$ showed a defect in T4P-dependent colony expansion (Fig. 2) as previously described for the $\Omega dmxA$ mutant (Skotnicka *et al.*, 2015). Previous studies on 1.5% agar had exclusively focused on the movement of single cells. While single $\Delta dmxA$ cells were still visible at the colony edge as observed for the $\Omega dmxA$ mutant (Skotnicka *et al.*, 2015), here we also observed that expansion of the $\Delta dmxA$ colony was reduced compared to WT. Importantly, the motility defect was partially complemented by ectopic expression of the full-length *dmxA* gene under the control of the native promoter, located upstream of *ftsB* (P_{ftsB}), on a plasmid integrated in a single copy at the Mx8 *attB* site (Fig. 2).

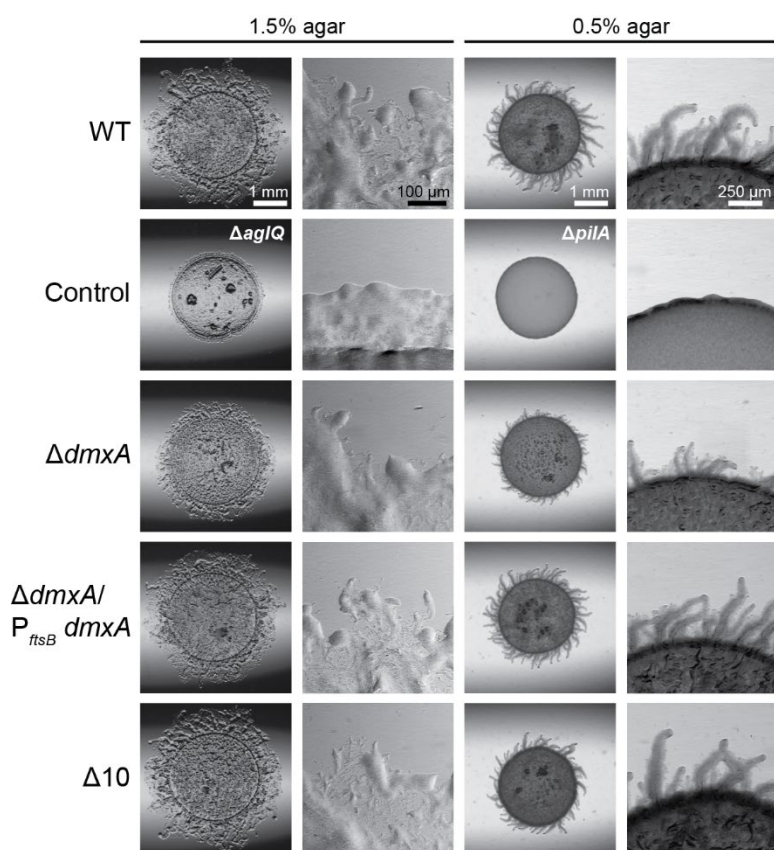


Figure 2. Gliding motility and T4P-dependent motility were analyzed on 1.5% and 0.5% agar respectively.

Interestingly, the *Myxococcus xanthus* genome encodes 18 GGDEF proteins (www.ncbi.nlm.nih.gov/Complete_Genomes/c-di-GMP). Among them 11, including DmxA, are putatively active. Single mutations in the remaining putatively active GGDEF proteins did not

affect motility (Skotnicka *et al.*, 2015). In order to understand whether DmxA was the only DGC involved in regulation of motility, we generated a mutant (henceforth, $\Delta 10$ mutant) in which all genes encoding active DGCs except *dmxA* were deleted. Interestingly, lack of the other 10 DGCs neither impacted the overall colony expansion on hard nor on soft agar. Thus, DmxA is the only active DGC that produces c-di-GMP involved in regulation of motility (Fig. 2).

The *dmxA* mutation negatively affects both motility systems

To confirm that lack of DmxA affects both motility systems, we generated double mutants, in which one of the motility systems was inactivated. $\Delta dmxA \Delta aglQ$ shows a stronger defect on 0.5% agar than $\Delta aglQ$ (Fig. 3). Similarly, $\Delta dmxA \Delta pilA$ shows a stronger defect on 1.5% agar than $\Delta pilA$ (Fig. 3). Thus, we can conclude that the *dmxA* mutation causes a defect in both motility systems.

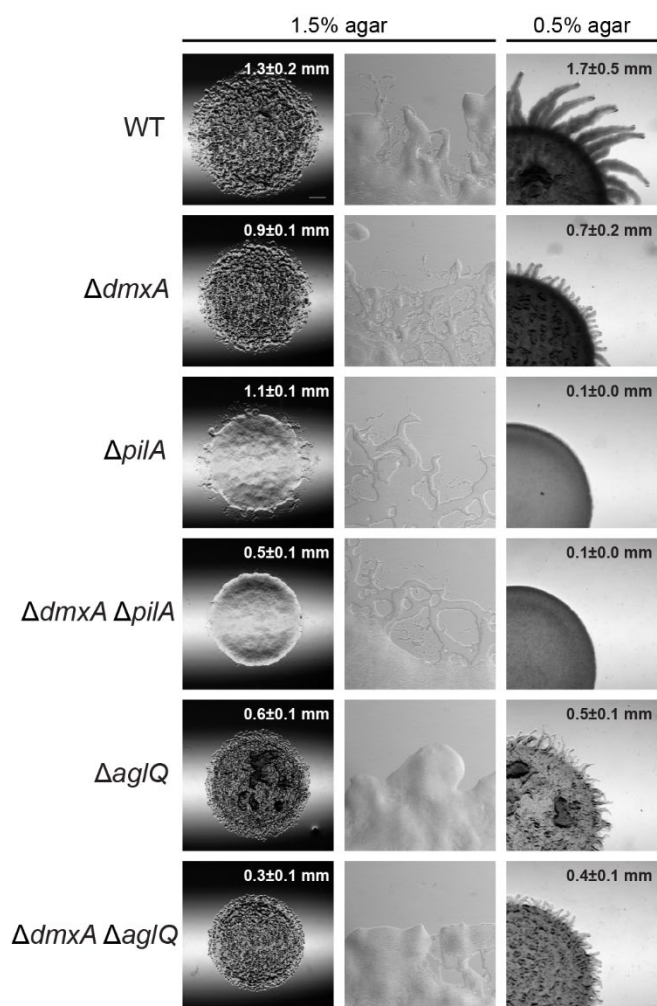


Figure 3. Gliding motility and T4P-dependent motility were analyzed on 1.5% and 0.5% agar respectively.

Lack of DmxA does not affect growth or cell morphology

Because *dmxA* forms an operon with the cell division *ftsB* gene (Fig. 1D), we first tested whether DmxA is implicated in cell growth. As shown in Figs. 4A and B, the $\Delta dmxA$ cells had a growth rate

and cell length distribution similar to WT cells supporting that DmxA is not implicated in cell growth or division.

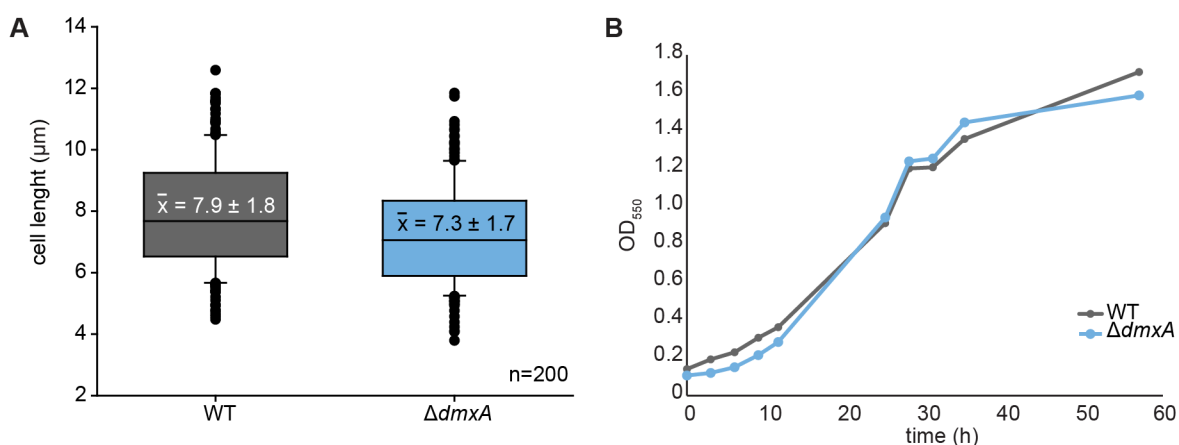


Figure 4. (A) Growth curve. Exponentially growing cells were diluted to a cell density of 1×10^8 and the optical density at 550 nm was measured over time. (B) Cell length determination. Cells were transferred from an exponential growing liquid culture to a thin TPM agarose pad and covered with a coverslip. n=200 cells per each strain were measured. The Y-axis corresponds to the cell length, boxes enclose the 25th and 75th percentile with the black line representing the mean and whiskers represent the 10th and 90th percentile and the black circles the outliers.

The $\Delta dmxA$ mutant is not affected in T4P accumulation and slightly affected in EPS synthesis

Previously it was proposed that the T4P-dependent motility defect of the $\Omega dmxA$ mutant arises from the increase in EPS accumulation caused by the high c-di-GMP level (Skotnicka *et al.*, 2015). Measurement of EPS accumulation in $\Delta dmxA$ cells using a plate-based colorimetric assay with Congo red and Trypan blue demonstrated that $\Delta dmxA$ cells had a slight increase in the EPS level compared to WT (Fig. 5A). Importantly, increased EPS was proposed to enhance T4P-dependent motility (Berleman *et al.*, 2016, Patra *et al.*, 2016). Because differences in the EPS level may arise from pleiotropic defects of the *dmxA* mutation (e.g. alterations in metabolism, variations in T4P assembly (see Chapter 3.3)), it is possible that the slightly increased EPS accumulation is not causing the motility defect of the $\Delta dmxA$ strain.

To test whether the altered EPS level was a result of an increase in T4P assembly, we performed a T4P shear off assay. The $\Delta dmxA$ mutant and WT assemble similar levels of T4P (Fig. 5B).

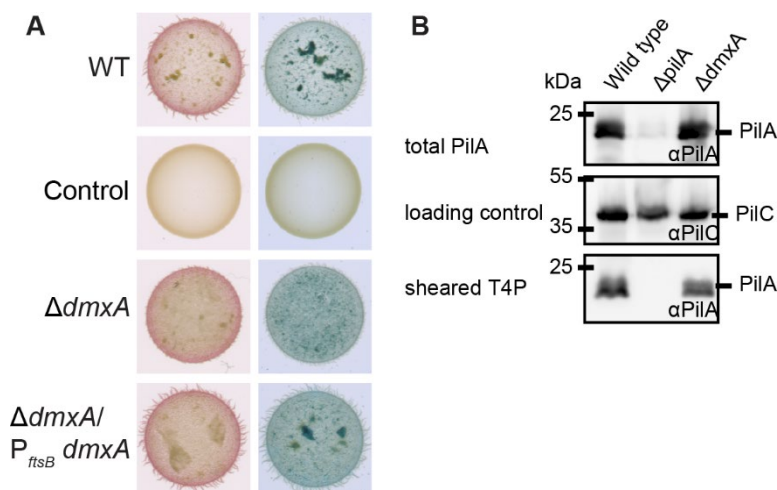


Figure 5. (A) EPS accumulation differences can be observed after spotting 7×10^9 cells ml^{-1} on 0.5% agar with 0.5% CTT and Congo Red or Trypan Blue and incubating for 24 h (Skotnicka *et al.*, 2015). $\Delta pilA$ does not accumulate EPS (Black *et al.*, 2006) and was used as negative control. (B) T4P shear off assay. Immunoblot detection of PilA in sheared T4P (bottom) and in total cell extract (top). Total protein was isolated from the indicated strains grown on 1% CTT 1.5% agar plates. In all three blots, protein from the same number of cells was loaded per lane. The total PilA fraction blot was probed with α -PilA antibodies and with α -PilC as a loading control. The sheared fraction blot was probed with α -PilA antibodies.

$\Delta dmxA$ cells show a polarity defect

Mutations affecting polarity and the reversal frequency can result in defects in both motility systems (Leonardy *et al.*, 2010, Zhang *et al.*, 2010). Therefore, we looked at the movement of single cells of the $\Delta dmxA$ mutant on hard agar to evaluate gliding motility and in 1% methylcellulose to study T4P-dependent motility.

Interestingly, we observed an increase in the reversal frequency of $\Delta dmxA$ cells moving by either motility system compared to WT (Figs. 6A and B). For gliding motility, the reversal defects was partially complemented by the ectopic expression of the *dmxA* gene under the control of the native promoter on a plasmid integrated at the Mx8 *attB* site (Fig. 6A). It would be interesting to evaluate whether a $\Delta dmxA \Delta pilA$ mutant hyper-reverses on hard agar and whether the defect of $\Delta dmxA$ cells in methylcellulose can be complemented.

Reversals in *M. xanthus* are mainly controlled by the Frz chemosensory system (Schumacher & Søgaard-Andersen, 2017). To determine whether the increase in the reversal frequency of the $\Delta dmxA$ cells depended on the Frz chemosensory system, we deleted the *frzE* gene, which encodes a CheA-CheY homolog. Interestingly, the $\Delta dmxA \Delta frzE$ colony showed additive motility defects compared to the single deletion mutants (Fig. 6C). Similarly, while the reversal frequency of $\Delta frzE$ cells was strongly reduced, $\Delta dmxA \Delta frzE$ single cells still reversed with a high frequency

in methylcellulose (Fig. 6D). Next, it should be evaluated whether this is also the case on hard surfaces. Altogether the results suggest that the motility defects of the $\Delta dmxA$ strain are caused by an increase in the reversal frequency that is independent of the Frz chemosensory system rather than *bona fide* motility defects.

Using time-lapse microscopy, we also observed that some cells were able to move forward by simultaneously using both poles pointing towards a defect in polarity. In agreement with this, we observed, using electron microscopy, that approx. 10% of $\Delta dmxA$ cells had pili at both poles (Fig. 6E and F) as was previously observed for other strains affected in polarity (Potapova personal communication).

Localization and accumulation of RomR-mCherry is affected in the $\Delta dmxA$ background

Polarity in *M. xanthus* depends on a protein module consisting of four proteins: The Ras-like GTPase MglA, the MglA GTPase Activating Protein (GAP) MglB, and the RomR/RomX complex, which is a MglA Guanine nucleotide Exchange Factor (GEF) complex (Szadkowski *et al.*, 2019, Schumacher & Sogaard-Andersen, 2017). Because the $\Delta dmxA$ mutant has a defect in polarity, we decided to look at the protein localization of the components that regulate polarity in *M. xanthus*. We started localizing RomR-mCherry, since RomR influences polar localization of the other three components (Szadkowski *et al.*, 2019, Schumacher & Sogaard-Andersen, 2017).

RomR-mCherry expressed from the native side in the $\Delta dmxA$ background localized in a bipolar asymmetric manner to the poles, similarly to that in WT (Fig. 7A). In moving WT cells, RomR-mCherry localizes preferentially at the lagging cell pole (Leonardy *et al.*, 2007). Interestingly, in the $\Delta dmxA$ background, RomR-mCherry localized not only at the lagging pole, but also mainly at the leading cell pole, symmetrically or diffusely (Fig. 7B). Moreover, in comparison to WT cells, RomR and RomR-mCherry accumulated to a higher level in the $\Delta dmxA$ background (Fig. 7C).

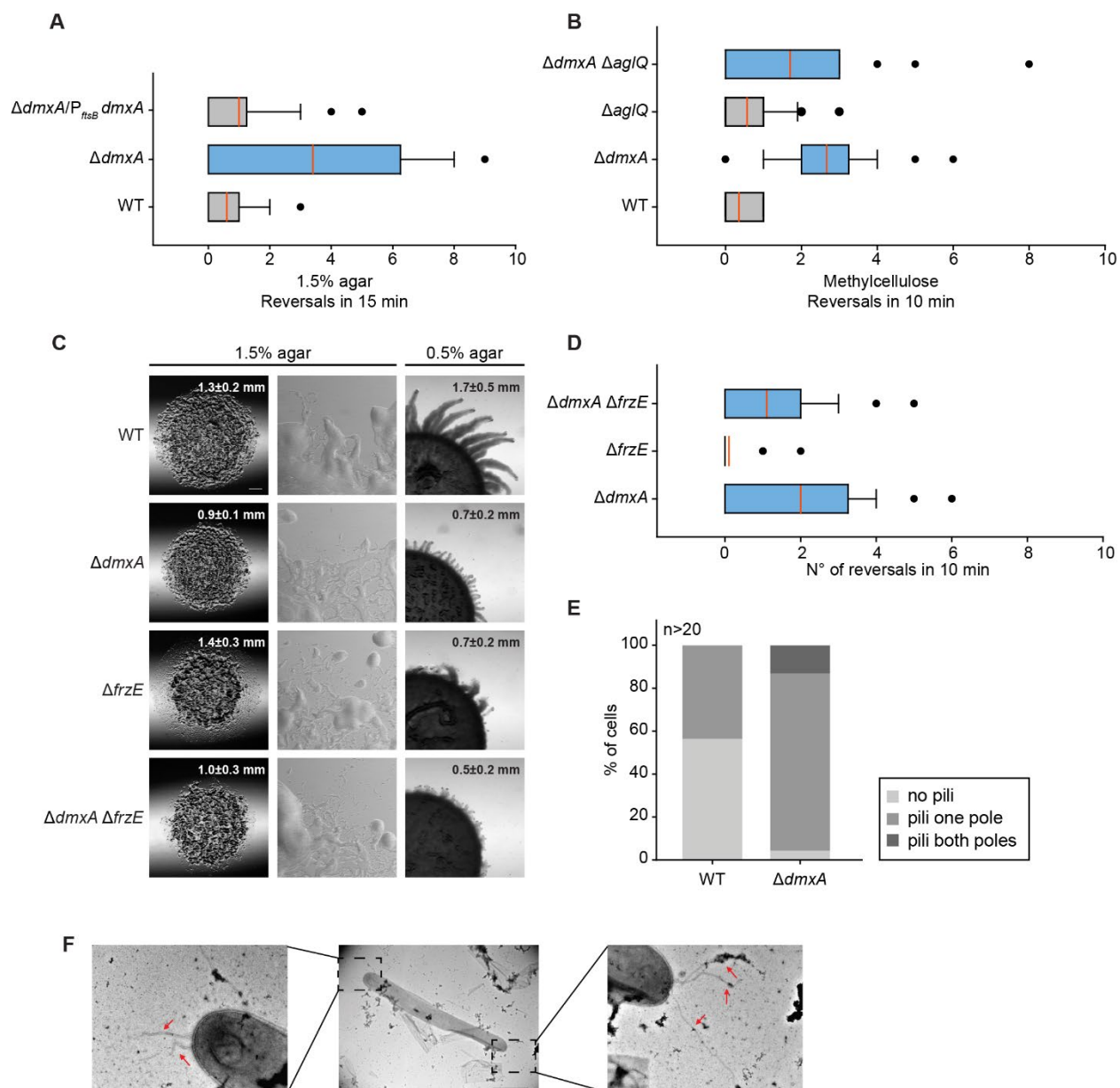


Figure 6. Characterization of the reversal frequency of the $\Delta dmxA$ strain. (A-B, D) Single cell analysis of the reversal frequency $\Delta dmxA$ cells by time-lapse microscopy. In the box plot, the X-axis corresponds to the number of reversals per time period. Boxes enclose the 25th and 75th percentile with the red line representing the mean. Whiskers represent the 10th and 90th percentile and the black circles the outliers. (A) Cells were transferred from a liquid culture to a thin TPM agar pad, covered with a coverslip, and imaged every 30 s for 15 min (n=50 per strain). (B) Cells in 1% methylcellulose were imaged for 10 min with 20 s intervals (n>30 per strain, except for WT where n=11). (C) Gliding motility and T4P-dependent motility were analyzed on 1.5% and 0.5% agar respectively. (D) Cells in 1% methylcellulose were imaged for 10 min with 20 s intervals (n=50 per strain). (E-F) Exponentially growing cells of $\Delta dmxA$ were visualized by electron microscopy and compared to WT. (E) Analysis of T4P at the poles (n>20 per strain). (D) Example of a $\Delta dmxA$ cell, which has assembled T4P at both poles. T4P are indicated by red arrows. The picture in the middle (size bar is 2 μ m) shows the complete cell and the pictures on the left and right (size bar is 500 nm) show the first and second pole.

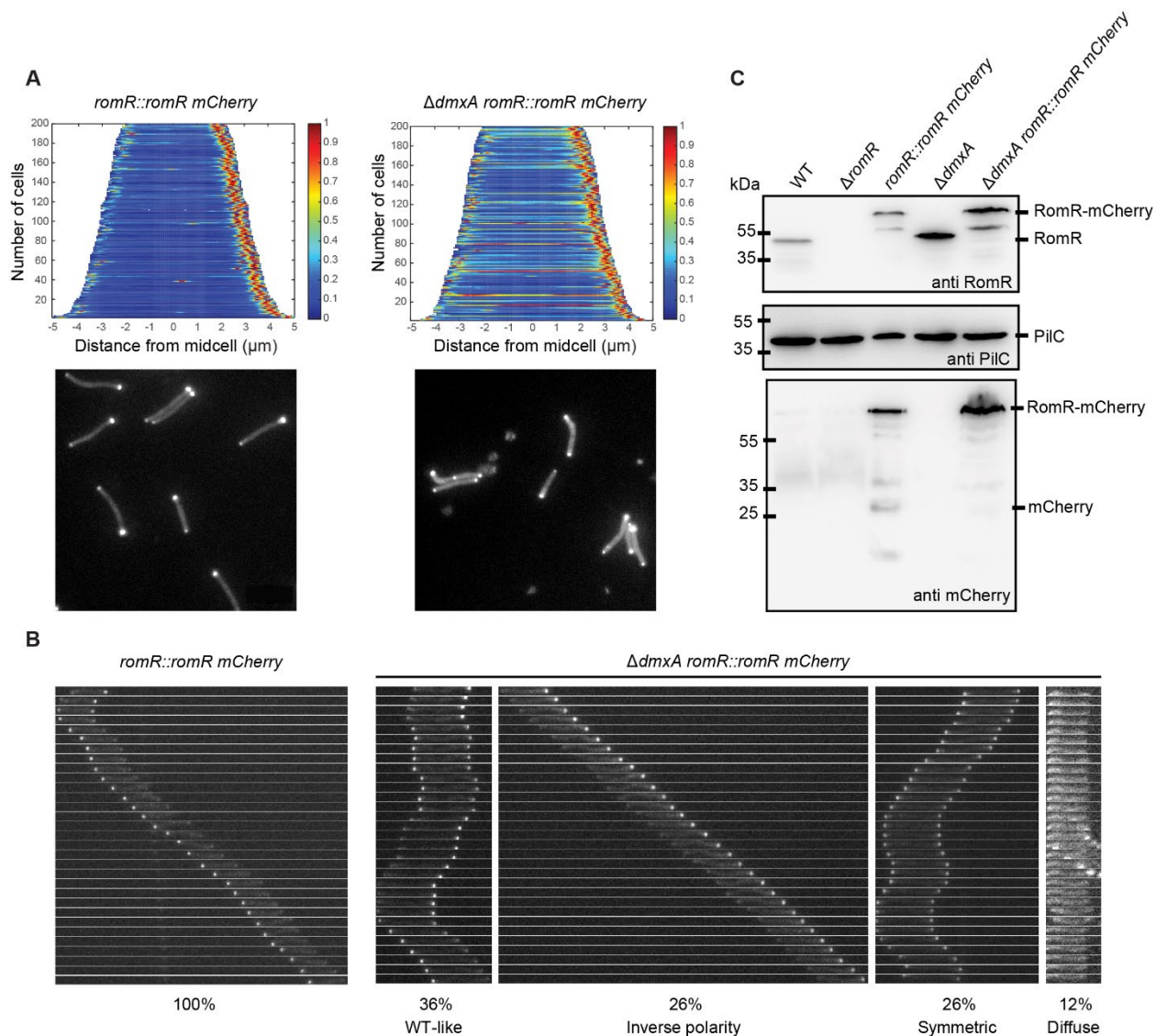


Figure 7. (A-B) Localization of RomR-mCherry by epifluorescence microscopy. Cells grown exponentially were transferred from a liquid culture to a thin 1.5% TPM agar pad supplemented with 0.2% CTT, covered with a coverslip and imaged. By time-lapse microscopy, cells were imaged every 30 s for 15 min and exposed to 100ms. (A) RomR mCherry localization in $\Delta dmxA$ and otherwise WT cells (bottom) and demograph (top) ($n=200$). (B) Time-lapse microscopy of strains expressing RomR-mCherry. (C) Immunoblot detection of RomR and RomR-mCherry. Total protein was isolated from exponential growing cells and the same number of cells was loaded per lane. The blot was probed with α -RomR, α -mCherry antibodies and with α -PilC as a loading control.

DmxA function in motility depends on DGC activity, but not on c-di-GMP binding

Because DmxA is an active DGC (Skotnicka *et al.*, 2015), we decided to study whether DGC activity and c-di-GMP synthesis are important for regulation of motility in *M. xanthus*. In order to test DGC activity of DmxA, a truncated cytoplasmic variant comprising the two GAF domains and the GGDEF domain was purified, mixed with [α - ^{32}P] GTP and tested for DGC activity *in vitro*.

While the DmxA variant is active (Skotnicka *et al.*, 2015) and synthesizes c-di-GMP, DmxA^{E626A}, which contains a mutation in the A site, is not (Skotnicka unpublished) (Fig. 8A).

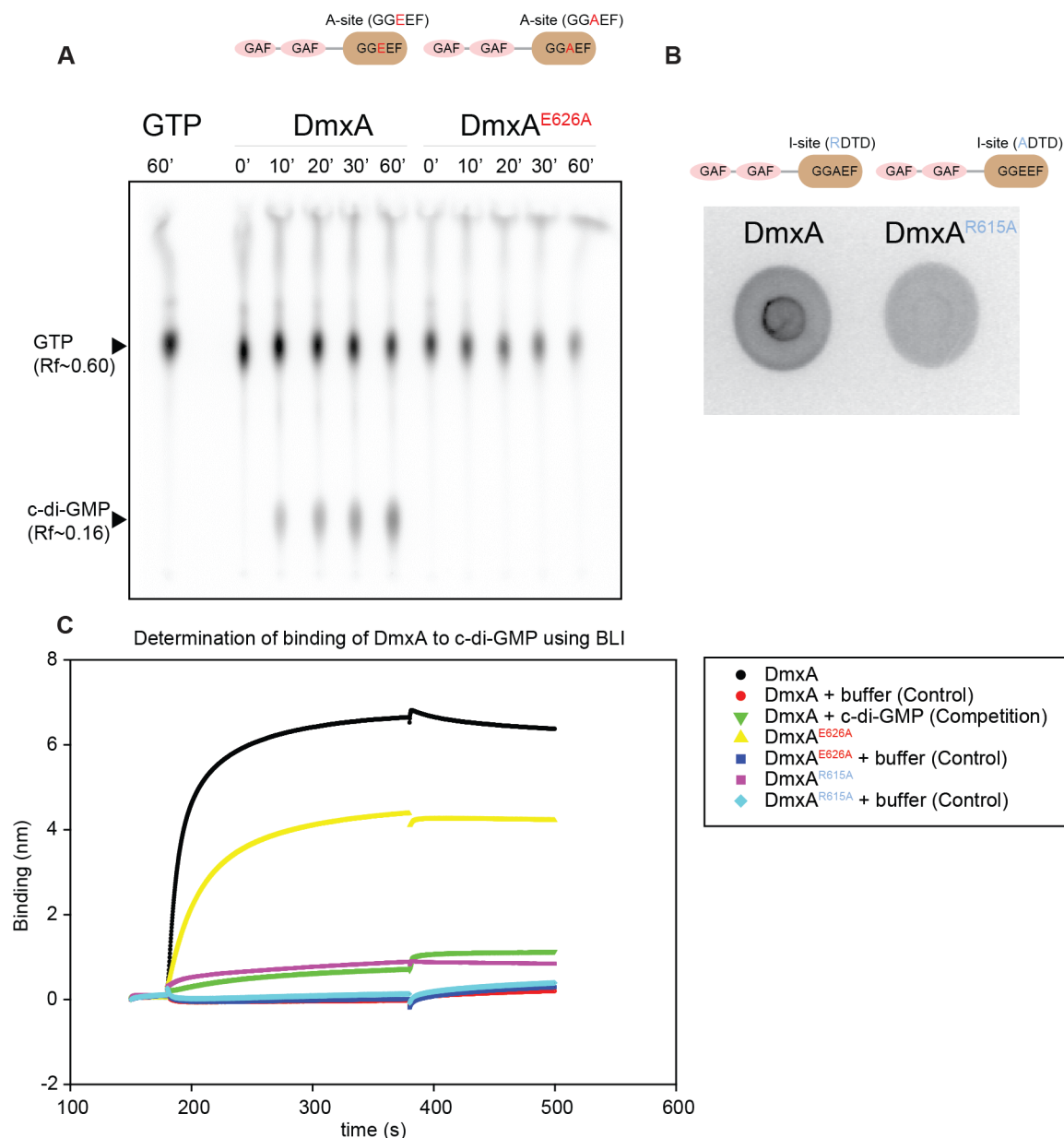


Figure 8. (A) *In vitro* DGC assay of DmxA and DmxA^{E626A}. DmxA and DmxA^{E626A} were incubated with [α -³²P] GTP for the indicated periods of time, followed by separation of nucleotides by thin-layer chromatography. Domain architectures of truncated DmxA and DmxA^{E626A} are shown as SMART images. GTP and c-di-GMP are indicated. (B) *In vitro* c-di-GMP binding assay. DRaCALA was used to detect specific c-di-GMP binding of DmxA. Purified DmxA and DmxA^{R615A} were incubated with [α -³²P]-labeled c-di-GMP. (C) BLI sensograms of binding of DmxA variant to 500nM biotinylated c-di-GMP. Equal concentrations of DmxA, DmxA^{R615A} and DmxA^{E626A} variants were used to determine their binding against biotinylated c-di-GMP immobilized on a streptavidin biosensor. Competition was tested by previously incubating DmxA variant with 1mM non biotinylated c-di-GMP for 30 min. Unspecific binding of DmxA to the streptavidin biosensor was tested by using buffer instead of biotinylated c-di-GMP.

Additionally, DmxA possesses an I-site that binds c-di-GMP (Skotnicka *et al.*, 2015) (Figs. 8B and C) and may potentially regulate DmxA activity. In order to determine the role of the I-site, we first tested whether a DmxA^{R615A} variant could bind c-di-GMP *in vitro*. As expected, in collaboration with Dorota Skotnicka, we observed that the R615A substitution in the I-site causes a reduction in c-di-GMP binding (Figs. 8B and C).

We next ectopically expressed both protein variants in the $\Delta dmxA$ mutant under the control of the *ftsB* promoter from a plasmid integrated at the Mx8 *attB* site. While expression of DmxA^{R615A} complements the motility phenotype, expression of DmxA^{E626A} did not (Fig. 9).

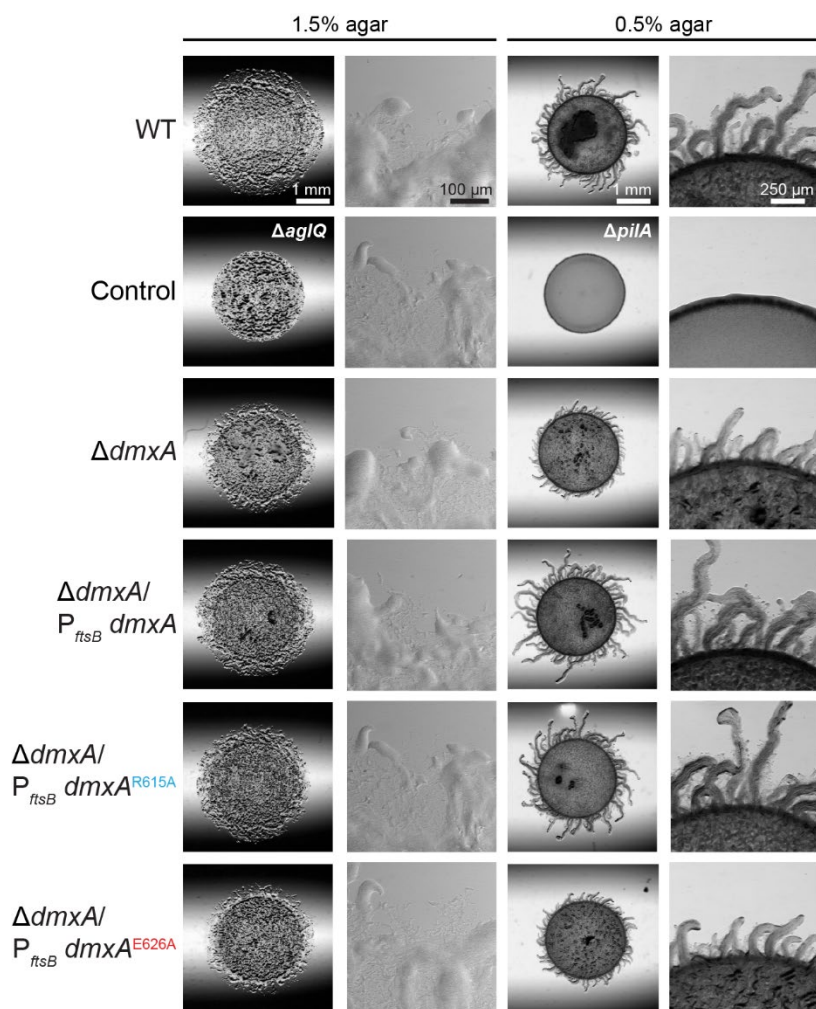


Figure 9. Gliding motility and T4P-dependent motility were analyzed on 1.5% and 0.5% agar respectively.

Lack of complementation of the DmxA^{E626A} variant could be caused by lack of DmxA^{E626A} accumulation. Therefore, in order to measure if both variant proteins were accumulating at the same level as the WT protein, the *dmxA* variants were fused to *mVenus* and were ectopically expressed under the control of the native promoter from a plasmid integrated at the Mx8 *attB* site. Importantly, similar motility results were obtained when expressing the tagged variants (Fig. 10A)

and, DmxA, DmxA^{E626A} and DmxA^{R615A} accumulated at a similar level (Fig. 10B). We conclude that regulation of motility by DmxA depends on DGC activity but not on the allosteric I-site. In other words, c-di-GMP synthesis is necessary for motility regulation.

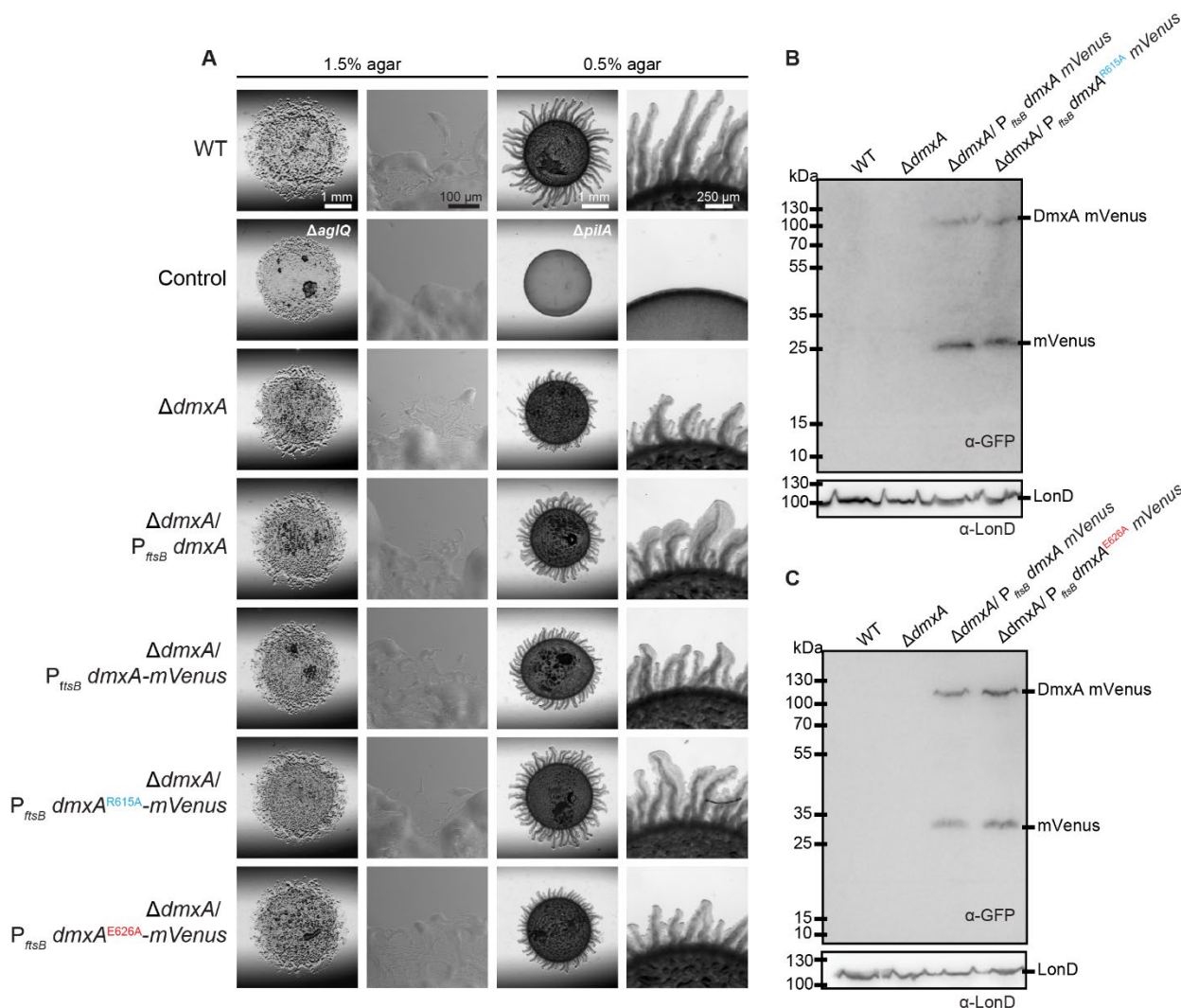


Figure 10. (A) Gliding motility and T4P-dependent motility were analyzed on 1.5% and 0.5% agar respectively. (B) Immunoblot of DmxA-mVenus and the A- and I-site variants. Same number of cells was separated by SDS-PAGE and analyzed by immunoblotting using anti GFP antibodies. As a loading control the membrane was probed with α -LonD antibodies.

Additionally to synthesis of c-di-GMP, GGDEF proteins may exert their function through protein-protein interactions (Römling *et al.*, 2013). In some cases, the DGC function can be replaced by a heterologous DGC (i.e. DmxB function, which is necessary for the increase of c-di-GMP during development, can be substituted by heterologous expression of DcgA from *C. crescentus* (Skotnicka *et al.*, 2016)). Following this reasoning, we tested whether a heterologous DGC, i.e. DcgA of *C. crescentus*, could complement the motility defect of $\Delta dmxA$ cells. We observed that a

$\Delta dmxA$ strain expressing DgcA showed a more pronounced motility defect on soft and hard agar than the single $\Delta dmxA$ mutation (Fig. 11A).

Given that DmxA is an active DGC, it was surprising that previous studies on $\Omega dmxA$ cells showed a 1.5-fold increase in the c-di-GMP level compared to WT (Skotnicka *et al.*, 2015). We decided to reevaluate, in collaboration with Prof. Dr. Volkhart Kaever, the measurement of c-di-GMP using the $\Delta dmxA$ mutant. The c-di-GMP level was measured in two different $\Delta dmxA$ clones and no difference was observed during growth in comparison to WT cells (Fig. 11B). The results suggest that although DmxA possesses DGC activity, it does not extensively contribute to the global level of c-di-GMP and its function may be restricted to a local pool.

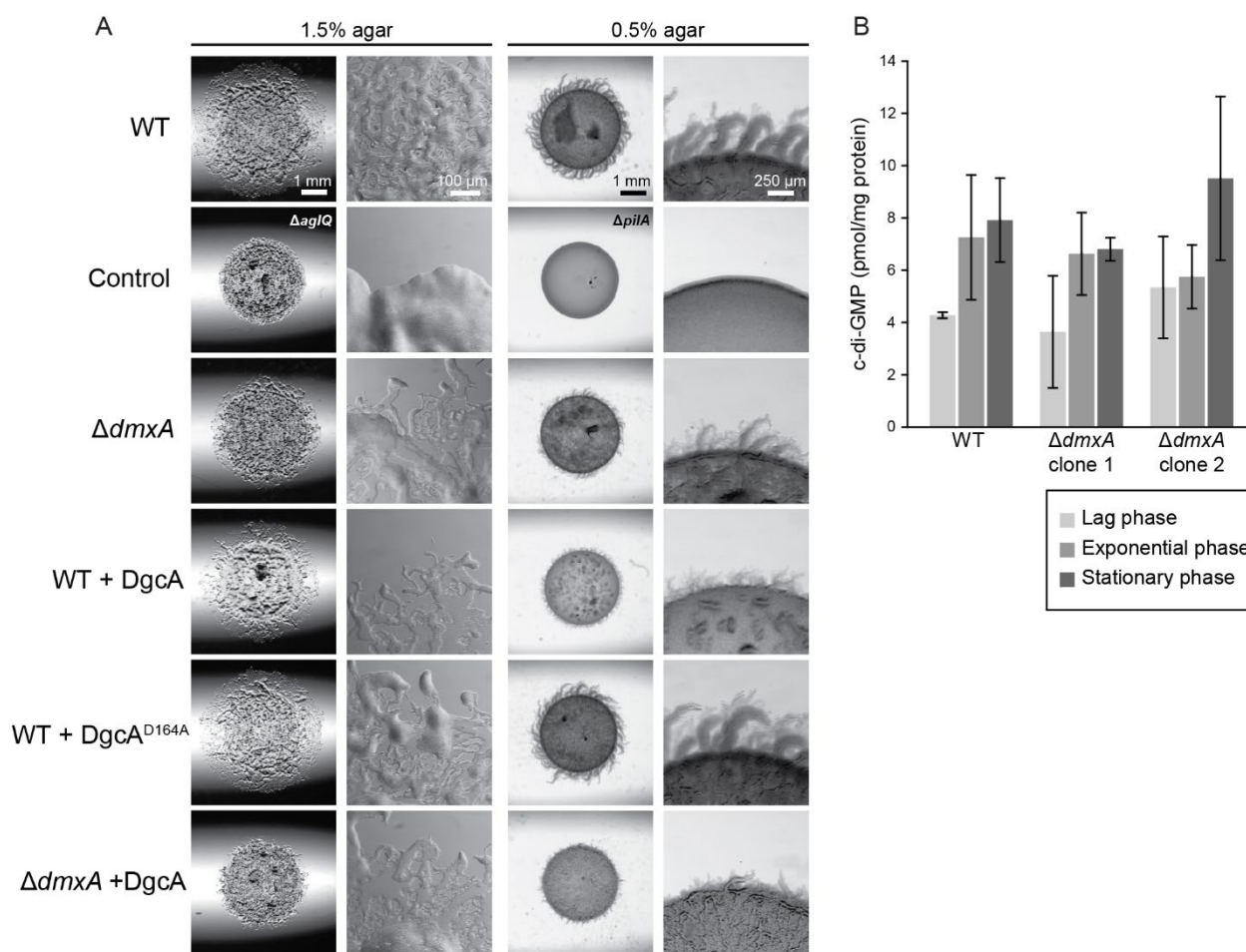


Figure 11. (A) Gliding motility and T4P-dependent motility were analyzed on 1.5% and 0.5% agar respectively. (B) c-di-GMP measurement of $\Delta dmxA$ during vegetative growth. Level of c-di-GMP is shown as the mean \pm SD from three technical replicates.

DmxA localizes to mid-cell during cell division and this depends on FtsZ

Because lack of DmxA causes a polarity defect, we decided to localize the protein by using fluorescence microscopy. To this end, we used the active DmxA-mVenus fusion expressed from the native promoter on a plasmid integrated at the Mx8 *attB* site. We observed localization of DmxA-mVenus to mid-cell (<5% of the population) late during cell division in cells with a visible cell constriction (Fig. 12A left), while protein localization was diffuse during the rest of the cell cycle. Similar results were obtained using DmxA^{E626A}-mVenus and DmxA^{R615A}-mVenus (Figs. 12B and C). Interestingly, treating the cells with the division inhibitor cephalixin to increase the number of cells with constrictions (Treuner-Lange *et al.*, 2013), resulted in an increase in the number of cells with a DmxA cluster at mid-cell (Figs. 12A right).

Because the signal of cells expressing DmxA-mVenus from the *att* site was relatively low, in order to perform time-lapse microscopy and improve visualization of the signal, we generated a strain expressing *dmxA-mVenus* from the native site. We observed that DmxA-mVenus expressed from the native site localized at mid-cell in 3% of the cells (Fig. 12D left) and the number of cells with a cluster increased in the presence of cephalixin (Fig. 12D right). The *dmxA::dmxA-mVenus* strain showed a higher fluorescence signal correlating with the higher protein level compared to a strain ectopically expressing DmxA-mVenus under the native promoter (Fig. 12E).

Using time-lapse microscopy and non-motile cells containing a $\Delta aglQ$ mutation, we observed the cluster dynamics during the cell cycle. The cluster formed at mid-cell after initiation of constriction and disappeared upon completion of cytokinesis (Fig. 12F left). *M. xanthus* cells' doubling time is around 5 h (Treuner-Lange *et al.*, 2013). Interestingly, the DmxA-mVenus cluster had a "lifetime" of ~20 min per cell cycle (Fig. 12F right), which nicely correlates with the low percentage of clusters observed in growing cell populations. Importantly, cluster formation was visible in each division event.

The FtsB protein forms part of the divisome and localizes to mid-cell during cell division in bacteria such as *C. crescentus* (Goley *et al.*, 2011), *E. coli* (Buddelmeijer *et al.*, 2002) and *Bacillus subtilis* (Katis *et al.*, 1997). FtsB forms a complex together with FtsQ and FtsL (Gonzalez & Beckwith, 2009, Kureisaite-Ciziene *et al.*, 2018, Choi *et al.*, 2018) that is suggested to recruit late components to the division site (LaPointe *et al.*, 2013). In *C. crescentus*, FtsB arrives to mid-cell after the core set of divisome proteins, immediately preceding initial invagination of the cell envelope (Goley *et al.*, 2011). Thus, it is compelling to hypothesize that the divisome and possibly FtsB, recruits DmxA to the division site.

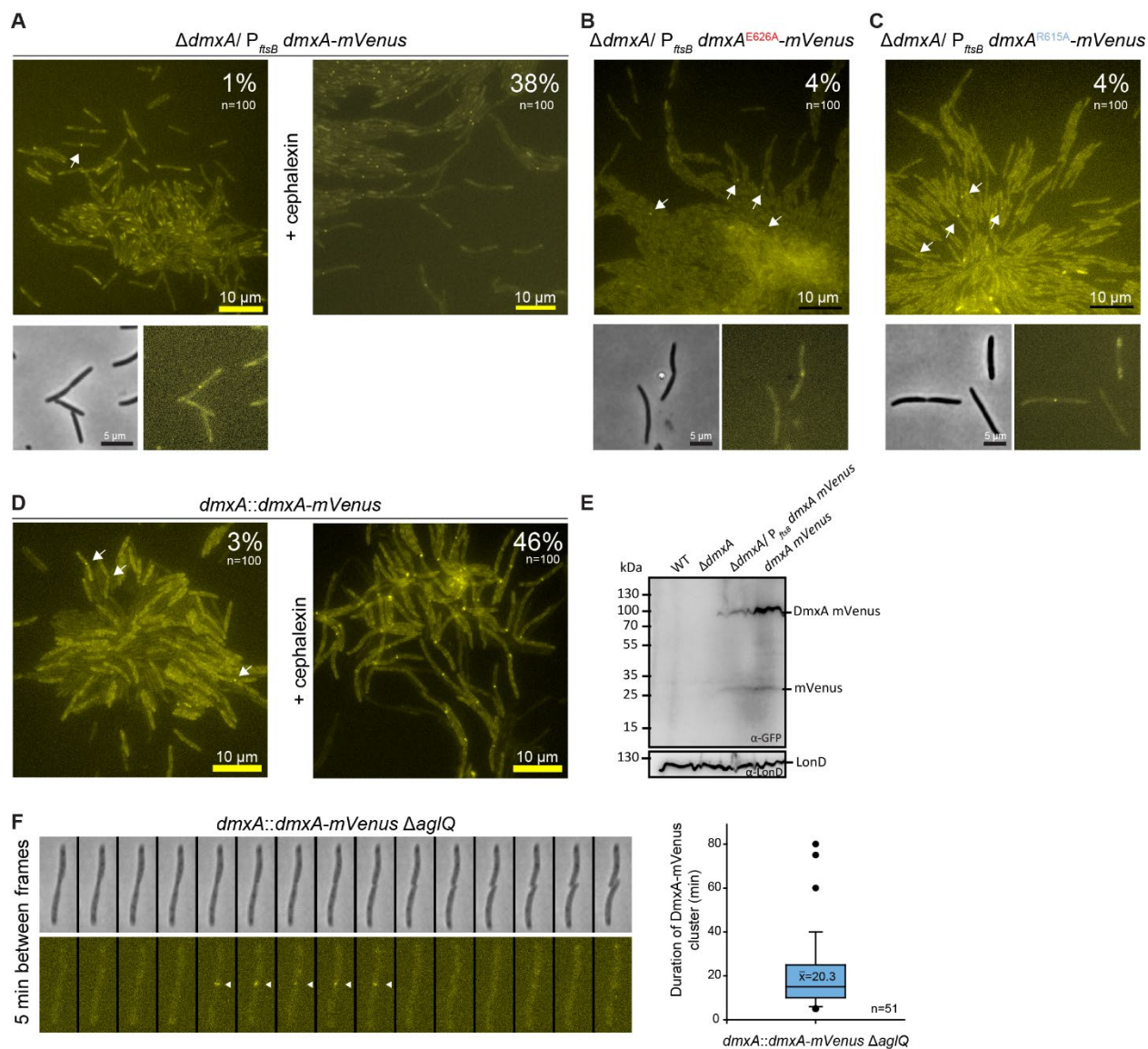


Figure 12. (A-E) Localization of DmxA-mVenus and its variants by epifluorescence microscopy. Cells grown exponentially in the presence or absence of cephalalexin for 6 h were transferred from a liquid culture to a thin 1.5% TPM agar pad supplemented with 0.2% CTT, covered with a coverslip and imaged. Cells were exposed for 1s. (F) Immunoblot detection of DmxA-mVenus. Total protein was isolated from exponential growing cells and the same number of cells was loaded per lane (5×10^9). The blot was probed with α -GFP antibodies, and with α -LonD as a loading control. (G) Phase contrast (top) and fluorescence (bottom) time-lapse microscopy of DmxA-mVenus clusters in non-motile cells containing a $\Delta aglQ$ mutation (left). Cells were imaged on 1.5% TPM agarose pad supplemented with 0.2% CTT at 32 °C. Determination of the duration of the cluster events (right).

To test whether DmxA localization to mid-cell depends on FtsB, we attempted to delete the *ftsB* gene. *ftsB* is essential in *B. subtilis* (Levin & Losick, 1994), *E. coli* and *V. cholerae* (Buddelmeijer *et al.*, 2002), but not in *C. crescentus* (Goley *et al.*, 2011), *Streptomyces coelicolor* (Bennett *et al.*, 2007) or *Streptococcus pneumoniae* (Le Gouellec *et al.*, 2008). However, attempts to delete or to

localize FtsB were not successful, suggesting that FtsB in *M. xanthus* is essential. Future work should focus on the generation of a depletion strain and the localization of FtsB during the cell cycle. Alternatively, we used an *ftsZ* depletion strain expressing *dmxA-mVenus* from its native site. While FtsZ localizes in a mid-cell cluster in around 50% of the cell population, which includes cells with and without constrictions (Treuner-Lange *et al.*, 2013), we observed that DmxA-mVenus exclusively localized in cells with constrictions and not all the cells with a constriction had a DmxA cluster. Interestingly, in the absence of FtsZ, DmxA did not localize to mid-cell, not even in the presence of cephalixin (Figs. 13A-D) despite the protein accumulating (Fig. 13E). Thus, DmxA localization to mid-cell depends on FtsZ and most probably on the assembly of the divisome during cell division.

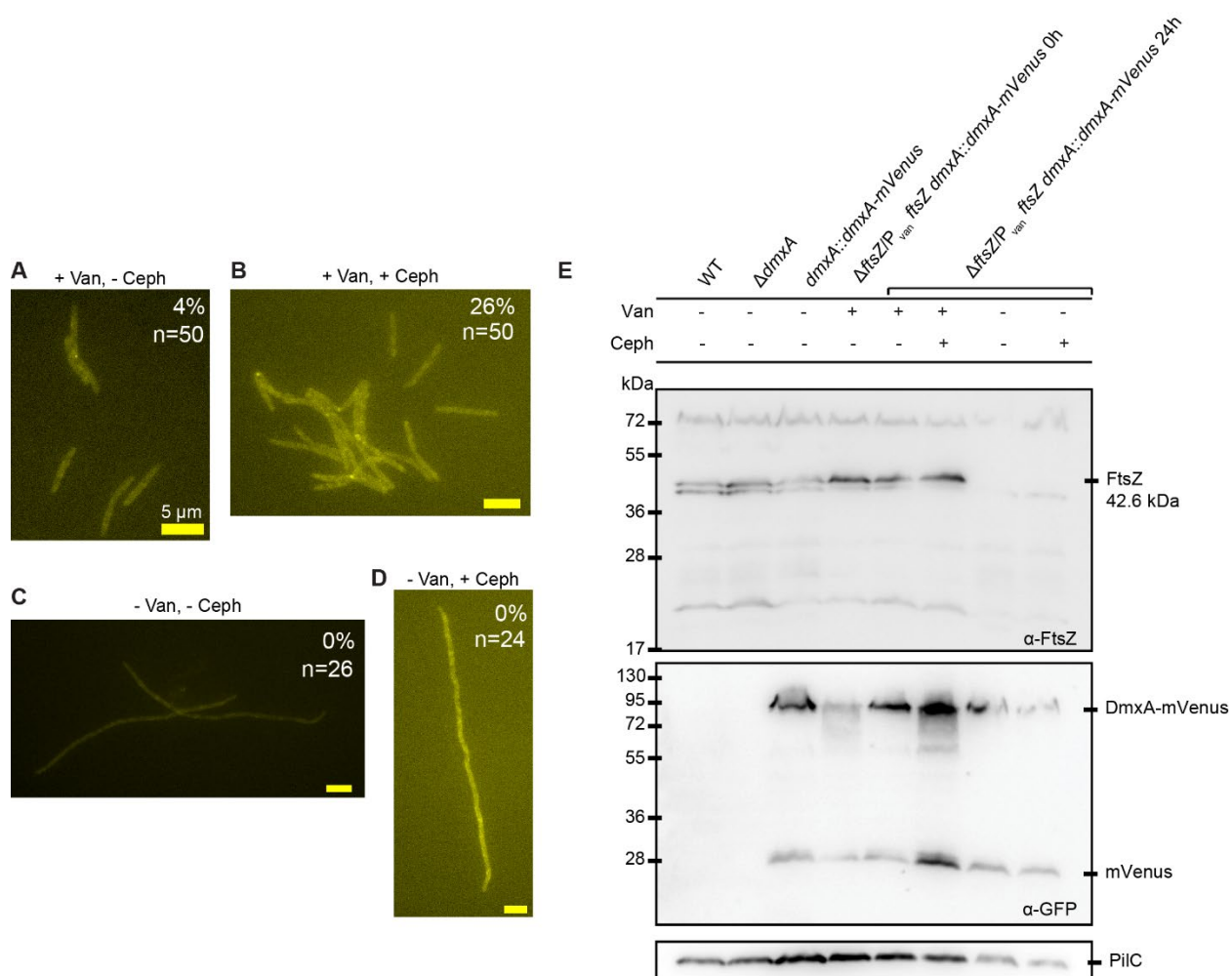


Figure 13. (A-D) Localization of DmxA-mVenus by epifluorescence microscopy in the presence and absence of vanillate and/or cephalixin. Cells grown exponentially for ~8 generations in the presence or absence of 10 μ M vanillate (Van) and in the presence or absence of cephalixin (Ceph) for 4 h were transferred from a liquid culture to a thin TPM agar pad and covered with a coverslip. Cells were exposed for 1s. (E) Immunoblot detection of FtsZ and DmxA-mVenus.

Total protein was isolated from exponential growing cells and the same number of cells was loaded per lane. The blot was probed with α -FtsZ, α -GFP antibodies and with α -LonD as a loading control.

3.4.2 Discussion

Our previous model suggested that a higher EPS accumulation caused by an increased c-di-GMP level in the Ω *dmxA* strain, was responsible for the higher stickiness of the cells and therefore of the reduction in T4P-dependent motility (Skotnicka *et al.*, 2015). Here, we showed, by generation of an in-frame deletion strain, that the active DGC DmxA is involved in motility regulation during growth in *M. xanthus*. We showed that not only T4P-dependent motility was affected, but also gliding motility, and that this defect is specific for DmxA, since none of the remaining putatively active DGC appear to be implicated in motility.

We have shown that the motility defects likely arise from an increase in the reversal frequency of Δ *dmxA* cells independently of the Frz chemosensory system. Because polarity of Δ *dmxA* cells is affected and mutant cells assemble pili at both poles in a significant number of cells, we suggest that the increase in the reversal frequency may partially depend on simultaneous activity of the pili at both poles. DGC activity is required for the regulation of motility, while DmxA does not contribute to the overall c-di-GMP pool. It would be interesting to test whether cells expressing the inactive DmxA variant also hyper-reverse. Additionally, because EPS and T4P regulate each other (see Chapter 3.3), it is possible that the defect in polarity may affect EPS synthesis.

Polarity in *M. xanthus* depends on RomR/RomX, MglA and MglB. Interestingly, the Δ *dmxA* mutant had a defect in the bipolar asymmetric localization of RomR-mCherry and an increase in the accumulation of RomR or RomR-mCherry. Because RomR, MglA and MglB influence localization of each other, it would be interesting to test whether MglA, MglB and RomX localization is affected in the Δ *dmxA* mutant. Similarly, it would be interesting to determine whether RomR/RomX, MglA or MglB affect localization of DmxA-mVenus.

We localized DmxA-mVenus to mid-cell posterior to the initiation of cell constriction. Recruitment of DmxA-mVenus to the division site depends on FtsZ and, most likely, on FtsB, because *ftsB* and *dmxA* form an operon. In agreement with this, FtsB from *C. crescentus* localizes to mid-cell anterior to membrane invagination (Goley *et al.*, 2011). In contrast, neither activity nor c-di-GMP binding were important for localization. Taking this in consideration, it is possible that (1) DmxA activity is regulated in space and time or (2) that DmxA is active during all the *M. xanthus* growth, but a larger amount of DmxA is needed during cell division at mid-cell to correctly sort/regulate polarity. Supporting the first hypothesis, DmxA contains two GAF domains. Such domains are

frequently found in cyclic nucleotide PDEs and are described to be involved in regulatory pathways through binding of cGMP or cAMP (Martinez *et al.*, 2002, Ho *et al.*, 2000). It would be interesting to identify the ligand of the GAF domains and to study whether the GAF domains regulate the activity of DmxA. Additionally, since DmxA does not influence the global c-di-GMP pool, but its DGC activity is essential for regulation of motility, it is possible that DmxA contributes to a local c-di-GMP pool through protein-protein interactions and/or compartmentalized localization as it was suggested for other c-di-GMP metabolizing proteins (Hengge, 2009).

3.4.3 Experimental procedures

Strains and cell growth. *M. xanthus* cells were grown at 32°C in 1% CTT (1% (w/v) Bacto Casitone, 10 mM Tris-HCl pH 8.0, 1 mM K₂HPO₄/KH₂PO₄ pH 7.6 and 8 mM MgSO₄) liquid medium or on 1.5% agar supplemented with 1% CTT (Hodgkin & Kaiser, 1977). Oxytetracycline, kanamycine and cephalixin at a concentration of 10 µg ml⁻¹, 50 µg ml⁻¹ and 35 µg ml⁻¹ respectively, were used when needed. All *M. xanthus* strains are derivatives of the WT strain DK1622 (Kaiser, 1979). The *M. xanthus* strains and plasmids used in this work are listed in Tables 1 and 2, respectively. The in-frame deletions were generated as described previously (Shi *et al.*, 2008) and plasmids for complementation experiments were integrated in a single copy by site specific recombination into the Mx8 *attB* site or by homologous recombination at the endogenous locus. All in-frame deletions and plasmid integrations were verified by PCR. Plasmids were propagated in *E. coli* Mach1.

Table 1. Strains used in this work.

Strain	Genotype	Reference
<i>M. xanthus</i>		
DK1622	Wildtype	(Kaiser, 1979)
DK10410	$\Delta pilA$	(Wu & Kaiser, 1997)
SA5923	$\Delta aglQ$	(Jakobczak <i>et al.</i> , 2015)
SA3543	<i>attB</i> ::pTP114 (<i>P_{pilA} dgcA^{WT}</i> -Strep-tag II)	(Skotnicka <i>et al.</i> , 2015)
SA3559	<i>attB</i> ::pTP131 (<i>P_{pilA}-dgcA^{D164A}</i> -Strep-tag II)	(Skotnicka <i>et al.</i> , 2015)
SA7507	<i>romR</i> :: <i>romR-mCherry</i>	(Szadkowski <i>et al.</i> , 2019)
SA8802	$\Delta frzE$	(Szadkowski <i>et al.</i> , 2019)
SA6755	$\Delta ftsZ mxan18-19$::pMAT86 (<i>P_{van ftsZ}</i>)	Anke Treuner-Lange
SA7442	$\Delta dmxA$	This study
SA7447	$\Delta dmxA attB$::pTP140 (<i>P_{ftsB dmxA}</i>)	This study
SA7449	$\Delta dmxA attB$::pTP114 (<i>P_{pilA dgcA^{WT}}</i> -Strep-tag II)	This study
SA7459	$\Delta dmxA romR$:: <i>romR mCherry</i>	This study
SA7461	$\Delta dmxA attB$::pMP088 (<i>P_{ftsB dmxA^{R615A}}</i>)	This study
SA7462	$\Delta dmxA attB$::pMP090 (<i>P_{ftsB dmxA^{E626A}}</i>)	This study
SA7465	$\Delta dmxA \Delta aglQ$	This study
SA7466	$\Delta dmxA \Delta pilA$	This study
SA7478	$\Delta dmxA attB$::pMP092 (<i>P_{ftsB dmxA-mVenus}</i>)	This study

SA7479	$\Delta dmxA \Delta frzE$	This study
SA7485	$dmxA:: dmxA\text{-}mVenus$	This study
SA7491	$\Delta dmxA attB:: pMP102 (P_{ftsB} dmxA^{R615A}\text{-}mVenus)$	This study
SA7492	$\Delta dmxA attB:: pMP101 (P_{ftsB} dmxA^{E626A}\text{-}mVenus)$	This study
SA8501	$dmxA:: dmxA\text{-}mVenus \Delta aglQ$	This study
SA8511	$\Delta ftsZ mxan18\text{-}19:: pMAT86 (P_{van} ftsZ) dmxA:: dmxA\text{-}mVenus$	This study
<i>E. coli</i>		
Mach1	$\Delta recA1398 endA1 tonA \Phi 80 \Delta lacM15 \Delta lacX74 hsdR(r_K^- m_K^+)$	Invitrogen
Rosetta (DE3)	$F^- ompT hsdS_B(r_B^- m_B^-) gal dcm (DE3) pRARE2$	Novagen/Merck

Table 2. Plasmids used in this work.

Plasmid	Description	Reference
pBJ114	<i>galK</i> Km ^r	(Julien <i>et al.</i> , 2000)
pSWU30	Tet ^r	(Wu & Kaiser, 1997)
pBJaglQ	pBJ114, in-frame deletion construct for <i>aglQ</i> Km ^r	(Sun <i>et al.</i> , 2011)
pTP114	pSW105, <i>dgcA</i> ^{WT} -Strep-tag II Kan ^r	(Skotnicka <i>et al.</i> , 2015)
pTP137	pET28a(+) <i>dmxA</i> ²²³⁻⁷²² Kan ^r	(Skotnicka <i>et al.</i> , 2015)
pTP139	pET28a(+) <i>dmxA</i> ^{223-722, E626A} Kan ^r	Tobi Petters
pTP140	pSWU30, $P_{ftsB}\text{-}dmxA$ Tet ^r	(Skotnicka <i>et al.</i> , 2015)
pMAT162	pBJ114, in-frame deletion construct for <i>pilA</i> Km ^r	(Szadkowski <i>et al.</i> , 2019)
pAP19	pBJ114, in-frame deletion construct for <i>frzE</i> Km ^r	Anna Potapova
pMP072	pBJ114, in-frame deletion construct for <i>dmxA</i> Km ^r	This work
pMP082	pET28a(+) <i>dmxA</i> ^{223-722, R615A} Kan ^r	This work
pMP088	pSWU30, $P_{ftsB} dmxA^{R615A}$ Tet ^r	This work
pMP090	pSWU30, $P_{ftsB} dmxA^{E626A}$ Tet ^r	This work
pMP092	pSWU30, $P_{ftsB} dmxA\text{-}mVenus$ Tet ^r	This work
pMP093	pBJ114, <i>dmxA</i> replacement by <i>dmxA-mVenus</i>	This work
pMP101	pSWU30, $P_{ftsB} dmxA^{E626A}\text{-}mVenus$ Tet ^r	This work
pMP102	pSWU30, $P_{ftsB} dmxA^{R615A}\text{-}mVenus$ Tet ^r	This work

Plasmid construction. All oligonucleotides used for plasmid construction are listed in Table 3 and all constructed plasmids were verified by DNA sequencing.

pMP072 (for generation of in-frame deletion of *dmxA*): up- and downstream fragments were amplified from genomic DNA of DK1622 using the primer pairs 3705_A/3705_B and 3705_C/3705_D, respectively, as described in (Shi *et al.*, 2008). Subsequently, the AB and CD fragments were used as templates to perform an overlapping PCR with the primer pair 3705_A/3705_D to generate the AD fragment. The AD fragment was digested with KpnI/XbaI and cloned in pBJ114.

pMP082 (expression of cytoplasmic *dmxA*^{223-722, R615A} from an IPTG inducible promoter): to introduce the R615A mutation to generate *dmxA*^{223-722, R615A}, two fragments were separately amplified with the primer combinations 3705 GAF1 forw NdeI/3705 R615A (-) and 3705 R615A (+)/3705 rev BamHI using pTP137 as DNA template. An overlapping

PCR with both fragments as DNA template and the primer pair 3705 GAF1 forw NdeI//3705 rev BamHI gave the *dmxA*^{223–722, R615A} fragment that was digested with NdeI/BamHI and cloned into pET28a(+).

pMP088 (expression of *P_{ftsB} dmxA*^{R615A} from the *attB* site): to introduce the R615A mutation in *P_{ftsB} dmxA*, two fragments were separately amplified with the primer combinations 3704 prmt forw +XbaI/3705 R615A (-) and 3705 R615A (+)/3705 rev BamHI using pTP140 as DNA template. An overlapping PCR with both fragments as DNA template and the primer pair 3704 prmt forw +XbaI/3705 rev BamHI gave the *P_{ftsB} dmxA*^{R615A} fragment that was digested with XbaI/BamHI and cloned into pSWU30.

pMP090 (expression of *P_{ftsB} dmxA*^{E626A} from the *attB* site): to introduce the E626A mutation in *P_{ftsB} dmxA*, two fragments were separately amplified with the primer combinations 3704 prmt forw +XbaI/3705 E626A (-) and 3705 E626A (+)/3705 rev BamHI using pTP140 as DNA template. An overlapping PCR with both fragments as DNA template and the primer pair 3704 prmt forw+XbaI/3705 rev BamHI gave the *P_{ftsB} dmxA*^{E626A} fragment that was digested with XbaI/BamHI and cloned into pSWU30.

pMP092 (expression of *P_{ftsB} dmxA-mVenus* from the *attB* site): *P_{ftsB} dmxA* and *mVenus* were separately amplified with 3704 prmt forw+XbaI/3705_rev no stop 1 and 3705_mVenus fw/mVenus_Kpn rev respectively by using pTP142 and pLC20 correspondingly as DNA template. An overlapping PCR with both fragments as DNA template and the primer pair 3704 prmt forw+XbaI/mVenus_Kpn rev gave the *P_{ftsB} dmxA-mVenus* fragment that was digested with XbaI/KpnI and cloned into pSWU30.

pMP093 (for substitution of native *dmxA* with *dmxA-mVenus*): up- and downstream fragments were amplified from genomic DNA of DK1622 using the primer pairs 3705_native forw/ 3705_rev no stop 1 and 3705_native middle fw/ 3705_native rev; and the *mVenus* fragment was amplified from pMP092 using the primer pair 3705_mVenus fw/ 3705_native middle rev. Subsequently, the DNA fragments were used as templates to perform an overlapping PCR with the primer pair 3705_native forw/ 3705_native rev to generate the insert fragment that was digested with KpnI/XbaI and cloned into pBJ114.

pMP101 (expression of *P_{ftsB} dmxA*^{E626A}-*mVenus* from the *attB* site): to introduce the E626A mutation in *P_{ftsB} dmxA-mVenus*, two fragments were separately amplified with the primer combinations 3704 prmt forw +XbaI/3705 E626A (-) and 3705 E626A (+)/mVenus_Kpn rev and using genomic DNA of DK1622 and pMP092 as DNA template, respectively. An overlapping PCR with both fragments as DNA template and the primer pair 3704 prmt forw+XbaI/ mVenus_Kpn rev gave the *P_{ftsB} dmxA*^{E626A}-*mVenus* fragment that was digested with XbaI/KpnI and cloned into pSWU30.

pMP102 (expression of *P_{ftsB} dmxA*^{R615A}-*mVenus* from the *attB* site): to introduce the R615A mutation in *P_{ftsB} dmxA-mVenus*, two fragments were separately amplified with the primer combinations 3704 prmt forw +XbaI/3705 R615A (-) and 3705 R615A (+)/mVenus_Kpn rev and using genomic DNA of DK1622 and pMP092 as DNA template, respectively. An overlapping PCR with both fragments as DNA template and the primer pair 3704 prmt forw +XbaI/ mVenus_Kpn rev gave the *P_{ftsB} dmxA*^{R615A}-*mVenus* fragment that was digested with XbaI/KpnI and cloned into pSWU30.

Table 3. Primers used in this work¹.

3705_A	ATCG <u>GGTACCA</u> AGGTGACGTGCACAAGAT
3705_B	CTTCAGCTGAGACGGAAACTCGGGAAG
3705_C	TTCCGTCTCAGCTGAAGGCGGCGAAC
3705_D	ATCGTCTAGACATCACCGGGTGGACCGTCA
3705_E	CGGCACCATCATCGAGTTCG
3705_F	TCCTCGGCTACCGGCTGCAG
3705_G	TGGTGACCCTGGGCGGTCCG
3705_H	CCAGGTCGATGAGCTGCTGC
3704 prmt forw +Xbal	ATCGTCTAGATTCTCAACGCGCTGGCGCTG
3705 E626A (+)	TACGGCGGCGCGGAGTTCGTC
3705 E626A (-)	GACGAACTCC G CGCCGCCGTA
3705 R615A (+)	GACGATGGCG G CCGATACGGAC
3705 R615A (-)	GTCCGTATCG G CCGCCATCGTC
3705 GAF1 forw NdeI	ATCGC <u>CATATG</u> GAGATCGAAGGCGCCGTGC
3705 rev BamHI	ATCGG <u>GATCCT</u> CAGGACGCGTTCGCCCG
3705_rev no stop 1	GCCGCCGCCggaacggttcgcccctcag
3705_mVenus fw	aacggtccGGCGGCGGCGGCTCCATGGTGAGCAAGGG
mVenus_Kpn rev	CGCGCCGGTAC <u>CTT</u> ACTTGTACAGCTCGTCCA
3705_native forw	ATATGGTAC <u>C</u> tcgctacggggcgccgctg
3705_native rev	CGCGTCTAGACATCCCCGAGTCGGCCATCG
3705_native middle rev	CCCGGCTGCATCAAGGACTTACTTGTACAGCTCGTC
3705_native middle fw	GACGAGCTGTACAAGTAAGTCCTTGTACAGCCGGG
3705_int.5	GAAGGCCGCGGAGATGAGCG
3704_A	TATAG <u>GTACC</u> AGATGGAGCTGTACGGCCTG
3704_B	GAAGACGAGCAACAGGAACTTTTCGCCT
3704_C	TTCCTGTTGCTCGTCTTCCACCTGGAG
3704_D	TATATCTAGACCCGCTCCTCCACCTCACGG
3704_E	AGCACGGCTTCAAGGTGACG
3704_F	GACACCAGCCGGAAGGTGCG
3704_G	AGCGGTAGGGGTGGCTGCGG
3704_H	GCCCCGGCTTACGAAGCCGA

¹ Underlined sequences indicate restriction sites and bold sequences indicate site directed mutagenesis.

Operon mapping. *ftsB-dmxA* operon mapping was performed by reverse-transcriptase analysis of the intergenic region indicated in Fig. 1D. RNA extracted as in (Overgaard *et al.*, 2006) and cDNA coming from growing *M. xanthus* cells were a gift of Dr. Sabrina Huneke-Vogt. cDNA, the mock control for which no reverse-transcriptase was added to the RNA sample, or genomic DNA was used as template for PCR using the primer combinations 3704_G/3704_H; 3704_G/3705_int.5 and 3705_G/3704_F (Table 3).

Cell length determination. 5 μ l aliquots of exponentially growing cultures were spotted on 1.5% agarose, immediately covered with a cover slide, and imaged using a DMI8 Inverted microscope and DFC9000 GT camera (Leica). To assess cell length, images were analysed Matlab R2018a (The MathWorks).

Detection of EPS accumulation. Exponentially growing cells were harvested, and resuspended in 1% CTT to a calculated density of 7×10^9 cells ml^{-1} . Twenty-microliter aliquots of the cell suspensions were placed on 0.5% CTT 0.5% agar supplemented with 20 $\mu\text{g ml}^{-1}$ Congo red or 40 $\mu\text{g ml}^{-1}$ Congo red. The plates were incubated at 32°C and documented at 24 h.

Motility assays. For population-based motility assays, exponentially growing cultures of *M. xanthus* were harvested (6000 g, room temperature (RT)) and resuspended in 1% CTT to a calculated density of 7×10^9 cells ml^{-1} . 5 μ l aliquots of cell suspensions were spotted on 0.5% and 1.5% agar supplemented with 0.5% CTT and incubated at 32°C. Cells were visualized after 24 h using a M205FA Stereomicroscope (Leica) and imaged using a Hamamatsu ORCA-flash V2 Digital CMOS camera (Hamamatsu Photonics). To quantify the movement of single cells, strains were imaged using a DMI8 Inverted microscope and FC9000 GT camera (Leica). For the visualization of single cells moving by T4P-dependent motility, exponentially growing cultures were diluted to 3×10^8 and 5 μ l cell suspension were placed in a 24-well polystyrene plate (Falcon) and incubated 10 min in the dark at RT. Then, 500 μ l of 1% methylcellulose in MMC buffer (10 mM MOPS, 4 mM MgSO_4 , 2 mM CaCl_2 , pH 7.6) were added and cells incubated for 30 min in the dark at RT. Cells were imaged for 10 min with 20 s intervals. To visualize individual cells moving by gliding motility, 5 μ l of exponentially growing cultures were spotted on 1.5% of agar plates supplemented with TPM buffer and immediately covered by a cover slide and then visualized for 15 min with 30 s intervals at 32°C. Pictures were analyzed using Metamorph® v 7.5 (Molecular Devices) and ImageJ (Schindelin *et al.*, 2012).

Epifluorescence microscopy. For epifluorescence microscopy, exponentially growing cells were placed on a thin TPM (10 mM Tris-HCl pH 8.0, 1 mM K₂HPO₄/KH₂PO₄ pH 7.6, 8 mM MgSO₄) 1.5% agar pad supplemented with 0.2% CTT on a glass slide and immediately covered with a coverslip.

For long time-lapse microscopy, growing cells were visualized overnight following a modified protocol (Schumacher & Søgaaard-Andersen, 2018). Briefly, 5 µl of exponentially growing cultures were spotted on a glass coverslip attached to a metal frame. Cells were covered with a thick pad (1% agar in TPM buffer supplemented with 0.2% casitone) and sealed with parafilm to reduce evaporation. Cells were imaged using a DMI8 inverted microscope and a Hamamatsu ORCA-Flash4.0 V2 Digital CMOS C11440 or a DFC9000 GT (Leica) camera. Data was analyzed using Oufi (Paintdakhi *et al.*, 2016), Metamorph® v 7.5 (Molecular Devices) and ImageJ (Schindelin *et al.*, 2012)

Negative stain transmission electron microscopy. Ten microliters of 5 mM magnesium acetate were placed on one side of the electron microscopy grid (Plano) and incubated for 15 min at room temperature. Liquid was blotted through the grid by capillarity by applying side of the grid on Whatman paper. Ten microliters of *M. xanthus* cells exponentially grown in liquid were placed on the grid and were incubated at 32° for 1 h. To avoid evaporation at this step, the grid was incubated in humid air conditions.

Cells were stained with a freshly prepared 2% uranyl acetate solution supplemented with 30 µg/ml bacitracin. Liquid was blotted and cells were washed once with double distilled H₂O to remove the excess of uranyl acetate. Electron microscopy was done with a CM120 electron microscope (FEI) at 100 kV.

Immunoblot analysis. Immunoblots were carried out as described (Sambrook & Russell, 2001). Rabbit polyclonal α-PilA (dilution: 1:2000), α-PilC (dilution: 1:2000) (Bulyha *et al.*, 2009), α-LonD (dilution: 1:5000) (Magdalena Anna Świątek-Połatyńska), α-FtsZ (dilution: 1:25000) (Treuner-Lange *et al.*, 2013), α-RomR (dilution: 1:5000) (Leonardy *et al.*, 2007) and α-mCherry (dilution: 1:1000) (BioVision), were used together with and horseradish peroxidase-conjugated goat α-rabbit immunoglobulin G (dilution: 1:15000) (Sigma) as secondary antibody respectively.

Mouse α-GFP antibodies (dilution: 1:2000) (Roche) were used together with horseradish peroxidase-conjugated sheep α-mouse immunoglobulin G (dilution: 1:2000) (GE Healthcare) as a secondary antibody. Blots were developed using Luminata crescendo Western HRP Substrate (Millipore) on a LAS-4000 imager (Fujifilm).

c-di-GMP quantifications. c-di-GMP quantifications of *M. xanthus* cells were done as in (Spangler *et al.*, 2010). Briefly, exponentially growing cells were diluted to OD 1×10^8 . Samples were harvested at the indicated time points by centrifugation at 4°C and 2,500 g for 20 min. Cells were mixed with 300 µl extraction buffer (high-pressure liquid chromatography [HPLC]-grade acetonitrile-methanol-water [2:2:1, v:v:v]), and incubated 15 min at 4°C. Extraction was performed at 95°C for 10 min. Samples were harvested at 4°C and 20,800 g for 10 min and supernatant was transferred into a new Eppendorf tube. The pellet was washed with 200 µl extraction buffer and harvested at 4°C and 20,800 g for 10 min. This step was repeated once more. The three supernatants were pooled and evaporated to dryness in a vacuum centrifuge. The pellets were dissolved in HPLC-grade water for analysis by liquid chromatography-coupled tandem mass spectrometry. For all samples, protein concentrations were determined in parallel using a Bradford assay (Bio-Rad).

Protein purification. For expression and purification of DmxA His₆-tagged and its variant proteins, proteins were expressed in *E. coli* Rosetta at 37°C and Ni-NTA purification was used. Cells were harvested, and resuspended in wash buffer (50 mM Tris, 150 mM NaCl, 10% glycerol, 10 mM imidazole, pH 7.5) supplemented with 1 mM dithiothreitol (DTT) and complete protease inhibitor (Roche). Cells were lysed using a French pressure cell and cell debris were removed by centrifugation (20 min, 40,000 × g, 4°C). The lysates were loaded on a 5 ml HiTrap™ Chelating HP column (GE Healthcare) preloaded with NiSO₄ as described by the manufacturer and pre-equilibrated in wash buffer. Following protein immobilization, the column was washed with 10 column volumes of wash buffer. Proteins were eluted with elution buffer A (50 mM Tris, 150 mM NaCl, 10% glycerol, 10-500 mM imidazole, pH 7.5) using a linear imidazole gradient from 10 to 500 mM.

In vitro nucleotide binding assay. c-di-GMP binding was determined using the differential radial capillary action of ligand assay DRaCALA as in (Roelofs *et al.*, 2011, Skotnicka *et al.*, 2015) and BLItz assays (Sultana & Lee, 2015).

For ligand assay DRaCALA, [α -³²P]-labeled c-di-GMP was prepared by incubating 10 µM His₆-DgcA^{WT} (final concentration) with 1 mM GTP/[α -³²P]-GTP (0.1 µCi/µl) in reaction buffer (50 mM Tris-HCl pH 8.0, 300 mM NaCl, 10 mM MgCl₂) in a total volume of 200 µl overnight at 30°C. The reaction mixture was then incubated with 5 units of calf intestine alkaline phosphatase (Fermentas) for 1 hr at 22°C to hydrolyze unreacted GTP. The reaction was stopped by incubation of the sample at 95°C for 10 min. The reaction was centrifuged (10 min, 15000× g, 20°C) and the supernatant was used for the assay. In the DRaCALA assay, reaction mixtures (50 µL) containing

[α - 32 P]-c-di-GMP and 20 μ M protein in binding buffer (10 mM Tris, pH 8.0, 100 mM NaCl, 5 mM MgCl₂) were incubated for 10 min at room temperature. Ten microliters of this reaction mixture was spotted onto a nitrocellulose membrane (GE Healthcare), and allowed to dry before exposing a phosphor-imaging screen using a STORM 840 scanner (Amersham Biosciences).

For the BLI binding measurements, c-di-GMP binding to DmxA was determined by BLI using the BLItz system (ForteBio) equipped with Streptavidin SA biosensor (ForteBio). Briefly, 500 nM biotinylated c-di-GMP in phosphate buffer supplemented with 0.01% (w/v) Tween 20 was immobilized onto the biosensors for 120 s, and unbound molecules were washed off for 30 s. Association and dissociation of the protein was carried out during 200 and 120 s respectively.

DGC activity assay. DGC activity was assessed as in (Skotnicka *et al.*, 2015, Bordeleau *et al.*, 2010). Briefly, 40 μ l of purified proteins (final concentration of 10 μ M) in reaction buffer (50 mM Tris-HCl pH 8.0, 300 mM NaCl, 10 mM MgCl₂) were pre-incubated for 5 min at 30°C. 1 mM GTP/[α - 32 P]-GTP (0.1 μ Ci/ μ l) was added to initiate the DGC reaction and samples were incubated at 30°C for the indicated periods of time.

Reaction products were analyzed by polyethyleneimine-cellulose TLC chromatography as described (Christen *et al.*, 2005). Plates were dried prior to exposing a phosphor-imaging screen (Molecular Dynamics) and documented using a STORM 840 scanner (Amersham Biosciences).

Bioinformatics. UniProt (The-UniProt-Consortium, 2019) and the KEGG databases were used to assign functions to proteins. KEGG SSDB was also used to identify homologs of *M. xanthus* proteins in other Myxococcales using a reciprocal best BlastP hit method. SMART (smart.embl-heidelberg.de) (Letunic *et al.*, 2015) was used to identify protein domains. Membrane topology was assessed by TMHMM v2.0 (Sonnhammer *et al.*, 1998).

The phylogenetic tree was prepared in MEGA7 (Kumar *et al.*, 2016) using the Neighbor-Joining method (Saitou & Nei, 1987). Bootstrap values (500 replicates) are shown next to the branches (Felsenstein, 1985).

4. Discussion of the study

The main objective of this study was to identify proteins involved in the synthesis of surface polysaccharides to study the function of LPS, spore coat polysaccharide and EPS in *M. xanthus*. Through bioinformatics, genetics, heterologous expression and biochemical experiments, we have identified and characterized key enzymes for biosynthesis of the three polysaccharides in *M. xanthus*. We have shown the existence of dedicated biosynthesis machineries and have proposed updated models for the three biosynthetic pathways. Having now discovered mutants affected at different steps of the EPS, LPS and spore coat polysaccharide biosynthesis, we have laid down the foundations to analyze in depth the synthesis, composition and structure of each of them.

Using selected mutants exclusively blocked in the synthesis of a specific polysaccharide, we have reevaluated the role of LPS, spore coat polysaccharide and EPS in *M. xanthus*. We have shown that intact LPS is important for development and gliding motility, but conditionally important for T4P-dependent motility. Spore coat polysaccharide is essential for the formation of starvation- and chemically-induced resistant spores, but not for aggregation into fruiting bodies in response to nutrient limitation. The function of EPS has been investigated in numerous studies. However, most of them had been performed using strains containing mutations in EPS regulatory genes rather than in the biosynthetic ones. Using Δeps mutants exclusively blocked in EPS synthesis, we have confirmed that EPS is important for cell cohesion, T4P-assembly and T4P-dependent motility and conditionally important for development. Additionally, despite different myxobacteria belonging to the three suborders form fruiting bodies and sporulate, the EPS, Exo and Nfs machineries are not conserved, supporting the notion that sporulation could occur by a different mechanism in sporulating Cystobacterineae compared to sporulating Nannocystineae and Sorangineae.

Moreover, because it had been suggested that c-di-GMP and the DGC DmxA regulated motility during growth via changes in the EPS synthesis, we sought to find the connection between c-di-GMP and EPS biosynthesis during growth. Although we showed that the level of EPS of the $\Delta dmxA$ cells is slightly increased, we suggest that DmxA does not directly regulate EPS, and that the EPS and motility defects may instead result from polarity defects. We have shown that there is a tight correlation between EPS synthesis and T4P assembly, pointing out that EPS synthesis and regulation of T4P-dependent motility are more complex than initially thought. It is possible that this may also depend on the regulation of polarity.

5. References

- Amikam, D., and Galperin, M.Y. (2006) PilZ domain is part of the bacterial c-di-GMP binding protein. *Bioinformatics* **22**: 3-6.
- Andrews, S.C., Robinson, A.K., and Rodríguez-Quiriones, F. (2003) Bacterial iron homeostasis. *FEMS Microbiol Rev* **27**: 215-237.
- Arnold, J.W., and Shimkets, L.J. (1988a) Cell surface properties correlated with cohesion in *Myxococcus xanthus*. *J Bacteriol* **170**: 5771-5777.
- Arnold, J.W., and Shimkets, L.J. (1988b) Inhibition of cell-cell interactions in *Myxococcus xanthus* by congo red. *J Bacteriol* **170**: 5765-5770.
- Beczala, A., Ovchinnikova, O.G., Datta, N., Mattinen, L., Knapska, K., Radziejewska-Lebrecht, J., Holst, O., and Skurnik, M. (2015) Structure and genetic basis of *Yersinia similis* serotype O:9 O-specific polysaccharide. *Innate Immun* **21**: 3-16.
- Behmlander, R.M., and Dworkin, M. (1991) Extracellular fibrils and contact-mediated cell interactions in *Myxococcus xanthus*. *J Bacteriol* **173**: 7810-7820.
- Behmlander, R.M., and Dworkin, M. (1994) Biochemical and structural analyses of the extracellular matrix fibrils of *Myxococcus xanthus*. *J Bacteriol* **176**: 6295-6303.
- Bellenger, K., Ma, X., Shi, W., and Yang, Z. (2002) A CheW homologue is required for *Myxococcus xanthus* fruiting body development, social gliding motility, and fibril biogenesis. *J Bacteriol* **184**: 5654-5660.
- Bennett, J.A., Aimino, R.M., and McCormick, J.R. (2007) *Streptomyces coelicolor* genes *ftsL* and *divIC* play a role in cell division but are dispensable for colony formation. *J Bacteriol* **189**: 8982-8992.
- Berleman, J.E., Vicente, J.J., Davis, A.E., Jiang, S.Y., Seo, Y.E., and Zusman, D.R. (2011) FrzS regulates social motility in *Myxococcus xanthus* by controlling exopolysaccharide production. *PLoS ONE* **6**: e23920.
- Berleman, J.E., Zemla, M., Remis, J.P., Liu, H., Davis, A.E., Worth, A.N., West, Z., Zhang, A., Park, H., Bosneaga, E., van Leer, B., Tsai, W., Zusman, D.R., and Auer, M. (2016) Exopolysaccharide microchannels direct bacterial motility and organize multicellular behavior. *ISME J* **10**: 2620-2632.
- Bischof, L.F., Friedrich, C., Harms, A., Søgaard-Andersen, L., and van der Does, C. (2016) The type IV pilus assembly ATPase PilB of *Myxococcus xanthus* interacts with the inner membrane platform protein PilC and the nucleotide-binding protein PilM. *J Biol Chem* **291**: 6946-6957.
- Black, W.P., Schubot, F.D., Li, Z., and Yang, Z. (2010) Phosphorylation and dephosphorylation among Dif chemosensory proteins essential for exopolysaccharide regulation in *Myxococcus xanthus*. *J Bacteriol* **192**: 4267-4274.
- Black, W.P., Wang, L., Davis, M.Y., and Yang, Z. (2015) The orphan response regulator EpsW is a substrate of the DifE kinase and it regulates exopolysaccharide in *Myxococcus xanthus*. *Sci Rep* **5**: 17831.
- Black, W.P., Wang, L.L., Jing, X., Saldana, R.C., Li, F., Scharf, B.E., Schubot, F.D., and Yang, Z.M. (2017) The type IV pilus assembly ATPase PilB functions as a signaling protein to regulate exopolysaccharide production in *Myxococcus xanthus*. *Sci Rep* **7**.
- Black, W.P., Xu, Q., Cadieux, C.L., Suh, S.J., Shi, W., and Yang, Z. (2009) Isolation and characterization of a suppressor mutation that restores *Myxococcus xanthus* exopolysaccharide production. *Microbiology* **155**: 3599-3610.
- Black, W.P., Xu, Q., and Yang, Z. (2006) Type IV pili function upstream of the Dif chemotaxis pathway in *Myxococcus xanthus* EPS regulation. *Mol Microbiol* **61**: 447-456.

- Black, W.P., and Yang, Z.M. (2004) *Myxococcus xanthus* chemotaxis homologs DifD and DifG negatively regulate fibril polysaccharide production. *J Bacteriol* **186**: 1001-1008.
- Bonner, P.J., Xu, Q., Black, W.P., Li, Z., Yang, Z., and Shimkets, L.J. (2005) The Dif chemosensory pathway is directly involved in phosphatidylethanolamine sensory transduction in *Myxococcus xanthus*. *Mol Microbiol* **57**: 1499-1508.
- Bontemps-Gallo, S., Cogez, V., Robbe-Masselot, C., Quintard, K., Dondeyne, J., Madec, E., and Lacroix, J.M. (2013) Biosynthesis of osmoregulated periplasmic glucans in *Escherichia coli*: the phosphoethanolamine transferase is encoded by *opgE*. *Biomed Res Int* **2013**: 371429.
- Bordeleau, E., Brouillette, E., Robichaud, N., and Burrus, V. (2010) Beyond antibiotic resistance: integrating conjugative elements of the SXT/R391 family that encode novel diguanylate cyclases participate to c-di-GMP signalling in *Vibrio cholerae*. *Environ Microbiol* **12**: 510-523.
- Bowden, M.G., and Kaplan, H.B. (1998) The *Myxococcus xanthus* lipopolysaccharide O-antigen is required for social motility and multicellular development. *Mol Microbiol* **30**: 275-284.
- Bretl, D.J., and Kirby, J.R. (2016) Molecular mechanisms of signaling in *Myxococcus xanthus* development. *J Mol Biol* **428**: 3805-3830.
- Bretl, D.J., Müller, S., Ladd, K.M., Atkinson, S.N., and Kirby, J.R. (2016) Type IV-pili dependent motility is co-regulated by PilSR and PilS2R2 two-component systems via distinct pathways in *Myxococcus xanthus*. *Mol Microbiol* **102**: 37-53.
- Buddelmeijer, N., Judson, N., Boyd, D., Mekalanos, J.J., and Beckwith, J. (2002) YgbQ, a cell division protein in *Escherichia coli* and *Vibrio cholerae*, localizes in codependent fashion with FtsL to the division site. *Proc Natl Acad Sci U S A* **99**: 6316-6321.
- Bui, N.K., Gray, J., Schwarz, H., Schumann, P., Blanot, D., and Vollmer, W. (2009) The peptidoglycan sacculus of *Myxococcus xanthus* has unusual structural features and is degraded during glycerol-induced myxospore development. *J Bacteriol* **191**: 494-505.
- Bulyha, I., Schmidt, C., Lenz, P., Jakovljevic, V., Hone, A., Maier, B., Hoppert, M., and Søggaard-Andersen, L. (2009) Regulation of the type IV pili molecular machine by dynamic localization of two motor proteins. *Mol Microbiol* **74**: 691-706.
- Burchard, R.P. (1974) Growth of surface colonies of the gliding bacterium *Myxococcus xanthus*. *Arch Microbiol* **96**: 247-254.
- Burchard, R.P. (1975) Myxospore induction in a nondispersed growing mutant of *Myxococcus xanthus*. *J Bacteriol* **122**: 302-306.
- Burrows, L.L., and Lam, J.S. (1999) Effect of *wzx* (*rfbX*) mutations on A-band and B-band lipopolysaccharide biosynthesis in *Pseudomonas aeruginosa* O5. *J Bacteriol* **181**: 973-980.
- Chang, B.Y., and Dworkin, M. (1994) Isolated fibrils rescue cohesion and development in the Dsp mutant of *Myxococcus xanthus*. *J Bacteriol* **176**: 7190-7196.
- Chang, Y.W., Rettberg, L.A., Treuner-Lange, A., Iwasa, J., Søggaard-Andersen, L., and Jensen, G.J. (2016) Architecture of the type IVa pilus machine. *Science* **351**: aad2001.
- Choi, Y., Kim, J., Yoon, H.J., Jin, K.S., Ryu, S., and Lee, H.H. (2018) Structural insights into the FtsQ/FtsB/FtsL complex, a key component of the divisome. *Sci Rep* **8**: 18061.
- Chojnacki, S., Cowley, A., Lee, J., Foix, A., and Lopez, R. (2017) Programmatic access to bioinformatics tools from EMBL-EBI update: 2017. *Nucleic Acids Res* **45**: W550-W553.
- Christen, M., Christen, B., Folcher, M., Schauerte, A., and Jenal, U. (2005) Identification and characterization of a cyclic di-GMP-specific phosphodiesterase and its allosteric control by GTP. *J Biol Chem* **280**: 30829-30837.
- Clarke, B.R., Cuthbertson, L., and Whitfield, C. (2004) Nonreducing terminal modifications determine the chain length of polymannose O antigens of *Escherichia coli* and couple chain termination to polymer export via an ATP-binding cassette transporter. *J Biol Chem* **279**: 35709-35718.

- Cohen, D., Mechold, U., Nevenzal, H., Yarmiyhu, Y., Randall, T.E., Bay, D.C., Rich, J.D., Parsek, M.R., Kaefer, V., Harrison, J.J., and Banin, E. (2015) Oligoribonuclease is a central feature of cyclic diguanylate signaling in *Pseudomonas aeruginosa*. *Proc Natl Acad Sci U S A* **112**: 11359-11364.
- Curtis, P.D., Atwood, J., 3rd, Orlando, R., and Shimkets, L.J. (2007) Proteins associated with the *Myxococcus xanthus* extracellular matrix. *J Bacteriol* **189**: 7634-7642.
- Cuthbertson, L., Kimber, M.S., and Whitfield, C. (2007) Substrate binding by a bacterial ABC transporter involved in polysaccharide export. *Proc Natl Acad Sci U S A* **104**: 19529-19534.
- Cuthbertson, L., Kos, V., and Whitfield, C. (2010) ABC transporters involved in export of cell surface glycoconjugates. *Microbiol Mol Biol Rev* **74**: 341-362.
- Cuthbertson, L., Powers, J., and Whitfield, C. (2005) The C-terminal domain of the nucleotide-binding domain protein Wzt determines substrate specificity in the ATP-binding cassette transporter for the lipopolysaccharide O-antigens in *Escherichia coli* serotypes O8 and O9a. *J Biol Chem* **280**: 30310-30319.
- Dana, J.R., and Shimkets, L.J. (1993) Regulation of cohesion-dependent cell interactions in *Myxococcus xanthus*. *J Bacteriol* **175**: 3636-3647.
- Dower, W.J., Miller, J.F., and Ragsdale, C.W. (1988) High efficiency transformation of *E. coli* by high voltage electroporation. *Nucleic Acids Res* **16**: 6127-6145.
- Downard, J., Ramaswamy, S.V., and Kil, K.S. (1993) Identification of *esg*, a genetic locus involved in cell-cell signaling during *Myxococcus xanthus* development. *J Bacteriol* **175**: 7762-7770.
- Du, S., and Lutkenhaus, J. (2017) Assembly and activation of the *Escherichia coli* divisome. *Mol Microbiol* **105**: 177-187.
- Ducret, A., Fleuchot, B., Bergam, P., and Mignot, T. (2013) Direct live imaging of cell-cell protein transfer by transient outer membrane fusion in *Myxococcus xanthus*. *elife* **2**: e00868.
- Ducret, A., Valignat, M.P., Mouhamar, F., Mignot, T., and Theodoly, O. (2012) Wet-surface-enhanced ellipsometric contrast microscopy identifies slime as a major adhesion factor during bacterial surface motility. *Proc Natl Acad Sci U S A* **109**: 10036-10041.
- Dworkin, M., and Gibson, S.M. (1964) A system for studying microbial morphogenesis: rapid formation of microcysts in *Myxococcus xanthus*. *Science* **146**: 243-244.
- Dworkin, M., and Voelz, H. (1962) The formation and germination of microcysts in *Myxococcus xanthus*. *J Gen Microbiol* **28**: 81-85.
- Faure, L.M., Fiche, J.-B., Espinosa, L., Ducret, A., Anantharaman, V., Luciano, J., Lhospice, S., Islam, S.T., Tréguier, J., Sotes, M., Kuru, E., Van Nieuwenhze, M.S., Brun, Y.V., Théodoly, O., Aravind, L., Nollmann, M., and Mignot, T. (2016) The mechanism of force transmission at bacterial focal adhesion complexes. *Nature* **539**: 530-535.
- Felsenstein, J. (1985) Confidence-limits on phylogenies - an approach using the bootstrap. *Evolution* **39**: 783-791.
- Fink, J.M., and Zissler, J.F. (1989a) Characterization of lipopolysaccharide from *Myxococcus xanthus* by use of monoclonal antibodies. *J Bacteriol* **171**: 2028-2032.
- Fink, J.M., and Zissler, J.F. (1989b) Defects in motility and development of *Myxococcus xanthus* lipopolysaccharide mutants. *J Bacteriol* **171**: 2042-2048.
- Finn, R.D., Coghill, P., Eberhardt, R.Y., Eddy, S.R., Mistry, J., Mitchell, A.L., Potter, S.C., Punta, M., Qureshi, M., Sangrador-Vegas, A., Salazar, G.A., Tate, J., and Bateman, A. (2016) The Pfam protein families database: towards a more sustainable future. *Nucleic Acids Res* **44**: D279-285.
- Flemming, H.C., Neu, T.R., and Wozniak, D.J. (2007) The EPS matrix: the "house of biofilm cells". *J Bacteriol* **189**: 7945-7947.
- Flemming, H.C., and Wingender, J. (2010) The biofilm matrix. *Nat Rev Microbiol* **8**: 623-633.

- Flemming, H.C., Wingender, J., Szewzyk, U., Steinberg, P., Rice, S.A., and Kjelleberg, S. (2016) Biofilms: an emergent form of bacterial life. *Nat Rev Microbiol* **14**: 563-575.
- Fluegel, W. (1963) Simple method for demonstrating myxobacterial slime. *J Bacteriol* **85**: 1173-1174.
- Franklin, M.J., Nivens, D.E., Weadge, J.T., and Howell, P.L. (2011) Biosynthesis of the *Pseudomonas aeruginosa* extracellular polysaccharides, alginate, Pel, and Psl. *Front Microbiol* **2**: 167.
- Friedrich, C., Bulyha, I., and Søgaard-Andersen, L. (2014) Outside-in assembly pathway of the type IV pilus system in *Myxococcus xanthus*. *J Bacteriol* **196**: 378-390.
- Furlong, S.E., Ford, A., Albarnez-Rodriguez, L., and Valvano, M.A. (2015) Topological analysis of the *Escherichia coli* WcaJ protein reveals a new conserved configuration for the polyisoprenyl-phosphate hexose-1-phosphate transferase family. *Sci Rep* **5**: 9178.
- Gibiansky, M.L., Hu, W., Dahmen, K.A., Shi, W., and Wong, G.C. (2013) Earthquake-like dynamics in *Myxococcus xanthus* social motility. *Proc Natl Acad Sci U S A* **110**: 2330-2335.
- Gloag, E.S., Turnbull, L., Javed, M.A., Wang, H., Gee, M.L., Wade, S.A., and Whitchurch, C.B. (2016) Stigmergy co-ordinates multicellular collective behaviours during *Myxococcus xanthus* surface migration. *Sci Rep* **6**: 26005.
- Goley, E.D., Yeh, Y.C., Hong, S.H., Fero, M.J., Abeliuk, E., McAdams, H.H., and Shapiro, L. (2011) Assembly of the *Caulobacter* cell division machine. *Mol Microbiol* **80**: 1680-1698.
- Gonzalez, M.D., and Beckwith, J. (2009) Divisome under construction: distinct domains of the small membrane protein FtsB are necessary for interaction with multiple cell division proteins. *J Bacteriol* **191**: 2815-2825.
- Greenfield, L.K., and Whitfield, C. (2012) Synthesis of lipopolysaccharide O-antigens by ABC transporter-dependent pathways. *Carbohydr Res* **356**: 12-24.
- Guo, D., Bowden, M.G., Pershad, R., and Kaplan, H.B. (1996) The *Myxococcus xanthus* *rfbABC* operon encodes an ATP-binding cassette transporter homolog required for O-antigen biosynthesis and multicellular development. *J Bacteriol* **178**: 1631-1639.
- Guzzo, C.R., Salinas, R.K., Andrade, M.O., and Farah, C.S. (2009) PilZ protein structure and interactions with PilB and the FimX EAL domain: implications for control of type IV pilus biogenesis. *J Mol Biol* **393**: 848-866.
- Harris, B.Z., Kaiser, D., and Singer, M. (1998) The guanosine nucleotide (p)ppGpp initiates development and A-factor production in *Myxococcus xanthus*. *Genes Dev* **12**: 1022-1035.
- He, K., and Bauer, C.E. (2014) Chemosensory signaling systems that control bacterial survival. *Trends Microbiol* **22**: 389-398.
- Hendrick, W.A., Orr, M.W., Murray, S.R., Lee, V.T., and Melville, S.B. (2017) Cyclic di-GMP binding by an assembly ATPase (PilB2) and control of type IV pilin polymerization in the Gram-positive pathogen *Clostridium perfringens*. *J Bacteriol* **199**.
- Hengge, R. (2009) Principles of c-di-GMP signalling in bacteria. *Nat Rev Microbiol* **7**: 263-273.
- Hillesland, K.L., and Velicer, G.J. (2005) Resource level affects relative performance of the two motility systems of *Myxococcus xanthus*. *Microb Ecol* **49**: 558-566.
- Ho, Y.S., Burden, L.M., and Hurley, J.H. (2000) Structure of the GAF domain, a ubiquitous signaling motif and a new class of cyclic GMP receptor. *EMBO J* **19**: 5288-5299.
- Hobley, L., Fung, R.K., Lambert, C., Harris, M.A., Dabhi, J.M., King, S.S., Basford, S.M., Uchida, K., Till, R., Ahmad, R., Aizawa, S., Gomelsky, M., and Sockett, R.E. (2012) Discrete cyclic di-GMP-dependent control of bacterial predation versus axenic growth in *Bdellovibrio bacteriovorus*. *PLoS Pathog* **8**: e1002493.
- Hodgkin, J., and Kaiser, D. (1977) Cell-to-cell stimulation of movement in nonmotile mutants of *Myxococcus*. *Proc Natl Acad Sci U S A* **74**: 2938-2942.
- Hodgkin, J., and Kaiser, D. (1979) Genetics of gliding motility in *Myxococcus xanthus* (Myxobacterales) - Two gene systems control movement. *Mol Gen Genet* **171**: 177-191.

- Holkenbrink, C., Hoiczky, E., Kahnt, J., and Higgs, P.I. (2014) Synthesis and assembly of a novel glycan layer in *Myxococcus xanthus* spores. *J Biol Chem* **289**: 32364-32378.
- Hu, W., Gibiansky, M.L., Wang, J., Wang, C., Lux, R., Li, Y., Wong, G.C., and Shi, W. (2016) Interplay between type IV pili activity and exopolysaccharides secretion controls motility patterns in single cells of *Myxococcus xanthus*. *Sci Rep* **6**: 17790.
- Hu, W., Hossain, M., Lux, R., Wang, J., Yang, Z., Li, Y., and Shi, W. (2011) Exopolysaccharide-independent social motility of *Myxococcus xanthus*. *PLoS ONE* **6**: e16102.
- Hu, W., Li, L., Sharma, S., Wang, J., McHardy, I., Lux, R., Yang, Z., He, X., Gimzewski, J.K., Li, Y., and Shi, W. (2012a) DNA builds and strengthens the extracellular matrix in *Myxococcus xanthus* biofilms by interacting with exopolysaccharides. *PLoS ONE* **7**: e51905.
- Hu, W., Lux, R., and Shi, W. (2013) Analysis of exopolysaccharides in *Myxococcus xanthus* using confocal laser scanning microscopy. *Methods Mol Biol* **966**: 121-131.
- Hu, W., Wang, J., McHardy, I., Lux, R., Yang, Z., Li, Y., and Shi, W. (2012b) Effects of exopolysaccharide production on liquid vegetative growth, stress survival, and stationary phase recovery in *Myxococcus xanthus*. *J Microbiol* **50**: 241-248.
- Hu, W., Yang, Z., Lux, R., Zhao, M., Wang, J., He, X., and Shi, W. (2012c) Direct visualization of the interaction between pilin and exopolysaccharides of *Myxococcus xanthus* with eGFP-fused PilA protein. *FEMS Microbiol Lett* **326**: 23-30.
- Hug, I., and Feldman, M.F. (2011) Analogies and homologies in lipopolysaccharide and glycoprotein biosynthesis in bacteria. *Glycobiology* **21**: 138-151.
- Hvorup, R.N., Winnen, B., Chang, A.B., Jiang, Y., Zhou, X.F., and Saier, M.H., Jr. (2003) The multidrug/oligosaccharidyl-lipid/polysaccharide (MOP) exporter superfamily. *Eur J Biochem* **270**: 799-813.
- Inouye, M., Inouye, S., and Zusman, D.R. (1979a) Biosynthesis and self-assembly of protein S, a development specific protein of *Myxococcus xanthus*. *Proc Natl Acad Sci U S A* **76**: 209-213.
- Inouye, M., Inouye, S., and Zusman, D.R. (1979b) Gene expression during development of *Myxococcus xanthus*: pattern of protein synthesis. *Dev Biol* **68**: 579-591.
- Islam, S.T., and Lam, J.S. (2014) Synthesis of bacterial polysaccharides via the Wzx/Wzy-dependent pathway. *Can J Microbiol* **60**: 697-716.
- Jain, R., Behrens, A.J., Kaever, V., and Kazmierczak, B.I. (2012) Type IV pilus assembly in *Pseudomonas aeruginosa* over a broad range of cyclic di-GMP concentrations. *J Bacteriol* **194**: 4285-4294.
- Jain, R., Sliusarenko, O., and Kazmierczak, B.I. (2017) Interaction of the cyclic-di-GMP binding protein FimX and the Type 4 pilus assembly ATPase promotes pilus assembly. *PLoS Pathog* **13**: e1006594.
- Jakobczak, B., Keilberg, D., Wuichet, K., and Søgaard-Andersen, L. (2015) Contact- and protein transfer-dependent stimulation of assembly of the gliding motility machinery in *Myxococcus xanthus*. *PLoS Genet* **11**: e1005341.
- Jakovljevic, V., Leonardy, S., Hoppert, M., and Søgaard-Andersen, L. (2008) PilB and PilT are ATPases acting antagonistically in type IV pilus function in *Myxococcus xanthus*. *J Bacteriol* **190**: 2411-2421.
- Jenal, U., Reinders, A., and Lori, C. (2017) Cyclic di-GMP: second messenger extraordinaire. *Nat Rev Microbiol* **15**: 271-284.
- Johns, S.J., TOPO2, Transmembrane protein display software (<http://www.sacs.ucsf.edu/TOPO2/>). In., pp.
- Jorgenson, M.A., Kannan, S., Laubacher, M.E., and Young, K.D. (2016) Dead-end intermediates in the enterobacterial common antigen pathway induce morphological defects in *Escherichia coli* by competing for undecaprenyl phosphate. *Mol Microbiol* **100**: 1-14.

- Jorgenson, M.A., and Young, K.D. (2016) Interrupting biosynthesis of O antigen or the lipopolysaccharide core produces morphological defects in *Escherichia coli* by sequestering undecaprenyl phosphate. *J Bacteriol* **198**: 3070-3079.
- Julien, B., Kaiser, A.D., and Garza, A. (2000) Spatial control of cell differentiation in *Myxococcus xanthus*. *Proc Natl Acad Sci U S A* **97**: 9098-9103.
- Kahnt, J., Aguiluz, K., Koch, J., Treuner-Lange, A., Konovalova, A., Huntley, S., Hoppert, M., Søgaard-Andersen, L., and Hedderich, R. (2010) Profiling the outer membrane proteome during growth and development of the social bacterium *Myxococcus xanthus* by selective biotinylation and analyses of outer membrane vesicles. *J Proteome Res* **9**: 5197-5208.
- Kaiser, D. (1979) Social gliding is correlated with the presence of pili in *Myxococcus xanthus*. *Proc Natl Acad Sci U S A* **76**: 5952-5956.
- Kaiser, D., and Crosby, C. (1983) Cell movement and its coordination in swarms of *Myxococcus xanthus*. *Cell Motility* **3**: 227-245.
- Kalynych, S., Morona, R., and Cygler, M. (2014) Progress in understanding the assembly process of bacterial O-antigen. *FEMS Microbiol Rev* **38**: 1048-1065.
- Kanehisa, M., and Goto, S. (2000) KEGG: kyoto encyclopedia of genes and genomes. *Nucleic Acids Res* **28**: 27-30.
- Kaplan, H.B., Kuspa, A., and Kaiser, D. (1991) Suppressors that permit A-signal-independent developmental gene expression in *Myxococcus xanthus*. *J Bacteriol* **173**: 1460-1470.
- Katis, V.L., Harry, E.J., and Wake, R.G. (1997) The *Bacillus subtilis* division protein DivIC is a highly abundant membrane-bound protein that localizes to the division site. *Mol Microbiol* **26**: 1047-1055.
- Kato, T., Shirakawa, Y., Takegawa, K., and Kimura, Y. (2015) Functional analysis of conserved motifs in a bacterial tyrosine kinase, BtkB, from *Myxococcus xanthus*. *J Biochem* **158**: 385-392.
- Kazmierczak, B.I., Lebron, M.B., and Murray, T.S. (2006) Analysis of FimX, a phosphodiesterase that governs twitching motility in *Pseudomonas aeruginosa*. *Mol Microbiol* **60**: 1026-1043.
- Kearns, D.B., Campbell, B.D., and Shimkets, L.J. (2000) *Myxococcus xanthus* fibril appendages are essential for excitation by a phospholipid attractant. *Proc Natl Acad Sci U S A* **97**: 11505-11510.
- Keenleyside, W.J., and Whitfield, C. (1996) A novel pathway for O-polysaccharide biosynthesis in *Salmonella enterica* serovar Borreze. *J Biol Chem* **271**: 28581-28592.
- Kim, S.H., Ramaswamy, S., and Downard, J. (1999) Regulated exopolysaccharide production in *Myxococcus xanthus*. *J Bacteriol* **181**: 1496-1507.
- Kimura, Y., Ishida, S., Matoba, H., and Okahisa, N. (2004) RppA, a transducer homologue, and MmrA, a multidrug transporter homologue, are involved in the biogenesis and/or assembly of polysaccharide in *Myxococcus xanthus*. *Microbiology* **150**: 631-639.
- Kimura, Y., Kato, T., and Mori, Y. (2012) Function analysis of a bacterial tyrosine kinase, BtkB, in *Myxococcus xanthus*. *FEMS Microbiol Lett* **336**: 45-51.
- Kimura, Y., Yamashita, S., Mori, Y., Kitajima, Y., and Takegawa, K. (2011) A *Myxococcus xanthus* bacterial tyrosine kinase, BtkA, is required for the formation of mature spores. *J Bacteriol* **193**: 5853-5857.
- Knirel, Y.A., and Valvano, M.A., (2013) Bacterial polysaccharide structure and biosynthesis. In: Encyclopedia of Biophysics. G.C.K. Roberts (ed). Springer, pp. 162.
- Komano, T., Furuichi, T., Teintze, M., Inouye, M., and Inouye, S. (1984) Effects of deletion of the gene for the development-specific protein S on differentiation in *Myxococcus xanthus*. *J Bacteriol* **158**: 1195-1197.
- Konovalova, A., Lobach, S., and Søgaard-Andersen, L. (2012) A RelA-dependent two-tiered regulated proteolysis cascade controls synthesis of a contact-dependent intercellular signal in *Myxococcus xanthus*. *Mol Microbiol* **84**: 260-275.

- Konovalova, A., Petters, T., and Søgaard-Andersen, L. (2010) Extracellular biology of *Myxococcus xanthus*. *FEMS Microbiol Revs* **34**: 89-106.
- Koontz, L. (2014) TCA precipitation. *Methods Enzymol* **541**: 3-10.
- Kottel, R.H., Bacon, K., Clutter, D., and White, D. (1975) Coats from *Myxococcus xanthus*: characterization and synthesis during myxospore differentiation. *J Bacteriol* **124**: 550-557.
- Kroos, L. (2017) Highly signal-responsive gene regulatory network governing *Myxococcus* development. *Trends Genet* **33**: 3-15.
- Kumar, S., Stecher, G., and Tamura, K. (2016) MEGA7: Molecular Evolutionary Genetics Analysis Version 7.0 for Bigger Datasets. *Mol Biol Evol* **33**: 1870-1874.
- Kureisaite-Ciziene, D., Varadajan, A., McLaughlin, S.H., Glas, M., Monton Silva, A., Luirink, R., Mueller, C., den Blaauwen, T., Grossmann, T.N., Luirink, J., and Lowe, J. (2018) Structural analysis of the interaction between the bacterial cell division proteins FtsQ and FtsB. *mBio* **9**.
- Kuspa, A., and Kaiser, D. (1989) Genes required for developmental signalling in *Myxococcus xanthus*: three *asg* loci. *J Bacteriol* **171**: 2762-2772.
- Lancero, H., Brofft, J.E., Downard, J., Birren, B.W., Nusbaum, C., Naylor, J., Shi, W., and Shimkets, L.J. (2002) Mapping of *Myxococcus xanthus* social motility *dsp* mutations to the *dif* genes. *J Bacteriol* **184**: 1462-1465.
- Lancero, H., Caberoy, N.B., Castaneda, S., Li, Y.N., Lu, A., Dutton, D., Duan, X.Y., Kaplan, H.B., Shi, W.Y., and Garza, A.G. (2004) Characterization of a *Myxococcus xanthus* mutant that is defective for adventurous motility and social motility. *Microbiology-Sgm* **150**: 4085-4093.
- Lancero, H.L., Castaneda, S., Caberoy, N.B., Ma, X., Garza, A.G., and Shi, W. (2005) Analysing protein-protein interactions of the *Myxococcus xanthus* Dif signalling pathway using the yeast two-hybrid system. *Microbiology* **151**: 1535-1541.
- LaPointe, L.M., Taylor, K.C., Subramaniam, S., Khadria, A., Rayment, I., and Senes, A. (2013) Structural organization of FtsB, a transmembrane protein of the bacterial divisome. *Biochemistry* **52**: 2574-2585.
- Le Gouellec, A., Roux, L., Fadda, D., Massidda, O., Vernet, T., and Zapun, A. (2008) Roles of pneumococcal DivIB in cell division. *J Bacteriol* **190**: 4501-4511.
- Lee, B., Mann, P., Grover, V., Treuner-Lange, A., Kahnt, J., and Higgs, P.I. (2011) The *Myxococcus xanthus* spore cuticula Protein C is a fragment of FibA, an extracellular metalloprotease produced exclusively in aggregated cells. *PLoS ONE* **6**.
- Lehrman, M.A. (1994) A family of UDP-GlcNAc/MurNAc: polyisoprenol-P GlcNAc/MurNAc-1-P transferases. *Glycobiology* **4**: 768-771.
- Leighton, T.L., Buensuceso, R.N., Howell, P.L., and Burrows, L.L. (2015) Biogenesis of *Pseudomonas aeruginosa* type IV pili and regulation of their function. *Environ Microbiol* **17**: 4148-4163.
- Leng, X., Zhu, W., Jin, J., and Mao, X. (2011) Evidence that a chaperone-usher-like pathway of *Myxococcus xanthus* functions in spore coat formation. *Microbiology* **157**: 1886-1896.
- Leonardy, S., Freymark, G., Hebener, S., Ellehauge, E., and Søgaard-Andersen, L. (2007) Coupling of protein localization and cell movements by a dynamically localized response regulator in *Myxococcus xanthus*. *EMBO J* **26**: 4433-4444.
- Leonardy, S., Miertzschke, M., Bulyha, I., Sperling, E., Wittinghofer, A., and Søgaard-Andersen, L. (2010) Regulation of dynamic polarity switching in bacteria by a Ras-like G-protein and its cognate GAP. *EMBO J* **29**: 2276-2289.
- Letunic, I., Doerks, T., and Bork, P. (2015) SMART: recent updates, new developments and status in 2015. *Nucleic Acids Res.* **43**: D257-260.
- Levin, P.A., and Losick, R. (1994) Characterization of a cell division gene from *Bacillus subtilis* that is required for vegetative and sporulation septum formation. *J Bacteriol* **176**: 1451-1459.

- Li, Y., Sun, H., Ma, X., Lu, A., Lux, R., Zusman, D., and Shi, W. (2003) Extracellular polysaccharides mediate pilus retraction during social motility of *Myxococcus xanthus*. *Proc Natl Acad Sci U S A* **100**: 5443-5448.
- Liang, Z.X. (2015) The expanding roles of c-di-GMP in the biosynthesis of exopolysaccharides and secondary metabolites. *Nat Prod Rep* **32**: 663-683.
- Licking, E., Gorski, L., and Kaiser, D. (2000) A common step for changing cell shape in fruiting body and starvation-independent sporulation in *Myxococcus xanthus*. *J Bacteriol* **182**: 3553-3558.
- Lombard, V., Ramulu, H.G., Drula, E., Coutinho, P.M., and Henrissat, B. (2014) The carbohydrate-active enzymes database (CAZy) in 2013. *Nucleic Acids Res* **42**: D490-D495.
- Lu, A., Cho, K., Black, W.P., Duan, X.Y., Lux, R., Yang, Z., Kaplan, H.B., Zusman, D.R., and Shi, W. (2005) Exopolysaccharide biosynthesis genes required for social motility in *Myxococcus xanthus*. *Mol Microbiol* **55**: 206-220.
- Luciano, J., Agrebi, R., Le Gall, A.V., Wartel, M., Fiegna, F., Ducret, A., Brochier-Armanet, C., and Mignot, T. (2011) Emergence and modular evolution of a novel motility machinery in bacteria. *PLoS Genet* **7**: e1002268.
- Lukose, V., Walvoort, M.T., and Imperiali, B. (2017) Bacterial phosphoglycosyl transferases: initiators of glycan biosynthesis at the membrane interface. *Glycobiology* **27**: 820-833.
- Luo, Y., Zhao, K., Baker, A.E., Kuchma, S.L., Coggan, K.A., Wolfgang, M.C., Wong, G.C., and O'Toole, G.A. (2015) A hierarchical cascade of second messengers regulates *Pseudomonas aeruginosa* surface behaviors. *mBio* **6**.
- Lux, R., Li, Y., Lu, A., and Shi, W. (2004) Detailed three-dimensional analysis of structural features of *Myxococcus xanthus* fruiting bodies using confocal laser scanning microscopy. *Biofilms* **1**.
- Maclean, L., Perry, M.B., Nossova, L., Kaplan, H., and Vinogradov, E. (2007) The structure of the carbohydrate backbone of the LPS from *Myxococcus xanthus* strain DK1622. *Carbohydr Res* **342**: 2474-2480.
- Manoil, C., and Kaiser, D. (1980) Guanosine pentaphosphate and guanosine tetraphosphate accumulation and induction of *Myxococcus xanthus* fruiting body development. *J Bacteriol* **141**: 305-315.
- Marczak, M., Dzwierzynska, M., and Skorupska, A. (2013) Homo- and heterotypic interactions between Pss proteins involved in the exopolysaccharide transport system in *Rhizobium leguminosarum* bv. *trifolii*. *Biol Chem* **394**: 541-559.
- Marolda, C.L., Lahiry, P., Vines, E., Saldias, S., and Valvano, M.A. (2006) Micromethods for the characterization of lipid A-core and O-antigen lipopolysaccharide. *Methods Mol Biol* **347**: 237-252.
- Marolda, C.L., Li, B., Lung, M., Yang, M., Hanuszkiewicz, A., Rosales, A.R., and Valvano, M.A. (2010) Membrane topology and identification of critical amino acid residues in the Wzx O-antigen translocase from *Escherichia coli* O157:H4. *J Bacteriol* **192**: 6160-6171.
- Marolda, C.L., Vicarioli, J., and Valvano, M.A. (2004) Wzx proteins involved in biosynthesis of O antigen function in association with the first sugar of the O-specific lipopolysaccharide subunit. *Microbiology* **150**: 4095-4105.
- Martinez, S.E., Wu, A.Y., Glavas, N.A., Tang, X.B., Turley, S., Hol, W.G., and Beavo, J.A. (2002) The two GAF domains in phosphodiesterase 2A have distinct roles in dimerization and in cGMP binding. *Proc Natl Acad Sci U S A* **99**: 13260-13265.
- McCarthy, R.R., Mazon-Moya, M.J., Moscoso, J.A., Hao, Y., Lam, J.S., Bordi, C., Mostowy, S., and Filloux, A. (2017) Cyclic-di-GMP regulates lipopolysaccharide modification and contributes to *Pseudomonas aeruginosa* immune evasion. *Nat Microbiol* **2**: 17027.
- McCleary, W.R., Esmon, B., and Zusman, D.R. (1991) *Myxococcus xanthus* protein C is a major spore surface protein. *J Bacteriol* **173**: 2141-2145.

- McDougald, D., Rice, S.A., Barraud, N., Steinberg, P.D., and Kjelleberg, S. (2012) Should we stay or should we go: mechanisms and ecological consequences for biofilm dispersal. *Nat Rev Microbiol* **10**: 39-50.
- Merritt, J.H., Brothers, K.M., Kuchma, S.L., and O'Toole, G.A. (2007) SadC reciprocally influences biofilm formation and swarming motility via modulation of exopolysaccharide production and flagellar function. *J Bacteriol* **189**: 8154-8164.
- Merroun, M.L., Ben Chekroun, K., Arias, J.M., and González-Muñoz, M.T. (2003) Lanthanum fixation by *Myxococcus xanthus*: cellular location and extracellular polysaccharide observation. *Chemosphere* **52**: 113-120.
- Milner, D.S., Till, R., Cadby, I., Lovering, A.L., Basford, S.M., Saxon, E.B., Liddell, S., Williams, L.E., and Sockett, R.E. (2014) Ras GTPase-like protein MglA, a controller of bacterial social-motility in Myxobacteria, has evolved to control bacterial predation by *Bdellovibrio*. *PLoS Genet* **10**: e1004253.
- Moak, P.L., Black, W.P., Wallace, R.A., Li, Z., and Yang, Z. (2015) The Hsp70-like StkA functions between T4P and Dif signaling proteins as a negative regulator of exopolysaccharide in *Myxococcus xanthus*. *PeerJ* **3**: e747.
- Mori, Y., Maeda, M., Takegawa, K., and Kimura, Y. (2012) PhpA, a tyrosine phosphatase of *Myxococcus xanthus*, is involved in the production of exopolysaccharide. *Microbiology* **158**: 2546-2555.
- Morona, R., Purins, L., Tocilj, A., Matte, A., and Cygler, M. (2009) Sequence-structure relationships in polysaccharide co-polymerase (PCP) proteins. *Trends Biochem Sci* **34**: 78-84.
- Morona, R., Van Den Bosch, L., and Daniels, C. (2000) Evaluation of Wzz/MPA1/MPA2 proteins based on the presence of coiled-coil regions. *Microbiology* **146** (Pt 1): 1-4.
- Müller, F.D., Schink, C.W., Hoiczky, E., Cserti, E., and Higgs, P.I. (2012) Spore formation in *Myxococcus xanthus* is tied to cytoskeleton functions and polysaccharide spore coat deposition. *Mol Microbiol* **83**: 486-505.
- Müller, F.D., Treuner-Lange, A., Heider, J., Huntley, S.M., and Higgs, P.I. (2010) Global transcriptome analysis of spore formation in *Myxococcus xanthus* reveals a locus necessary for cell differentiation. *BMC Genomics* **11**: 264.
- Müller, S., Strack, S.N., Ryan, S.E., Shawgo, M., Walling, A., Harris, S., Chambers, C., Boddicker, J., and Kirby, J.R. (2016) Identification of functions affecting predator-prey interactions between *Myxococcus xanthus* and *Bacillus subtilis*. *J Bacteriol* **198**: 3335-3344.
- Nan, B., Bandaria, J.N., Moghtaderi, A., Sun, I.-H., Yildiz, A., and Zusman, D.R. (2013) Flagella stator homologs function as motors for myxobacterial gliding motility by moving in helical trajectories. *Proc Natl Acad Sci U S A* **110**: E1508-E1513.
- Navarro, M.V., De, N., Bae, N., Wang, Q., and Sondermann, H. (2009) Structural analysis of the GGDEF-EAL domain-containing c-di-GMP receptor FimX. *Structure* **17**: 1104-1116.
- Nudleman, E., Wall, D., and Kaiser, D. (2006) Polar assembly of the type IV pilus secretin in *Myxococcus xanthus*. *Mol Microbiol* **60**: 16-29.
- O'Connor, K.A., and Zusman, D.R. (1991a) Behavior of peripheral rods and their role in the life cycle of *Myxococcus xanthus*. *J Bacteriol* **173**: 3342-3355.
- O'Connor, K.A., and Zusman, D.R. (1991b) Development in *Myxococcus xanthus* involves differentiation into two cell types, peripheral rods and spores. *J Bacteriol* **173**: 3318-3333.
- Okuda, S., Sherman, D.J., Silhavy, T.J., Ruiz, N., and Kahne, D. (2016) Lipopolysaccharide transport and assembly at the outer membrane: the PEZ model. *Nat Rev Microbiol* **14**: 337-345.
- Orr, M.W., Donaldson, G.P., Severin, G.B., Wang, J., Sintim, H.O., Waters, C.M., and Lee, V.T. (2015) Oligoribonuclease is the primary degradative enzyme for pGpG in *Pseudomonas aeruginosa* that is required for cyclic-di-GMP turnover. *Proc Natl Acad Sci U S A* **112**: E5048-5057.

- Overgaard, M., Wegener-Feldbrugge, S., and Søgaard-Andersen, L. (2006) The orphan response regulator DigR is required for synthesis of extracellular matrix fibrils in *Myxococcus xanthus*. *J Bacteriol* **188**: 4384-4394.
- Paintdakhi, A., Parry, B., Campos, M., Irnov, I., Elf, J., Surovtsev, I., and Jacobs-Wagner, C. (2016) Oufiti: an integrated software package for high-accuracy, high-throughput quantitative microscopy analysis. *Mol Microbiol* **99**: 767-777.
- Palsdottir, H., Remis, J.P., Schaudinn, C., O'Toole, E., Lux, R., Shi, W., McDonald, K.L., Costerton, J.W., and Auer, M. (2009) Three-dimensional macromolecular organization of cryofixed *Myxococcus xanthus* biofilms as revealed by electron microscopic tomography. *J Bacteriol* **191**: 2077-2082.
- Pan, H., He, X., Lux, R., Luan, J., and Shi, W. (2013) Killing of *Escherichia coli* by *Myxococcus xanthus* in aqueous environments requires exopolysaccharide-dependent physical contact. *Microb Ecol* **66**: 630-638.
- Panasenko, S.M. (1985) Methylation of macromolecules during development in *Myxococcus xanthus*. *J Bacteriol* **164**: 495-500.
- Panasenko, S.M., Jann, B., and Jann, K. (1989) Novel change in the carbohydrate portion of *Myxococcus xanthus* lipopolysaccharide during development. *J Bacteriol* **171**: 1835-1840.
- Patel, K.B., Furlong, S.E., and Valvano, M.A. (2010) Functional analysis of the C-terminal domain of the WbaP protein that mediates initiation of O antigen synthesis in *Salmonella enterica*. *Glycobiology* **20**: 1389-1401.
- Patel, K.B., Toh, E., Fernandez, X.B., Hanuszkiewicz, A., Hardy, G.G., Brun, Y.V., Bernards, M.A., and Valvano, M.A. (2012) Functional characterization of UDP-glucose:undecaprenyl-phosphate glucose-1-phosphate transferases of *Escherichia coli* and *Caulobacter crescentus*. *J Bacteriol* **194**: 2646-2657.
- Patra, P., Kisson, K., Cornejo, I., Kaplan, H.B., and Igoshin, O.A. (2016) Colony expansion of socially motile *Myxococcus xanthus* cells is driven by growth, motility, and exopolysaccharide production. *PLoS Comput Biol* **12**: e1005010.
- Pérez-Burgos, M., García-Romero, I., Jung, J., Valvano, M.A., and Søgaard-Andersen, L. (2019) Identification of the lipopolysaccharide O-antigen biosynthesis priming enzyme and the O-antigen ligase in *Myxococcus xanthus*: Critical role of LPS O-antigen in motility and development. *Mol Microbiol* **112**: 1178-1198.
- Pérez-Burgos, M., García-Romero, I., Valvano, M.A., and Søgaard-Andersen, L. (2020) Identification of the Wzx flippase, Wzy polymerase and sugar-modifying enzymes for spore coat polysaccharide biosynthesis in *Myxococcus xanthus*. *Mol Microbiol*.
- Pérez-Burgos, M., and Søgaard-Andersen, L., (2020) Regulation by cyclic di-GMP in *Myxococcus xanthus*. In: *Microbial Cyclic Di-Nucleotide Signaling*. S.-H. Chou, N. Guilian, V.T. Lee & U. Römling (eds). Cham: Springer International Publishing, pp. 293-309.
- Petters, T., Zhang, X., Nesper, J., Treuner-Lange, A., Gomez-Santos, N., Hoppert, M., Jenal, U., and Søgaard-Andersen, L. (2012) The orphan histidine protein kinase SgmT is a c-di-GMP receptor and regulates composition of the extracellular matrix together with the orphan DNA binding response regulator DigR in *Myxococcus xanthus*. *Mol Microbiol* **84**: 147-165.
- Pham, V.D., Shebelut, C.W., Mukherjee, B., and Singer, M. (2005) RasA is required for *Myxococcus xanthus* development and social motility. *J Bacteriol* **187**: 6845-6848.
- Plamann, L., Davis, J.M., Cantwell, B., and Mayor, J. (1994) Evidence that *asgB* encodes a DNA-binding protein essential for growth and development of *Myxococcus xanthus*. *J Bacteriol* **176**: 2013-2020.
- Raetz, C.R., and Whitfield, C. (2002) Lipopolysaccharide endotoxins. *Annu Rev Biochem* **71**: 635-700.

- Ramaswamy, S., Dworkin, M., and Downard, J. (1997) Identification and characterization of *Myxococcus xanthus* mutants deficient in calcofluor white binding. *J Bacteriol* **179**: 2863-2871.
- Ranjit, D.K., and Young, K.D. (2016) Colanic acid intermediates prevent *de novo* shape recovery of *Escherichia coli* spheroplasts, calling into question biological roles previously attributed to colanic acid. *J Bacteriol* **198**: 1230-1240.
- Rehm, B.H. (2010) Bacterial polymers: biosynthesis, modifications and applications. *Nat Rev Microbiol* **8**: 578-592.
- Reichenbach, H. (1999) The ecology of the myxobacteria. *Environ Microbiol Rep* **1**: 15-21.
- Reid, A.N., and Cuthbertson, L. (2012) Biosynthesis of Capsular Polysaccharides and Exopolysaccharides. *Bacterial glycomics: current research, technology and applications*: 27-54.
- Reid, A.N., and Szymanski, C.M., (2010) Biosynthesis and assembly of capsular polysaccharides. In: *Microbial Glycobiology*. P.J.B. Otto Holst, Mark von Itzstein, Anthony P. Moran (ed). Academic Press, pp. 351-373.
- Remis, J.P., Wei, D., Gorur, A., Zemla, M., Haraga, J., Allen, S., Witkowska, H.E., Costerton, J.W., Berleman, J.E., and Auer, M. (2014) Bacterial social networks: structure and composition of *Myxococcus xanthus* outer membrane vesicle chains. *Environ Microbiol* **16**: 598-610.
- Rodriguez-Soto, J.P., and Kaiser, D. (1997) Identification and localization of the Tgl protein, which is required for *Myxococcus xanthus* social motility. *J Bacteriol* **179**: 4372-4381.
- Roelofs, K.G., Wang, J., Sintim, H.O., and Lee, V.T. (2011) Differential radial capillary action of ligand assay for high-throughput detection of protein-metabolite interactions. *Proc Natl Acad Sci U S A* **108**: 15528-15533.
- Römling, U., Galperin, M.Y., and Gomelsky, M. (2013) Cyclic di-GMP: the first 25 years of a universal bacterial second messenger. *Microbiol Mol Biol Rev* **77**: 1-52.
- Ross, P., Weinhouse, H., Aloni, Y., Michaeli, D., Weinberger-Ohana, P., Mayer, R., Braun, S., de Vroom, E., van der Marel, G.A., van Boom, J.H., and Benziman, M. (1987) Regulation of cellulose synthesis in *Acetobacter xylinum* by cyclic diguanylic acid. *Nature* **325**: 279-281.
- Ruiz, N., Kahne, D., and Silhavy, T.J. (2009) Transport of lipopolysaccharide across the cell envelope: the long road of discovery. *Nat Rev Microbiol* **7**: 677-683.
- Saitou, N., and Nei, M. (1987) The Neighbor-Joining Method - a New Method for Reconstructing Phylogenetic Trees. *Mol Biol Evol* **4**: 406-425.
- Saldías, M.S., Patel, K., Marolda, C.L., Bittner, M., Contreras, I., and Valvano, M.A. (2008) Distinct functional domains of the *Salmonella enterica* WbaP transferase that is involved in the initiation reaction for synthesis of the O antigen subunit. *Microbiology* **154**: 440-453.
- Sambrook, J., and Russell, D.W., (2001) *Molecular cloning : a laboratory manual*. Cold Spring Harbor Laboratory Press, Cold Spring Harbor, N.Y.
- Schäffer, C., Wugeditsch, T., Messner, P., and Whitfield, C. (2002) Functional expression of enterobacterial O-polysaccharide biosynthesis enzymes in *Bacillus subtilis*. *Appl Environ Microbiol* **68**: 4722-4730.
- Schindelin, J., Arganda-Carreras, I., Frise, E., Kaynig, V., Longair, M., Pietzsch, T., Preibisch, S., Rueden, C., Saalfeld, S., Schmid, B., Tinevez, J.Y., White, D.J., Hartenstein, V., Eliceiri, K., Tomancak, P., and Cardona, A. (2012) Fiji: an open-source platform for biological-image analysis. *Nat Methods* **9**: 676-682.
- Schmid, J., Sieber, V., and Rehm, B. (2015) Bacterial exopolysaccharides: biosynthesis pathways and engineering strategies. *Front Microbiol* **6**.
- Schumacher, D., Bergeler, S., Harms, A., Vonck, J., Huneke-Vogt, S., Frey, E., and Søggaard-Andersen, L. (2017) The PomXYZ proteins self-organize on the bacterial nucleoid to stimulate cell division. *Dev Cell* **41**: 299-314 e213.

- Schumacher, D., and Søgaard-Andersen, L. (2017) Regulation of cell polarity in motility and cell division in *Myxococcus xanthus*. *Annu Rev Microbiol* **71**: 61-78.
- Schumacher, D., and Søgaard-Andersen, L. (2018) Fluorescence live-cell imaging of the complete vegetative cell cycle of the slow-growing social bacterium *Myxococcus xanthus*. *J Vis Exp*.
- Shi, W., Yang, Z., Sun, H., Lancero, H., and Tong, L. (2000) Phenotypic analyses of *frz* and *dif* double mutants of *Myxococcus xanthus*. *FEMS Microbiol Lett* **192**: 211-215.
- Shi, W., and Zusman, D.R. (1993) The two motility systems of *Myxococcus xanthus* show different selective advantages on various surfaces. *Proc Natl Acad Sci U S A* **90**: 3378-3382.
- Shi, X., Wegener-Feldbrugge, S., Huntley, S., Hamann, N., Hedderich, R., and Søgaard-Andersen, L. (2008) Bioinformatics and experimental analysis of proteins of two-component systems in *Myxococcus xanthus*. *J Bacteriol* **190**: 613-624.
- Shimkets, L.J. (1986a) Correlation of energy-dependent cell cohesion with social motility in *Myxococcus xanthus*. *J Bacteriol* **166**: 837-841.
- Shimkets, L.J. (1986b) Role of cell cohesion in *Myxococcus xanthus* fruiting body formation. *J Bacteriol* **166**: 842-848.
- Siewering, K., Jain, S., Friedrich, C., Webber-Birungi, M.T., Semchonok, D.A., Binzen, I., Wagner, A., Huntley, S., Kahnt, J., Klingl, A., Boekema, E.J., Søgaard-Andersen, L., and van der Does, C. (2014) Peptidoglycan-binding protein Tsap functions in surface assembly of type IV pili. *Proc Natl Acad Sci U S A* **111**: E953-961.
- Silhavy, T.J., Kahne, D., and Walker, S. (2010) The bacterial cell envelope. *Cold Spring Harb Perspect Biol* **2**: a000414.
- Singer, M., and Kaiser, D. (1995) Ectopic production of guanosine penta- and tetraphosphate can initiate early developmental gene expression in *Myxococcus xanthus*. *Genes Dev* **9**: 1633-1644.
- Skotnicka, D., Petters, T., Heering, J., Hoppert, M., Kaefer, V., and Søgaard-Andersen, L. (2015) c-di-GMP regulates type IV pili-dependent-motility in *Myxococcus xanthus*. *J Bacteriol* **198**: 77-90.
- Skotnicka, D., Smaldone, G.T., Petters, T., Trampari, E., Liang, J., Kaefer, V., Malone, J.G., Singer, M., and Søgaard-Andersen, L. (2016) A minimal threshold of c-di-GMP is essential for fruiting body formation and sporulation in *Myxococcus xanthus*. *PLoS Genet* **12**: e1006080.
- Sobhanifar, S., King, D.T., and Strynadka, N.C. (2013) Fortifying the wall: synthesis, regulation and degradation of bacterial peptidoglycan. *Curr Opin Struct Biol* **23**: 695-703.
- Sonnhammer, E.L., von Heijne, G., and Krogh, A. (1998) A hidden Markov model for predicting transmembrane helices in protein sequences. *Proc Int Conf Intell Syst Mol Biol* **6**: 175-182.
- Spangler, C., Bohm, A., Jenal, U., Seifert, R., and Kaefer, V. (2010) A liquid chromatography-coupled tandem mass spectrometry method for quantitation of cyclic di-guanosine monophosphate. *J Microbiol Methods* **81**: 226-231.
- Sprecher, K.S., Hug, I., Nesper, J., Potthoff, E., Mahi, M.A., Sangermani, M., Kaefer, V., Schwede, T., Vorholt, J., and Jenal, U. (2017) Cohesive properties of the *Caulobacter crescentus* holdfast adhesin are regulated by a novel c-di-GMP effector protein. *mBio* **8**.
- Steiner, S., Lori, C., Boehm, A., and Jenal, U. (2013) Allosteric activation of exopolysaccharide synthesis through cyclic di-GMP-stimulated protein-protein interaction. *EMBO J* **32**: 354-368.
- Stoodley, P., Sauer, K., Davies, D.G., and Costerton, J.W. (2002) Biofilms as complex differentiated communities. *Annu Rev Microbiol* **56**: 187-209.
- Sultana, A., and Lee, J.E. (2015) Measuring protein-protein and protein-nucleic acid interactions by bilayer interferometry. *Curr Protoc Protein Sci* **79**: 19 25 11-19 25 26.

- Sun, M., Wartel, M., Cascales, E., Shaevitz, J.W., and Mignot, T. (2011) Motor-driven intracellular transport powers bacterial gliding motility. *Proc Natl Acad Sci U S A* **108**: 7559-7564.
- Sutherland, I.W. (1976) Novel surface polymer changes in development of *Myxococcus* spp. *Nature* **259**: 46-47.
- Sutherland, I.W., and Thomson, S. (1975) Comparison of polysaccharides produced by *Myxococcus* strains. *J Gen Microbiol* **89**: 124-132.
- Szadkowski, D., Harms, A., Carreira, L.A.M., Wigbers, M., Potapova, A., Wuichet, K., Keilberg, D., Gerland, U., and Sogaard-Andersen, L. (2019) Spatial control of the GTPase MglA by localized RomR-RomX GEF and MglB GAP activities enables *Myxococcus xanthus* motility. *Nat Microbiol* **4**: 1344-1355.
- The-UniProt-Consortium (2019) UniProt: a worldwide hub of protein knowledge. *Nucleic Acids Res* **47**: D506-515.
- Thomasson, B., Link, J., Stassinopoulos, A.G., Burke, N., Plamann, L., and Hartzell, P.L. (2002) MglA, a small GTPase, interacts with a tyrosine kinase to control type IV pili-mediated motility and development of *Myxococcus xanthus*. *Mol Microbiol* **46**: 1399-1413.
- Treuner-Lange, A., Aguiluz, K., van der Does, C., Gomez-Santos, N., Harms, A., Schumacher, D., Lenz, P., Hoppert, M., Kahnt, J., Muñoz-Dorado, J., and Sogaard-Andersen, L. (2013) PomZ, a ParA-like protein, regulates Z-ring formation and cell division in *Myxococcus xanthus*. *Mol Microbiol* **87**: 235-253.
- Treuner-Lange, A., Macia, E., Guzzo, M., Hot, E., Faure, L.M., Jakobczak, B., Espinosa, L., Alcor, D., Ducret, A., Keilberg, D., Castaing, J.P., Lacas Gervais, S., Franco, M., Sogaard-Andersen, L., and Mignot, T. (2015) The small G-protein MglA connects to the MreB actin cytoskeleton at bacterial focal adhesions. *J Cell Biol* **210**: 243-256.
- Tytgat, H.L., and Lebeer, S. (2014) The sweet tooth of bacteria: common themes in bacterial glycoconjugates. *Microbiol Mol Biol Rev* **78**: 372-417.
- Ueki, T., and Inouye, S. (2005) Identification of a gene involved in polysaccharide export as a transcription target of FruA, an essential factor for *Myxococcus xanthus* development. *J Biol Chem* **280**: 32279-32284.
- Valvano, M.A. (2008) Undecaprenyl phosphate recycling comes out of age. *Mol Microbiol* **67**: 232-235.
- Valvano, M.A. (2011) Common themes in glycoconjugate assembly using the biogenesis of O-antigen lipopolysaccharide as a model system. *Biochemistry (Mosc)* **76**: 729-735.
- Valvano, M.A., Furlong, S.E., and Patel, K.B., (2011) Genetics, biosynthesis and assembly of O-antigen. In: *Bacterial lipopolysaccharides: structure, chemical synthesis, biogenesis and interaction with host cells*. Y.A. Knirel & M.A. Valvano (eds). Vienna: Springer Vienna, pp. 275-310.
- Vassallo, C., Pathak, D.T., Cao, P., Zuckerman, D.M., Hoiczyk, E., and Wall, D. (2015) Cell rejuvenation and social behaviors promoted by LPS exchange in myxobacteria. *Proc Natl Acad Sci U S A* **112**: E2939-2946.
- Velicer, G.J., and Yu, Y.T. (2003) Evolution of novel cooperative swarming in the bacterium *Myxococcus xanthus*. *Nature* **425**: 75-78.
- Vollmer, W., Blanot, D., and de Pedro, M.A. (2008) Peptidoglycan structure and architecture. *FEMS Microbiol Rev* **32**: 149-167.
- Wall, D., Kolenbrander, P.E., and Kaiser, D. (1999) The *Myxococcus xanthus pilQ (sglA)* gene encodes a secretin homolog required for type IV pilus biogenesis, social motility, and development. *J Bacteriol* **181**: 24-33.
- Wall, D., Wu, S.S., and Kaiser, D. (1998) Contact stimulation of Tgl and type IV pili in *Myxococcus xanthus*. *J Bacteriol* **180**: 759-761.
- Wallace, R.A., Black, W.P., Yang, X., and Yang, Z. (2014) A CRISPR with roles in *Myxococcus xanthus* development and exopolysaccharide production. *J Bacteriol* **196**: 4036-4043.

- Wang, Y.C., Chin, K.H., Tu, Z.L., He, J., Jones, C.J., Sanchez, D.Z., Yildiz, F.H., Galperin, M.Y., and Chou, S.H. (2016) Nucleotide binding by the widespread high-affinity cyclic di-GMP receptor MshEN domain. *Nat Commun* **7**: 12481.
- Wartel, M., Ducret, A., Thutupalli, S., Czerwinski, F., Le Gall, A.V., Mauriello, E.M., Bergam, P., Brun, Y.V., Shaevitz, J., and Mignot, T. (2013) A versatile class of cell surface directional motors gives rise to gliding motility and sporulation in *Myxococcus xanthus*. *PLoS Biol* **11**: e1001728.
- Weimer, R.M., Creighton, C., Stassinopoulos, A., Youderian, P., and Hartzell, P.L. (1998) A chaperone in the HSP70 family controls production of extracellular fibrils in *Myxococcus xanthus*. *J Bacteriol* **180**: 5357-5368.
- Whitfield, C. (2006) Biosynthesis and assembly of capsular polysaccharides in *Escherichia coli*. *Annu Rev Biochem* **75**: 39-68.
- Whitfield, C. (2010) Glycan chain-length control. *Nat Chem Biol* **6**: 403-404.
- Whitfield, C., and Larue, K. (2008) Stop and go: regulation of chain length in the biosynthesis of bacterial polysaccharides. *Nat Struct Mol Biol* **15**: 121-123.
- Whitfield, C., and Trent, M.S. (2014) Biosynthesis and export of bacterial lipopolysaccharides. *Annu Rev Biochem* **83**: 99-128.
- Whitney, J.C., and Howell, P.L. (2013) Synthase-dependent exopolysaccharide secretion in Gram-negative bacteria. *Trends Microbiol* **21**: 63-72.
- Willis, L.M., and Whitfield, C. (2013a) KpsC and KpsS are retaining 3-deoxy-D-manno-oct-2-ulosonic acid (Kdo) transferases involved in synthesis of bacterial capsules. *Proc Natl Acad Sci U S A* **110**: 20753-20758.
- Willis, L.M., and Whitfield, C. (2013b) Structure, biosynthesis, and function of bacterial capsular polysaccharides synthesized by ABC transporter-dependent pathways. *Carbohydr Res* **378**: 35-44.
- Wilson, W.A., Roach, P.J., Montero, M., Baroja-Fernandez, E., Munoz, F.J., Eydallin, G., Viale, A.M., and Pozueta-Romero, J. (2010) Regulation of glycogen metabolism in yeast and bacteria. *FEMS Microbiol Rev* **34**: 952-985.
- Wireman, J.W., and Dworkin, M. (1977) Developmentally induced autolysis during fruiting body formation by *Myxococcus xanthus*. *J Bacteriol* **129**: 796-802.
- Wolgemuth, C., Hoiczky, E., Kaiser, D., and Oster, G. (2002) How myxobacteria glide. *Curr Biol* **12**: 369-377.
- Wu, S.S., and Kaiser, D. (1995) Genetic and functional evidence that Type IV pili are required for social gliding motility in *Myxococcus xanthus*. *Mol Microbiol* **18**: 547-558.
- Wu, S.S., and Kaiser, D. (1996) Markerless deletions of *pil* genes in *Myxococcus xanthus* generated by counterselection with the *Bacillus subtilis sacB* gene. *J Bacteriol* **178**: 5817-5821.
- Wu, S.S., and Kaiser, D. (1997) Regulation of expression of the *pilA* gene in *Myxococcus xanthus*. *J Bacteriol* **179**: 7748-7758.
- Wu, S.S., Wu, J., and Kaiser, D. (1997) The *Myxococcus xanthus pilT* locus is required for social gliding motility although pili are still produced. *Mol Microbiol* **23**: 109-121.
- Xu, Q., Black, W.P., Cadieux, C.L., and Yang, Z. (2008) Independence and interdependence of Dif and Frz chemosensory pathways in *Myxococcus xanthus* chemotaxis. *Mol Microbiol* **69**: 714-723.
- Xu, Q., Black, W.P., Nascimi, H.M., and Yang, Z. (2011) DifA, a methyl-accepting chemoreceptor protein-like sensory protein, uses a novel signaling mechanism to regulate exopolysaccharide production in *Myxococcus xanthus*. *J Bacteriol* **193**: 759-767.
- Xu, Q., Black, W.P., Ward, S.M., and Yang, Z. (2005) Nitrate-dependent activation of the Dif signaling pathway of *Myxococcus xanthus* mediated by a NarX-DifA interspecies chimera. *J Bacteriol* **187**: 6410-6418.

- Yan, J., Garza, A.G., Bradley, M.D., and Welch, R.D. (2012) A Clp/Hsp100 chaperone functions in *Myxococcus xanthus* sporulation and self-organization. *J Bacteriol* **194**: 1689-1696.
- Yang, Z., Geng, Y., and Shi, W. (1998a) A DnaK homolog in *Myxococcus xanthus* is involved in social motility and fruiting body formation. *J Bacteriol* **180**: 218-224.
- Yang, Z., Geng, Y., Xu, D., Kaplan, H.B., and Shi, W. (1998b) A new set of chemotaxis homologues is essential for *Myxococcus xanthus* social motility. *Mol Microbiol* **30**: 1123-1130.
- Yang, Z., Guo, D., Bowden, M.G., Sun, H., Tong, L., Li, Z., Brown, A.E., Kaplan, H.B., and Shi, W. (2000a) The *Myxococcus xanthus* *wbgB* gene encodes a glycosyltransferase homologue required for lipopolysaccharide O-antigen biosynthesis. *Arch Microbiol* **174**: 399-405.
- Yang, Z., and Li, Z. (2005) Demonstration of interactions among *Myxococcus xanthus* Dif chemotaxis-like proteins by the yeast two-hybrid system. *Arch Microbiol* **183**: 243-252.
- Yang, Z., Ma, X., Tong, L., Kaplan, H.B., Shimkets, L.J., and Shi, W. (2000b) *Myxococcus xanthus* *dif* genes are required for biogenesis of cell surface fibrils essential for social gliding motility. *J Bacteriol* **182**: 5793-5798.
- Youderian, P., Burke, N., White, D.J., and Hartzell, P.L. (2003) Identification of genes required for adventurous gliding motility in *Myxococcus xanthus* with the transposable element mariner. *Mol Microbiol* **49**: 555-570.
- Youderian, P., and Hartzell, P.L. (2006) Transposon insertions of magellan-4 that impair social gliding motility in *Myxococcus xanthus*. *Genetics* **172**: 1397-1410.
- Yu, R., and Kaiser, D. (2007) Gliding motility and polarized slime secretion. *Mol Microbiol* **63**: 454-467.
- Zhang, Y., Ducret, A., Shaeviz, J., and Mignot, T. (2012) From individual cell motility to collective behaviors: insights from a prokaryote, *Myxococcus xanthus*. *FEMS Microbiol Revs* **36**: 149-164.
- Zhang, Y., Franco, M., Ducret, A., and Mignot, T. (2010) A bacterial Ras-like small GTP-binding protein and its cognate GAP establish a dynamic spatial polarity axis to control directed motility. *PLoS Biol* **8**: e1000430.
- Zhou, T., and Nan, B. (2017) Exopolysaccharides promote *Myxococcus xanthus* social motility by inhibiting cellular reversals. *Mol Microbiol* **103**: 729-743.
- Zusman, D.R., Scott, A.E., Yang, Z., and Kirby, J.R. (2007) Chemosensory pathways, motility and development in *Myxococcus xanthus*. *Nat Rev Microbiol* **5**: 862-872.

Acknowledgments

In first instance, I would like to sincerely express my gratitude to my supervisor, Prof. Dr. Lotte Søgaaard-Andersen, for welcoming me into her group, for her advice and supervision that made me improve as a scientist and grow as a person, and for giving me the freedom and support to develop my scientific interests.

I would like to mention the people who brought me to this step of my life whom I would like to genuinely thank. Mr. Javier Igual and Mr. Jordi Bley transmitted to me their passion for biology and chemistry back in my school days, which convinced me to pursue a scientific career. Prof. Elena Mercadé and Prof. Francisco Congregado introduced me to the world of microorganisms and glycans and Dr. Faïza Diaba, who taught me about scientific writing and synthesis of natural molecules.

During my project, I was surrounded by amazing people in the lab who spiced my daily routine. I would like to thank Dr. Dorota Skotnicka, who trained me at the beginning of the PhD project until the day I became an “independent scientist” and Dr. Magdalena Połatyńska, who was always there for me to listen and discuss my scientific theories. Also, I was greatly inspired by Dr. Nuria Gómez Santos. Further, it was a great pleasure to work with, teach and supervise Jana Jung and Eugenia Schanders’s lab work.

My project would not have been the same without the help of Dr. Dobromir Szadkowski. He could always fix a broken microscope, sometimes it took just his physical presence in the room. I would like to express my gratitude to Dr. Anke Treuner-Lange for her patience in answering all my questions about myxobacteria and Marco Herfurth for daydreaming about random scientific topics with me. Also, I would like to thank the remaining members of “lab 1”, with whom I spend most of my time in the last years, for being there when I needed help, support or sweets: Dr. Deepak Anand, Dr. Sofya Kuzmich, Memduha Muratoglu, Ahmet Tekin, Michel Oklitschek, Janina Foronda and Dr. Anna McLoon. I am happy to have had Luis Carreira keeping me company in the lab at all hours of the day and night, including the weekends. I could always count on Dr. Anna Potapova to distract me and cheer me up when something was not working, either by having a coffee, dinner, going to the cinema or to sport class.

Many thanks also go to Susanne Kneip, Steffi Lindow, Andrea Harms, Yvonne Ried and Elizabeth Ried. The five of you were and are essential for the proper running of the lab and I could always count on you when I needed new materials, technical help or huge amounts of CTT media. Also

big thanks to Tobi Bender, Dr. Dominik Schumacher, Dr. Sabrina Huneke-Vogt, Franziska Müller and Michael Seidel.

To have been in the Cell surfaces-Gordon conference in 2018 was one of the best experiences during the project, since I got to know Prof. Dr. Miguel Valvano who later, and together with Dr. Inmaculada García Romero, collaborated with us. It was an amazing experience to work with you and learn so much from you. Of course, I would also like to thank the lab of Prof. Dr. Volkhard Kaefer for helping us to measure c-di-GMP, the members of my Thesis Advisory Committee for the help during the project: Prof. Dr. Anke Becker, Prof. Dr. Tobi Erb, Prof. Dr. Erhard Bremer and Dr. Alexander Elsholz, as well as my Thesis Committee for evaluating my thesis: Prof. Dr. Erhard Bremer, Prof. Dr. Lars-Oliver Essen and Prof. Dr. Hans-Ulrich Mösch.

My work was supported by the Deutsche Forschungsgemeinschaft (DFG, German Research Council) within the framework of the SFB987 'Microbial Diversity in Environmental Signal Response'.

Finally, I am very thankful to my family for supporting my decisions and always being there taking care of me. Especially, I would like to thank my parents, and my aunts Carmen and Matilde for always keeping an eye on me and worrying for me. As last, I would like to express my gratefulness to Joachim, who constantly supported me, took care of me and accompanied me in this PhD adventure.

List of publications

Pérez-Burgos, M. & Søgaaard-Andersen, L. (2020). Regulation by c-di-GMP in *Myxococcus xanthus*. In: Microbial Cyclic Di-Nucleotide Signaling. S.-H. Chou, N. Guiliani, V.T. Lee & U. Römling (eds). Cham: Springer International Publishing, pp. 293-309.

Pérez-Burgos, M., García-Romero, I., Jung, J. Valvano, M.A. & Søgaaard-Andersen, L. (2019). Identification of the lipopolysaccharide O-antigen biosynthesis priming enzyme and the O-antigen ligase in *Myxococcus xanthus*: Critical role of LPS O-antigen in motility and development. Mol Microbiol, 112, 1178-1198

Pérez-Burgos M., García-Romero I., Valvano M.A., Søgaaard-Andersen L. Identification of the Wzx flippase, Wzy polymerase and sugar-modifying enzymes for spore coat polysaccharide biosynthesis in *Myxococcus xanthus*. Mol Microbiol (in press)

Pérez-Burgos M., García-Romero I., Jung J., Schander E., Valvano M.A., Søgaaard-Andersen L. Identification of the exopolysaccharide biosynthesis pathway in *Myxococcus xanthus* (in preparation)